ANL/NE-12/4

The SAS4A/SASSYS-1 Safety Analysis Code System

Nuclear Engineering Division

ANL/NE-12/4

The SAS4A/SASSYS-1 Safety Analysis Code System

Chapter 10:
SSCOMP: Pre-Transient Characterization of Metallic Fuel Pins

Kalimullah
Nuclear Engineering Division
Argonne National Laboratory

January 31, 2012

TABLE OF CONTENTS

Table of Contents 10-iii

List of Figures 10-v

List of Tables 10-xi

Nomenclature 10-xiii

SSCOMP: Pre-Transient Characterization of Metallic Fuel Pins 10-1

10.1 Introduction and Overview 10-1
10.2 The Earlier SSCOMP Model and Current Capability 10-3
10.3 Thermal Properties of U-Pu-Zr and U-Zr Alloy Fuels as a Function of Composition 10-4
10.3.1 Temperature-Dependent Tables 10-11
10.3.2 Regionwise Interpolation of IFR Handbook Data 10-11
10.3.2.1 Enthalpy of U-Pu-Zr Fuel 10-14
10.3.2.2 Specific Heat of U-Pu-Zr Fuel 10-44
10.3.2.3 Theoretical Density of U-Pu-Zr Fuel 10-57
10.3.2.4 Thermal Expansion of U-Pu-Zr Fuel 10-69
10.3.2.5 Thermal Conductivity of Unirradiated 100% Dense U-Pu-Zr Fuel 10-87
10.3.2.6 Burnup or Porosity Correction of Thermal Conductivity 10-115
10.3.2.7 Uncertainties of U-Pu-Zr Fuel Thermal Conductivity 10-121
10.3.3 Correlations of the Report ANL/RAS 85-19 10-124
10.3.3.1 Theoretical Density of U-Pu-Zr Fuel at 298K 10-124
10.3.3.2 Thermal Expansion of U-Pu-Zr Fuel 10-126
10.3.3.3 Enthalpy and Specific Heat of U-Pu-Zr Fuel 10-127
10.3.3.4 Thermal Conductivity of U-Pu-Zr Fuel 10-128
10.3.3.5 Porosity Correction of Fuel Thermal Conductivity 10-147
10.3.4 Properties of Some Specific Fuels 10-147
10.3.5 Computer Implementation 10-149
10.3.5.1 List of Fuel Thermal Property Subroutines 10-150
10.3.5.2 Input Data Related to Fuel Thermal Properties 10-151
10.4 Future Directions for Modeling Efforts 10-155
10.4.1 Fuel constituent Radial Migration 10-155
10.4.2 Fission Gas Behavior, and Porosity Formation and Distribution 10-156
10.4.3 Irradiation-Induced Radial and Axial Swelling of Fuel and Cladding 10-156

References 10-159

APPENDIX 10.1: Equivalency of Interpolation in Terms of Weight Fractions and Atom Fractions 10-163

APPENDIX 10.2: Correlations in the IFR Handbook and Some Other Sources 10-165

LIST OF FIGURES

Fig. 10.3-1. Flow Diagram of Subroutine CFUEL for Fuel Specific Heat 10-5
Fig. 10.3-2. Flow Diagram of Function Subprogram RHOF for Fuel Theoretical Density 10-6
Fig. 10.3-3. Flow Diagram of Function subprogram FK for Thermal Conductivity of a Single Fuel Radial Node 10-7
Fig. 10.3-4. Flow Diagram of Subroutine KFUEL for Thermal Conductivity of All Fuel Radial Nodes in a Pin Axial Segment 10-9
Fig. 10.3-5. Flow Diagram of Subroutine PRECA1 to Pre-Calculate Parameters Stored for Fast Evaluation of U-Pu-Zr Specific Heat, Theoretical Density and Thermal Conductivity by Fuel Type 10-12
Fig. 10.3-6. Diagram Showing Enthalpy Interpolation Regions for Solid U-Pu-Zr Ternary Alloy 10-16
Fig. 10.3-7. Enthalpy of U-15Pu-10Zr Obtained from Eqs. (10.3-2) to (10.3-5) That is Used as Database 1 in Regions 1, 2 and 3; and its Comparison with Metallic Fuels Handbook Data 10-20
Fig. 10.3-8. Enthalpy of U Metal Obtained From Eqs. (10.3-2) and (10.3-6) That is used as Database 1 in Region 4; and its Comparison With Metallic Fuels handbook Data 10-21
Fig. 10.3-9. Enthalpy of U-5.4Zr Obtained From Eqs. (10.3-2), (10.3-4) and (10.3-7) That is Used as Database 2 in Regions 1, 2 and 4; and its Comparison With Metallic Fuels Handbook Data 10-22
Fig. 10.3-10. Enthalpy of U-10Zr Obtained from Eqs. (10.3-2), (10.3-4) and (10.3-7) That is Used as Database 2 in Regions 1, 2 and 4; and its Comparison With Metallic Fuels Handbook Data 10-23
Fig. 10.3-11. Enthalpy of U-21.1Zr Obtained From Eqs. (10.3-2), (10.3-4) and (10.3-7) That is Used as Database 2 in Region 1; and its Comparison With Metallic Fuels Handbook Data 10-24
Fig. 10.3-12. Enthalpy of U-37.6Zr Obtained From Eqs. (10.3-2),v(10.3-4) and (10.3-7) That is Used as Database 2 in Regions 1 and 3; and its Comparison With Metallic Fuels Handbook Data 10-25
Fig. 10.3-13. Enthalpy of Pu Metal Obtained From Eqs. (10.3-3) and (10.3-8) That is Used as Database 3 in Regions 2, 3 and 4; and its Comparison With Metallic Fuels Handbook Data 10-26
Fig. 10.3-14. Flow Diagram of Subroutine HFUEL1 for U-Pu-Zr Enthalpy 10-35
Fig. 10.3-15. Diagram Showing the 9 Parameters (ACPF1 to ACPF7, and Solidus and Liquidus Temperatures) Pre-Calculated and Stored for Each U-Pu-Zr Fuel Type for Fast Evaluation of Specific Heat 10-36
Fig. 10.3-16. Comparison of Calculated Enthalpy of U-Pu-10Zr Fuel With the IFR Metallic Fuels Handbook Data 10-37
Fig. 10.3-17. Comparison of Calculated Enthalpy of U-10Zr Fuel With the

Handbook Data (Input KBASE to Subroutine HFUEL1-1) 10-38
Fig. 10.3-18. Comparison of Calculated Enthalpy of Uranium Metal with the IFR Metallic Fuels Handbook Data 10-39
Fig. 10.3-19. Comparison of Calculated Enthalpy of Plutonium Metal with the IFR Metallic Fuels Handbook Data 10-40
Fig. 10.3-20. Variation of U-5Pu-Zr Alloy Fuel Enthalpy With Composition Obtained From Subroutine HFUEL1 Based on the Method of Regionwise Interpolation 10-41
Fig. 10.3-21. Variation of U-20Pu-Zr Alloy Fuel Enthalpy With Composition Obtained From Subroutine HFUEL1 Based on the Method of Regionwise Interpolation 10-42
Fig. 10.3-22. Variation of U-30Pu-Zr Alloy Fuel Enthalpy With Composition Obtained From Subroutine HFUEL1 Based on the Method of Regionwise Interpolation 10-43
Fig. 10.3-23. Flow Diagram of Subroutine CFUEL1 for U-Pu-Zr Specific Heat 10-46
Fig. 10.3-24. Detailed Variation of U-Pu-2Zr Fuel Specific Heat Obtained by Regionwise Interpolation of Metallic Fuels Handbook Data 10-47
Fig. 10.3-25. Detailed Variation of U-Pu-10Zr Fuel Specific Heat Obtained by Regionwise Interpolation of Metallic Fuels Handbook Data 10-48
Fig. 10.3-26. Detailed Variation of U-Pu-25Zr Fuel Specific Heat Obtained by Regionwise Interpolation of Metallic Fuels Handbook Data 10-49
Fig. 10.3-27. Specific Heat of Mark-V (U-20Pu-10Zr) Fuel Obtained by Regionwise Interpolation of Metallic Fuels Handbook Data 10-50
Fig. 10.3-28. Specific Heat of U-Pu-2Zr Alloy Fuel Obtained By Regionwise Interpolation of Metallic Fuels Handbook Data 10-51
Fig. 10.3-29. Specific Heat of U-Pu-2Zr Alloy Fuel Obtained by Regionwise Interpolation of Metallic Fuels Handbook Data (Enlarged) 10-52
Fig. 10.3-30. Specific Heat of U-Pu-10Zr Alloy Fuel Obtained by Regionwise Interpolation of Metallic Fuels Handbook Data 10-53
Fig. 10.3-31. Specific Heat of U-Pu-10Zr Alloy Fuel Obtained by Regionwise Interpolation of Metallic Fuels Handbook Data (Enlarged). 10-54
Fig. 10.3-32. Specific Heat of U-Pu-25Zr Alloy Fuel Obtained by Regionwise Interpolation of Metallic Fuels Handbook Data 10-55
Fig. 10.3-33. Specific Heat of U-Pu-25Zr Alloy Fuel Obtained by Regionwise Interpolation of Metallic Fuels Handbook Data (Enlarged) 10-56
Fig. 10.3-34. Flow Diagram of subroutine PHOFM for U-Pu-Zr Fuel Theoretical Density 10-64
Fig.. 10.3-35. Theoretical Density of U-Pu Fuel Without Fission Products, Obtained from Regionwise Interpolation 10-65
Fig. 10.3-36. Theoretical Density of U-Pu-10Zr Fuel Without Fission Products, Obtained From Regionwise Interpolation of IFR Handbook Data 10-66

Fig. 10.3-37. Theoretical Density of U-Pu-20Zr Fuel Without Fission Products, Obtained from Regionwise Interpolation of IFR Handbook Data....10-67
Fig. 10.3-38. Theoretical Density of U-Pu-30Zr Fuel Without Fission Products, Obtained from Regionwise interpolation of IFR Handbook Data....10-68
Fig. 10.3-39. Diagram Showing Thermal Expansion Interpolation Regions for Solid U-Pu-Zr Alloy Fuels....10-70
Fig. 10.3-40. Flow Diagram of Subroutine THEXP2 for U-Pu-Zr Thermal Expansion....10-75
Fig. 10.3-41. Comparison of Uranium Metal Linear Thermal Expansion Data in IFR Handbook With Those Calculated by the Regionwise Interpolation Subroutine THEXP1....10-76
Fig. 10.3-42. Comparison of U-10Zr Alloy Linear Thermal Expansion Data in IFR Handbook With Those Calculated by the Regionwise Interpolation Subroutine THEXP1....10-77
Fig. 10.3-43. Comparison of U-20Zr Alloy Linear Thermal Expansion Data in IFR Handbook With those Calculated by the Regionwise Interpolation Subroutine THEXP1....10-78
Fig. 10.3-44. Comparison of Zirconium Metal Linear Thermal Expansion Data in IFR Handbook With Those Calculated by the Regionwise Interpolation Subrountine THEXP1....10-79
Fig. 10.3-45. Comparison of U-15Pu-10Zr Linear Thermal Expansion Data in IFR Handbook With Those Calculated by the Regionwise Interpolation Subroutine THEXP1....10-80
Fig. 10.3-46. Comparison of U-19Pu-10Zr Linear Thermal Expansion Data in IFR Handbook With Those Calculated by the Regionwise Interpolation Subroutine THEXP1....10-81
Fig. 10.3-47. Comparison of U-26Pu-10Zr Linear Thermal expansion Data in IFR Handbook With those Calculated by the Regionwise Interpolation Subroutine THEXP1....10-82
Fig. 10.3-48. Comparison of Plutonium Metal Liner Thermal Expansion Data in IFR Handbook With Those calculated by the Regionwise Interpolation Subroutine THEXP1....10-83
Fig. 10.3-49. Linear Thermal Expansion of U-Pu Fuel Without Fission Products, Obtained From Regionwise Interpolation of IFR Handbook Data....10-84
Fig. 10.3-50. Linear Thermal Expansion of U-Pu-10Zr fuel Without Fission Products, Obtained From Regionwise Interpolation of IFR Handbook Data....10-85
Fig. 10.3-51. Linear Thermal Expansion of U-Pu-30Zr Fuel Without Fission Products, Obtained From Regionwise Interpolation of IFR Handbook Data....10-86
Fig. 10.3-52. Diagram Showing Thermal Conductivity Interpolation Regions for 100% Dense Solid U-Pu-Zr Fuels....10-89

Fig. 10.3-53. Flow Diagram of Subroutine KFUEL1 for 100% Dense U-Pu-Zr Thermal Conductivity 10-100
Fig. 10.3-54. Comparison of 100% Dense Uranium Metal Thermal Conductivity Data in IFR Handbook With Those Calculated by Subroutine KFUEL1 10-101
Fig. 10.3-55. Comparison of 100% Dense U-1.5Zr Fuel thermal Conductivity Data in IFR Handbook With Those Calculated by Subroutine KFUEL1 10-102
Fig. 10.3-56. Comparison of 100% Dense U-5.9Zr Fuel Thermal Conductivity Data in IFR Handbook With Those Calculated by Subroutine KFUEL1 10-103
Fig. 10.3-57. Comparison of 100% Desense U-11.4Zr Fuel Thermal Conductivity Data in IFR Handbook With Those Calculated by Subroutine KFUEL1 10-104
Fig. 10.3-58. Comparison of 100% Dense U-20Zr Fuel Thermal Conductivity Data in IFR Handbook With Those Calculated by Subroutine KFUEL1 10-105
Fig. 10.3-59. Comparison of 100% Dense U-40Zr Fuel Thermal Conductivity Data in IFR Handbook With Those Calculated by Subroutine KFUEL1 10-106
Fig. 10.3-60. Comparison of 100% Dense U-14.7Pu-9.7Zr Fuel Thermal Conductivity Data in IFR Handbook With Those Calculated by Subroutine KFUEL1 10-107
Fig. 10.3-61. Comparison of 100% Dense U-18.4Pu-11.5Zr Fuel Thermal Conductivity Data in IFR Handbook With Those Calculated by Subroutine KFUEL1 10-108
Fig. 10.3-62. Comparison of 100% Dense U-16.2Pu-6.2Zr Fuel Thermal Conductivity Data in IFR Handbook With Those Calculated by Subroutine KFUEL1 10-109
Fig. 10.3-63. Comparison of 100% Dense U-10Pu Fuel Thermal Conductivity Data With Those Calculated by Subroutine KFUEL1 10-110
Fig. 10.3-64. Comparison of 100% Dense Pu Metal Thermal Conductivity Data in Plutonium Handbook With Those Calculated by Subroutine KFUEL1 10-111
Fig. 10.3-65. Thermal Conductivity of 100% Dense U-Pu-1.0Zr Alloy Fuel, Obtained From Regionwise Interpolation of IFR Handbook Data 10-112
Fig. 10.3-66. Thermal Conductivity of 100% Dense U-Pu-10Zr Alloy Fuel, Obtained From Regionwise Interpolation of IFR Handbook Data 10-113
Fig. 10.3-67. Thermal Conductivity of 100% Dense U-Pu-30Zr Alloy Fuel, Obtained From Regionwise Interpolation IFR Handbook Data 10-114
Fig. 10.3-68. A Unit Cell of Porous Metallic Fuel Containing a Sodium-Filled Pore and a Gas-Filled Pore (Only One Pore is Shown for Clarity) 10-118
Fig. 10.3-69. Uranium Specific Heat Correlation Including the Heats of Solid-State Transformations 10-131
Fig. 10.3-70. Plutonium Specific Heat Correlation Including the Heats of Solid-State Temperature 10-132
Fig. 10.3-71. Zirconium Specific Heat Correlation Including the Heats of Solid-State Transformations 10-133
Fig. 10.3-72. Uranium Enthalpy Obtained by Integrating its Specific Heat

Correlation 10-136
Fig. 10.3-73. Plutonium Enthalpy Obtained by Integrating its Specific Heat Correlation 10-137
Fig. 10.3-74. Zirconium Enthalpy Obtained by Integrating its Specific Heat Correlation 10-138
Fig. 10.3-75. Thermal Conductivity of the Uranium-Zirconium Binary Alloy for the Full Range of Composition 10-139
Fig. 10.3-76. Plot of Coefficient C vs. Temperature Obtained from Thermal Conductivity Data for U-Pu-Zr Samples D-44, D-54 and D-50 10-142
Fig. 10.3-77. Comparison of the Thermal Conductivity Correlation Eqs. (10.3-102) and (10.3-104) with the Data for the U-Pu-Zr Sample D-44 10-144
Fig. 10.3-78. Comparison of the Thermal Conductivity Correlation Eqs. (10.3-102) and (10.3-104) with the Data for the U-Pu-Zr Sample D-54 10-145
Fig. 10.3-79. Comparison of the Thermal Conductivity Correlation Eqs. (10.3-102) and (10.3-104) with the Data for the U-Pu-Zr Sample D-50 10-146

LIST OF TABLES

Table 10.3-1. Basic Alloys Whose IFR Handbook Enthalphy Data are Combined to Obtain the Enthalpy of a Desired U-Pu-Zr Alloy Composition 10-18
Table 10.3-2. Comparison of Measured and Calculated Theoretical Densities of U-Pu-Zr Alloys at 293K 10-59
Table 10.3-3. Linear Thermal Expansion Data of the 8 Basic Solid Alloys or Components Used in the Method of Regionwise Interpolation 10-72
Table 10.3-4. Thermal Conductivity Data of the 9 100%-Dense Basic Solid Alloys/Components Used in the Method of Regionwise Interpolation 10-92
Table 10.3-5. Coefficients of Quadratic Functions of Temperature Fitted to Thermal Conductivity Data of the 9 100%-Dense Basic Solid Alloys/Components Used in the Method of Regionwise Interpolation 10-93
Table 10.3-6. Estimation of 100%-Dense Molten Uranium Thermal Conductivity Using Wiedermann-Lorenz Law 10-98
Table 10.3-7. Accuracy of Unirradiated 100% Dense U-Pu-Zr Alloy/Component Thermal Conductivity Data Used in the Method of Regionwise Interpolation 10-122
Table 10.3-8. Comparison of Measured and Estimated Theoretical Densities of U-Pu-Zr Alloy at 298K 10-126
Table 10.3-9. Enthalpy and Specific Heat Data of Uranium Metal [10-10] 10-129
Table 10.3-10. Enthalpy and Specific Heat Data of Plutonium Metal [10-10] 10-130
Table 10.3-11. Enthalpy and Specific Heat Data for Zirconium Metal [10-10] 10-130
Table 10.3-12. Thermal Conductivity Data for Three U-Pu-Zr Alloys Prepared in Casting Numbers D-44, D-54 and D50 10-135
Table 10.3-13. Comparison of Thermal Conductivity Evaluated Using Eq. (10.3-101) With the Data [10-18] for U-20Zr Binary Alloy 10-140
Table 10.3-14. Temperature Variation of the Plutonium Alloying Coefficient C Evaluated from the Thermal Conductivity Data for Three U-Pu-Zr Alloys Prepared in Casting Numbers D-44, D-54 and D-50 10-141
Table 10.3-15. Input Data Required to Use IFR Handbook U-Pu-Zr Fuel Properties Data and Multiple Radial Fuel Zones Option 10-152
Table 10.4-1. Internal Arrays Required for Implementing IFR Handbook U-Pu-Zr Fuel Properties Data and Multiple Radial Fuel Zones Option 10-156

NOMENCLATURE

Symbols	Definition	Units
A	Atom fraction, e.g., Eq. (10.3-7) or coefficients of the quadratic function of temperature for fuel thermal conductivity, e.g., Eqs. (10.3-52) and (10.3-61).	
a	Atomic weight	
B	Coefficient of the quadratic function of temperature for fuel thermal conductivity, e.g., Eqs. (A10.2-1) to (A10.2-3)	
Bu	Fuel burnup	atom %
C	Plutonium alloying coefficient in thermal conductivity Eq. (10.3-102)	
C_p	Specific heat	J/kg-K
c	Coefficient of the quadratic term in the simplified enthalpy Eq. (10.3-26)	
D	Value of determinants in Cramer's rule for solving a system of linear algebraic equations	
f_o	Heavy-metal mass fissioned expressed as a percentage of U-Pu-Zr alloy post-irradiation mass	
H	Enthalpy	J/mol
h	Enthalpy	J/kg
K	Thermal Conductivity	W/m-K
K_{pt1}	Thermal conductivity of a pore tube containing a fission gas-filled pore	W/m-K
K_{pt2}	Thermal conductivity of a pore tube containing a logged sodium-filled pore	W/m-K
L	Length, e.g., Eq. (10.3-44) or Lorenz number in Q. (10.3-68)	m W-Ω/K^2
M	Mass	kg
m_a	One atomic mass unit, 1.6592828 x 10^{-27} kg	kg
N	Number of atoms, e.g., Eq. (10.3-34) or number of fissions, e.g., Eq. (10.3-35) or number of pairs of temperature and enthalpy values, e.g., Eq. (10.3-37)	
Na	Avogadro's number, 6.02472 x 10^{26} mulecules/kg-mole	/kg-mole
P′	Porosity fraction relative to the 100%-dense volume	
P_{c1}	Areal fraction of a face of a unit cell that is occupied by a sodium-filled pore, e.g., Eq. (10.3-72)	

Symbols	Definition	Units
P_{c2}	Areal fraction of a face of a unit cell that is occupied by a sodium-filled pore, e.g., Eq. (10.3-72)	
P_g	Gas-filled porosity fraction relative to the swollen fuel volume	
$P_{I,1}$	Fraction of the side (in heat flow direction) of a unit cell that is occupied by a gas-filled pore	
$P_{I,2}$	Fraction of the side (in heat flow direction) of a unit cell that is occupied by a sodium-filled pore	
P_{Na}	Sodium-filled porosity fraction relative to the swollen fuel volume	
T	Temperature	K
V	Volume	m^3
v	Characteristic volume of an atom	m^3
W	Weight fraction	
X_i	Weight fractions of the 3 database alloys to be mixed to produce the desired fuel composition	
x	Zr weight fraction in the U-Zr binary database alloy used in enthalpy region 1 or thermal conductivity region 3	
Y_i	Atom fractions of the 3 database alloys to be mixed to produce the desired fuel composition	
α	Coefficient of linear thermal expansion	per K
ΔL	Linear thermal expansion from 293K	m
ρ	Density, e.g., Eq. (10.3-32) or electrical resistivity in Eq. (10.3-68)	kg/m^3 Ω-m
σ	Standard deviation	
Subscripts:		
a	Desired alloy or desired database alloy	
c	Centigrade temperature scale	
f	Fission, e.g., Eq. (10.3-38) or solid fission products, e.g., Eq. (10.3-40) or desired fuel, e.g., Eq. (10.3-61)	
g	Fission gas	
h	Heavy metals	
i	Index for fuel constituents (I – U, Pu, Zr) or index for the 3 database alloys of a region of interpolation	
ℓ	Liquidus or molten liquid	
Na	Sodium	

Symbols	Definition	Units
o	Fabricated condition, e.g., Eq. (10.3-33) or 100%-dense unirradiated condition, e.g., Eq. (10.3-72) or a specified temperature, e.g., Eq. (10.3-44)	
p	Plutonium	
s	Solidus	
sfp	Solid fission products	
th	Theoretical	
u	Uranium	
uz	U-Zr binary alloy	
u50	U-50 atom % Zr binary alloy	
z	Zirconium	
α	Lowest-temperature solid-state phase (α-phase)	
γ	Highest-temperature solid-state phase (γ-phase)	

SSCOMP: PRE-TRANSIENT CHARACTERIZATION OF METALLIC FUEL PINS

10.1 Introduction and Overview

The Integral Fast Reactor (IFR) Program [10-1] at Argonne National Laboratory is developing an advanced liquid-metal-cooled nuclear reactor (LMR) that uses U-Pu-Zr metallic alloy fuel due to a number of safety and economic benefits. The post-irradiation examination of U-Pu-Zr fuel pins irradiated in EBR-II shows the formation of three annular zones (central, middle and outer) of considerably different alloy compositions, fuel porosities and densities [10-2, 10-3]. The uranium in the fuel migrates from the central and outer zones to the middle zone, and the zirconium and fission products migrate in the opposite directions, i.e., from the middle zone to the central and outer zones [10-3]. Due to zirconium depletion the middle zone has a solidus temperature significantly lower than that of the central or outer zone. The zonal fuel densities have been measured to vary from about 8000 kg/m^3 in the central zone to about 16000 kg/m^3 in the middle zone [10-3]. The average porosity of each zone is also found to be significantly different from each other [10-4]. This radial redistribution of fuel constituents and annular zone formation has a considerable effect on the thermal behavior of U-Pu-Zr fuel pins because the thermal conductivity, specific heat and density of the fuel all vary with composition and porosity. The radial power shape within the fuel pin is also changed by fissile (i.e., U and Pu) redistribution.

During steady-state irradiation, the buildup of fission gas within the metal fuel produces considerably more fuel swelling than is observed in oxide fuel. As the steady-state irradiation proceeds in metal fuel, the fission gas is initially all retained in the fuel matrix. Grain boundary bubbles gradually form, producing fuel swelling. As the porosity continues to increase, the grain boundary bubbles can become interlinked, producing a long-range interlinked porosity that offers a path for fission gas release to pin plenum [10-4]. When metallic fuel was first used in EBR-II, a peak burnup of only 1 at. % was considered a reasonable objective because of the extensive fuel swelling caused by grain boundary bubbles. Once it was determined that this "breakaway" swelling appeared to be self-limiting, and if enough space (~25 to 30% of fabricated fuel volume) was provided in the fuel-cladding gap, the result was very little stress on the cladding and high burnups could be achieved [10-5]. In order to calculate the steady-state behavior of metal fuel, it is therefore necessary to model the fuel swelling due to grain boundary bubbles and the associated fission gas release in a consistent manner.

Listed below are the important in-pin phenomena (including the two described above) occurring during steady-state irradiation, that need to be modeled in order to characterize a U-Pu-Zr fuel pin at the beginning of a transient calculation:

1. Thermal expansion of fuel and cladding,
2. Fuel constituent radial migration,
3. Fission gas behavior, and porosity formation and distribution,
4. Irradiation-induced radial and axial swelling of fuel and cladding,

5. Bond sodium migration into fuel and pin plenum,
6. Cladding constituent migration into fuel.

The modeling of these phenomena in the SSCOMP module will provide SAS4A and SASSYS-1 codes with the capability to describe the transition of the fuel pin form cold clean as-manufactured conditions to hot irradiated swollen initial conditions for the transient fuel mechanics module FPIN2 [10-6]. The modeling of the following aspects of fission gas behavior (phenomenon 3 listed above) is required for calculating the initial conditions of FPIN2 transient calculation: (a) fission gas generation, (b) fission gas retained within grains, (c) fission gas retained in grain boundary bubbles that are not linked, (d) fission gas contained in grain boundary bubbles that are interlinked, and (e) fission gas released to pin plenum. The need for modeling these three types of fission gas contained in fuel (gas within grains, in unlinked grain boundary bubbles, and in interlinked grain boundary bubbles) has also been expressed by the pre-failure in-pin fuel motion module PINACLE development [10-7]. Regarding irradiation induced fuel swelling (phenomenon 4 listed above), axial swelling will contribute to pre-transient fuel column length, a needed initial condition for the FPIN2 module. Radial swelling of fuel and cladding will determine fuel-cladding gap closure and bond sodium migration into pin plenum, a needed initial condition for the FPIN2 module. The modeling of fuel swelling phenomenon has two important aspects: swelling due to solid fission products, and fission gas-induced swelling. Swelling of a cladding material is mainly determined by neutron fluence which is also a parameter in determining cladding rupture life used in the FPIN2 transient fuel mechanics calculation.

The SSCOMP module is being developed to model the above listed in-pin phenomena during steady-state irradiation of metallic fuel pins. After the fuel pin has been characterized at the end of steady-state irradiation, the calculation of the relevant ones of these phenomena during the transient will be performed by the DEFORM-5 model. The purpose of this chapter is to present the current status and future modeling needs of the SSCOMP module. As discussed in Section 10.2, the zone formation calculation method of the earlier SSCOMP model [10-4] is not incorporated into SAS4A/SASSYS-1 Version 3.0 code due to its limitations. The study of fuel constituent radial migration leading to zone formation was not at that time developed to a state where an appropriate dynamic model could be developed. At present, the data needed to account for the effects of zone formation on pin transient temperature calculation are specified through input data controlled by the input parameter IFUELC. As a starting point for SSCOMP development, Section 10.3 describes thermal properties of U-Pu-Zr metallic alloy fuel as a function of composition and temperature. These properties are needed in the analysis of the Mark-V fuel (U-20Pu-10Zr), and other metallic alloy fuels of different compositions, especially the different fuel compositions across the pin radius resulting from fuel constituent migration during steady-state irradiation. The implementation of the thermal properties data of the IFR Metallic Fuels Handbook [10-8], using a method of regionwise interpolation, is an important part of Section 10.3. Thermal properties of mixed-oxide fuel are described in Section 3.15, and not here. Future directions for modeling efforts are discussed in Section 10.4.

10.2 The Earlier SSCOMP Model and Current Capability

Assuming chemical equilibrium at annular zone boundaries and mass conservation of fuel constituents, a model was developed earlier [10-4] to directly calculate zone formation at the end of steady-state irradiation. This model was also calibrated using zone formation data obtained for the cross section at the mid-height of a U-Pu-Zr alloy fuel pin in an EBR-II steady-state irradiation experiment [10-3]. This earlier SSCOMP model calculates the alloy compositions of the zones, the boundary radii of the zones, and the resulting in-pin power radial profile. The earlier model does not calculate the time-development of the fuel zones from the fabricated condition to the end-of-steady-state irradiation condition. This is so because the study of fuel constituent radial migration leading to zone formation was not at that time developed to a state where an appropriate dynamic model could be developed.

The zone formation calculation method of the earlier SSCOMP model is not incorporated into SAS4A/SASSYS-1 Version 3.x codes due to its limitations. Some of its limitations are:

1. The earlier SSCOMP model directly calculates the fuel compositions and boundary radii of the zones based on chemical equilibrium under end-of-steady-state reactor operating conditions, and does not calculate the migration of fuel constituents with time during steady-state irradiation. Reactor operating conditions usually change during the steady-state irradiation of a fuel pin, and therefore, chemical equilibrium under end-of-steady-state operating conditions may not have been attained if the operating conditions changed during a (fuel constituent) migration time constant before the end of steady-state irradiation.
2. The earlier SSCOMP does not model other important pre-transient phenomena such as irradiation-induced fuel swelling, fission gas generation, retention and release to pin plenum, etc. These phenomena are important for characterizing a fuel pin at the beginning of a transient as noted in Section 10.1.
3. The earlier SSCOMP model is not well validated by analysis of experimental data for zone formation.

Therefore, after evaluating the earlier SSCOMP in light of new data on zone formation and current understanding of phenomena causing it (zone formation), the earlier model or another more advanced model will be incorporated into SAS4A/SASSYS-1 codes, and this will be done in the framework of models for other important pre-transient phenomena that characterize the fuel pin at the beginning of transient calculation. At present, the zone formation data (such as zonal U-Pu-Zr alloy compositions, boundary radii of the zones, etc.) are supplied to the code as input data, and used in pin transient temperature calculation. This multiple radial fuel zone option is controlled by the input parameter IFUELC.

10.3 Thermal Properties of U-Pu-Zr and U-Zr Alloy Fuels as a Function of Composition

The fuel thermal properties described in this section are used in all modules of SAS4A and SASSYS-1 codes, and not only in the SSCOMP module. The fuel thermal properties include its specific heat, theoretical density and thermal conductivity. A U-Zr binary alloy is treated as a special case of the U-Pu-Zr ternary alloy. In the SAS4A/SASSYS-1 codes, one of the following four options are used for providing fuel thermal properties of a channel: (1) temperature-dependent property tables prepared by the user, and supplied to the code as input data, (2) regionwise interpolation of IFR Metallic Fuels Handbook data (as explained in Section 10.3.2, region here implies a triangular part of the U-Pu-Zr ternary system composition triangle), (3) composition- and temperature-dependent fuel property correlations of the report ANL/RAS 85-19 developed before IFR Metallic Fuels Handbook [10-9] in course of the earlier SSCOMP model development [10-4], and (4) Billone's correlations for Mark-V (i.e., U-20Pu-10Zr) and U-10Zr fuels based on IFR Handbook data. The options available for providing mixed-oxide fuel properties to the codes are described in Section 3.15, and not in the present section.

The specific heat of both metallic and oxide fuels is calculated in subroutine CFUEL, the theoretical density in subroutine RHOF, and the thermal conductivity in subroutines FK and KFUEL. The difference between the two thermal conductivity subroutines FK and KFUEL is that FK is used to calculate the thermal conductivity of a single fuel radial node during steady-state heat transfer calculation, whereas KFUEL is used to calculate the thermal conductivities of all fuel radial modes in a pin axial segment (in a single call, for computational efficiency) during transient heat transfer calculation. The flow diagrams of these subroutines are shown in Figs. 10.3-1 to 10.3-4. The above mentioned four options for providing fuel thermal properties along with some other options related to fuel properties, are controlled through the following six input parameters: IRHOK, IMETAL, IFUELM, IFUELC, KFIRR and KDENBU. The input parameter IMETAL>1 implies U-Pu-Zr alloy fuel.

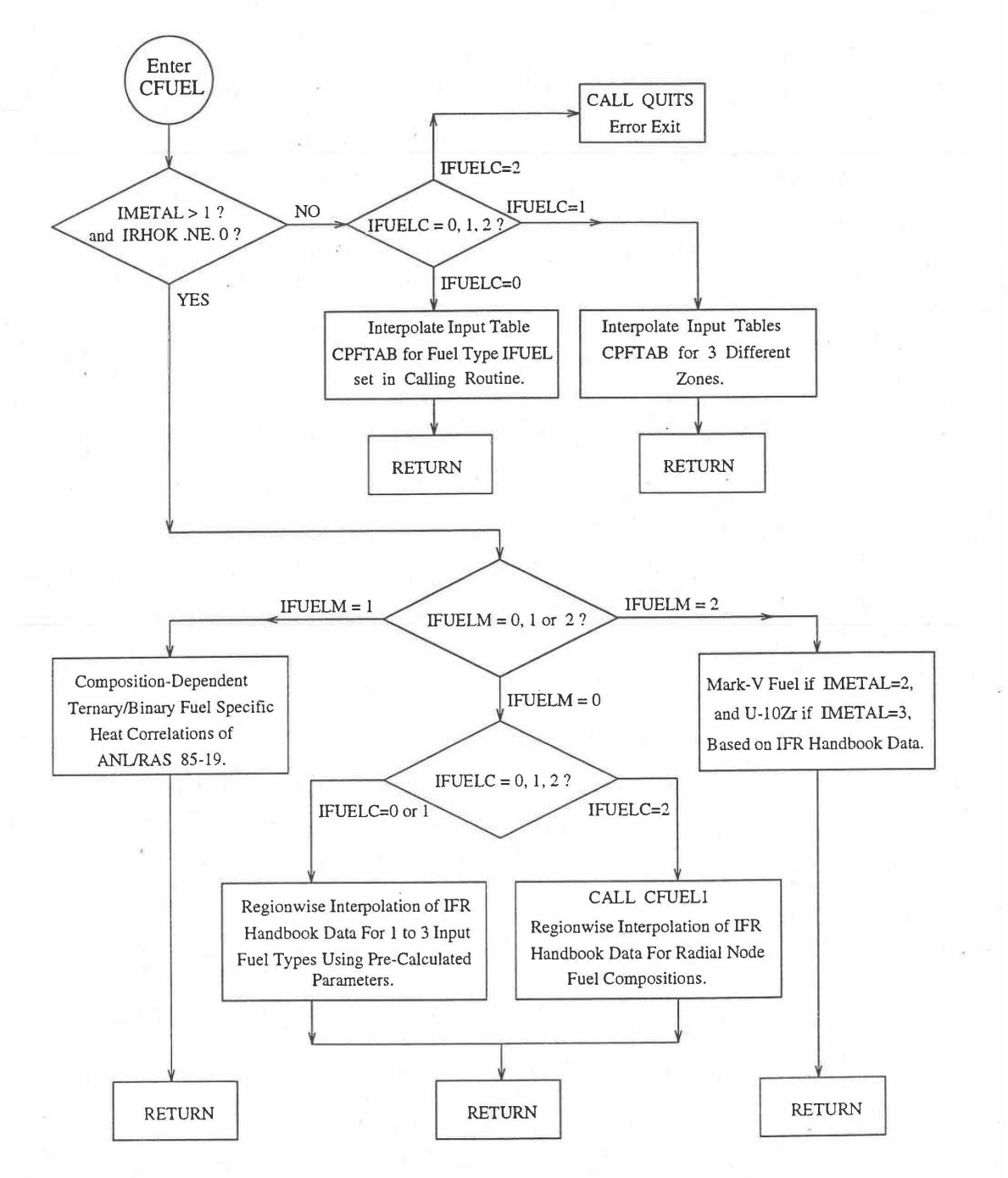

Fig. 10.3-1. Flow Diagram of Subroutine CFUEL for Fuel Specific Heat

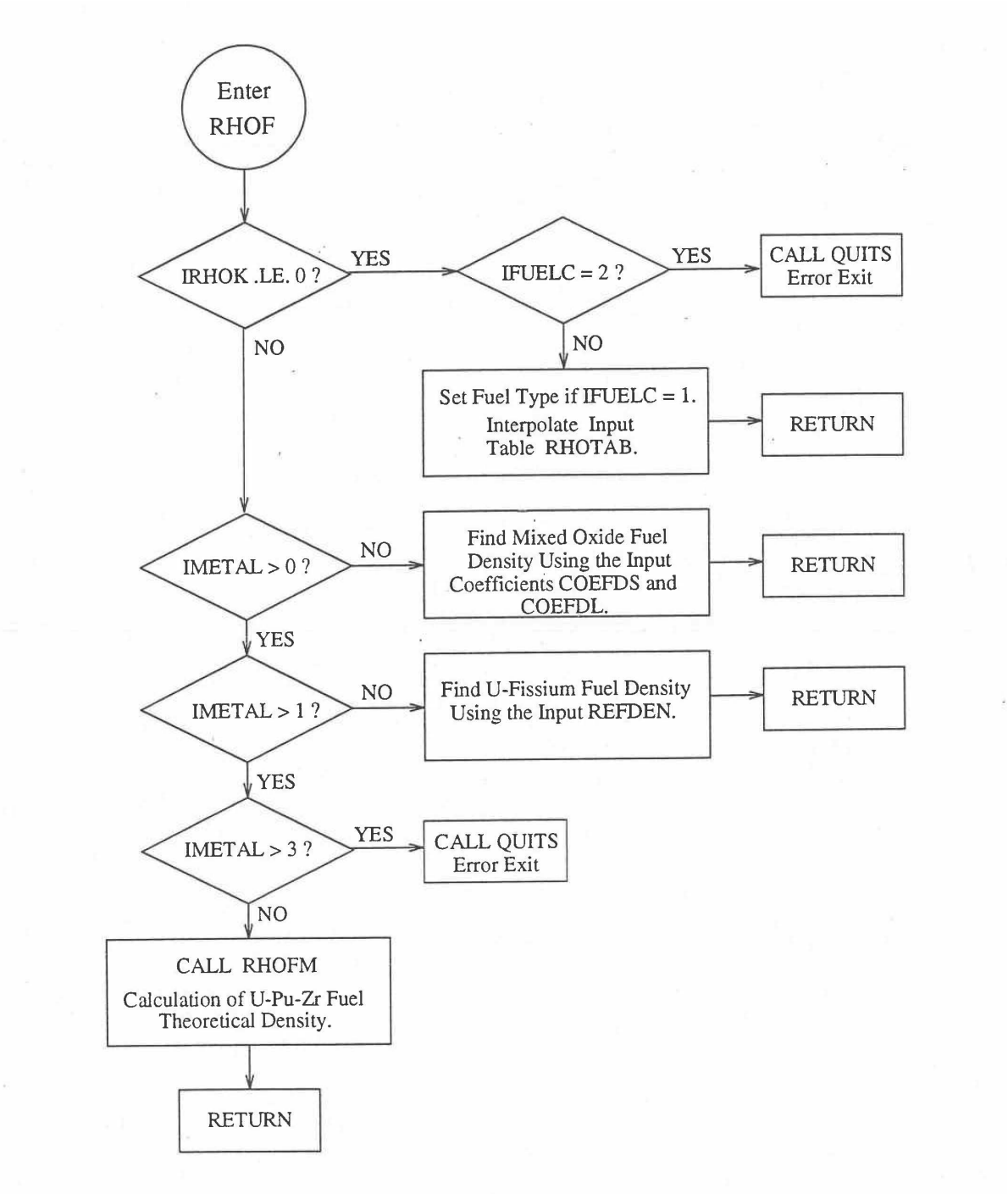

Fig. 10.3-2. Flow Diagram of Function Subprogram RHOF for Fuel Theoretical Density

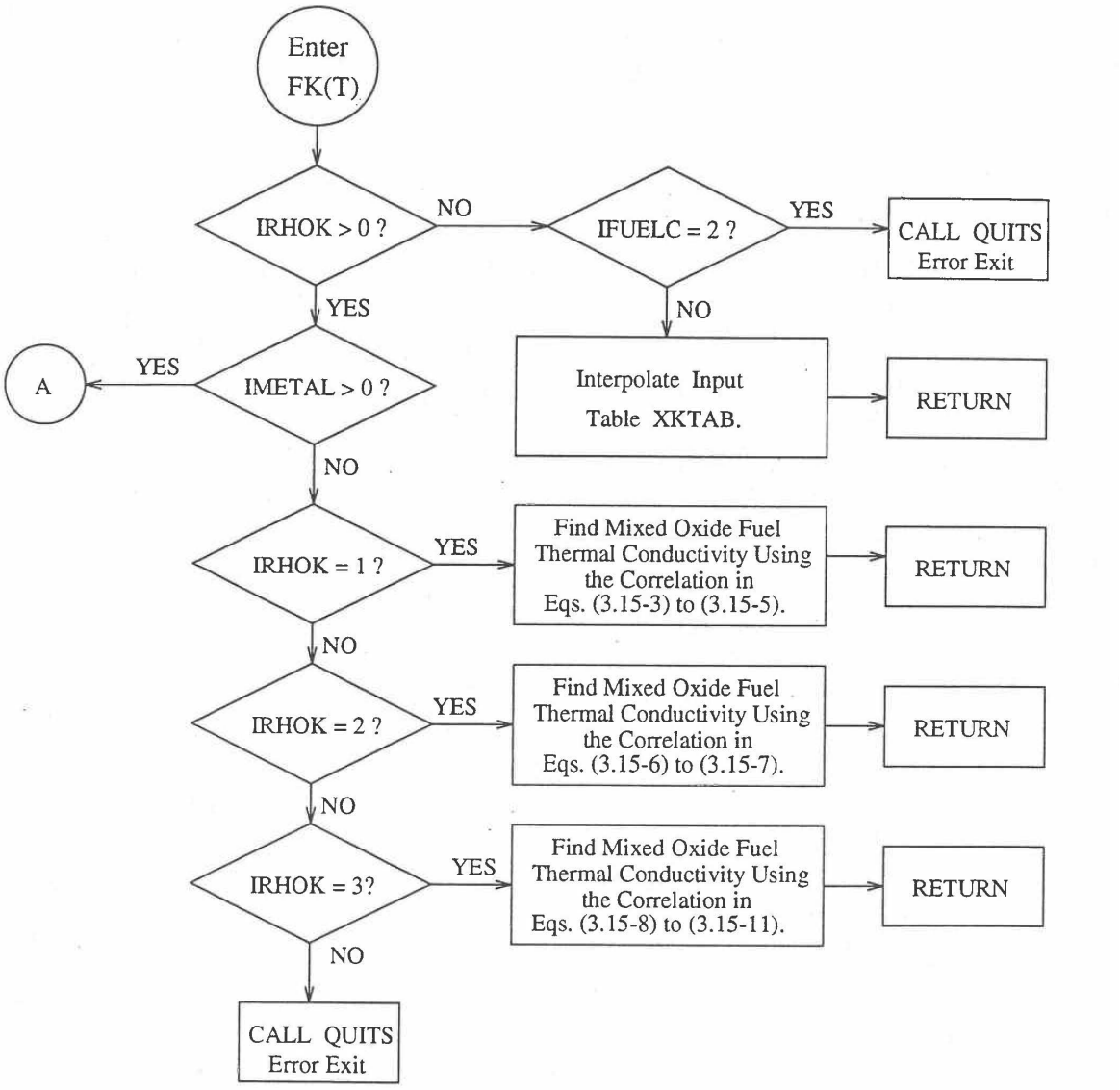

Fig. 10.3-3. Flow Diagram of Function subprogram FK for Thermal Conductivity of a Single Fuel Radial Node

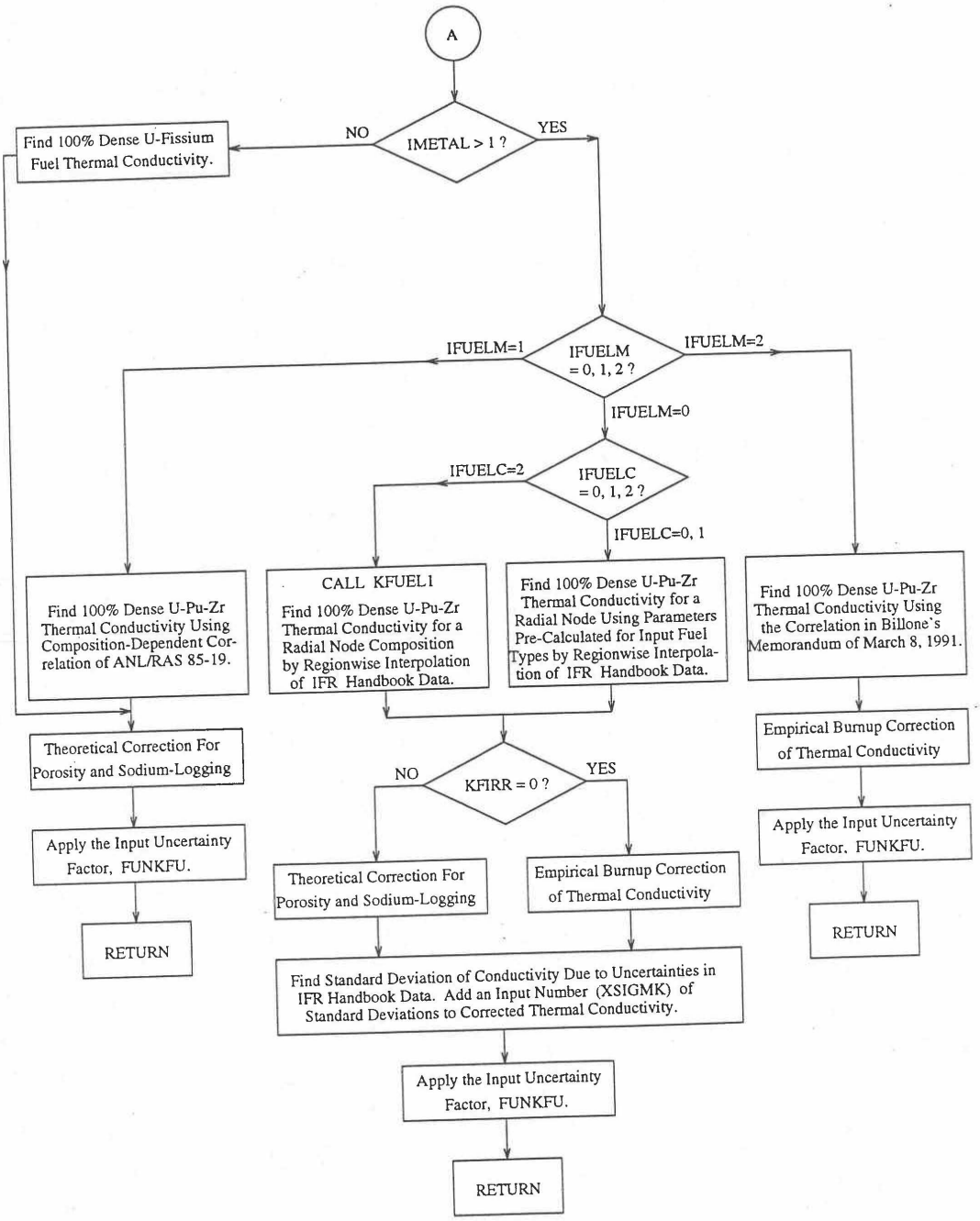

Fig. 10.3-3. Flow Diagram of Function subprogram FK for Thermal Conductivity of a Single Fuel Radial Node (Cont'd)

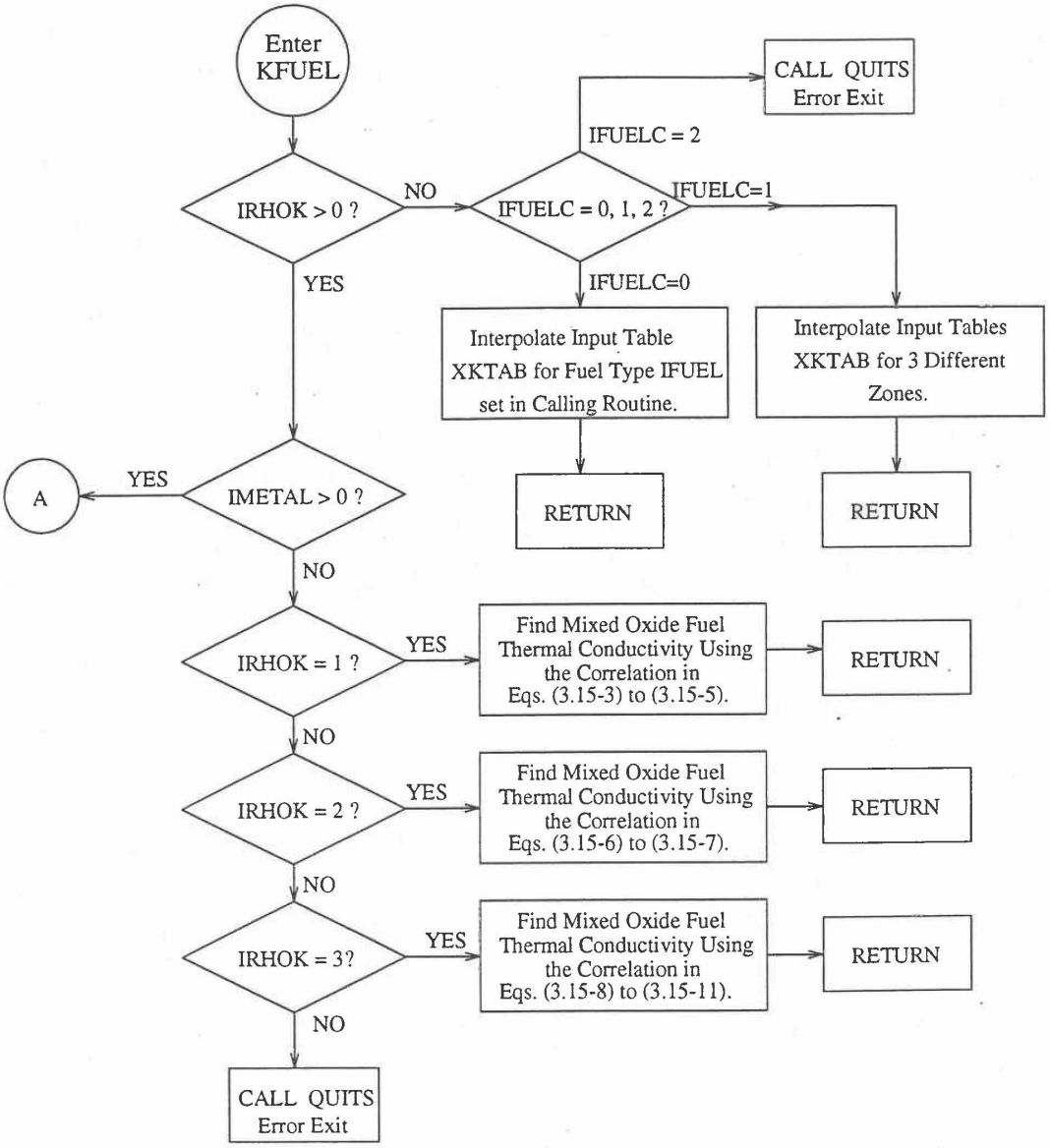

Fig. 10.3-4. Flow Diagram of Subroutine KFUEL for Thermal Conductivity of All Fuel Radial Nodes in a Pin Axial Segment

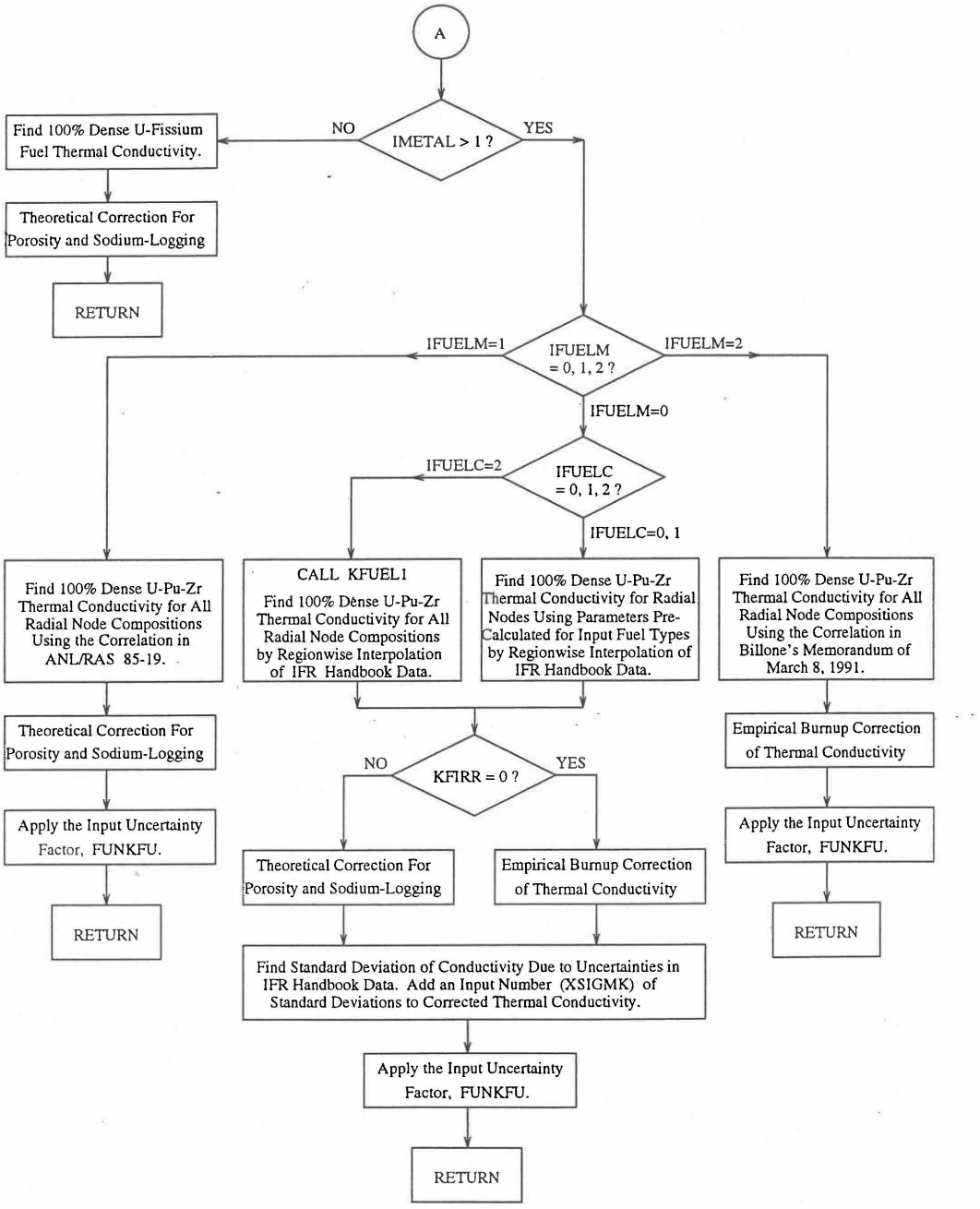

Fig. 10.3-4. Flow Diagram of Subroutine KFUEL for Thermal Conductivity of All Fuel Radial Nodes in a Pin Axial Segment (Cont'd)

10.3.1 Temperature-Dependent Tables

The input parameter IRHOK=0 in a channel implies that temperature-dependent tables of specific heat, theoretical density and thermal conductivity of U-Pu-Zr alloy fuels of a maximum of 8 different alloy compositions (called fuel types in the input description given in Chapter 2) have been prepared by the user and supplied to the code as input data, and one of these tables is to be used in the channel. The core and blanket fuel types to be used in a channel are specified through the input variables IFUELV and IFUELB if the channel has a single radial fuel zone (indicated by the input parameter IFUELC=0). The fuel types are specified through the input array MFTZN if the channel has multiple radial fuel zones (indicated by the input parameter IFUELC=1). The compositions of the U-Pu-Zr metallic alloy fuel types are specified through the input array PUZRTP.

10.3.2 Regionwise Interpolation of IFR Handbook Data

The SAS4A and SASSYS-1 codes are being developed to perform calculations for the Mark-V fuel (U-20Pu-10Zr) and other metallic alloy fuels of different compositions, especially the different fuel compositions across the pin radius resulting form the migration of fuel constituents during steady-state reactor operation. There is thus a need for modeling and correlation development for the thermal properties of U-Pu-Zr alloy fuels as a function of composition. This is so because the IFR Metallic Fuels Handbook [10-8, 10-9] presents thermal properties data for the 3 constituents and certain specific alloys only, and does not always present correlations with their coefficients and transition temperatures as functions of composition. Using the thermal properties data presented in the IFR Metallic Fuels Handbook, a method of regionwise interpolation in the U-Pu-Zr ternary composition triangle has been developed to estimate thermal properties of U-Pu-Zr alloy fuels as a function of composition and temperature. This method of evaluating fuel thermal properties is specified by setting the input parameter IRHOK=1 and the input parameter IFUELM=0 in a channel, and this is the recommended option among the built-in fuel thermal properties options.

Figure 10.3-5 shows the flow diagram of a subroutine PRECAL that is called by the input driver routine INPDRV (see flow diagram of Fig. 2.2-2) to pre-calculate, using the method of regionwise interpolation, certain parameters (described below) stored for fast evaluation of U-Pu-Zr alloy fuel thermal properties by fuel type. Fuel thermal properties by fuel type can be used only in case of a single radial fuel zone (IFUELC=0), or multiple (i.e., up to 3) radial fuel zones (IFUELC=1), but not when each fuel radial mesh interval is a unique zone of a different alloy composition (IFUELC=2). In the latter case, fuel thermal properties are evaluated directly using the fuel compositions of the mesh intervals. The pre-calculated parameters by fuel type evaluated by the subroutine PRECAL are not used when IFUELC=2.

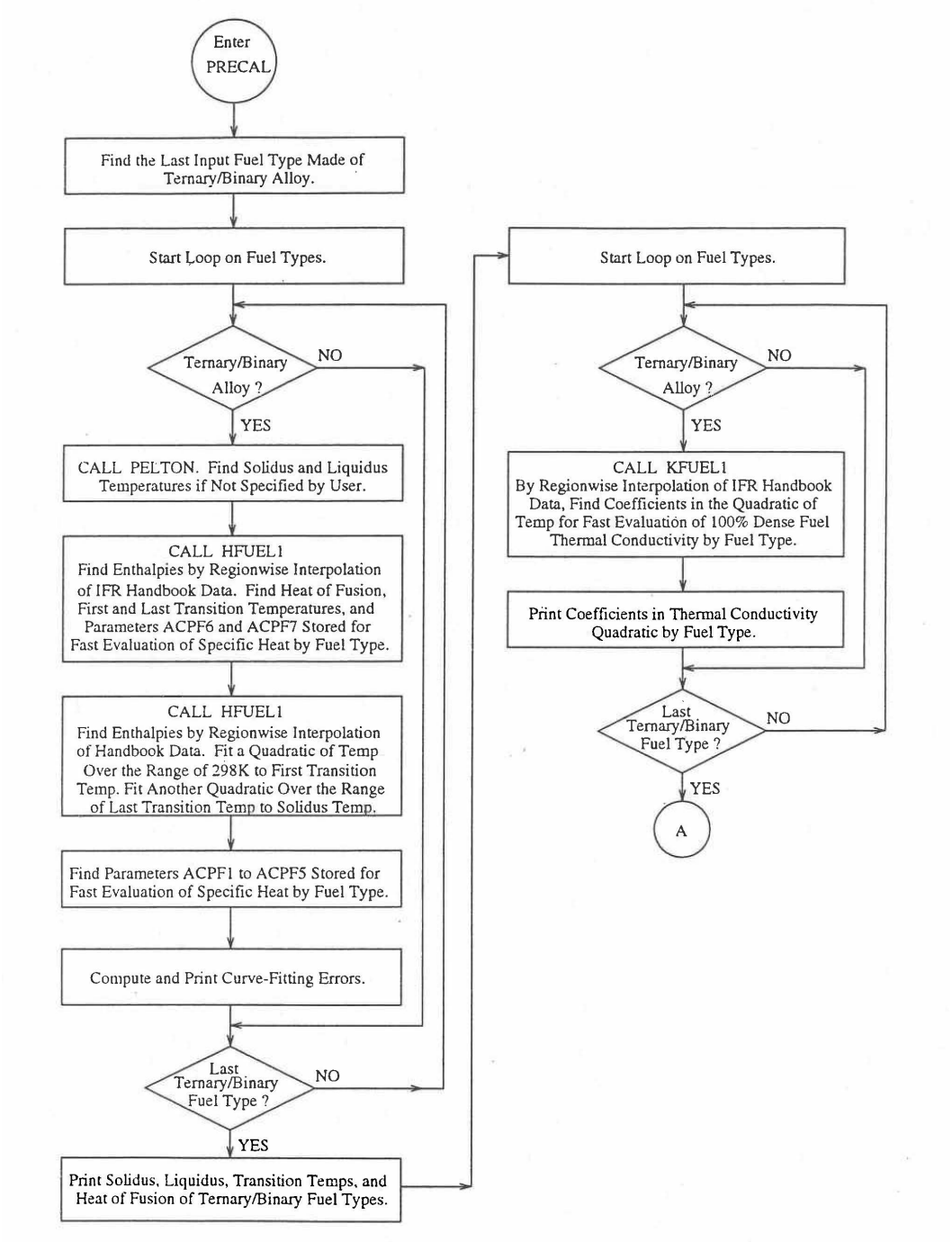

Fig. 10.3-5. Flow Diagram of Subroutine PRECA1 to Pre-Calculate Parameters Stored for Fast Evaluation of U-Pu-Zr Specific Heat, Theoretical Density and Thermal Conductivity by Fuel Type

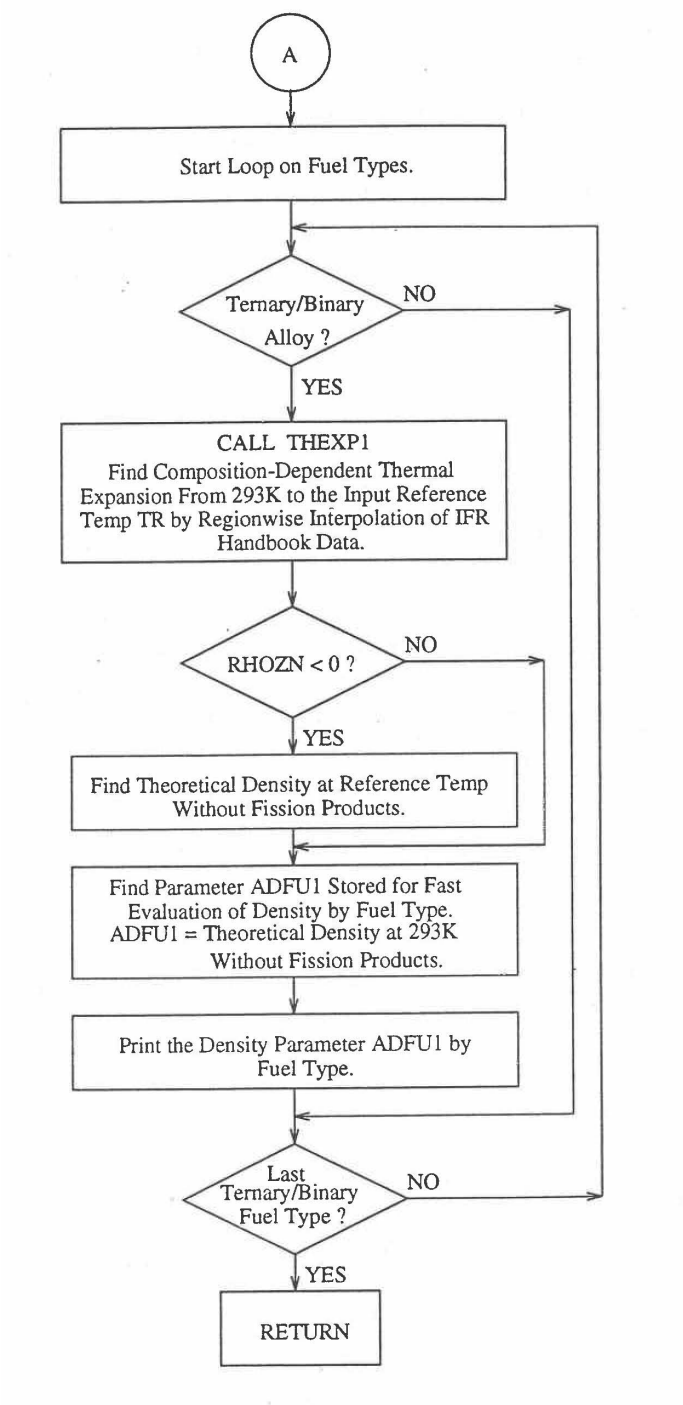

Fig. 10.3-5. Flow Diagram of Subroutine PRECA1 to Pre-Calculate Parameters Stored for Fast Evaluation of U-Pu-Zr Specific Heat, Theoretical Density and Thermal Conductivity by Fuel Type (Cont'd)

10.3.2.1 Enthalpy of U-Pu-Zr Fuel

10.3.2.1.1 Introduction

The IFR Metallic Fuels Handbook presents enthalpy and specific heat data for the 3 constituents and certain specific alloys only, and does not present correlations with their coefficients and transition temperatures as functions of composition.

Earlier, before the preparation of the Metallic Fuels Handbook [10-9], a method was developed to estimate the composition-dependent enthalpy of solid U-Pu-Zr alloy fuel by mass-weighted averaging of the enthalpy data of the 3 constituents, i.e., U, Pu and Zr metals [10-4]. Each of the constituent metals undergoes certain crystallographic phase transitions in the solid state that require considerable heat addition (causing an enthalpy jump) at the transition temperatures, but the alloy itself has no sharp transition temperature or enthalpy jump. A drawback of this method [10-4] of estimating U-Pu-Zr enthalpy is that the enthalpy jumps in the constituent metals data are required to be spread over an arbitrarily chosen temperature range containing the transition temperatures. Another drawback is that the enthalpy data for the constituent metals was obtained from a source [10-10] other than the Metallic Fuels Handbook.

The method that is used in the FPIN2 code [10-11] to estimate the composition-dependent specific heat of U-Pu-Zr alloy fuel is also based on mass-weighted averaging of the 3 constituent specific heats. In this method, each constituent specific heat is assumed to be constant over the range of room temperature to the melting point of the constituent metal; and this assumption is tantamount to spreading the enthalpy jumps (due to solid-state phase transitions) over the same temperature range.

Recently, Billone has suggested that the enthalpy of solid U-Pu-Zr alloy fuel as a function of composition could be obtained by mixing the following 3 alloys rather than the 3 constituent metals [10-12]:

(1) U-15 wt % Pu-10 wt % Zr ternary alloy.

(2) U-(10 ± 5) wt % Zr binary alloy, and

(3) Pu metal.

The enthalpy data of U-15Pu-10Zr ternary, U-10Zr binary and Pu metal have been reported in the Metallic Fuels Handbook. The enthalpy of U-Zr binary alloy as a function of Zr content (in the neighborhood of 10 wt %) has also been correlated [10-12] by Billone using data for some binary alloys reported in the Metallic Fuels Handbook, i.e., 87 at. % U-Zr (U-5.4 wt. % Zr), U-10 wt % Zr, 59 at. % U-Zr (U-21.1 wt % Zr), and 39 at. % U-Zr (U-37.6 wt % Zr). The suggestion of mixing the 3 alloys rather than the 3 constituents provides a number of benefits. It removes the drawback of spreading the enthalpy jumps (due to solid-state phase transitions) over an arbitrarily chosen temperature range. The heats of solid-state transitions are naturally spread over the correct temperature range and included in the enthalpy data of the alloys that are mixed. The suggestion also improves the accuracy of the calculated enthalpy of the

desired U-Pu-Zr alloy by choosing the 3 basic alloy compositions (that are mixed) in the neighborhood of the desired alloy composition.

Based on (a) this suggestion for obtaining the enthalpy of solid U-Pu-Zr alloy fuel, and (b) the assumption of ideal solution of molten U, Pu and Zr (used in the Metallic Fuels Handbook to obtain U-10Zr and U-15Pu-10Zr enthalpies at and above their liquidus temperatures) for obtaining the enthalpy of liquid U-Pu-Zr fuel, a method of regionwise interpolation and a subroutine HFUEL1 based on it have been developed and incorporated into the SAS4A/SASSYS-1 codes. This method exactly reproduces enthalpy data in the Handbook for molten U-15Pu-10Zr, U-10Zr, U, Pu and Zr liquids. The enthalpy data in the Handbook for solid U-15Pu-10 Zr, U-5.4Zr, U-10Zr, U-21.1Zr, U-37.6Zr alloys, and solid U and Pu metals are also accurately reproduced by this method.

10.3.2.1.2 Description of the Method

Figure 10.3-6 shows the U-Pu-Zr ternary system composition triangle. To perform design and safety calculations for the Mark-V fuel and other metallic alloy fuels important in the IFR program, including the different fuel compositions across the pin radius caused by migration of fuel constituents during reactor operation, it is sufficient to be able to evaluate enthalpy of alloy compositions (represented by points) located in a small region, equal in area to about one-third of the whole composition triangle, in the U corner of the triangle. The present method models and evaluates the enthalpy of all alloy compositions located in the triangular region UEPu of Fig. 10.3-6.

The enthalpy of a molten alloy (at and above its liquidus temperature) as a function of composition is evaluated in the present method by assuming the molten alloy to be an ideal solution of the 3 liquid components U, Pu and Zr. The enthalpy evaluation approach for the molten alloy is changed from that for the solid alloy because (1) the IFR Metallic Fuels Handbook uses this 3-component ideal solution assumption for evaluating enthalpy of molten U-10Zr, and U-15Pu-10Zr, and recommends this assumption for other alloy compositions, and (2) the solid-state phase structure is lost after melting, i.e., the liquid obtained after melting is the same irrespective of the solid phase which melted; the alternate approach of arriving at the enthalpy at liquidus by adding the heat of fusion and the sensible heat (required for raising temperature form solidus to liquidus) to the enthalpy at solidus contains uncertainties which can be avoided by using the 3-liquid ideal solution assumption. Between the solidus and liquidus temperatures, the enthalpy of the alloy is linearly interpolated as recommended in the Metallic Fuels Handbook. The solidus and liquidus temperatures required in the present method may be either obtained from experimental measurements for the desired alloy, if available, or calculated using a subroutine developed by Pelton [10-13] and incorporated into the SAS4A/SASSYS-1 codes.

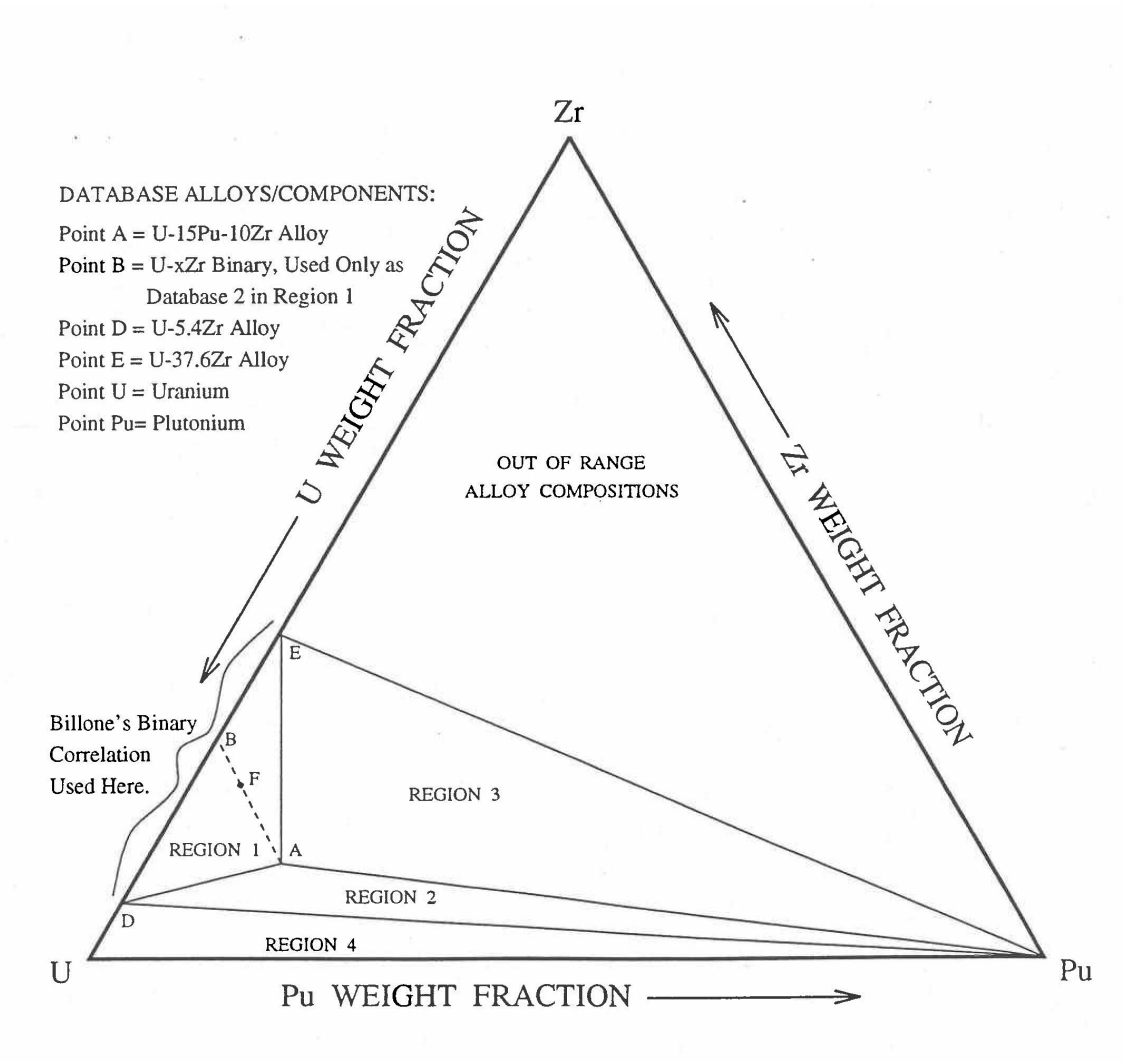

Fig. 10.3-6. Diagram Showing Enthalpy Interpolation Regions for Solid U-Pu-Zr Ternary Alloy

Base on the enthalpy data available in the IFR Handbook, the present method divides the triangular region UEPu, i.e., the region representing all those alloy compositions whose enthalpy in the solid state can be evaluated by the present method, into four regions as shown in Fig. 10.3-6. There are data in the Handbook for solid U, Pu, U-15Pu-10Zr (represented by point A in Fig. 10.3-6), and six U-Zr binary alloys with Zr content ranging form 5.4 wt % (point D) to 75.7 wt %. Because the IFR program deals with fuels having a limited amount of Zr, the highest Zr content U-Zr binary alloy data used in the method is that of U-37.6 wt % Zr (point E). In region 1 given by triangle ADE of Fig. 10.3-6, the enthalpy of a solid U-Pu-Zr alloy of a desired composition represented by point F is obtained by mixing or linearly interpolating between the database alloys A (i.e., U-15Pu-10Zr) and B (i.e., the U-Zr binary defined by the point of intersection of line AF). The Zr content of binary alloy B is given in Section D, and the enthalpy of this binary alloy is found form a correlation by Billone [10-12] of all the enthalpy data in the Handbook for U-Zr alloys between points D and E. The coefficients of this correlation are composition-dependent. By comparison with data in the Handbook, this U-Zr enthalpy correlation has been found to be accurate.

The enthalpy of a solid U-Pu-Zr alloy of a desired composition represented by a point inside region 2 (given by triangle ADPu of Fig. 10.3-6 is obtained by mixing the 3 database alloys A, D (i.e., U-5.4Zr) and Pu metal. The enthalpy of a solid U-Pu-Zr alloy of a desired composition represented by a point inside region 3 (given by triangle AEPu) is obtained by mixing the 3 database alloys A, E (i.e., U-37.6Zr) and Pu as shown in Table 10.3-1. Regions 1, 2 and 3 are all in the vicinity of the important ternary fuel U-15Pu-10Zr, and in the present method the enthalpy data for this fuel has a proportional influence on the interpolated enthalpy for any desired alloy composition in these three regions. The enthalpy of a solid U-Pu-Zr alloy of a desired composition represented by a point inside region 4 (given by triangle UDPu) is obtained by mixing the database alloy D, and U and Pu metals. The enthalpy of U metal used in the present method is obtained from data and correlation given in the Handbook because an extrapolation of the U-Zr binary alloy enthalpy correlation does not produce an accurate U metal enthalpy. The enthalpies of the database alloys used in the interpolation are given in Section C. The proportions or weight fractions of the 3 database alloys in mixing are given in Section D.

Between the first and the last solid-state phase transition temperatures, 873 K and 923 K, the specific heat of database alloy A (i.e., U-15Pu-10Zr) is much higher than the specific heat above and below this temperature range. These transition temperatures, denoted by T_α and T_γ, are required for the other database alloys and the desired U-Pu-Zr alloy in order to accurately account for the specific heat variation over this temperature range. In the present method, these transition temperatures for the U-Zr binary alloys used as database, and for all U-Pu-Zr ternary alloy compositions in regions 1, 2 and 3 are assumed to be equal to those of database alloy A because of lack of composition-dependent correlations for the transition temperatures. Such an assumption was suggested by Billone [10-12] for U-Pu-Zr alloys in the vicinity of U-15Pu-10Zr, and for U-Zr binary alloys used in mixing calculations. The choice of T_α and T_γ for Pu metal is immaterial because its enthalpy data, after the simplification suggested by Billone [10-12] and described in Section C, does not have any temperature range of abruptly high specific heat. In region 4 of Fig. 10.3-6, the average specific heat of U metal between its first and last transition temperatures is abruptly high, and therefore,

T_α is interpolated between the value of T_α (942 K) for U metal [10-8] and the assumed value for other databases (873 K); and T_γ is interpolated between the value of T_γ (1049 K) for U metal [10-8] and the assumed value for other databases (923 K). These transition temperatures are summarized in Table 10.3-1.

Section C describes the enthalpy correlations for the basic alloys and their comparison with the data in the Handbook. Section D describes the equations used for interpolating between the database alloys. Section E summarizes the variation of fuel enthalpy with composition computed using the subroutine HFUEL1 based on this method.

Table 10.3-1. Basic Alloys Whose IFR Handbook Enthalphy Data are Combined to Obtain the Enthalpy of a Desired U-Pu-Zr Alloy Composition

	Database Alloys				
Region[a]	1	2	3	Desired Alloy T_α, K[(b)]	Desired Alloy T_γ, K[(b)]
Region 1	U-15Pu-10Zr	U-xZr[c]	not required	873	923
Region 2	U-15Pu-10Zr	U-5.4455Zr	Pu metal	873	923
Region 3	U-15Pu-10Zr	U-37.6105Zr	Pu metal	873	923
Region 4	U metal	U-5.4455Zr	Pu metal	873 to 942[d]	923 to 1049[e]

[a] These regions are shown on the U-Pu-Zr ternary composition triangle in Fig. 10.3-6.

[b] T_α and T_γ denote the first and the last solid-state phase transition temperatures of the alloy. T_α and T_γ of alloy compositions in the vicinity of U-15Pu-10Zr are assumed to be equal to those of U-15Pu-10Zr, i.e., 873 K and 923 K, as suggested by Billone [10-12].

[c] The weight fraction x of Zr is selected such that the point representing U-xZr binary lies on the line joining the points representing the desired alloy composition and U-15Pu-10Zr database alloy on the ternary composition triangle shown in Fig. 10.3-6.

[d] Interpolated between 942 K (the value for U metal) and 873 K (the assumed value for other databases, see footnote b).

[e] Interpolated between 1049 K (the value for U metal) and 923 K (the assumed value for other databases, see footnote b).

10.3.2.1.3 Enthalpy Correlations of Database Alloys

Figures 10.3-7 to 10.3-13 show the temperature dependence of the enthalpy of all the basic alloys used in the present method. The difference in behavior of a database alloy when mixed to produce a desired alloy composition, e.g., U-20Pu-20Zr, as compared to its behavior in isolation is also clarified by these figures. For this purpose, the comparison of enthalpy of the basic alloy in isolation, evaluated from the correlations used in the present method, with the data in the Metallic Fuels Handbook [10-8] is also shown. These plots cover the entire temperature range from 298 K (zero enthalpy reference temperature) to 2000 K, a temperature well beyond the liquidus. In the following sections, the enthalpy correlations of the database alloys for use in solid and liquid phases are separately described.

1. Database Used in Liquid Phase

The enthalpy of a molten U-Pu-Zr alloy fuel (at and above its liquidus temperature) is evaluated by assuming the molten alloy to be an ideal solution of the 3 liquid components U, Pu and Zr. Thus the enthalpies of the 3 liquid components as functions of temperature from the database. Based on the data for enthalpy at U liquidus and specific heat of liquid U given in the Handbook [10-8], the enthalpy of liquid U can be written as

$$H_{lu} = 58347 + 48.66(T - 1408) \qquad (10.3\text{-}1)$$

where

H_{lu} = enthalpy of liquid U, J/mol

T = temperature of liquid U, K

58347 = liquid U enthalpy (J/mol) at its melting point 1408 K,

48.66 = liquid U specific heat, J/mol-K.

Eq. (10.3-1) simplifies to

$$H_{lu} = 48.66T - 10166.28 \qquad (10.3\text{-}2)$$

Similarly, based on the data for enthalpy at liquidus and specific heat of the liquid phase given in the Handbook for Pu and Zr, the following equations for liquid phase enthalpy are obtained:

$$H_{lp} = 42.258T - 7291.55 \qquad (10.3\text{-}3)$$

$$H_{lz} = 33.5T + 6116.5 \qquad (10.3\text{-}4)$$

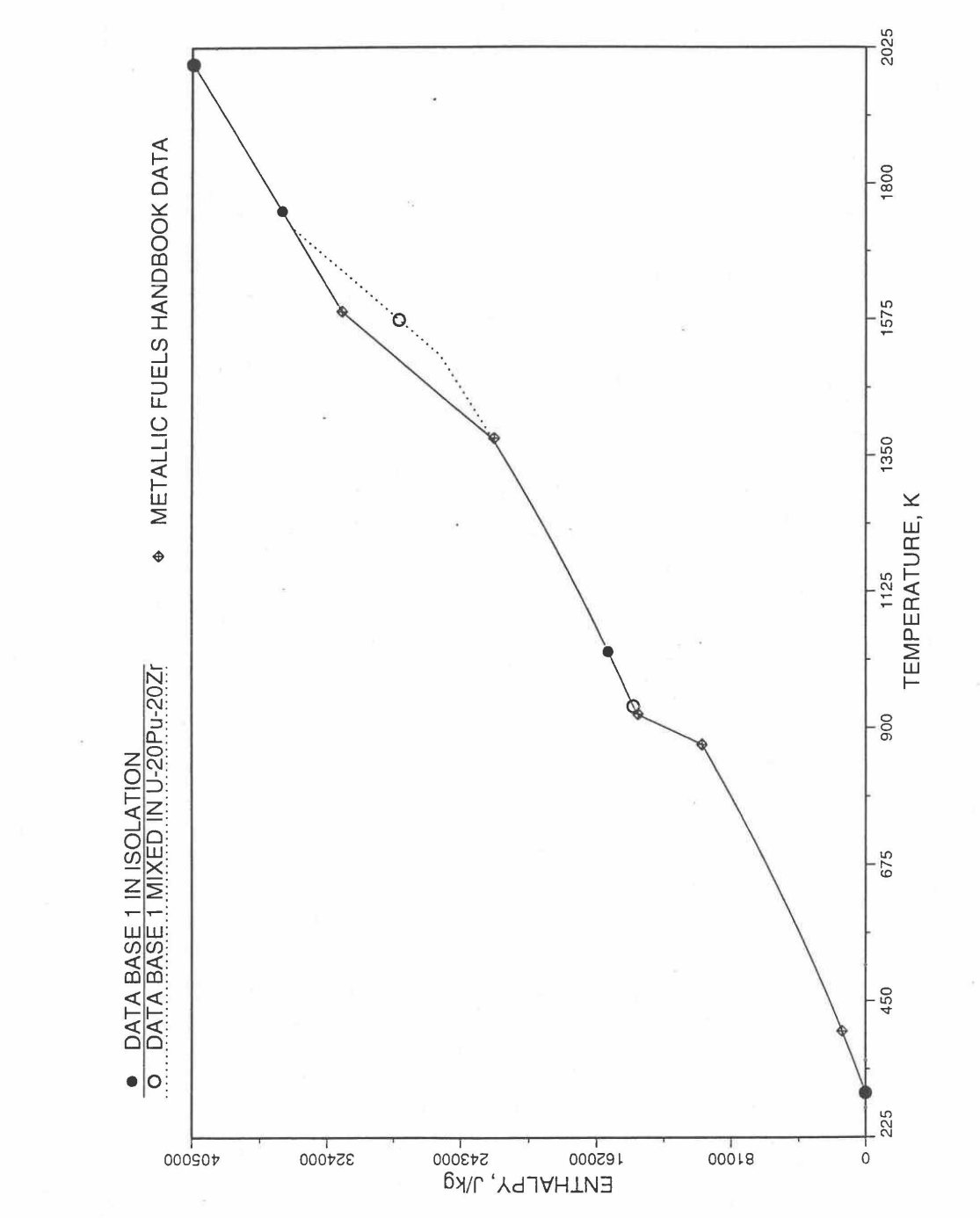

Fig. 10.3-7. Enthalpy of U-15Pu-10Zr Obtained from Eqs. (10.3-2) to (10.3-5) That is Used as Database 1 in Regions 1, 2 and 3; and its Comparison with Metallic Fuels Handbook Data

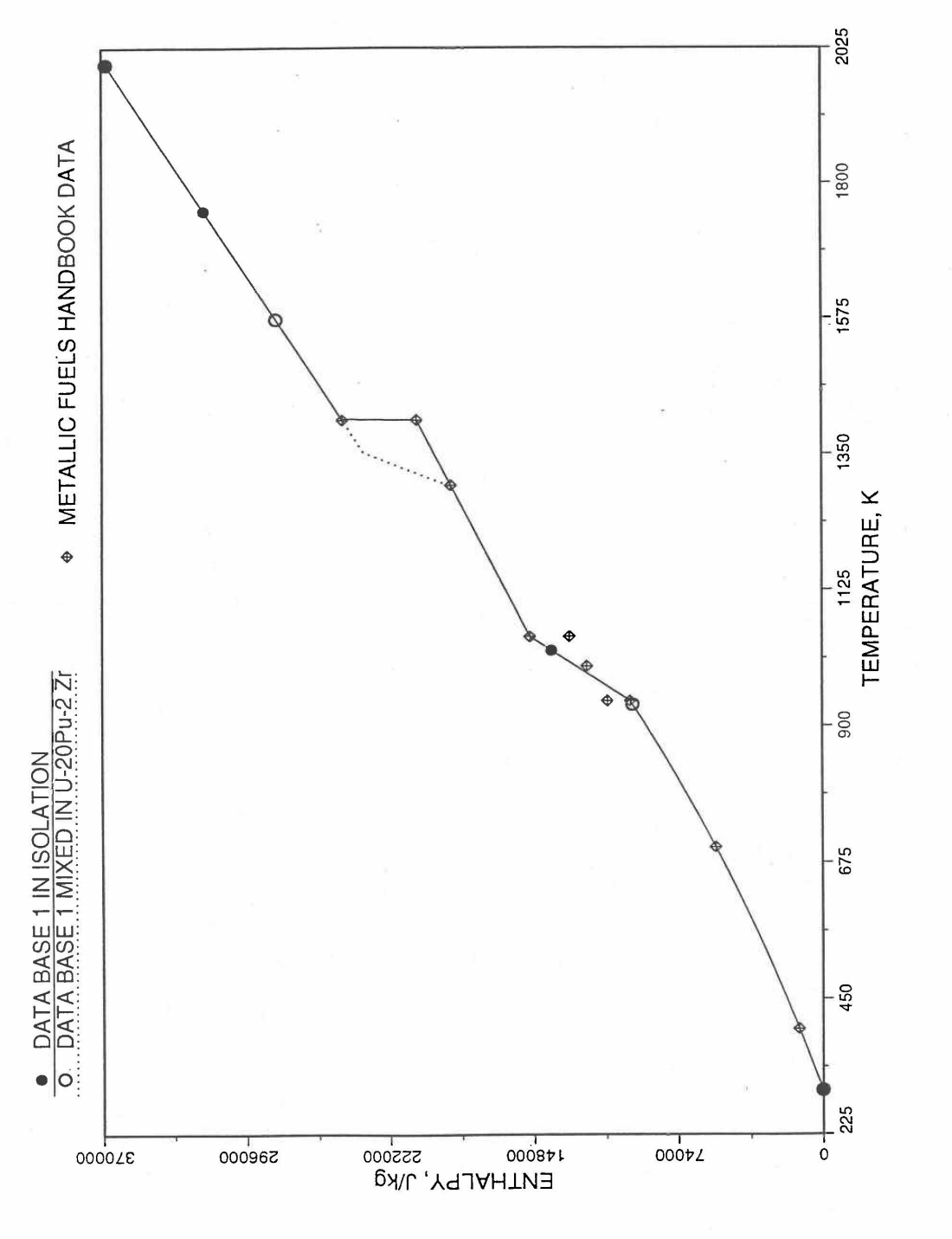

Fig. 10.3-8. Enthalpy of U Metal Obtained From Eqs. (10.3-2) and (10.3-6) That is used as Database 1 in Region 4; and its Comparison With Metallic Fuels handbook Data

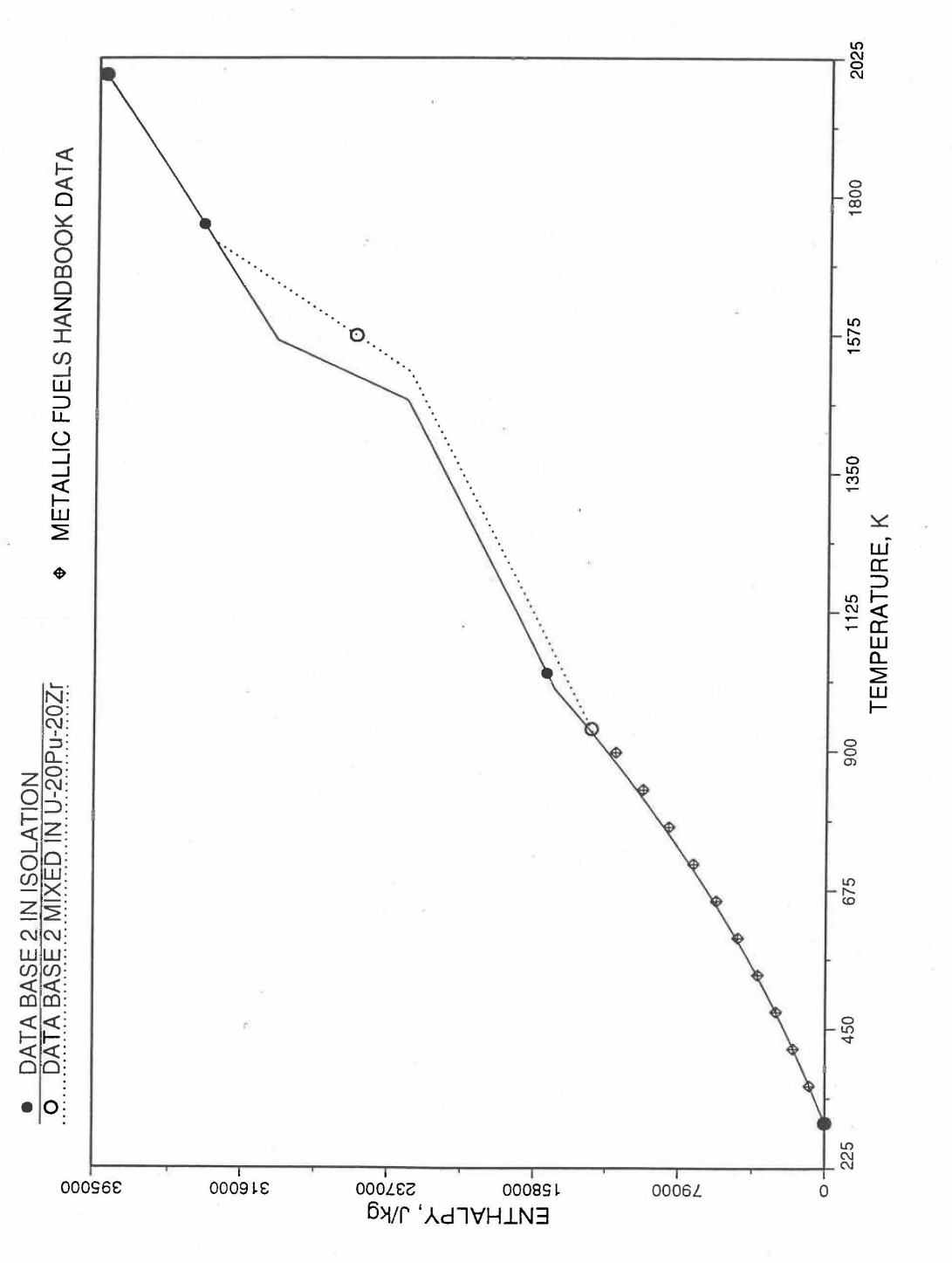

Fig. 10.3-9. Enthalpy of U-5.4Zr Obtained From Eqs. (10.3-2), (10.3-4) and (10.3-7) That is Used as Database 2 in Regions 1, 2 and 4; and its Comparison With Metallic Fuels Handbook Data

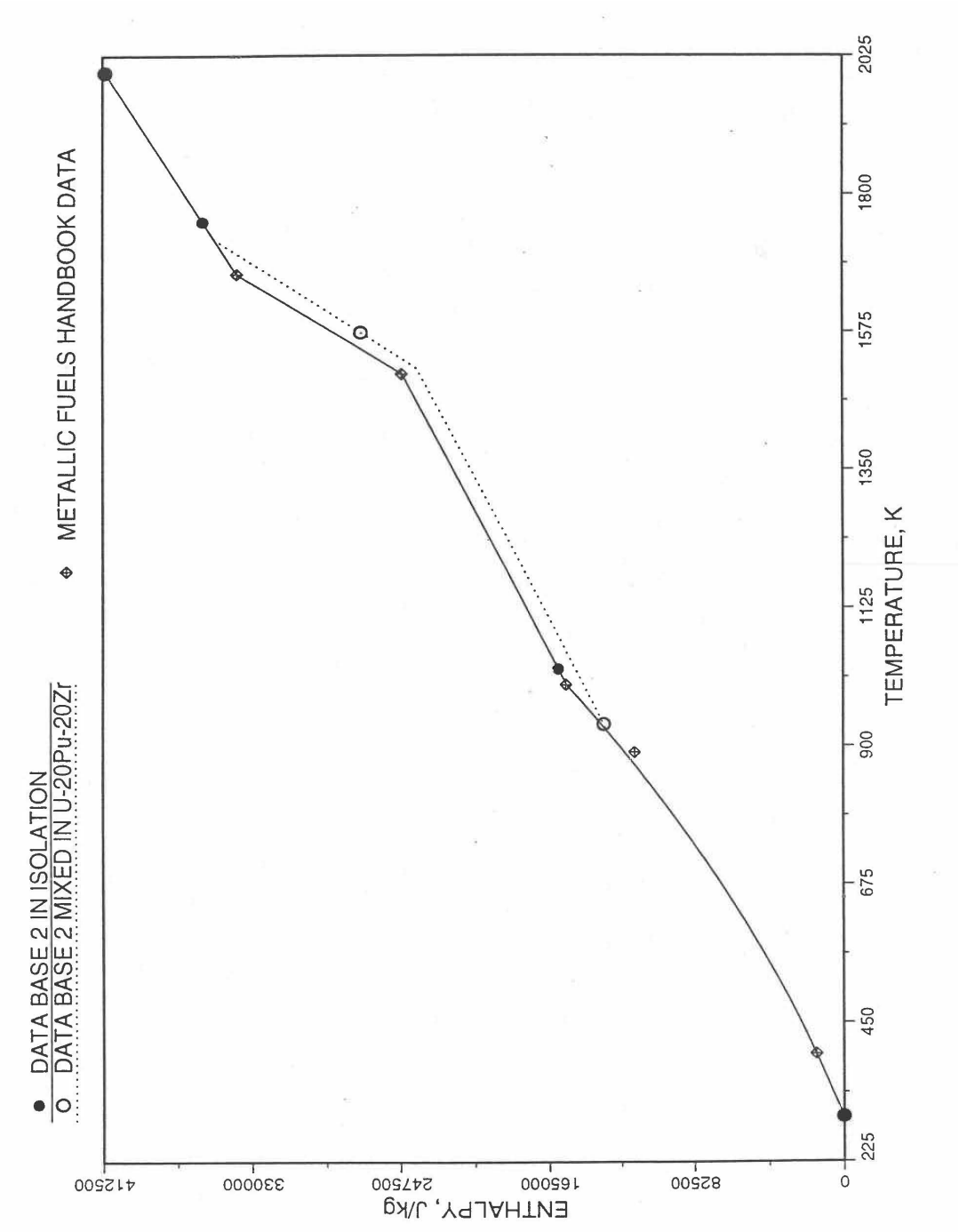

Fig. 10.3-10. Enthalpy of U-10Zr Obtained from Eqs. (10.3-2), (10.3-4) and (10.3-7) That is Used as Database 2 in Regions 1, 2 and 4; and its Comparison With Metallic Fuels Handbook Data

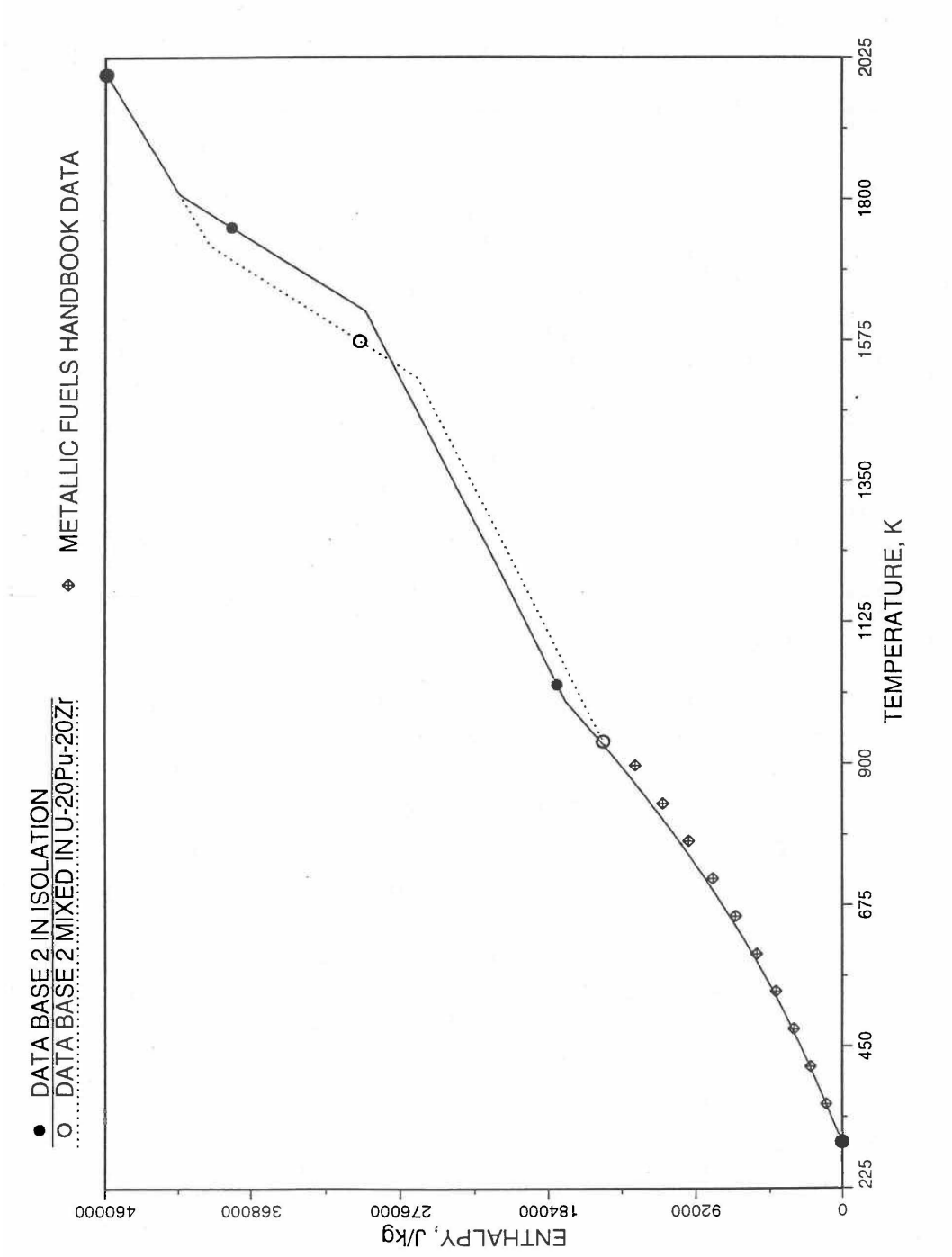

Fig. 10.3-11. Enthalpy of U-21.1Zr Obtained From Eqs. (10.3-2), (10.3-4) and (10.3-7) That is Used as Database 2 in Region 1; and its Comparison With Metallic Fuels Handbook Data

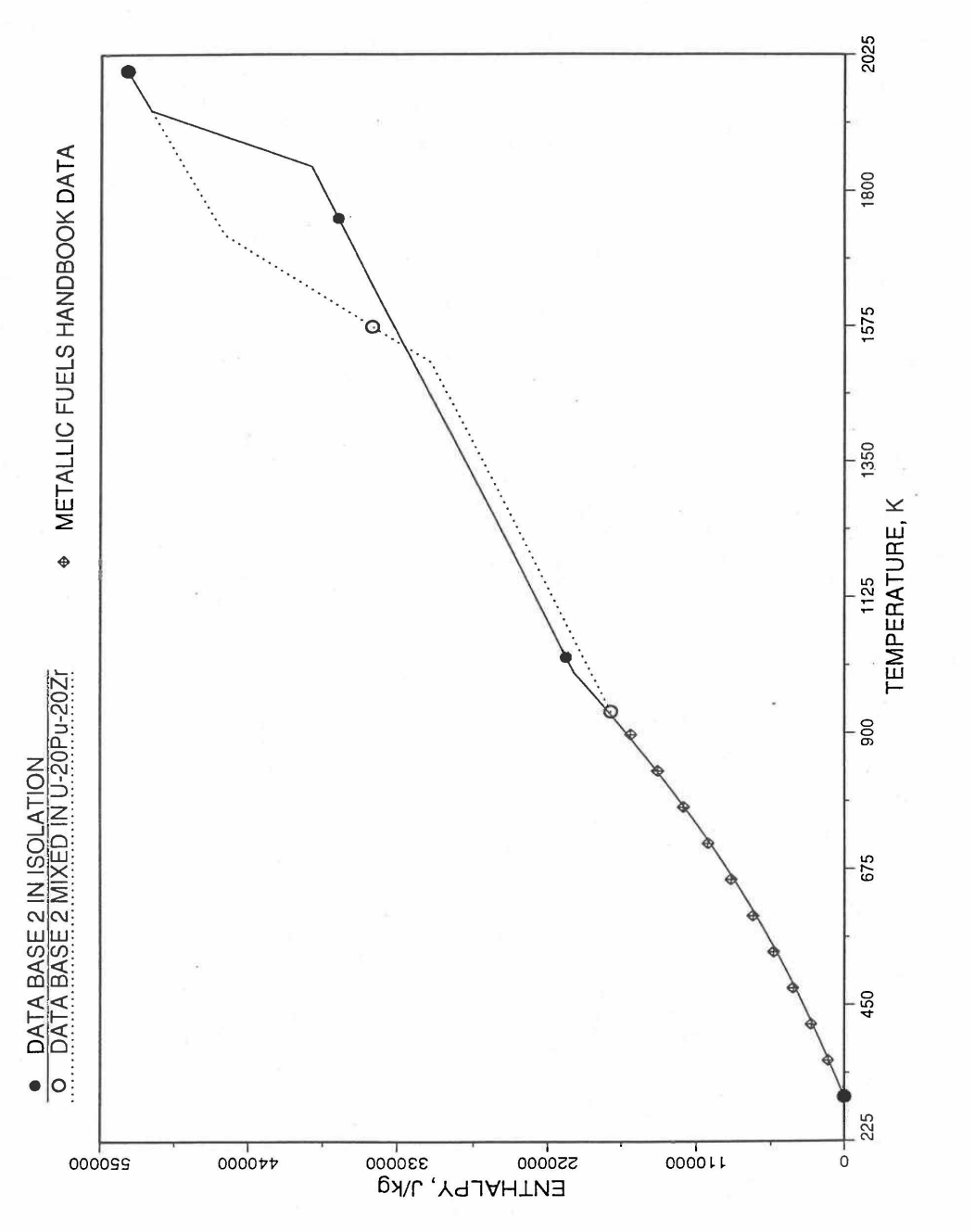

Fig. 10.3-12. Enthalpy of U-37.6Zr Obtained From Eqs. (10.3-2),v(10.3-4) and (10.3-7) That is Used as Database 2 in Regions 1 and 3; and its Comparison With Metallic Fuels Handbook Data

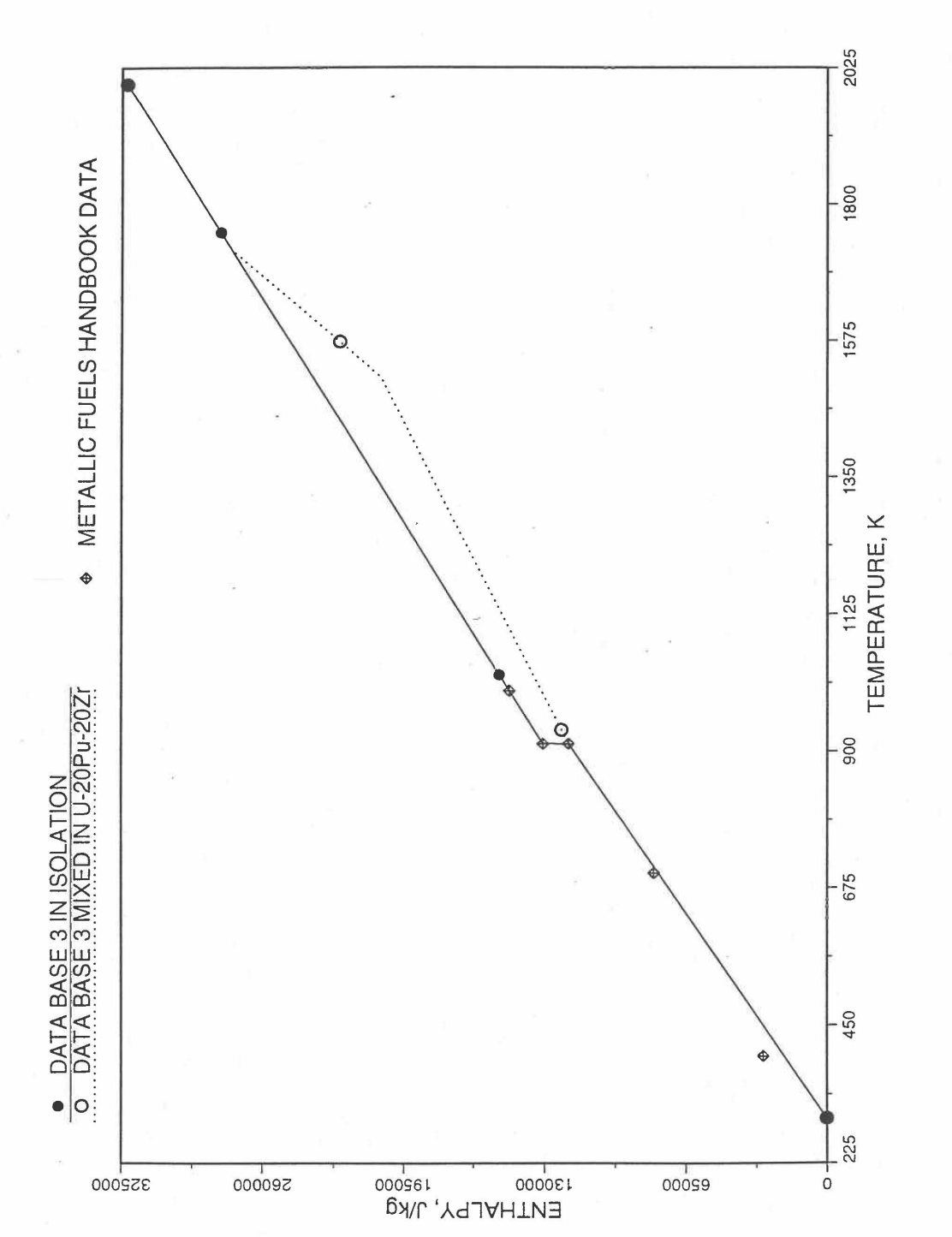

Fig. 10.3-13. Enthalpy of Pu Metal Obtained From Eqs. (10.3-3) and (10.3-8) That is Used as Database 3 in Regions 2, 3 and 4; and its Comparison With Metallic Fuels Handbook Data

where

H_{lp}, H_{lz} = enthalpies of liquid *Pu* and liquid *Zr*, J/mol

T = temperature of the liquid phase, K.

When mixed to form a *U-Pu-Zr* molten mixture, Eqs. (10.3-2) to (10.3-4) are used for all temperatures at and above the liquidus temperature of the *U-Pu-Zr* alloy, even if the liquidus temperature is below the melting point of U, *Pu* or *Zr*.

2. Database 1 Used in Solid Phase

As described in Section B, the ternary fuel U-15Pu-10Zr is used as database 1 in regions 1, 2 and 3 of Fig. 10.3-6; and the U metal is used as database 1 in region 4. The enthalpy data and correlation for U-15Pu-10Zr presented in the Metallic Fuels Handbook [10-8] and in the memorandum by Billone [10-12] can be written as

$$H_a(T)=\begin{cases} 19.34(T-298)+0.0133\left(T^2-298^2\right), & T\le 873\,K \quad \text{(10.3-5a)} \\ H_a(873)+162(T-873), & 873<T\le 943\,K \quad \text{(10.3-5b)} \\ H_a(923)+8.752(T-923)+0.01304\left(T^2-923^2\right), & 943<T\le 1379\,K \quad \text{(10.3-5c)} \\ H_a(1379)+89.95(T-1379), & 1379<T\le 1588\,K \quad \text{(10.3-5d)} \\ H_a(1588)+44.4(T-1588), & T>1588\,K \quad \text{(10.3-5e)} \end{cases}$$

where

H_a = enthalpy of U-15Pu-10Zr alloy, J/mol

T = temperature of the alloy, K

Here 1379 K and 1588 K are the solidus and liquidus temperatures of this alloy. In the present method, Eqs. (10.3-5d) and (10.3-5e) are never required. Equation (10.3-5b) covers the temperature range containing solid-state phase transitions. When mixed to form a desired U-Pu-Zr alloy composition, Eq. (10.3-5c) for the enthalpy in the temperature range above the solid-state phase transitions is extended up to the solidus temperature of the desired alloy. This difference in behavior of U-15Pu-10Zr when mixed to produce a desired alloy composition, e.g., U-20Pu-20Zr, as compared to its behavior in isolation is shown in Fig. 10.3-7.

The enthalpy data and correlation for U metal (used as database 1 in region 4) presented in the Metallic Fuels Handbook [10-8] can be written as

$$H_u(T)=\begin{cases} 26.92(T-298)-1.251x10^{-3}\left(T^2-298^2\right)+8.852\,x10^{-6}\left(T^3-298^3\right) \\ \quad -7.7\,x10^{4}\left[\dfrac{1}{298}-\dfrac{1}{T}\right] & T\le 942\,K \quad (10.3\text{-}6a) \\ H_u(942)+113.467(T-942), & 942<T\le 1049\,K \quad (10.3\text{-}6b) \\ H_u(1049)+38.284(T-1049), & 1049<T\le 1408\,K \quad (10.3\text{-}6c) \\ H_u(1408)+9142+48.66(T-1408), & T>1408\,K \quad (10.3\text{-}6d) \end{cases}$$

where

$H_u(T)$ = enthalpy (J/mol) of U metal at temperature T(K).

Here 942 K and 1049 K are the first and the last solid-state phase transition temperatures of U metal, and 1408 K is the melting point. The average specific heat [10-8] over the solid-state phase transition range is 113.467 J/mol-K as used in Eq. (10.3-6b). In the present method, Eq. (10.3-6d) is never required. When mixed to form a desired U-Pu-Zr alloy composition, Eq. (10.3-6c) for the enthalpy in the temperature range above the solid-state phase transitions is extended up to the solidus temperature of the desired alloy. This difference in behavior of U metal when mixed to produce a desired alloy composition, e.g., U-20Pu-2Zr, as compared to its behavior in isolation is shown in Fig. 10.3-8.

3. Database 2 Used in Solid Phase

As described in Section B, U-Zr binary alloys of 5.4 to 37.6 wt % Zr content are used as database 2 in different regions as given in Table 10.3-1. The enthalpy data and correlations for 87 at.% U-Zr (U-5.4wt %Zr), U-10 wt %Zr, 59 at.% U-Zr (U-21.1wt %Zr), and 39 at.% U-Zr (U-37.6wt %Zr) presented in the Metallic Fuels Handbook have been correlated by Billone [10-12] into the following single equation with composition-dependent coefficients. Here the relationships between atom fractions and weight fractions were derived using an average atomic weight of 236.678 for U (based on a U-235 enrichment of 0.478 weight fraction as done by Billone for Mark-V fuel), an atomic weight of 91.22 from Zr, and an atomic weight of 239.13 for Pu.

$$H_{uz}(T)=\begin{cases}1.594\left(A_u+0.3219A_z\right)\left(T-298\right)+0.03235\left(A_u+0.8495A_z\right)\left(T^2-298^2\right) \\ +928700\left(A_u+1.0243A_2\right)\left(\dfrac{1}{298}-\dfrac{1}{T}\right), T\le T_\gamma & \text{(10.3-7a)}\\ H_{uz}\left(T_\gamma\right)+38.28\left(A_u+0.8203A_z\right)\left(T-T_\gamma\right), T_\gamma<T\le T_s & \text{(10.3-7b)}\\ H_{uz}\left(T_s\right)+9142\left(A_u+5.938A_z\right)\left(T-T_s\right)/\left(T_\ell-T_s\right), T_s<T\le T_\ell & \text{(10.3-7c)}\\ H_{uz}\left(T_\ell\right)+48.66\left(A_u+0.6885A_z\right)\left(T-T_\ell\right), T>T_\ell & \text{(10.3-7d)}\end{cases}$$

where

$H_{uz}(T)$ = enthalpy (J/mol) of the U-Zr binary alloy at temperature T (K),

A_u, A_z = atom fractions of U and Zr in the alloy,

T_γ = the highest solid-state phase (γ-phase) transition temperature,

T_s, T_ℓ = solidus and liquidus temperatures of the U-Zr binary alloy.

For the U-Zr binary alloy, the temperatures T_γ, T_s and T_ℓ should be taken form the U-Zr phase diagram. For U-10wt %Zr, the temperatures T_γ, T_s and T_ℓ are 1000 K, 1506 K and 1669 K. In the present method, Eqs. (10.3-7c) and (10.3-7d) are never required. When mixed to form a desired U-Pu-Zr alloy composition, the temperatures T_γ, T_s and T_ℓ for the U-Pu-Zr ternary alloy are to be used in Eq. (10.3-7) as suggested by Billone [10-12]. In the present method, this amounts to (1) lowering T_γ from the U-Zr value of about 1000 K to the U-Pu-Zr alloy value of 923 K (see Table 10.3-1), and (2) extending Eq. (10.3-7b) for U-Zr enthalpy in the γ-phase temperature range to the solidus temperature of the desired U-Pu-Zr alloy composition. This difference in behavior of four U-Zr alloys (database 2 alloys) when mixed to produce a desired alloy composition, e.g., U-20Pu-20Zr, as compared to their behavior in isolation is shown in Figs. 10.3-9 to 10.3-12. These plots also show the agreement between the enthalpy of U-Zr alloys in isolation, evaluated from this correlation, with the data in the Metallic Fuels Handbook [10-8].

4. Database 3 Used in Solid Phase

As described in Section B, the Pu metal is used as database 3 in regions 2, 3, and 4. Region 1 does not require this database. The enthalpy data for Pu metal presented in the Metallic Fuels Handbook [10-8] has a number of solid-state phase transitions causing relatively small enthalpy jumps at the transition temperatures. As suggested by Billone [10-12], the following equation is a simplified representation of Pu metal enthalpy data [10-8], in the spirit of mixing to produce a desired U-Pu-Zr alloy

composition (the value of the average Pu specific heat from the reference temperature of 298 K to Pu melting point of 913 K has been corrected):

$$H_p(T)=\begin{cases} 46.286(T-298), & T\le 913K \quad \text{(10.3-8a)} \\ H_p(913)+34.434(T-913), & 913<T\le T_s \quad \text{(10.3-8b)} \\ H_p(913)+34.434(T-913)+2824(T-T_s)/(T_\ell-T_s), & T_s<T\le T_\ell \quad \text{(10.3-8c)} \\ H_p(T_\ell)+42.258(T-T_\ell), & T>T_\ell \quad \text{(10.3-8d)} \end{cases}$$

where

$H_p(T)$ = enthalpy (J/mol) of Pu metal at temperature T,

913 K = the melting point of Pu metal

T_s, T_ℓ = solidus and liquidus temperatures of the desired U-Pu-Zr alloy composition, and not of pure Pu metal.

Here 46.286 J/mol-K is the average Pu specific heat between 298 K and 913 K, and 34.434 J/mol-K is the specific heat of the last solid-stat phase (ε-phase) of Pu metal that is extended up to the liquidus temperature of the desired U-Pu-Zr alloy composition to account for the sensible heat absorbed by Pu. Equation (10.3-8c) indicates that the Pu heat of fusion required for solid-to-liquid phase transition is added linearly between the solidus and liquidus temperatures of the desired U-Pu-Zr alloy composition. In the present method, Eqs. (10.3-8c) and (10.3-8d) are never required. The difference in behavior of Pu metal when mixed to produce a desired alloy composition, e.g., U-20Pu-20Zr, as compared to its behavior in isolation is shown in Fig. 10.3-13. This plot also shows the comparison between the enthalpy of Pu metal in isolation with the date in Metallic Fuels Handbook [10-8]. In Fig. 10.3-13, the Pu enthalpy above the solidus temperature of the desired U-Pu-Zr alloy composition was obtained by linearly joining the enthalpy at solidus evaluated from Eq. (10.3-8b) with the enthalpy at liquidus evaluated from Eq. (10.3-3) as mentioned in Section B.

It should be noted that the contribution of Pu enthalpy to U-Pu-Zr fuel compositions in the vicinity of U-15Pu-10Zr (point A of Fig. 10.3-6) is small because the corner Pu of the ternary composition triangle is far removed from point A and the point representing the desired fuel composition. The major contribution comes from U-15Pu-10Zr enthalpy.

10.3.2.1.4 Method of Interpolation Between Database

As described in Section B, the enthalpy of a desired U-Pu-Zr fuel composition at and above its liquidus temperature is evaluated by assuming it to be an ideal solution of the

3 liquid components U, Pu and Zr whose enthalpies are given by Eqs. (10.3-2) to (10.3-4). This method is tantamount to mass-weighted averaging of the component enthalpies.

$$h_\ell(T) = 1000\left(W_u H_{\ell u}/a_u + W_p H_{\ell p}/a_p + W_z H_{\ell z}/a_z\right) \tag{10.3-9}$$

where

$h_\ell(T)$ = enthalpy (J/kg) of a U-Pu-Zr fuel composition at a temperature T, at and above its liquidus,

W_u, W_p, W_z = weight fractions of U, Pu and Zr in the U-Pu-Zr fuel composition

$H_{\ell u}, H_{\ell p}, H_{\ell z}$ = enthalpies (J/mol) of U, Pu and Zr metals in the liquid phase

a_u, a_p, a_z = atomic weight of U, Pu and Zr,

1000 = conversion factor from J/gm to J/kg.

The method of interpolation to evaluate the enthalpy of a U-Pu-Zr fuel composition at and below its solidus temperature consists of first determining the region of the ternary composition triangle (shown in Fig. 10.3-6) in which the desired fuel composition lies, and then finding the weight fractions in which the 3 database alloys of the region are required to be mixed to obtain the desired fuel composition. The mass balance of he 3 constituents requires that the following 3 equations be satisfied by the weight fractions of the 3 database alloys.

$$W_{u1} X_1 + W_{u2} X_2 + W_{u3} X_3 = W_u \tag{10.3-10}$$

$$W_{p1} X_1 + W_{p2} X_2 + W_{p3} X_3 = W_p \tag{10.3-11}$$

$$W_{z1} X_1 + W_{z2} X_2 + W_{z3} X_3 = W_z \tag{10.3-12}$$

where

W_{u1}, W_{p1}, W_{z1} = weight fractions of U, Pu and Zr in database alloy 1 of the region in which the desired fuel composition lies,

W_{u2}, W_{p2}, W_{z2} = weight fractions of U, Pu and Zr is database alloy 2 of the region,

W_{u3}, W_{p3}, W_{z3} = weight fractions of U, Pu and Zr in database alloy 3 of the region,

W_u, W_p, W_z = weight fractions of U, Pu and Zr in the desired fuel composition,

X_1, X_2, X_3 = weight fractions of database alloys 1, 2, and 3 in which they must be mixed.

It should be noted that the sum of U, Pu and Zr weight fractions in each database alloy is 1.

$$W_{u,i} + W_{p,i} + W_{z,i} = 1, \quad i = 1,2,3 \tag{10.3-13}$$

Adding Eqs. (10.3-10) to (10.3-12), and substituting Eq. (10.3-13), one obtains

$$X_1 + X_2 + X_3 = 1 \tag{10.3-14}$$

Equations (10.3-11), (10.3-12) and (10.3-14) provide a set of 3 linear equations in the variables X_1, X_2 and X_3. The solution of this set is given by

$$X_i = D_i / D, \; i = 1,2,3 \tag{10.3-15}$$

where

$$D = (W_{z1} - W_{z2})(W_{p3} - W_{p1}) - (W_{p1} - W_{p2})(W_{z3} - W_{z1}) \tag{10.3-16}$$

$$D_1 = (W_z - W_{z2})(W_{p3} - W_p) - (W_p - W_{p2})(W_{z3} - W_z) \tag{10.3-17}$$

$$D_2 = (W_{z1} - W_z)(W_{p3} - W_{p1}) - (W_{p1} - W_p)(W_{z3} - W_{z1}) \tag{10.3-18}$$

$$D_3 = (W_{z1} - W_{z2})(W_p - W_{p1}) - (W_{p1} - W_{p2})(W_z - W_{z1}) \tag{10.3-19}$$

The sum of X_1, X_2 and X_3 is always 1. In case of interpolation, the values of X_1, X_2 and X_3 are always positive. If any extrapolation were involved, the value of at least one weight fraction becomes negative which is entirely avoided in the present method. For region 4 of Fig. 10.3-6, the mixing fractions of the database alloys given by Eqs. (10.3-15) to (10.3-19) simplify to the following:

$$X_2 = W_z / W_{z2} \tag{10.3-20}$$

$$X_3 = W_p \tag{10.3-21}$$

$$X_1 = 1 - X_2 - X_3 \tag{10.3-22}$$

The Zr weight fraction of database alloy 2 to be used in region 1 of Fig. 10.3-6 is found by writing the general equation of the line joining points A and F, i.e., the points representing the U-15Pu-10Zr database and the desired fuel composition.

$$W_z' = W_{z1} + \frac{(W_z - W_{z1})}{(W_p - W_{p1})}(W_p' - W_{p1}) \tag{10.3-23}$$

where

W_p', W_z' = weight fractions of Pu and Zr corresponding to any point on the line AF.

The Zr weight fraction of database alloy 2 is then found by setting $W_p' = 0$ in Eq. (10.3-23) because database 2 is a U-Zr binary alloy.

$$x = W_{z1} - \frac{(W_z - W_{z1})}{(W_p - W_{p1})} W_{p1} \tag{10.3-24}$$

where

x = Zr weight fraction of database alloy 2 to be used in region 1.

The enthalpy of the desired U-Pu-Zr fuel composition at and below its solidus temperature is then evaluated by mass-weighted averaging of the enthalpies of the 3 database alloys of the region in which the desired fuel composition lies.

$$h(T) = 1000\left(X_1 H_1 / a_1 + X_2 H_2 / a_2 + X_3 H_3 / a_3\right) \tag{10.3-25}$$

where

$h(T)$ = enthalpy (J/kg) of the U-Pu-Zr fuel composition at a temperature T, at and below its solidus,

H_1, H_2, H_3 = enthalpies (J/mol) of the 3 database alloys at temperature T,

a_1, a_2, a_3 = average atomic weights of the 3 database alloys,

1000 = conversion factor from J/gm to J/kg.

10.3.2.1.5 Subroutine HFUEL1 and Specific Heat by Fuel Type

Figure 10.3-14 shows flow diagram of the subroutine HFUEL1 for calculating the enthalpy, based on this method of regionwise interpolation, of a U-Pu-Zr alloy fuel as a function of composition and temperature. The specific heat of each input fuel type of U-Pu-Zr alloy is evaluated using the 9 parameters defined in Fig. 10.3-15 that are calculated using the subroutine HFUEL1 as described in this section. Figures 10.3-16 to

10.3-19 show the comparison of calculated enthalpy with all the data in the Metallic Fuels Handbook for U-15Pu-10Zr and U-10Zr alloys, and U and Pu metals. Figures 10.3-20 to 10.3-22 show the variation of U-Pu-Zr alloy fuel enthalpy with composition obtained from this subroutine. The Zr content varies from 2 to 20 wt % and the Pu content varies from 5 to 30 wt % in the U-Pu-Zr alloy fuels plotted in these figures. The solidus and liquidus temperature required as input to the HFUEL1 subroutine were calculated using the subroutine developed by Pelton [10-13].

The subroutine is used in the SAS4A/SASSYS-1 codes by the subroutine PRECAl (see flow diagram of Fig. 10.3-5), before the steady state calculation, to pre-calculate coefficient of a simplified specific heat equation to be used in the steady state and transient calculations of the codes. These coefficients or parameters are defined in Fig. 10.3-15, and are pre-calculated for each fuel type that use the regionwise interpolated U-Pu-Zr thermal properties (input option IFUELM=0). This pre-calculation of the coefficients or parameters of the simplified specific heat equation should increase the computational speed of the codes. For this pre-calculation, a sufficient number of pairs of temperature and enthalpy values for the pre-transition solid U-Pu-Zr alloy (see Fig. 10.3-15) are obtained from the subroutine HFUEL1. The following enthalpy equation, basically a quadratic function of temperature that is constrained to exactly reproduce the first and last pairs of values, is then fitted by the method of least squares.

$$h(T) = f(T) + c(T - T_1)(T - T_N) \tag{10.3-26}$$

$$f(T) = h_1 + \frac{h_N - h_1}{T_N - T_1}(T - T_1) \tag{10.3-27}$$

where

T_i, h_i = ith pair of temperature and enthalpy values,

N = number of pairs of values,

c = coefficient of the quadratic term in the simplified enthalpy equation, to be determines by the method of least squares.

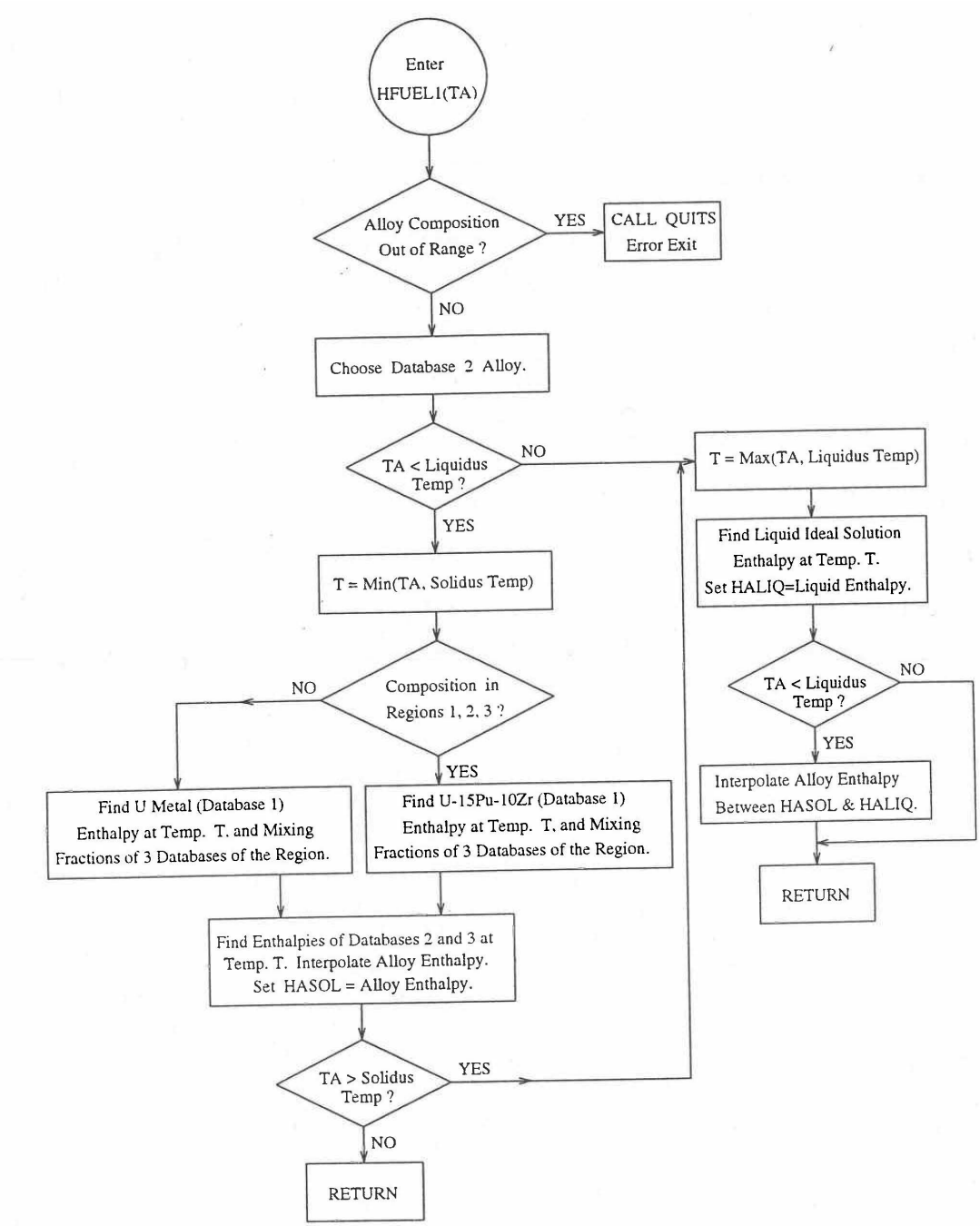

Fig. 10.3-14. Flow Diagram of Subroutine HFUEL1 for U-Pu-Zr Enthalpy

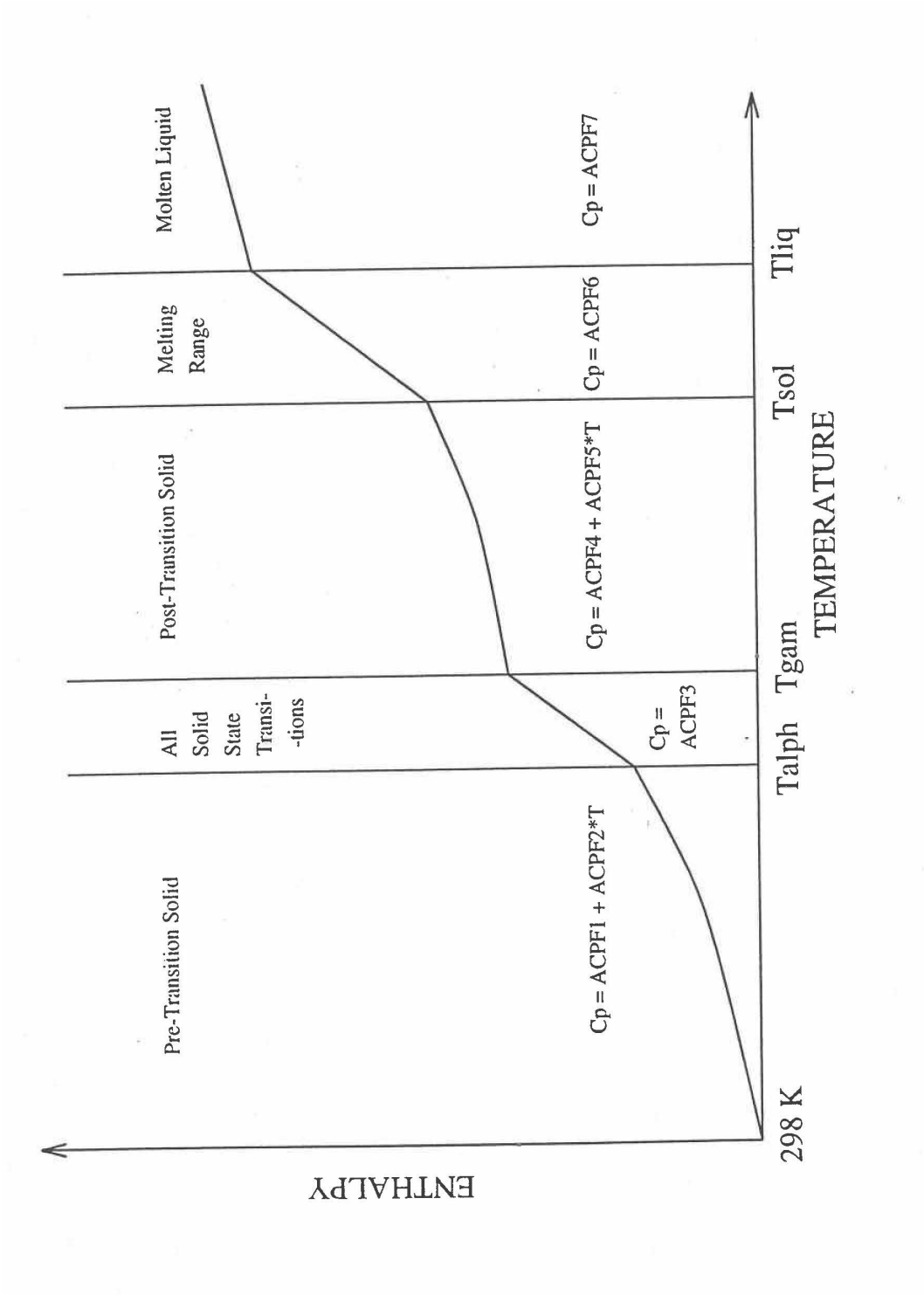

Fig. 10.3-15. Diagram Showing the 9 Parameters (ACPF1 to ACPF7, and Solidus and Liquidus Temperatures) Pre-Calculated and Stored for Each U-Pu-Zr Fuel Type for Fast Evaluation of Specific Heat

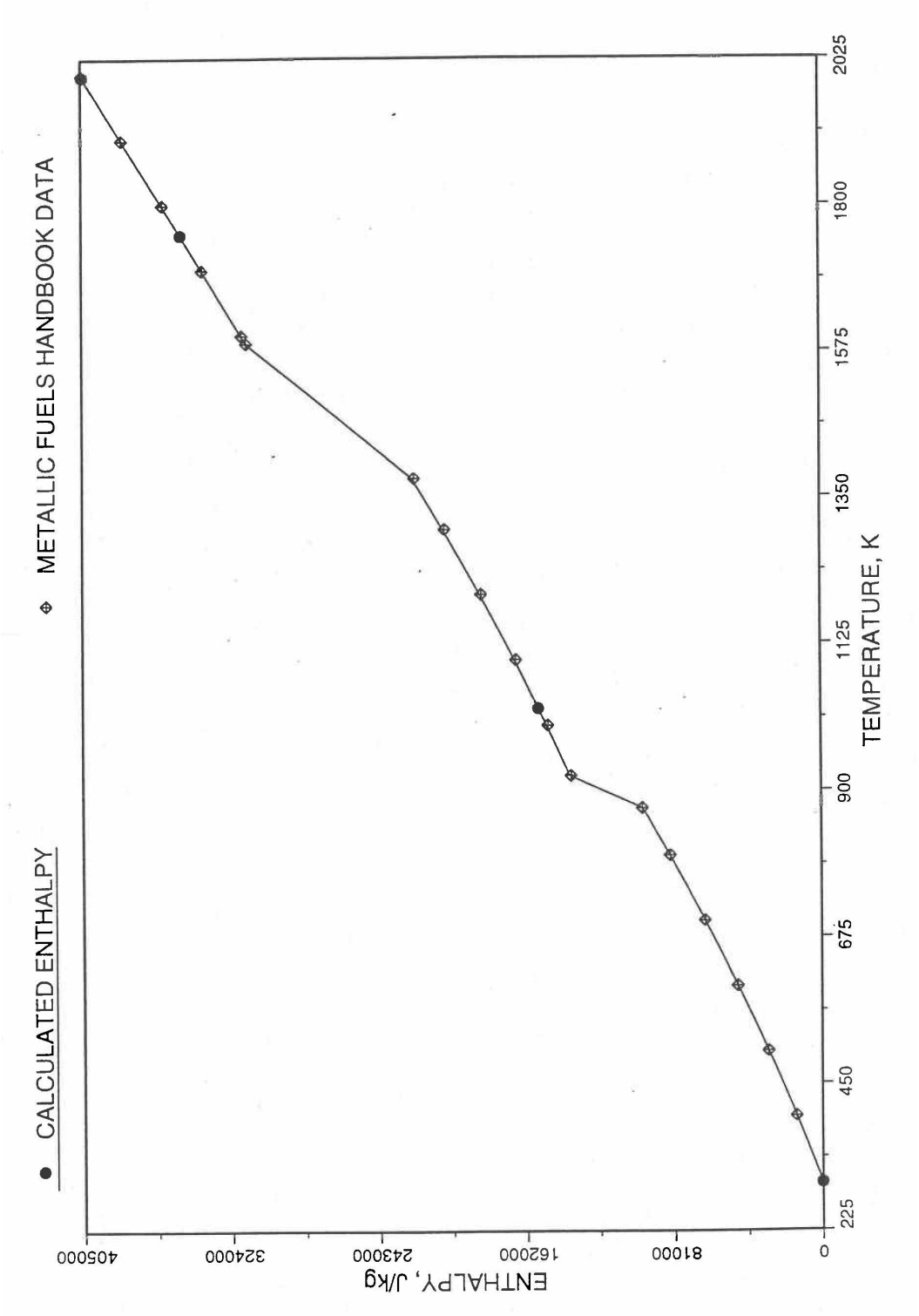

Fig. 10.3-16. Comparison of Calculated Enthalpy of U-Pu-10Zr Fuel With the IFR Metallic Fuels Handbook Data

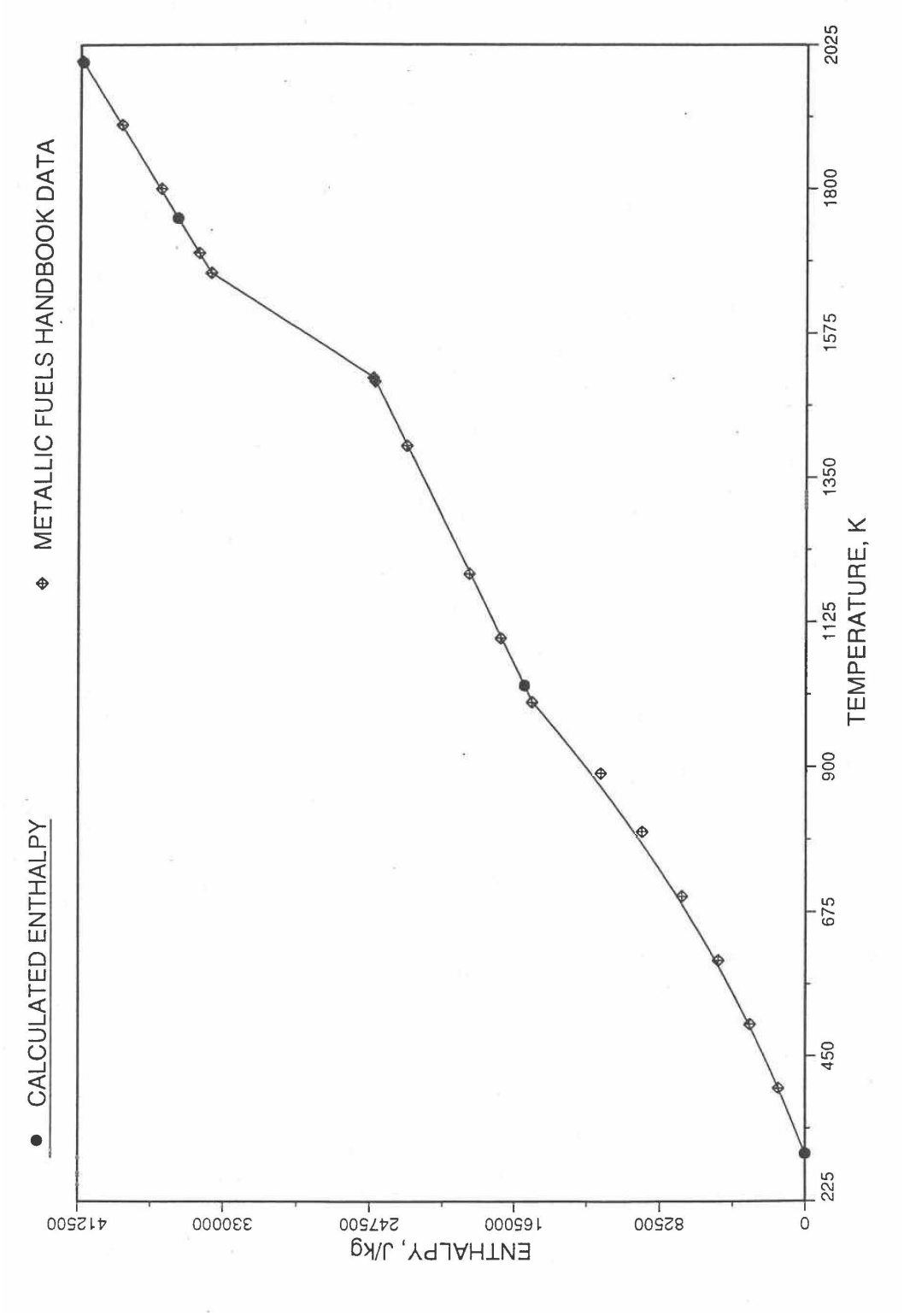

Fig. 10.3-17. Comparison of Calculated Enthalpy of U-10Zr Fuel With the Handbook Data (Input KBASE to Subroutine HFUEL1-1)

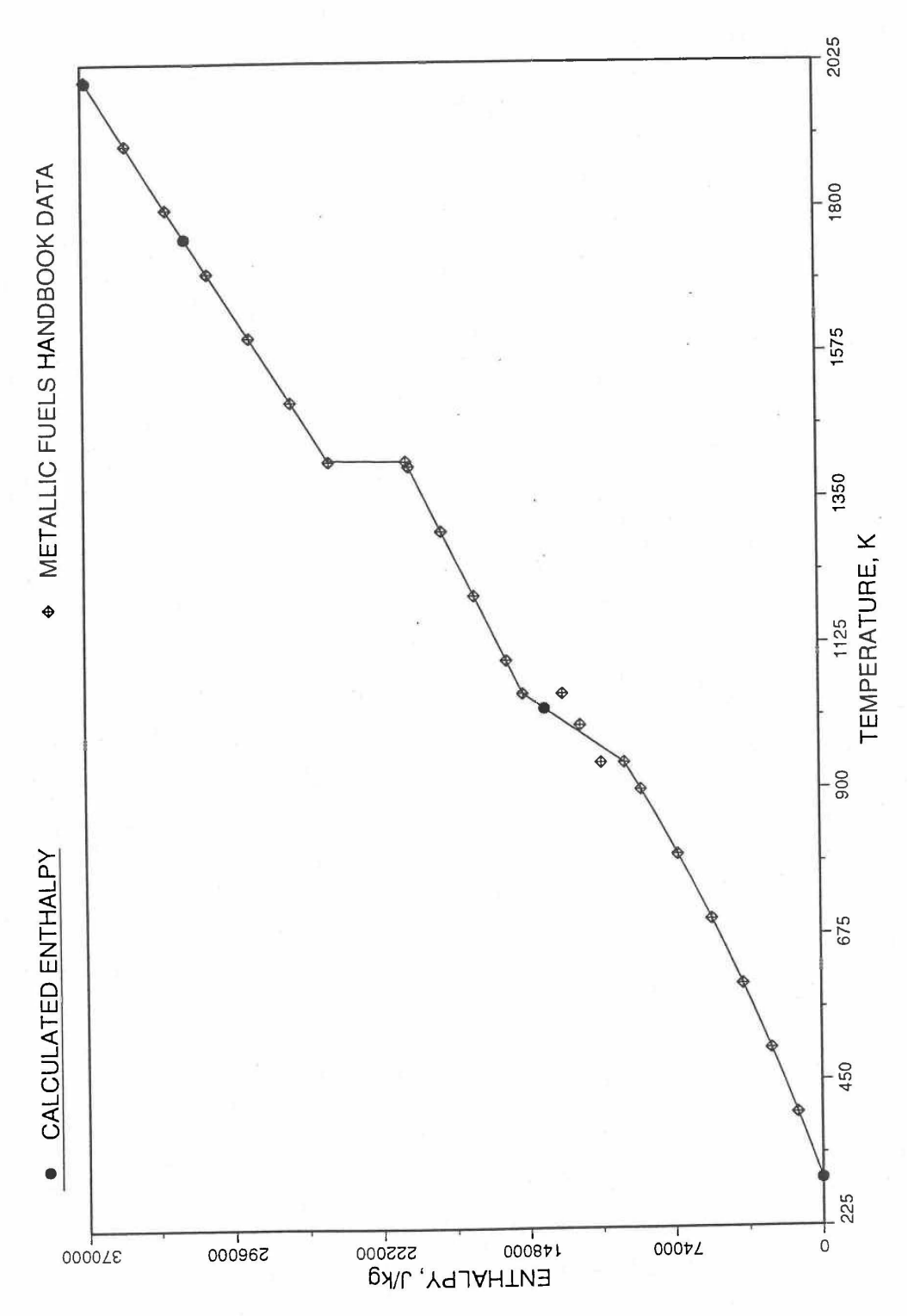

Fig. 10.3-18. Comparison of Calculated Enthalpy of Uranium Metal with the IFR Metallic Fuels Handbook Data

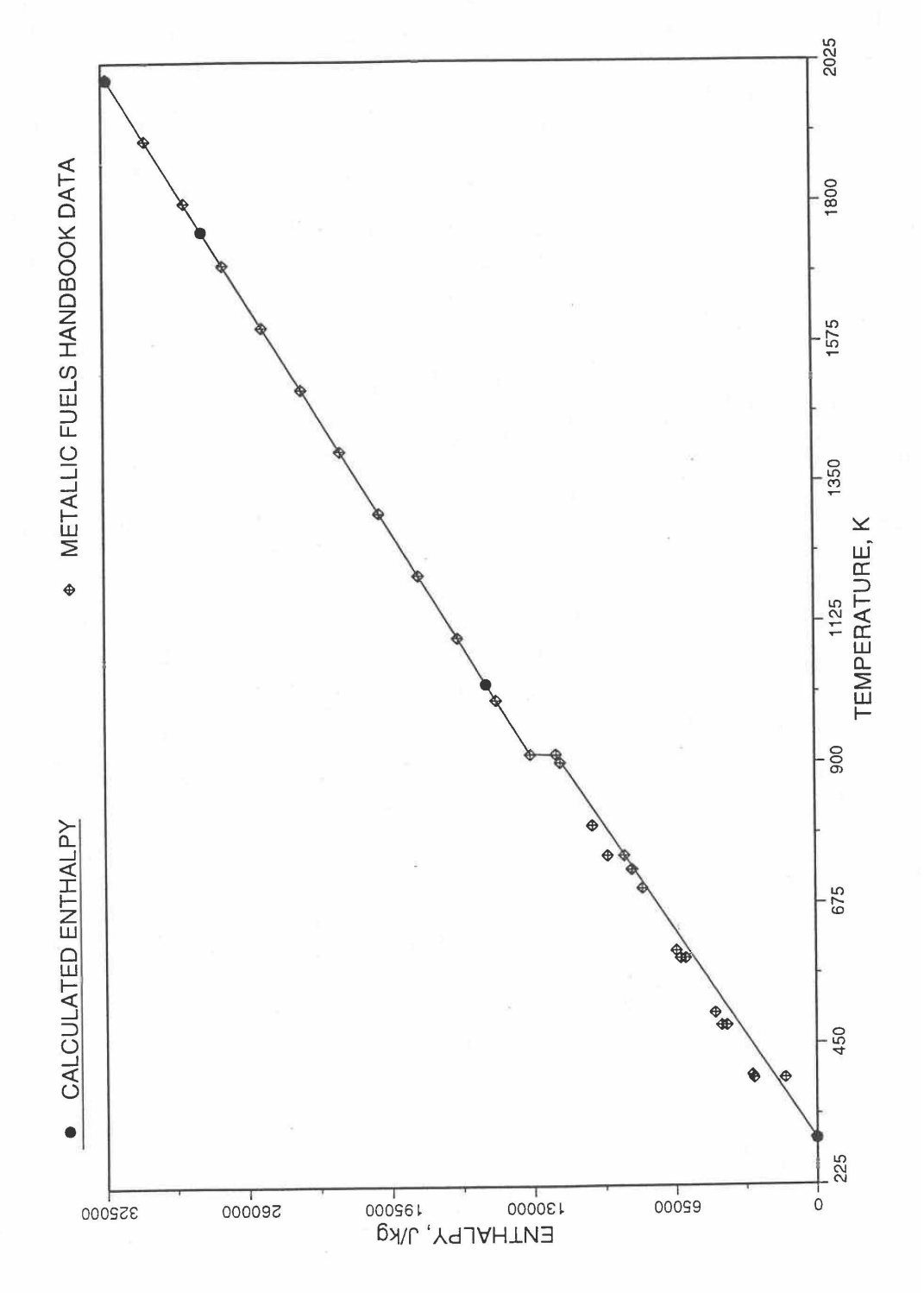

Fig. 10.3-19. Comparison of Calculated Enthalpy of Plutonium Metal with the IFR Metallic Fuels Handbook Data

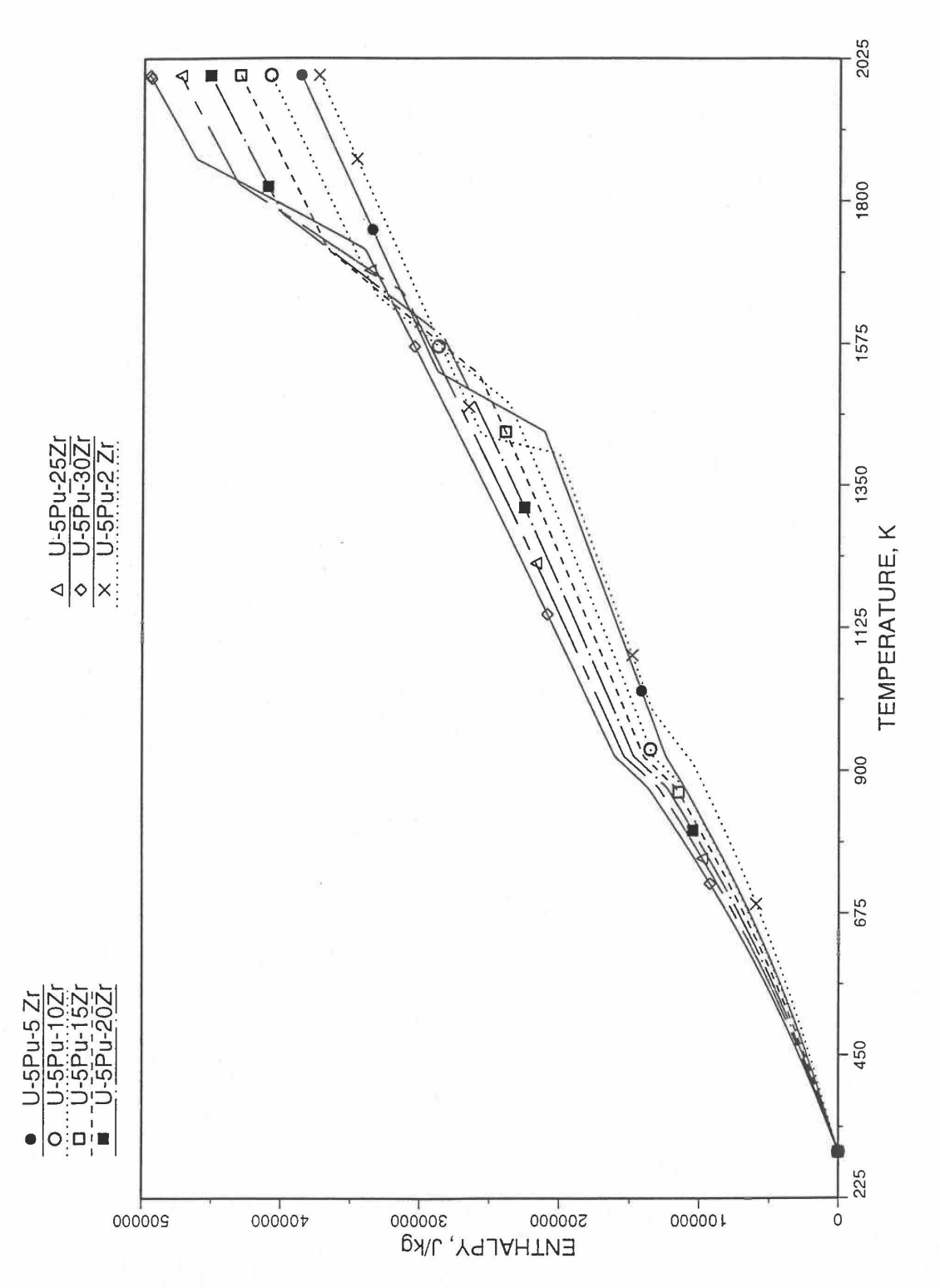

Fig. 10.3-20. Variation of U-5Pu-Zr Alloy Fuel Enthalpy With Composition Obtained From Subroutine HFUEL1 Based on the Method of Regionwise Interpolation

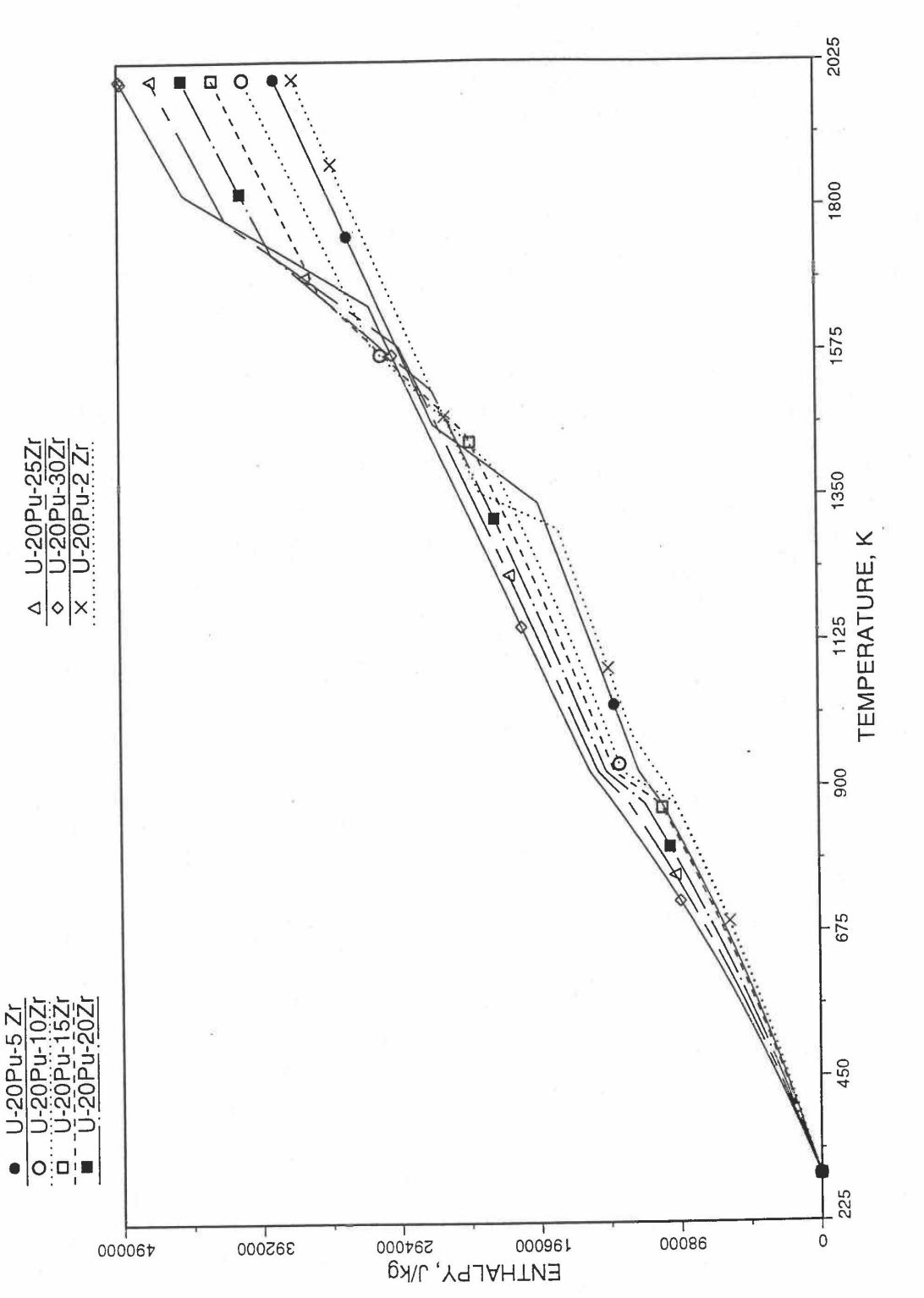

Fig. 10.3-21. Variation of U-20Pu-Zr Alloy Fuel Enthalpy With Composition Obtained From Subroutine HFUEL1 Based on the Method of Regionwise Interpolation

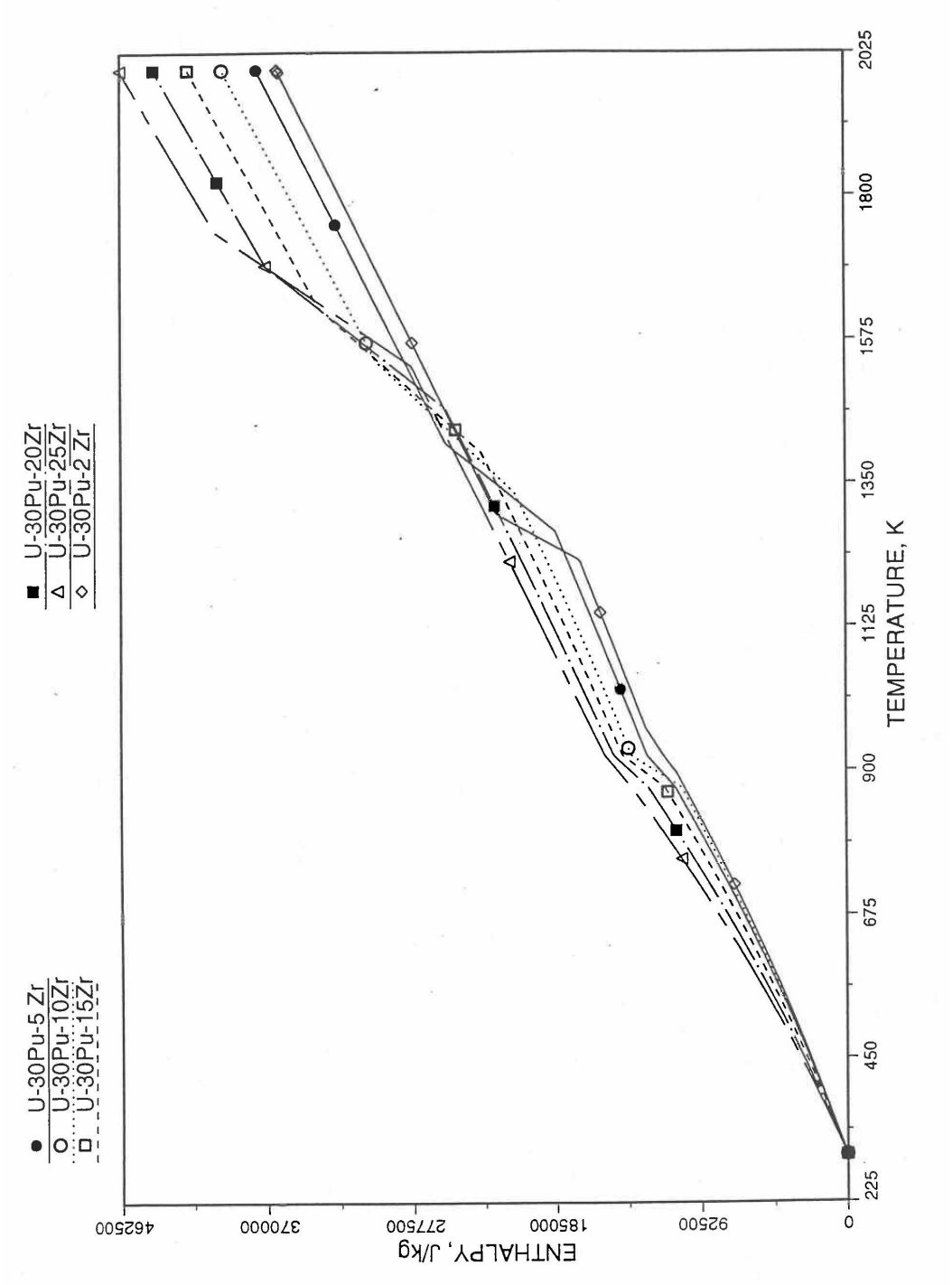

Fig. 10.3-22. Variation of U-30Pu-Zr Alloy Fuel Enthalpy With Composition Obtained From Subroutine HFUEL1 Based on the Method of Regionwise Interpolation

Minimizing the sum of squared errors, $\sum_{i=1}^{N}\left[h(T_i)-h_i\right]^2$, one obtains the following value of the quadratic term coefficient.

$$c=\frac{\sum_i\left[h_i-f(T_i)\right](T_i-T_1)(T_i-T_N)}{\sum_i(T_i-T_1)^2(T_i-T_N)^2} \tag{10.3-28}$$

Differentiating Eq. (10.3-26) with respect to temperature, one obtains the following values of the coefficients of the simplified specific heat equation for the pre-transition solid U-Pu-Zr alloy (see Fig. 10.3-15).

$$C_p = ACPF1 + ACPF2 * T \tag{10.3-29}$$

$$ACPF1=(h_N-h_i)/(T_N-T_1)-c(T_1+T_N) \tag{10.3-30}$$

$$ACPF2=2C \tag{10.3-31}$$

The least-squares fitting procedure is repeated for the post-transition solid U-Pu-Zr alloy (see Fig. 10.3-15) to obtain the coefficients its simplified specific heat equation. In each of the remaining temperature ranges of Fig. 10.3-15, the specific heat is assumed to be a constant.

It is important to note that, in order to be consistent with the method of Section 3.3.5 for adjusting fuel temperature (computed without accounting for heat of fusion during the main heat transfer calculation) to account for heat of fusion at any radial mesh interval that is going through the melting range, the actual specific heat ACPF6 (see Fig. 10.3-15) over the melting range is replaced in subroutine CFUEL by a value linearly interpolated between (i) the post-transition solid U-Pu-Zr specific heat at the solidus temperature, and (ii) the molten liquid solution specific heat, ACPF7, at the liquidus temperature.

This approach of calculating U-Pu-Zr fuel specific heat by fuel type is used only in case of a single radial fuel zone (IFUELC=0), or multiple (i.e., up to 3) radial fuel zones (IFUELC=1). When each fuel radial mesh interval is a unique zone of a different alloy composition (IFUELC=2), then use is made of another subroutine CFUEL1 that calculates U-Pu-Zr alloy specific heat as a function of composition, directly by regionwise interpolation of the temperature-derivative of enthalpies of database alloys, as described in the next section.

10.3.2.2 Specific Heat of U-Pu-Zr Fuel

When each fuel radial mesh interval is a unique zone of a different alloy composition (input parameter IFUELC = 2), then it is difficult to use specific heat by fuel type

because only 8 fuel types are currently allowed in the SAS4A/SASSYS-1 codes. The situation becomes even more difficult after in-pin fuel melting, and mixing of fuel radial mesh intervals in the molten fuel cavity produces new alloy compositions. In this case, use is made of another subroutine CFUEL1 that calculates U-Pu-Zr alloy specific heat as a function of composition, directly by regionwise interpolation of the temperature-derivatives of enthalpies of database alloys, given by Eqs. (10.3-2) to (10.3-8). The regionwise interpolation of the derivatives in subroutine CFUEL1 is performed following exactly the same logic as that used in the regionwise interpolation of enthalpies in the subroutine HFUEL1. This makes the two subroutines consistent. Figure 10.3-23 shows flow diagram of the subroutine CFUEL1.

The calculation begins with the evaluation of the first and last solid-state transition temperatures based on data in Table 10.3-1. The bold-boundary rectangular box in the flow diagram of Fig. 10.3-23 represents the most major part of the subroutine CFUEL1, the part that performs regionwise interpolation of the temperature-derivatives of enthalpies of database alloys in the temperature range of pre-transition and post-transition solid fuels. These temperature ranges are defined in Fig. 10.3-15. Between the first and last transition temperatures, the subroutine HFUEL1 is used to find the enthalpies at the first and last transition temperatures, and the fuel specific heat is set equal to the average slope of enthalpy between these two temperatures. The detailed variation of specific heat between the first and last transition temperatures was studied using a modified version of CFUEL1 and found to be small (see Figs. 10.3-24 to 10.3-26) and inappropriate for inclusion in the heat transfer calculation of the SAS4A/SASSYS-1 codes. In that modified version of CFUEL1, the regionwise interpolation of derivatives represented by the bold-boundary rectangular box of Fig. 10.3-23 was used instead of the average slope. At and above the liquidus temperature of the desired U-Pu-Zr alloy, the specific heat as a function of composition is evaluated by assuming the molten alloy to be an ideal solution of the 3 liquid components U, Pu and Zr. Between the solidus and liquidus temperatures of the desired U-Pu-Zr alloy, the actual specific heat (obtained by following the dashed part of the CFUEL1 flow diagram shown in Fig. 10.3-23) over the melting range is replaced by a value linearly interpolated between (i) the post-transition solid U-Pu-Zr specific heat (CPSOL in Fig. 10.3-23) at the solidus temperature, and (ii) the molten liquid solution specific heat (CPLIQ in Fig. 10.3-23) at the solidus temperature. This replacement is required in order to be consistent with the method of Section 3.3.5 for adjusting fuel temperature (computed without accounting for heat of fusion during the main heat transfer calculation) to account for heat of fusion at any radial mesh interval that is going through the melting range.

Figure 10.3-17 shows the variation of Mark-V (U-20Pu-10Zr), U-15Pu-10Zr and U-10Zr fuel specific heats with temperature, obtained from this subroutine. Figures 10.3-28 to 10.3-33 show the variation of U-Pu-Zr alloy fuel specific heat with composition. The Zr content varies from 2 to 25 wt %, and the Pu content varies from 5 to 30 wt % in the U-Pu-Zr alloy fuels plotted in these figures. Figures 10.3-29, 10.3-31 and 10.3-33 simply show an enlargement of the solid-stat transition region of Figs. 10.3-28, 10.3-30 and 10.3-32. The solidus and liquidus temperatures required as input to the CFUEL1 subroutine were obtained using the subroutine developed by Pelton [10-13].

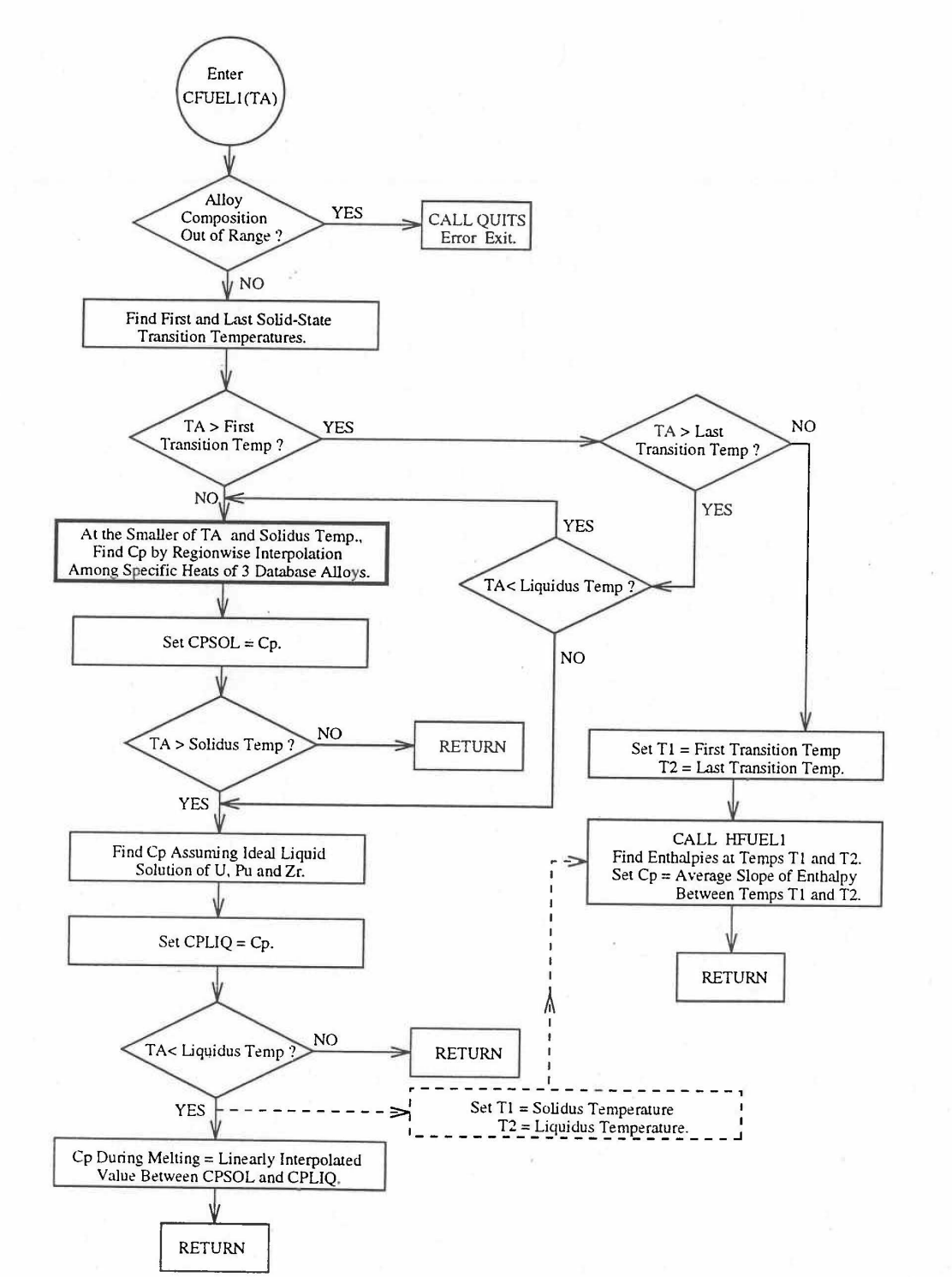

Fig. 10.3-23. Flow Diagram of Subroutine CFUEL1 for U-Pu-Zr Specific Heat

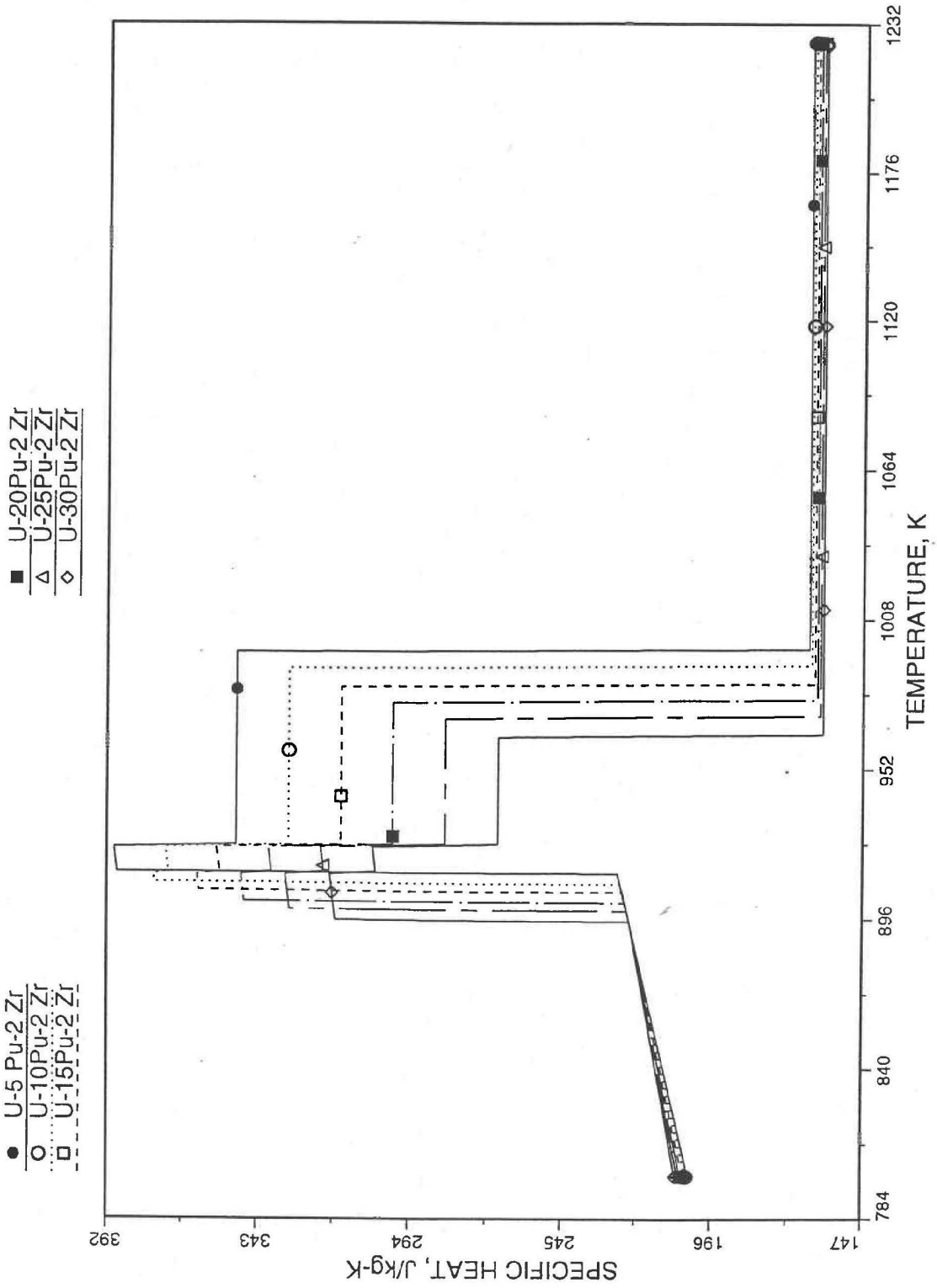

Fig. 10.3-24. Detailed Variation of U-Pu-2Zr Fuel Specific Heat Obtained by Regionwise Interpolation of Metallic Fuels Handbook Data

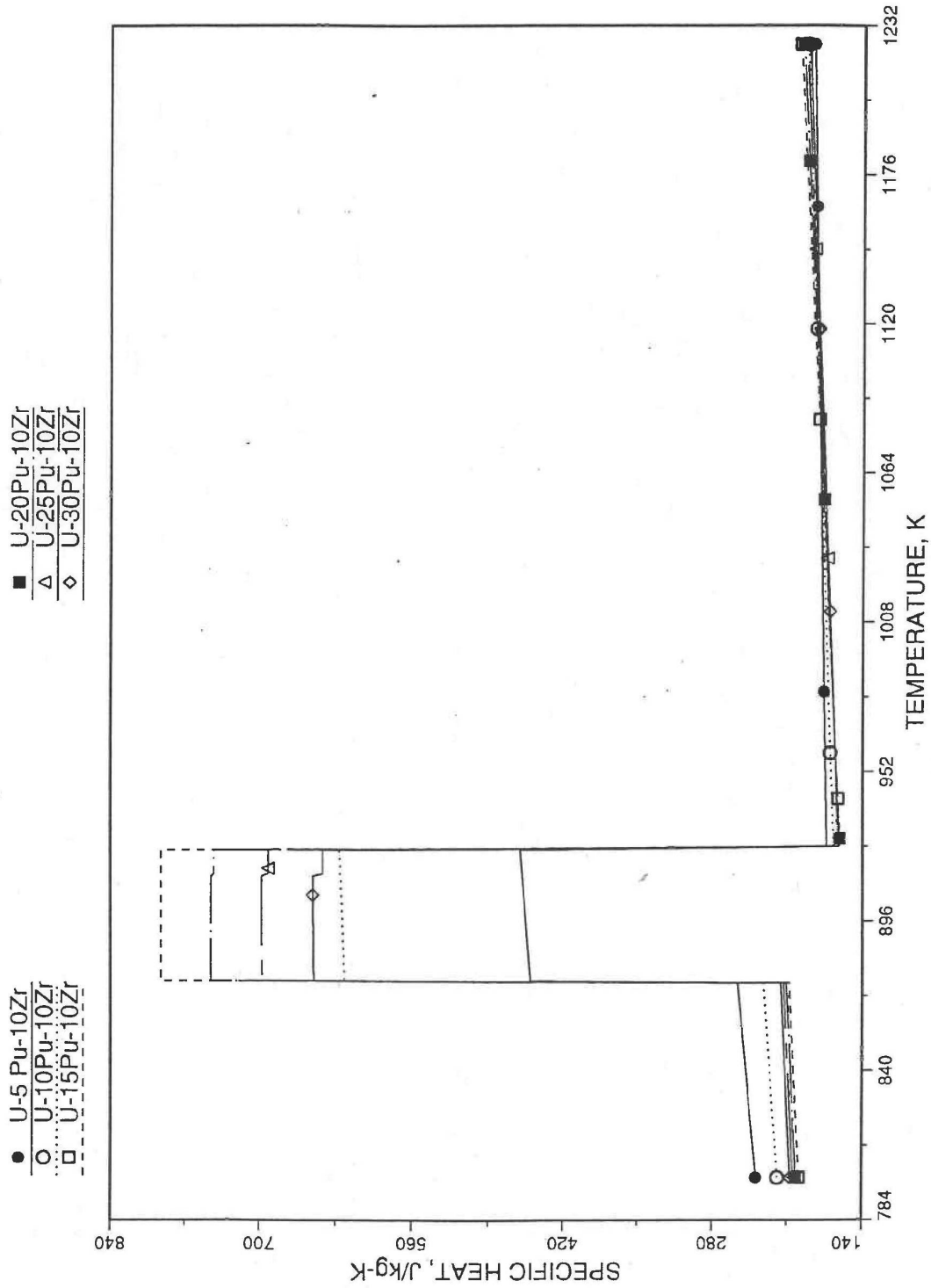

Fig. 10.3-25. Detailed Variation of U-Pu-10Zr Fuel Specific Heat Obtained by Regionwise Interpolation of Metallic Fuels Handbook Data

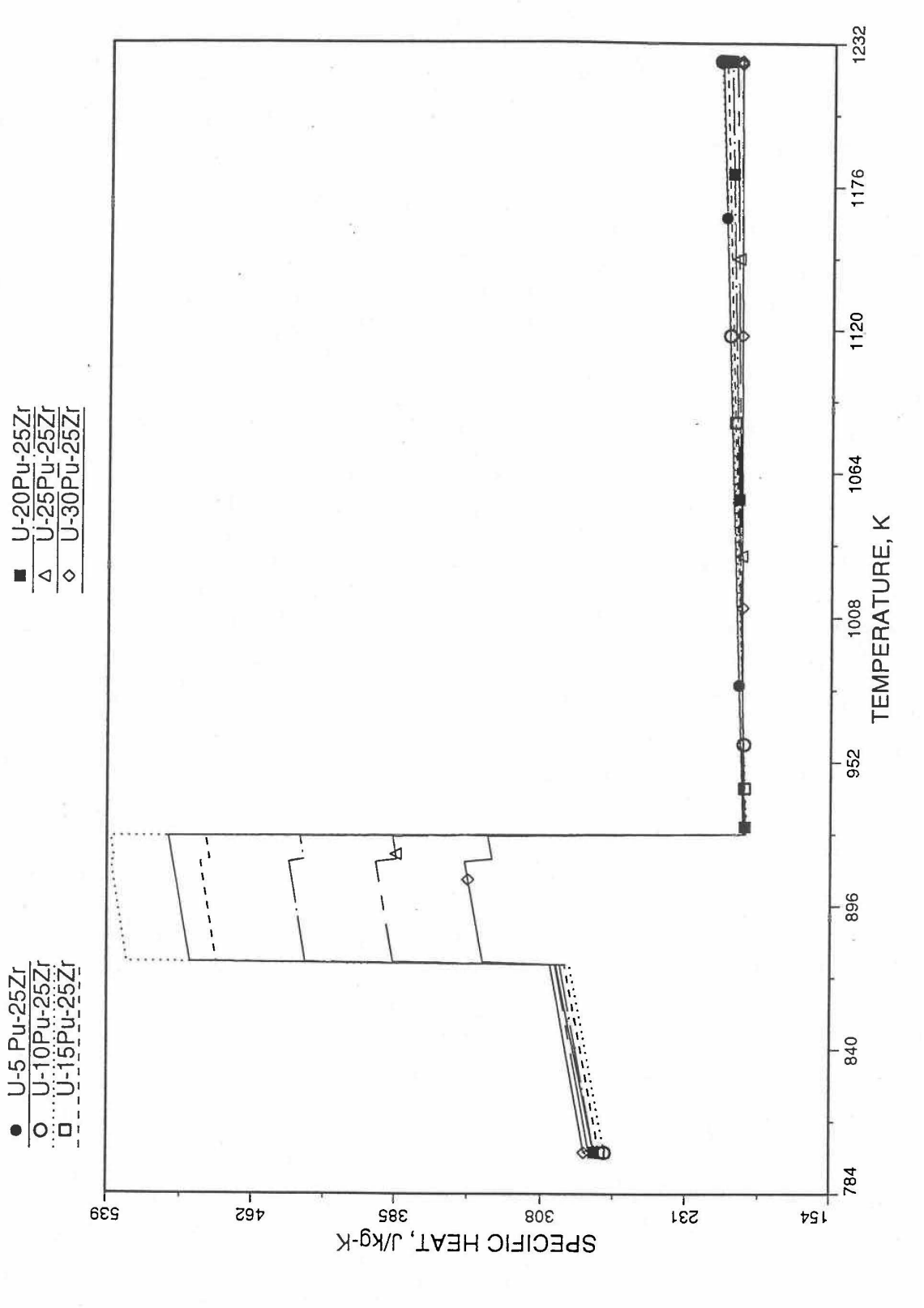

Fig. 10.3-26. Detailed Variation of U-Pu-25Zr Fuel Specific Heat Obtained by Regionwise Interpolation of Metallic Fuels Handbook Data

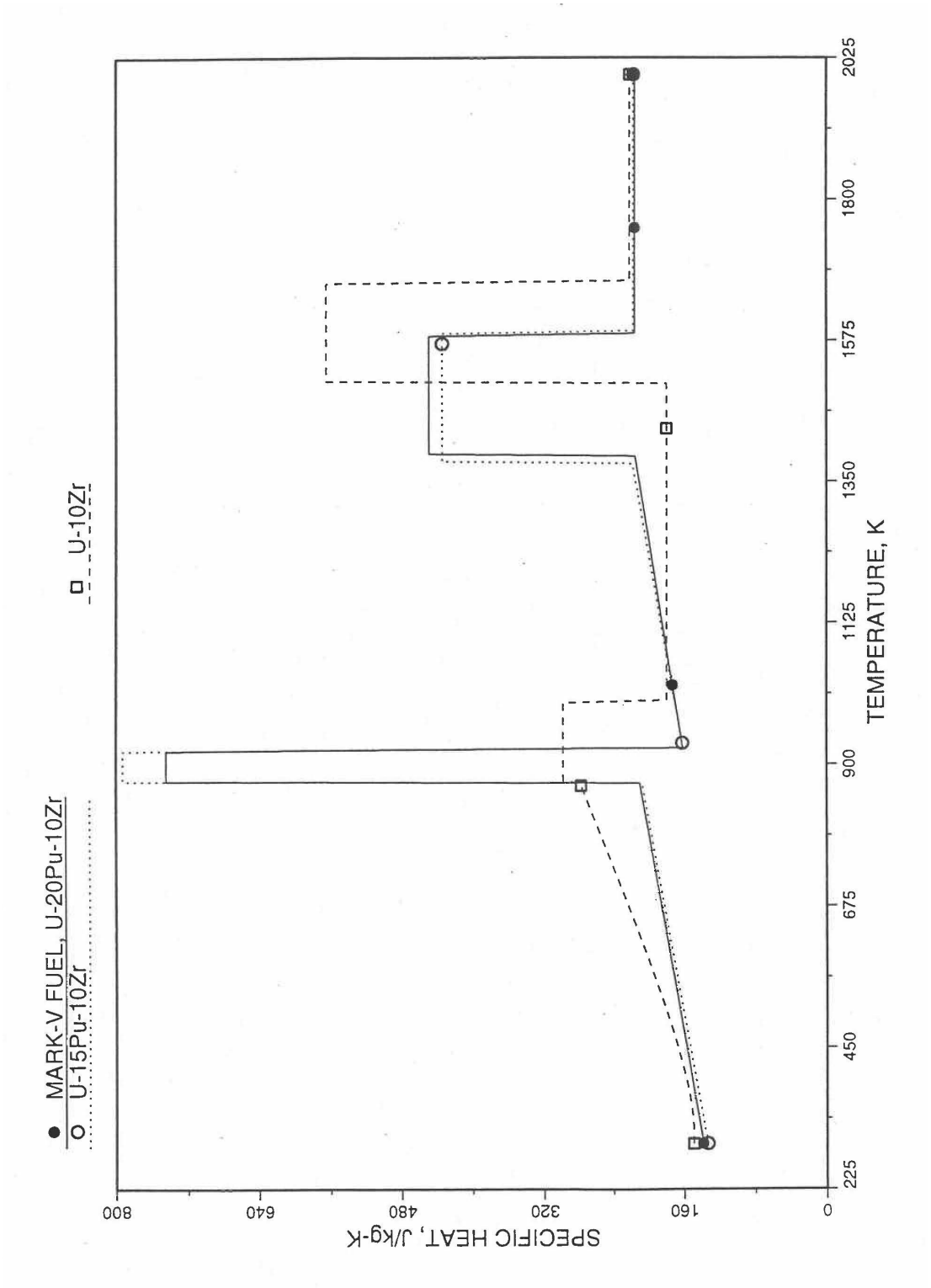

Fig. 10.3-27. Specific Heat of Mark-V (U-20Pu-10Zr) Fuel Obtained by Regionwise Interpolation of Metallic Fuels Handbook Data

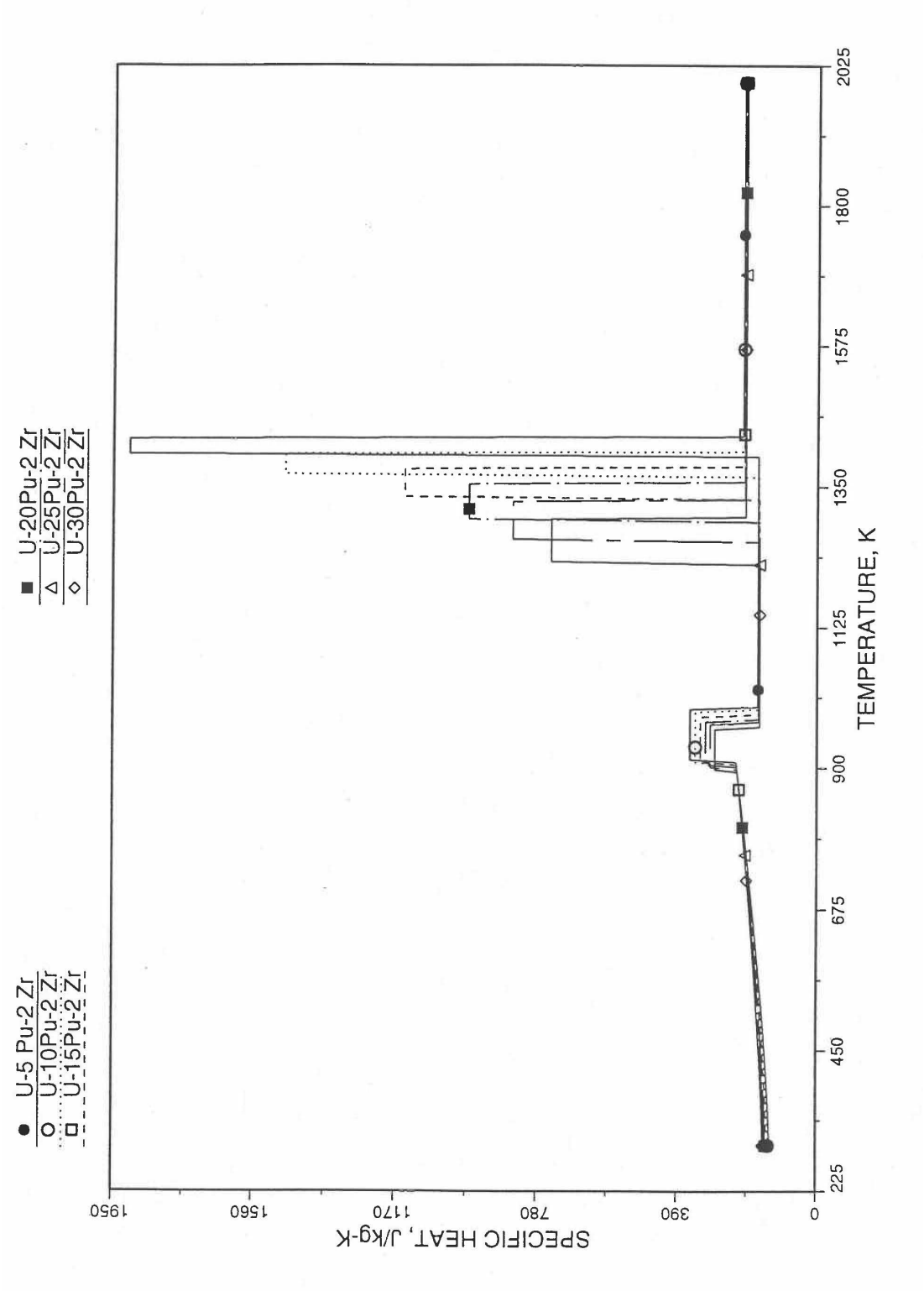

Fig. 10.3-28. Specific Heat of U-Pu-2Zr Alloy Fuel Obtained By Regionwise Interpolation of Metallic Fuels Handbook Data

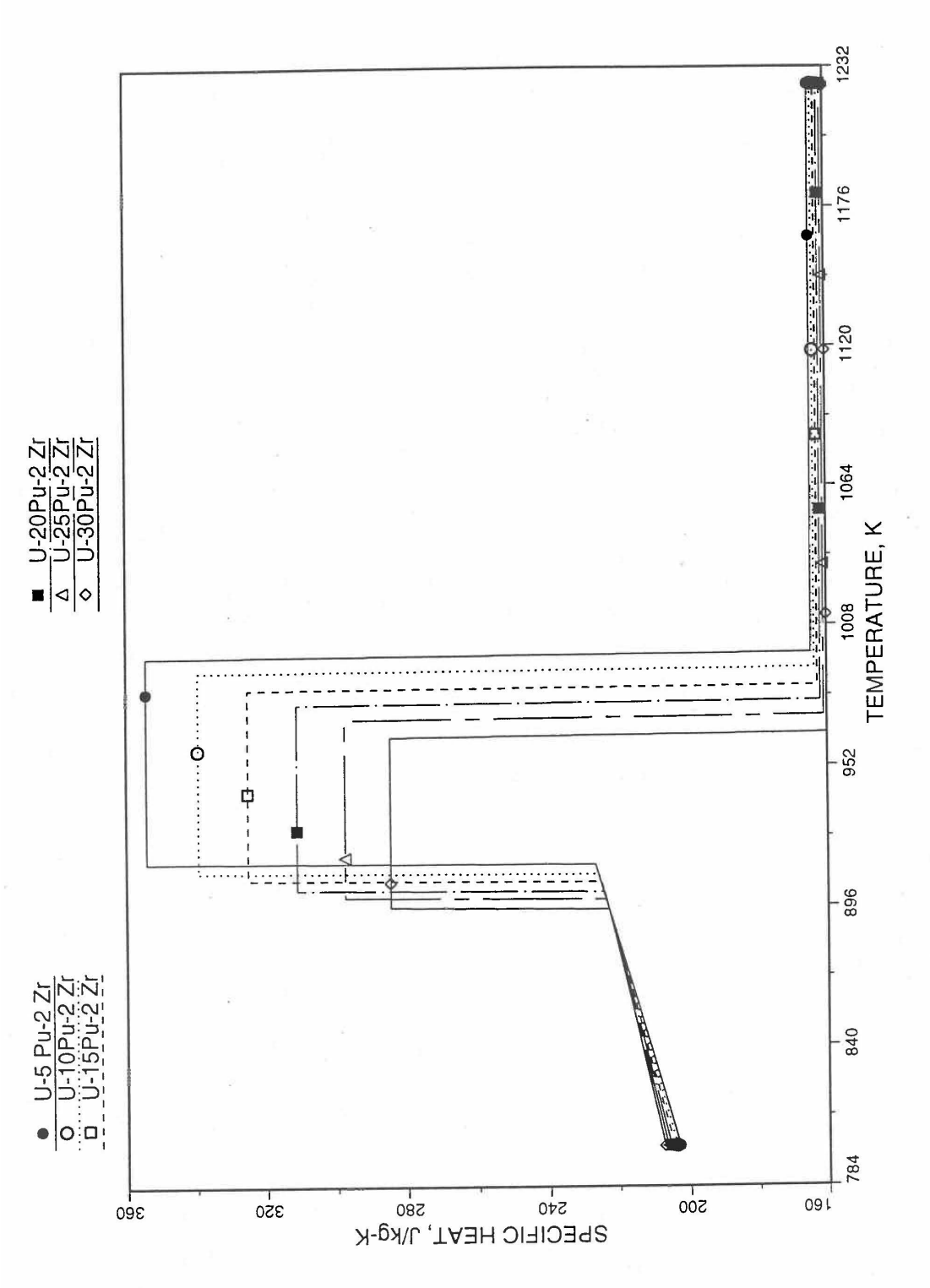

Fig. 10.3-29. Specific Heat of U-Pu-2Zr Alloy Fuel Obtained by Regionwise Interpolation of Metallic Fuels Handbook Data (Enlarged)

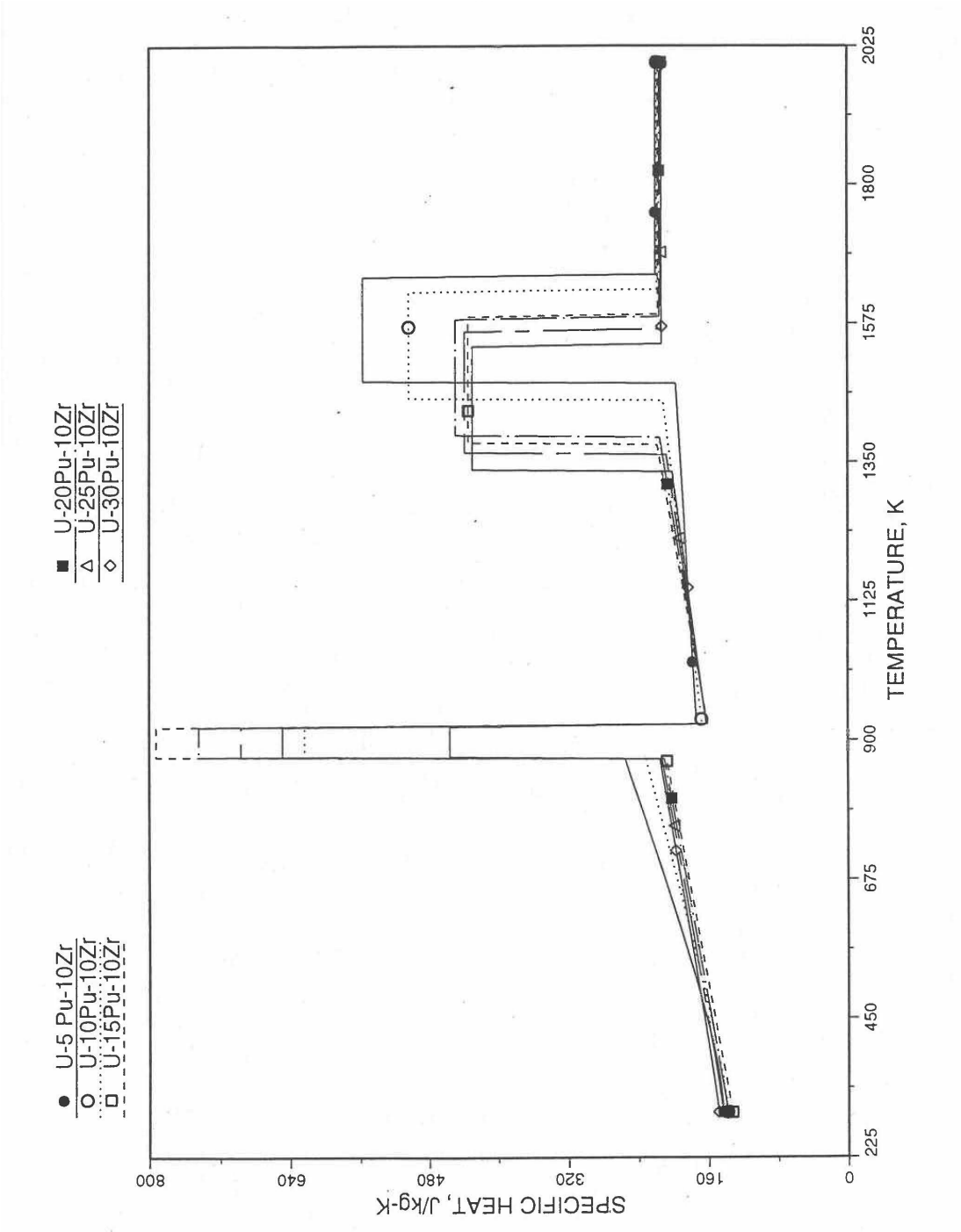

Fig. 10.3-30. Specific Heat of U-Pu-10Zr Alloy Fuel Obtained by Regionwise Interpolation of Metallic Fuels Handbook Data

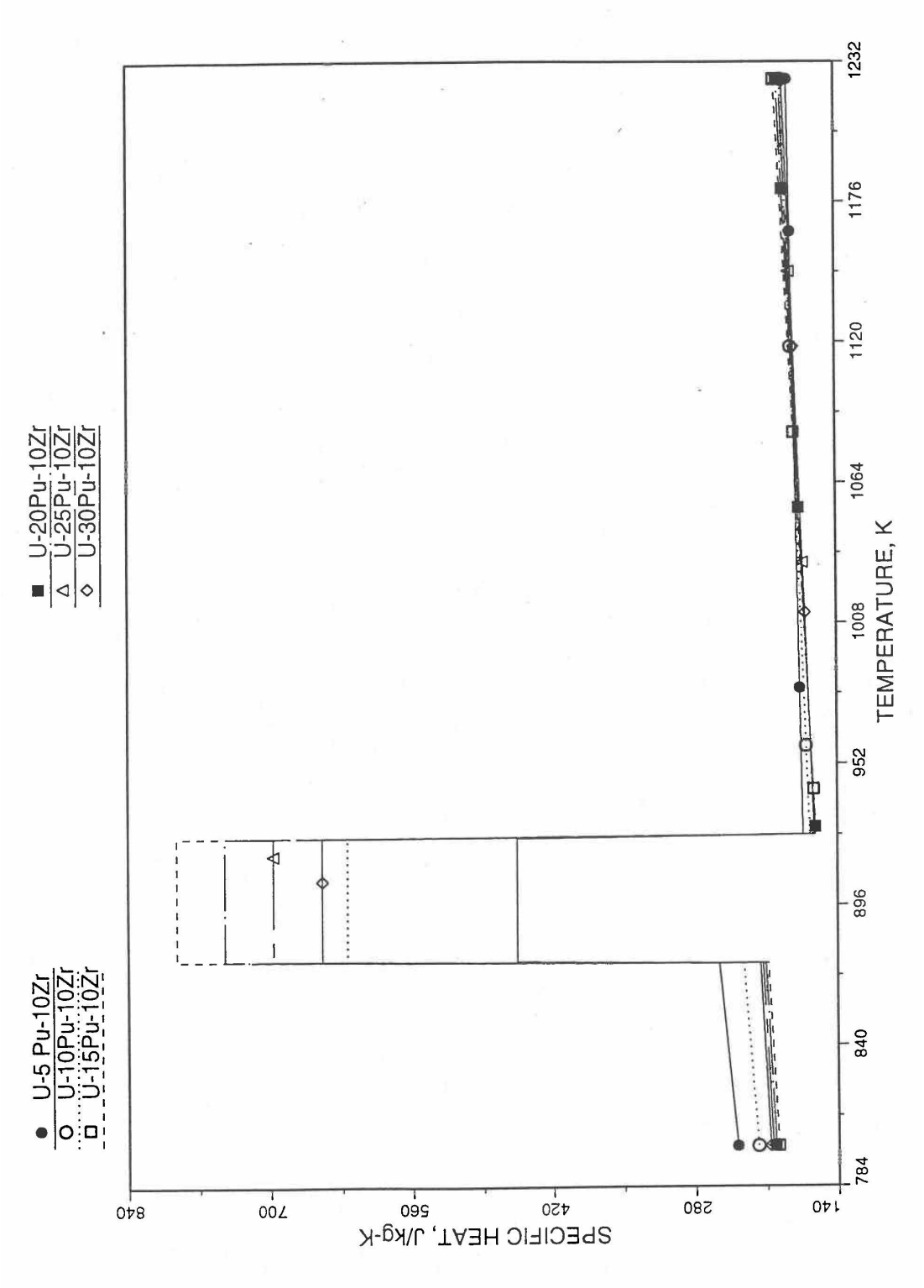

Fig. 10.3-31. Specific Heat of U-Pu-10Zr Alloy Fuel Obtained by Regionwise Interpolation of Metallic Fuels Handbook Data (Enlarged).

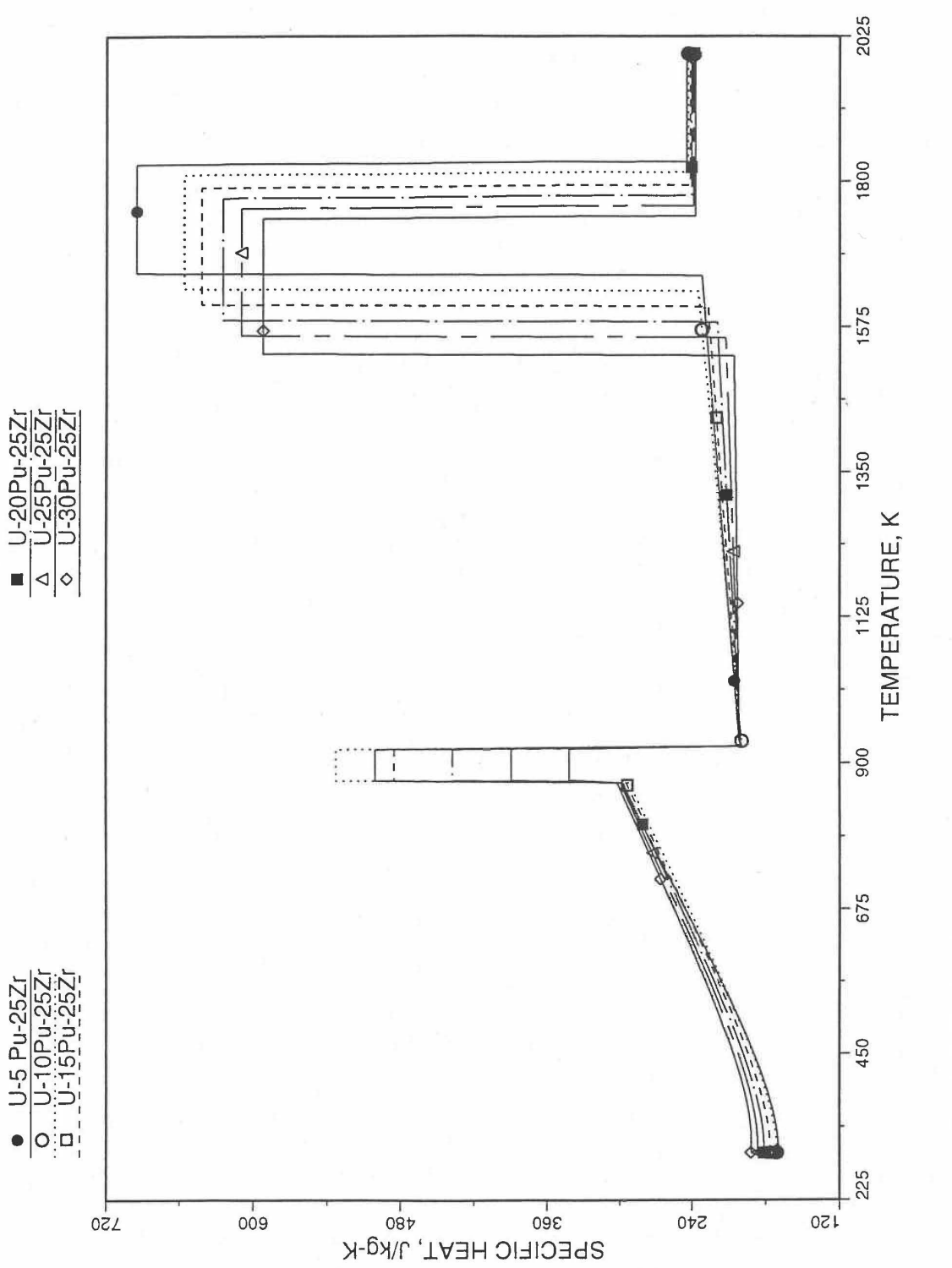

Fig. 10.3-32. Specific Heat of U-Pu-25Zr Alloy Fuel Obtained by Regionwise Interpolation of Metallic Fuels Handbook Data

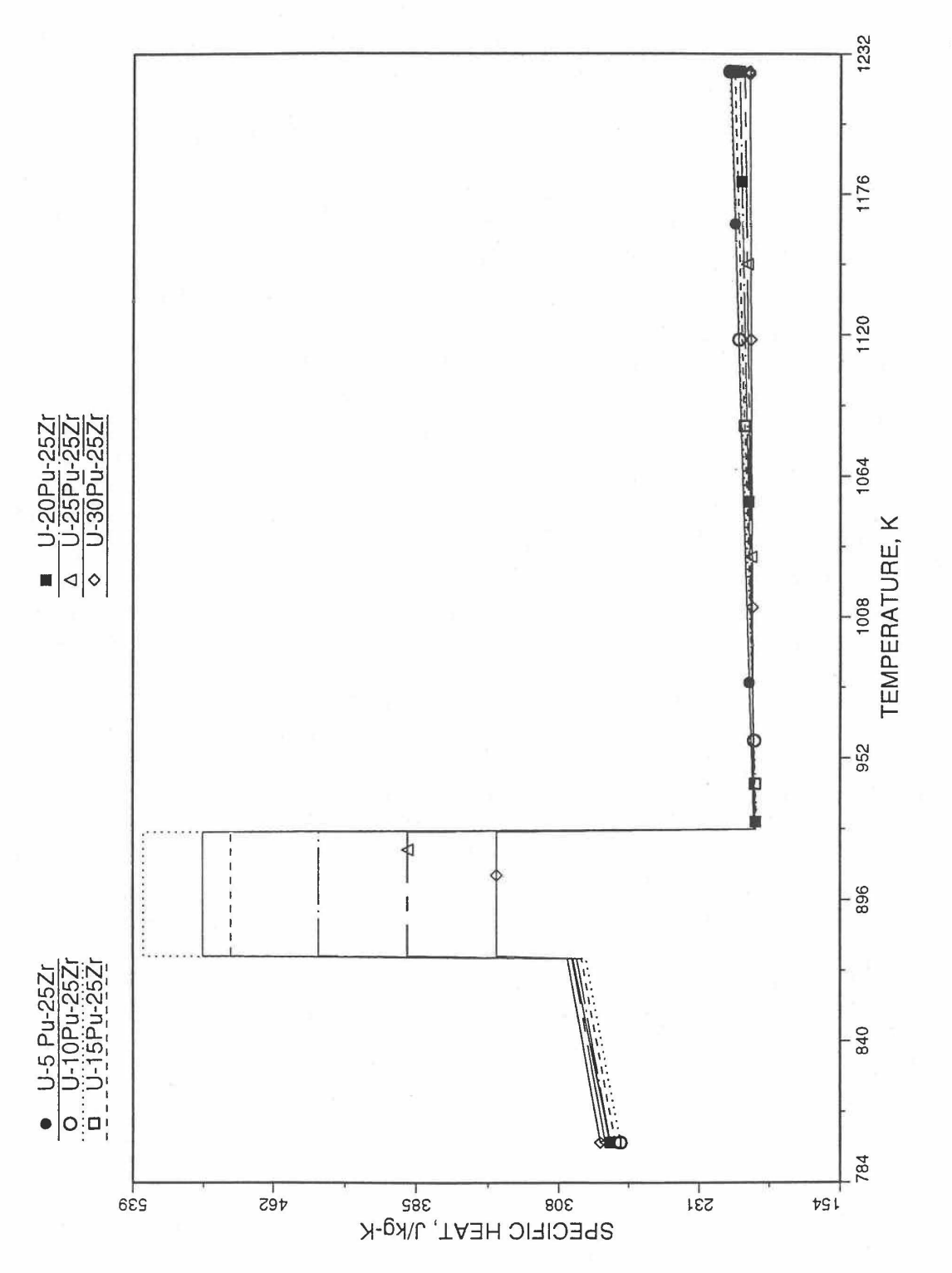

Fig. 10.3-33. Specific Heat of U-Pu-25Zr Alloy Fuel Obtained by Regionwise Interpolation of Metallic Fuels Handbook Data (Enlarged)

10.3.2.3 Theoretical Density of U-Pu-Zr Fuel

10.3.2.3.1 Introduction

The IFR Metallic Fuels Handbook presents density and thermal expansion data for the 3 constituents and certain specific alloys only, and does not present correlations with their coefficients and transition temperatures as functions of composition.

Earlier, before the preparation of the Metallic Fuels Handbook [109], a method was developed to estimate the composition- and temperature-dependent theoretical density of solid U-Pu-Zr alloy fuel [10-4]. In this method, the theoretical density was first evaluated at a fixed temperature of 298K from the theoretical densities of the 3 constituents, i.e., U, Pu and Zr metals, by assuming that there is no volume change due to alloying of the constituents. This U-Pu-Zr theoretical density was adjusted for thermal expansion from 298K to the desired temperature, assuming thermal expansion to be independent of alloy composition and using the U-15Pu-10ZR alloy thermal expansion data for all alloy compositions. A drawback of this method [10-4] of estimating U-Pu-Zr theoretical density is that the dependence of thermal expansion on alloy composition is left unaccounted. Another drawback is that the data for the theoretical densities of the constituent metals and the thermal expansion of U-15Pu-10Zr were obtained from sources [10-14, 10-15] other than the Metallic Fuels Handbook.

A similar method is used in the FPIN2 code [10-11] to estimate the composition- and temperature-dependent theoretical density of U-Pu-Zr alloy fuel. The theoretical density is first evaluated at a fixed temperature of 293K from the theoretical density data in the Handbook of the 3 constituent metals, by assuming that there is no volume change due to alloying of the constituents. The U-Pu-Zr density is then adjusted for temperature difference, using a composition-independent thermal expansion data. This data is obtained simply by averaging the thermal expansion data of U-5Fs, U-10Zr and U-15Pu-10Zr. The dependence of thermal expansion on alloy composition is here also left unaccounted.

Recently, new experimental thermal expansion data for U-19Pu-10Zr and U-26Pu-10Zr alloys have been reported in the IFR Handbook [10-8]. Prompted b this new data, the method of estimating U-Pu-Zr alloy enthalpy by regionwise interpolation has been extended to estimate linear thermal expansion of U-Pu-Zr alloy fuels as a function of composition. A subroutine THEXP1 based on this method to calculate the composition-dependent thermal expansion has been developed and incorporated into the SAS4a/SASSYS-1 codes. The subroutine makes use of the thermal expansion data of all the 8 alloys/components reported in the Handbook [10-8]. The 8 basic alloy compositions are used to divide the ternary composition triangle into 9 regions of interpolation as described in Section 10.3.2.4. The method is flexible enough to make use of the thermal expansion data of additional alloys (as they become available) to divide the composition triangle into a larger number of smaller regions, thus improving its accuracy. The U-Pu-Zr theoretical density is now adjusted for temperature difference using composition-dependent thermal expansion calculated for the desired alloy instead of using an arbitrarily assumed composition-independent thermal expansion data. Also, an approximate technique to correct the theoretical density for

the presence of fission products, which remains valid even if annular composition zones have been formed due to radial redistribution of alloy constituents, has been developed and incorporated into the SAS4A/SASSYS-1 codes. This technique is applied by a code user option.

10.3.2.3.2 Theoretical Density of U-Pu-Zr Fuel at 293K

The theoretical density of U-Pu-Zr fuel at a fixed temperature of 293K is calculated form the theoretical densities of U, Pu and Zr by assuming that there is no volume change due to alloying of the constituents. This assumption has been referred to as the ideal-solution approximation, and recommended in the IFR Handbook. The recommended theoretical densities of U, Pu and Zr at 293K are 19070, 19750 and 6570 kg/m^3. The volume of one kilogram of U-Pu-Zr alloy can be found by summing the volumes of its constituents, and the reciprocal of this volume equals theoretical density.

$$\rho_{th}\left(0, 293K, W_p, W_z\right) = 1.\left(\frac{W_u}{19070} + \frac{W_p}{19750} + \frac{W_z}{6570}\right) \qquad (10.3\text{-}32)$$

where

$\rho_{th}(Bu,T,W_p,W_z)$ = theoretical density of U-Pu-Zr alloy at temperature T°K after a burnup of Bu atom percent, kg/m^3,

W_u, W_p, W_z = weight fractions of U, Pu and Zr in the alloy.

Table 10.3-2 shows a comparison of all the measured densities reported in the IFR Handbook with the theoretical densities calculated using Eq. (10.3-32). The comparison gives a maximum error of 2.45% with an average error of 1.1%. The comparison is satisfactory for these alloy compositions. The small differences may be due to measurement error, small voids left during the alloy preparation or some volume change taking place during alloying. Equation (10.3-32) does not account for the effect of isotopic compositions of U and Pu on theoretical density, and some of the difference between the measured and calculated densities may be caused by this effect.

10.3.2.3.3 Correction for the Presence of Fission Products

Equation (10.3-32) gives the theoretical density of unirradiated U-Pu-Zr fuel at a fixed temperature of 293K. This section presents the effect of the presence of fission products, and the next section presents the effect of temperature on U-Pu-Zr fuel theoretical density. The effect of burnup on U-Pu-Zr fuel density was studied earlier [10-16], and the following equation for the theoretical density of irradiated fuel at a fixed temperature of 293K was obtained in terms of fabricated fuel composition and burnup.

Table 10.3-2. Comparison of Measured and Calculated Theoretical Densities of U-Pu-Zr Alloys at 293K

		Density, kg/m^3		
No.	Alloy	Handbook	Calculated Using Eq. 10.3-32	% Error
1	U	19070	19070	0.0
2	U-10Zr	16020	16022	0.01
3	U-20Zr	13810	13814	0.03
4	Zr	6570	6570	0.0
5	U-15Pu-10Zr	15800	16092	1.85
6	U-19Pu-10Zr	--	16110	--
7	U-26Pu-10Zr	--	16143	--
8	Pu	19750	19750	0.0
9	U-20Pu-10Zr	15730	16115	2.45
10	U-11.1Pu-6.3Zr	16800	17087	1.71
11	U-18.5Pu-14.1Zr	14800	15112	2.11
12	U-15Pu-6.8Zr	16600	16963	2.19
13	U-15Pu-13.5Zr	15000	15235	1.57

$$\rho_{th}\left(Bu, 293K, W_p', W_z'\right) = \frac{\rho_{th}\left(0, 293K, W_{po}, W_{zo}\right)\left[1 - 9.026\times10^{-6}\, Bu\left(W_{uo}+W_{po}\right)\right]}{1+1.190\times10^{-6}\,\rho_{th}\left(0, 293K, W_{po}, W_{zo}\right) Bu\left(W_{uo}+W_{po}\right)} \qquad (10.3\text{-}33)$$

where

W_{uo}, W_{po}, W_{zo} = fabricated weight fractions of U, Pu and Zr in the unirradiated U-Pu-Zr alloy,

W_u', W_p', W_z' = weight fractions of U, Pu and Zr in the irradiated alloy after a burnup of Bu atom percent, without any radial migration of alloy constituents.

This change in alloy composition is only due to fission and breeding. The value of the fabricated alloy theoretical density required for the evaluation of the right hand side of

Eq. (10.3-33) can be obtained from Eq. (10.3-32), using the fabricated weight fractions in place of the present weight fractions of the alloy.

In this section we want to express the irradiated fuel theoretical density in terms of zonal fuel composition (resulting from fission, breeding and also migration of constituents) and burnup. For this purpose, we need to know the amount of fission products the present fuel contains. During irradiation, uranium migrates to the middle radial composition zone while plutonium, zirconium and fission products migrate out of the middle radial composition zone. Thus the fuel constituents and their generated fission products do not remain together. This makes it difficult to calculate the amount of fission products mixed in a given zonal fuel composition. Lacking a modeling and calculation of the radial migration of fission products in a fuel pin, it is assumed that the fission products are uniformly distributed over the pin cross section, on a per unit U-Pu-Zr alloy post-irradiation mass basis. The total amount of fission products is obtained from the radially averaged atom percent burnup and the fabricated pin composition. Due to radial migration of heavy metal constituents, it is difficult to define a radial variation of atom percent burnup. The fabricated composition and not the irradiated (zonal0 composition is the basis of atom percent burnup reported in literature and, therefore, the fabricated composition should be used in evaluating the total amount of fission products. The number of heavy-metal atoms, N_{ho}, per unit fabricated U-Pu-Zr alloy mass is given by

$$N_{ho} = \frac{W_{uo}\, Na}{a_u} + \frac{W_{po}\, Na}{a_p} \tag{10.3-34}$$

where

a_u, a_p = uranium and plutonium atomic weights,

$Na = 6.02472 \times 10^{26}$ = Avogadro's number, molecules/kg-mole.

The number of fissions, N_{fo}, per unit fabricated mass equals the product of burnup and heavy-metal atoms.

$$N_{fo} = \frac{Na\, Bu}{100}\left(\frac{W_{uo}}{a_u} + \frac{W_{po}}{a_p}\right) \tag{10.3-35}$$

Assuming $a_u \approx a_p$, the mass of heavy-metals fissioned, M_{fo}, per unit fabricated U-Pu-Zr alloy mass is given by

$$M_{fo} = N_{fo}\frac{a_u}{Na} \tag{10.3-36}$$

Substituting Eq. (10.3-35), Eq. (10.3.-36) becomes

$$M_{fo} = 0.01\,Bu\left(W_{uo} + W_{po}\right) \tag{10.3-37}$$

The mass of U-Pu-Zr alloy left after irradiation per unit fabricated mass is given by (1-M_{fo}). Therefore, the average number of fissions, N_f, per unit U-Pu-Zr alloy post-irradiation mass is obtained by dividing Eq. (10.3-35) by (1-M_{fo}).

$$N_f = \frac{0.01\,Bu\,Na\left(W_{uo} + W_{po}\right)/a_u}{1 - 0.01\,Bu\left(W_{uo} + W_{po}\right)} \tag{10.3-38}$$

Equation (10.3-38) determines the assumed uniform distribution of fission products over the pin cross section, on a per unit U-Pu-Zr alloy post-irradiation mass basis. As discussed above, the amount of fission products determined by Eq. (10.3-38) is used to correct U-Pu-Zr alloy theoretical density for the presence of fission products as follows.

Considering the mass-plus-energy conservation of a nuclear power reactor with negligible neutron leakage and capture in coolant and structure, all neutrons emitted by fuel are absorbed in the fuel itself. Therefore, the mass of fission products equals the mass of heavy-metals fissioned minus the mass-equivalent of fission energy released. The mass of fission products, M_f, per unit U-Pu-Zr alloy post-irradiation mass is given by

$$M_f = \frac{N_f\,a_u}{Na} - \frac{200\,m_a}{931}N_f \tag{10.3-39}$$

where

m_a = 1 atomic mass unit = 1.659828×10^{-27} kilogram,

200 = energy released per fission in MeV units,

931 = energy-equivalent (in MeV units) of 1 atomic mass unit.

Following Ref. [10-16], the volume of fission products, V_f, per unit U-Pu-Zr alloy post-irradiation mass is given by

$$V_f = N_f\,v_{sfp} \tag{10.3-40}$$

where

v_{sfp} = characteristic volume of the solid fission products per fission = 6.772565×10^{-29} m^3.

This value of v_{sfp} has been found from pure uranium swelling data to be 4.70×10^{-29} m^3/fission over and above the characteristic volume of uranium atom [10-16]. Using Eqs. (10.3-39) and (10.3-40), the theoretical density of irradiated fuel at a fixed

temperature of 293K, after correction for the presence of fission products, is obtained as

$$\rho_{th}\left(Bu,293K,W_p,W_z\right)=\frac{1+N_f\,a_u/Na-200\,m_a\,N_f/931}{\left(\frac{W_u}{19070}+\frac{W_p}{19750}+\frac{W_z}{6570}\right)+N_f\,v_{sfp}} \tag{10.3-41}$$

where

W_u, W_p, W_z = weight fractions of U, Pu and Zr in the irradiated U-Pu-Zr alloy.

Using a value of 238 for a_u, and noting that m_a is the reciprocal of Na, Eq. (10.3-41) becomes

$$\rho_{th}\left(Bu,293K,W_p,W_z\right)=\frac{1+0.009991\,f_o}{\left(\frac{W_u}{19070}+\frac{W_p}{19750}+\frac{W_z}{6570}\right)+1.7144\times10^{-6}\,f_o} \tag{10.3-42}$$

where

$$f_o=\frac{Bu\left(W_{uo}+W_{po}\right)}{1-0.01Bu\left(W_{uo}+W_{po}\right)} \tag{10.3-43}$$

The quantity f_o is the heavy-metal mass fissioned expressed as a percentage of U-Pu-Zr alloy post-irradiation mass. This approximate technique to correct the theoretical density for the presence of fission products, which remains valid even after annular zone formation (W_u, W_p, W_z are then zonal weight fractions) due to radial migration of alloy constituents, is incorporated into the SAS4A/SASSYS-1 codes and is applied by a code user option.

10.3.2.3.4 Theoretical Density of Irradiated U-Pu-Zr Fuel

Equations (10.3-42) and (10.3-43) give the theoretical density of irradiated U-Pu-Zr fuel at a fixed temperature of 293K. In the next section, a method of interpolating the linear thermal expansion from 293K to any desired temperature T as a function of fuel composition is described. Using this thermal expansion, the following equation can be written for the theoretical density of irradiated U-Pu-Zr fuel at any desired temperature T:

$$\rho_{th}\left(Bu,T,W_p,W_z\right)=\frac{\left(1+0.009991\,f_o\right)\left[1+\Delta L\left(T,W_p,W_z\right)/Lo\right]^{-3}}{\left(\frac{W_u}{19070}+\frac{W_p}{19750}+\frac{W_z}{6570}\right)+1.7144\times10^{-6}\,f_o} \tag{10.3-44}$$

where

$\Delta L(T,\ W_p,\ W_z)/L_o$ = linear thermal expansion from 293K to temperature T, expressed as a fraction of length L_o at the temperature 293K, for a U-Pu-Zr alloy with U, Pu, and Zr weight fractions equal to W_u, W_p and W_z.

Figure 10.3-34 shows the flow diagram of a subroutine RHOFM for calculating the theoretical density, based on this method, of irradiated U-Pu-Zr alloy fuel as a function of composition and temperature. For improving the computational speed of the SAS4A/SASSYS-1 codes, the theoretical density without fission products at 293K of each U-Pu-Zr fuel type (that uses the regionwise interpolation thermal properties, i.e., input option IFUELM = 0) is precalculated in subroutine PRECAL before steady state calculation, and used later in the steady state and transient calculation of the codes.

Figures (10.3-35) to (10.3-38) show the variation of theoretical density (without fission products) with temperature for 28 alloy compositions, calculated using Eq. (10.3-44). The thermal expansion required on the right hand side of Eq. (10.3-44) was obtained using the subroutine THEXP1 described below. The Pu and Zr contents each vary from zero to 30 at % in the alloy compositions plotted in these figures.

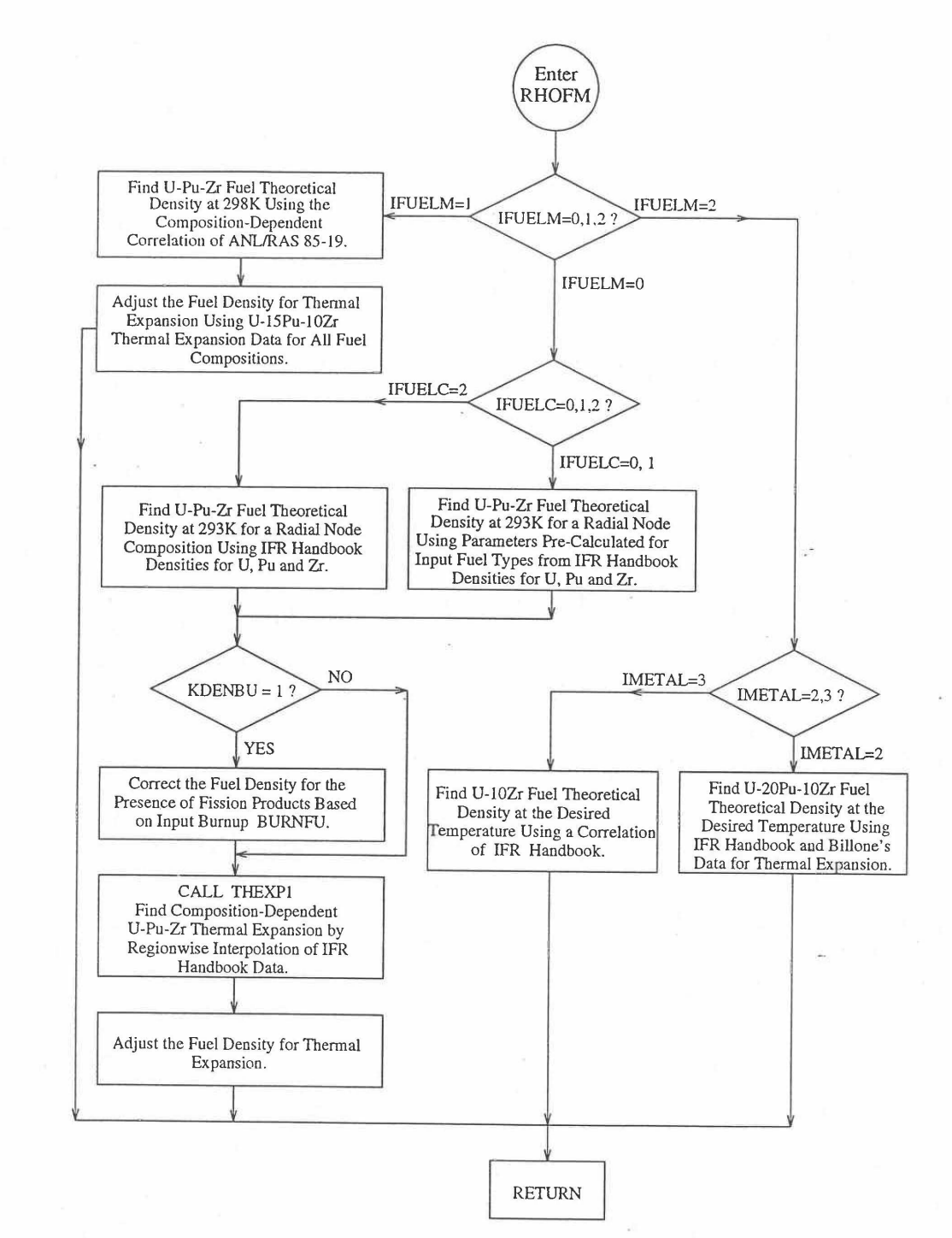

Fig. 10.3-34. Flow Diagram of subroutine PHOFM for U-Pu-Zr Fuel Theoretical Density

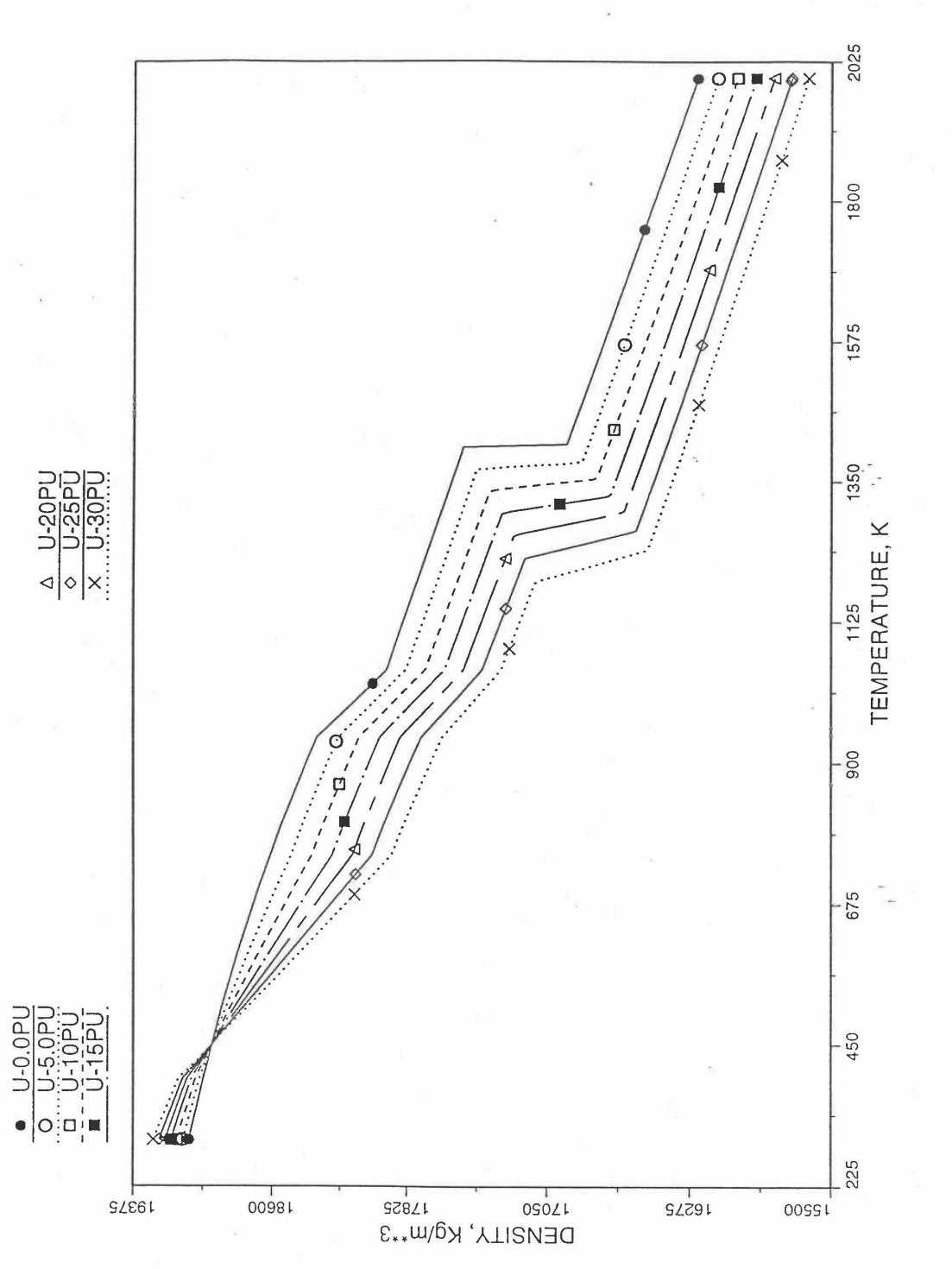

Fig.. 10.3-35. Theoretical Density of U-Pu Fuel Without Fission Products, Obtained from Regionwise Interpolation

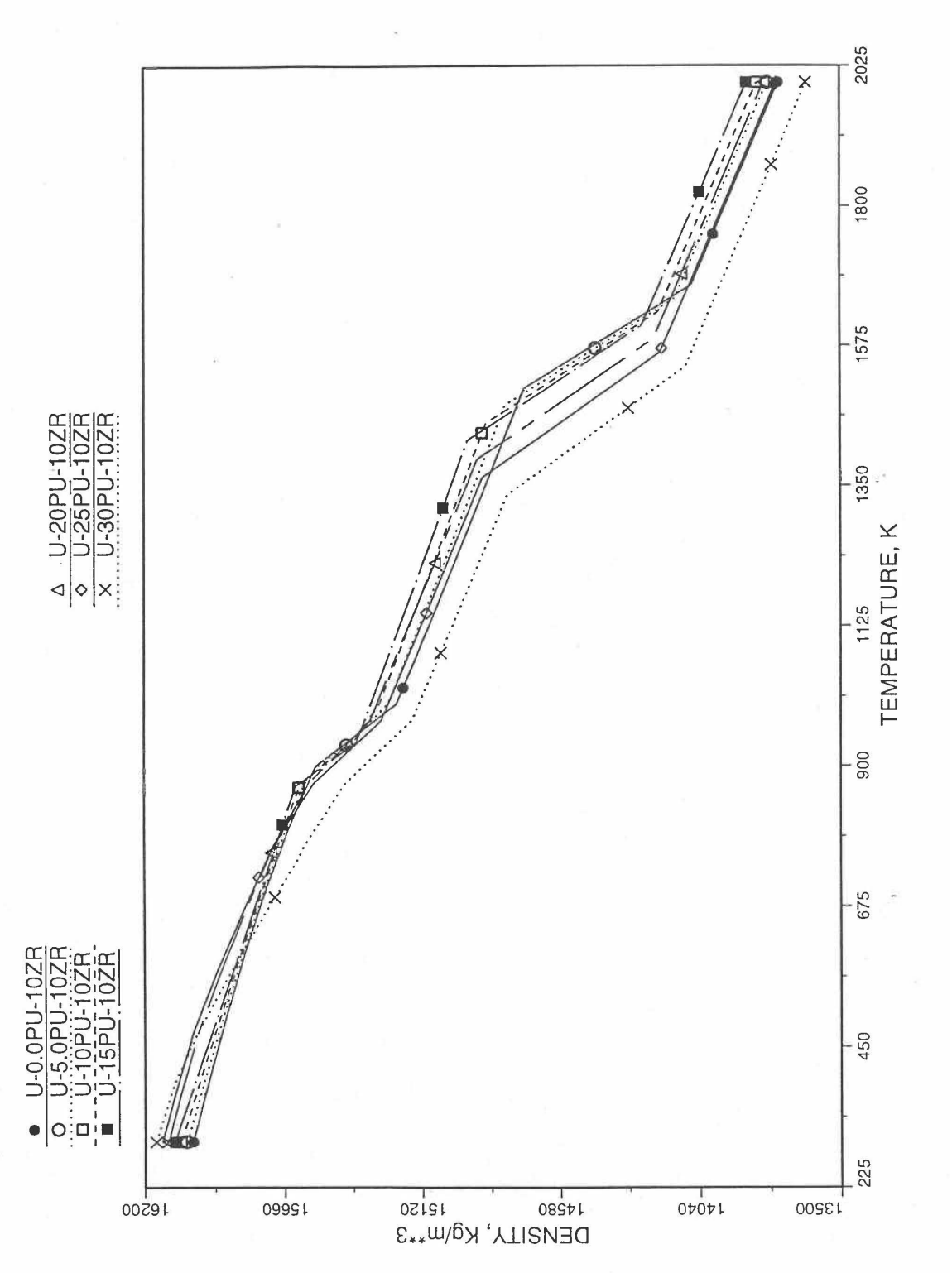

Fig. 10.3-36. Theoretical Density of U-Pu-10Zr Fuel Without Fission Products, Obtained From Regionwise Interpolation of IFR Handbook Data

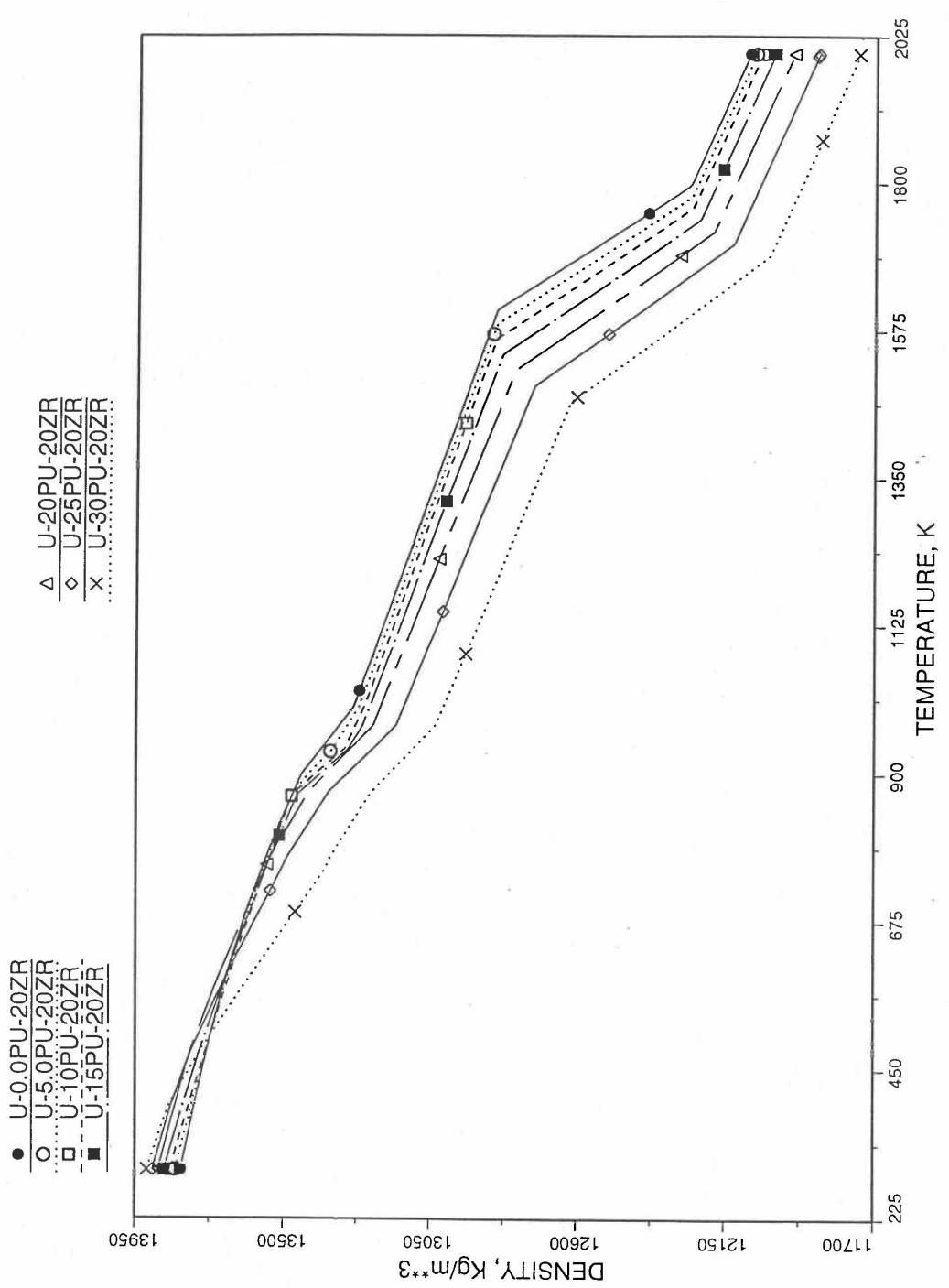

Fig. 10.3-37. Theoretical Density of U-Pu-20Zr Fuel Without Fission Products, Obtained from Regionwise Interpolation of IFR Handbook Data

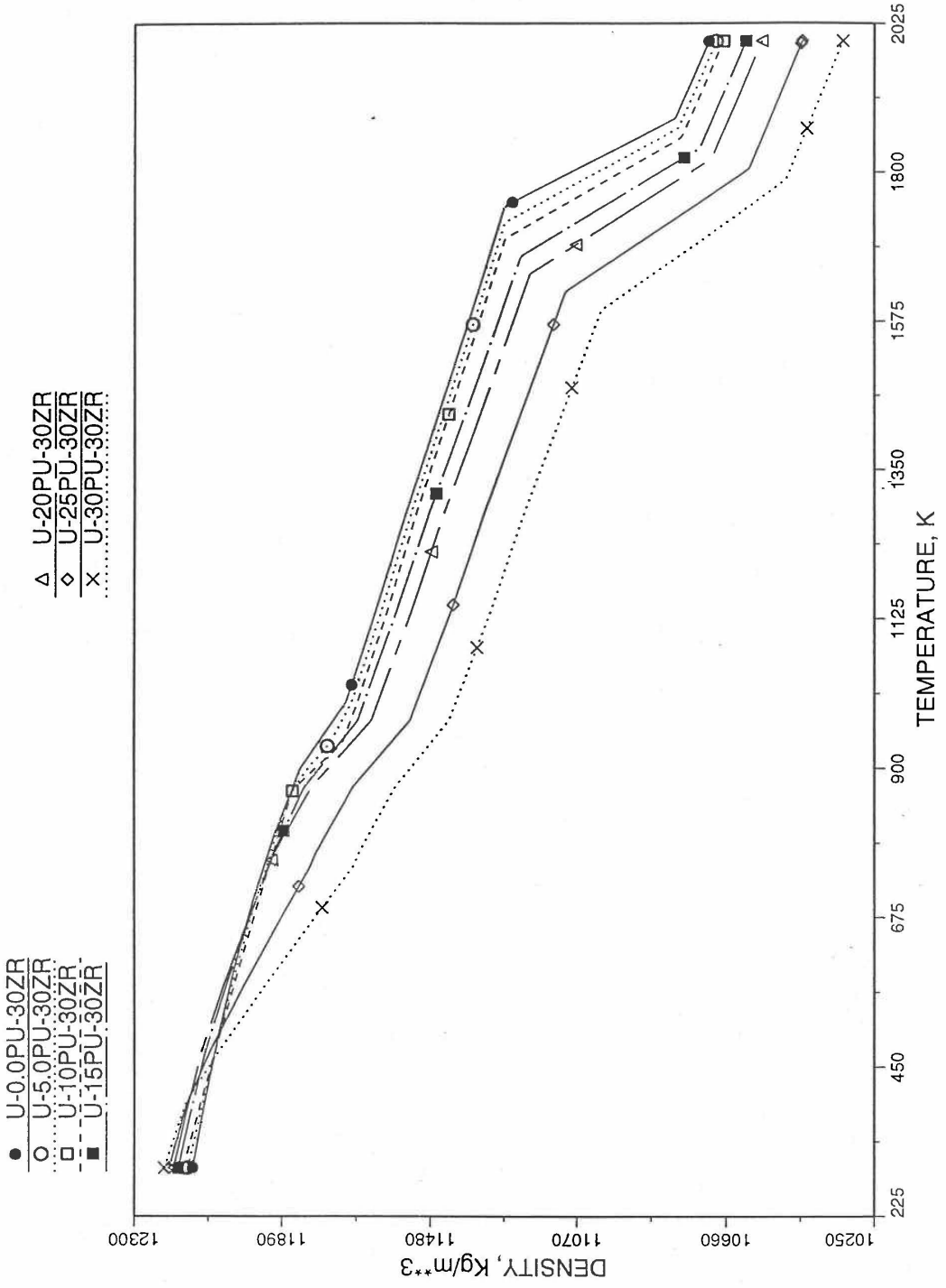

Fig. 10.3-38. Theoretical Density of U-Pu-30Zr Fuel Without Fission Products, Obtained from Regionwise interpolation of IFR Handbook Data

10.3.2.4 Thermal Expansion of U-Pu-Zr Fuel

In this section, a method of interpolating the linear thermal expansion of U-Pu-Zr fuel form 293K to any desired temperature T as a function of fuel composition is described. Only the U, Pu and Zr weight fractions are considered and the effect of fission products on thermal expansion is ignored. This thermal expansion is used in the evaluation of theoretical density of irradiated U-Pu-Zr fuel at any desired temperature, as explained in Section 10.3.2.3.

10.3.2.4.1 Description of the Method

Figure 10.3-39 shows the U-Pu-Zr ternary composition triangle marked with the points representing all the 8 alloys/components for which thermal expansion data re reported in the IFR Handbook [10-8]. The composition points of these 8 database alloys/components are used to divide the whole ternary composition triangle into 9 triangular regions of interpolation. For evaluating the linear thermal expansion of a desired solid U-Pu-Zr alloy represented by a point located in any region of interpolation, the method consists of mixing the 3 database alloys represented by the corners of the region of interpolation. The proportions or weight fractions of the 3 database alloys in mixing are so calculated in the method that the resulting mixture has the composition of the desired alloy. The calculated mixing fractions are then used as weight factors in making a linear combination of (or liner interpolation between) thermal expansions of the 3 database alloys corresponding to the desired temperature, and the value of the linear combination is the interpolated thermal expansion of the desired alloy. It should be noted that the calculated mixing fractions are never negative and the linear combination never requires extrapolation because the desired alloy composition point is always inside the triangle with corners at the 3 database alloy points. If the desired alloy composition point were outside this triangle, the linear combination would involve negative mixing fractions and extrapolation which are avoided entirely in the present method.

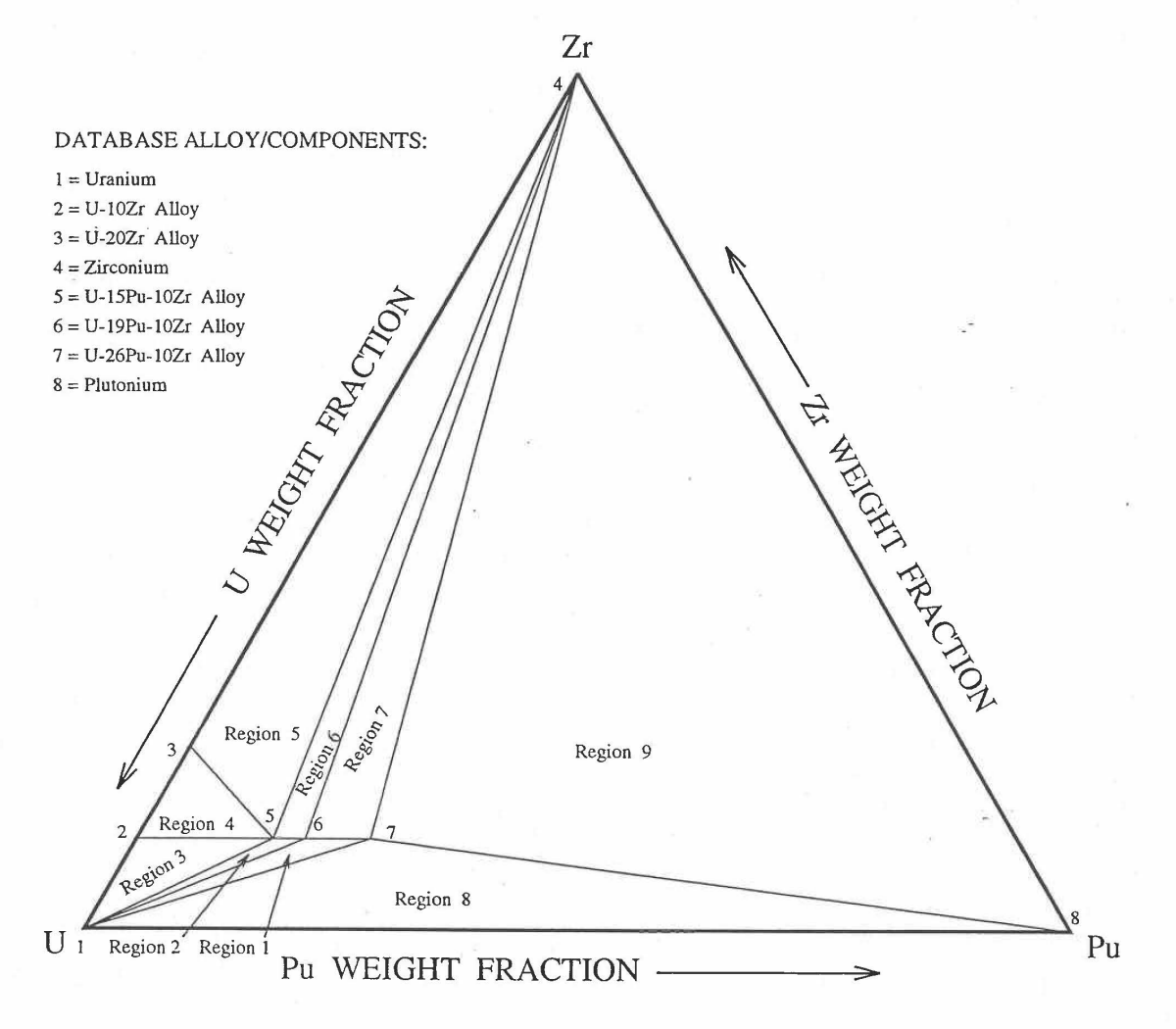

Fig. 10.3-39. Diagram Showing Thermal Expansion Interpolation Regions for Solid U-Pu-Zr Alloy Fuels

10.3.2.4.2 Thermal Expansion Data of Basic Alloys

Table 10.3-3 gives the linear thermal expansion data of the 8 basic solid alloys or components that are used in the present method of evaluating composition-dependent thermal expansion of a U-Pu-Zr alloy. The 8 basic alloys/components are: (1) U metal, (2) U-10Zr, (3) U-20Zr, (4) Zr metal, (5) U-15Pu-10Zr, (6) U-19Pu-10Zr, (7) U-26Pu-10Zr, and (8) Pu metal. The data have all been taken from the Metallic Fuels Handbook [10-8] with the modification that the thermal expansion data of U, Pu and Zr metals between their first and last solid-state transition temperatures are not included in Table 10.3-3, and not used in the present method. The thermal expansion data of U, Pu and Zr metals at their first and last transition temperatures are included in Table 10.3-3, and the thermal expansion is assumed to vary linearly with temperature between the first and last transition temperatures. This is reasonable because the sharp jumps (i.e., discontinuities) in thermal expansion data of U, Pu and Zr metals, over the temperature range of solid-state transitions, are not exhibited by alloys. The value of thermal expansion at 2500K shows in Table 10.3-3, for each database alloy/component has been obtained from the Handbook data for percent thermal expansion and coefficient of thermal expansion at the highest temperature available. A warning message is printed by the SAS4A/SASSYS1 codes if the thermal expansion value at 2500K of any database alloy is ever used in computation. The uranium thermal expansion data at 1500K, 1600K and 2500K (above its melting point) in Table 10.3-3 have been obtained by subtracting the thermal expansion due to melting (i.e., 1.14%) from the data given in the Handbook. This is done because the data in Table 10.3-3 is used in the present method to interpolate the thermal expansion of a desired U-Pu-Zr alloy up to its solidus temperature only. The evaluation of thermal expansion above the solidus temperature is described below in Section D.

10.3.2.4.3 Method of Interpolation

The method of interpolation to evaluate the linear thermal expansion of a U-Pu-Zr fuel composition at and below its solidus temperature consists of first determining the region of the ternary composition triangle (shown in Fig. 10.3-39) in which the desired fuel composition lies, and then finding the weight fractions in which the 3 database alloys of the region are required to be mixed to obtain the desired fuel composition. From the mass balance of U, Pu and Zr, the following equations have been obtained in Section 10.3.2.1 for the mixing fractions, X_i, of the database alloys that are assumed to be numbered 1, 2 and 3:

Table 10.3-3. Linear Thermal Expansion Data of the 8 Basic Solid Alloys or Components Used in the Method of Regionwise Interpolation

	1. Uranium		2. U-10Zr		3. U-20Zr		4. Zirconium		5. U-15Pu-10Zr		6. U-19Pu-10Zr		7. U-26Pu-10Zr		8. Plutonium	
No.	Temp, K	$\Delta L/L_o$, %	Temp, K	$\Delta L/L_o$, %	Temp, K	$\Delta L/L_o$, %	Temp, K	$\Delta L/L_o$, %	Temp, K	$\Delta L/L_o$, %	Temp, K	$\Delta L/L_o$, %	Temp, K	$\Delta L/L_o$, %	Temp, K	$\Delta L/L_o$, %
1	293	0	293	0	293	0	293	0	293	0	293	0	293	0	293	0
2	400	0.157	400	0.142	400	0.107	400	0.06	400	0.18	373	0.103	373	0.108	350	0.279
3	500	0.315	500	0.281	500	0.219	500	0.123	500	0.356	473	0.242	473	0.253	395	0.502
4	600	0.494	600	0.433	600	0.348	600	0.192	600	0.532	573	0.431	573	0.455	753	6.287
5	700	0.697	700	0.603	700	0.5	700	0.265	700	0.708	673	0.638	673	0.683	800	6.459
6	800	0.924	800	0.799	800	0.681	800	0.343	800	0.884	773	0.86	773	0.924	2500	12.68
7	900	1.186	900	1.027	900	0.899	900	0.442	868	1.004	873	1.146	873	1.276		
8	941	1.3	1000	1.725	1000	1.3	1000	0.505	938	1.524	973	1.662	973	1.868		
9	1048	2.05	1100	1.95	1100	1.487	1100	0.586	1000	1.649	1073	1.881	1073	2.095		
10	1100	2.168	1200	2.175	1200	1.674	1137	0.617	1100	1.85	1173	2.104	1173	2.327		
11	1200	2.398	2500	5.1	2500	4.105	1284	0.617	1200	2.051	1273	2.334	1233	2.464		
12	1400	2.855					1400	0.725	1300	2.252	2500	5.113	2500	5.386		
13	1408	2.866					1600	0.922	1378	2.409						
14	1500	3.092					1800	1.138	2500	4.664						
15	1600	3.362					2500	1.803								
16	2500	5.657														

$$X_i = D_i / D,\ i = 1, 2, 3 \tag{10.3-45}$$

$$D = \left(W_{z1} - W_{z2}\right)\left(W_{p3} - W_{p1}\right) - \left(W_{p1} - W_{p2}\right)\left(W_{z3} - W_{z1}\right) \tag{10.3-46}$$

$$D_1 = \left(W_z - W_{z2}\right)\left(W_{p3} - W_p\right) - \left(W_p - W_{p2}\right)\left(W_{z3} - W_z\right) \tag{10.3-47}$$

$$D_2 = \left(W_{z1} - W_z\right)\left(W_{p3} - W_{p1}\right) - \left(W_{p1} - W_p\right)\left(W_{z3} - W_{z1}\right) \tag{10.3-48}$$

$$D_3 = \left(W_{z1} - W_{z2}\right)\left(W_p - W_{p1}\right) - \left(W_{p1} - W_{p2}\right)\left(W_z - W_{z1}\right) \tag{10.3-49}$$

where

W_{ui}, W_{pi}, W_{zi} = weight fractions of U, Pu and Zr in database alloy I of the region in which the desired fuel compositions lies,

W_u, W_p, W_z = weight fractions of U, Pu and Zr in the desired fuel composition.

The sum of X_1, X_2 and X_3 is always 1. In case of interpolation, the values of X_1, X_2 and X_3 are always positive. If any extrapolation were involved, the value of at least one weight fraction would be negative which is entirely avoided in the present method. The linear thermal expansion of the desired U-Pu-Zr fuel composition from 293K to a temperature T at or below its solidus is then evaluated by mass-weighted averaging of the thermal expansions of the 3 database alloys from 293K to the same temperature T.

$$\frac{\Delta L\left(T, W_p, W_z\right)}{L_o} = X_1 \frac{\Delta L_1}{L_o} + X_2 \frac{\Delta L_2}{L_o} + X_3 \frac{\Delta L_3}{L_o} \tag{10.3-50}$$

where

$\frac{\Delta L_i}{L_o}$ = linear thermal expansion from 293K to temperature T of the database alloy i of the region in which the desired fuel composition lines.

10.3.2.4.4 Thermal Expansion During and After Melting

Thermal expansion data during and after melting is available for none of the database alloys except uranium metal. Therefore, the thermal expansion of all alloy compositions above their solidus temperatures is evaluated using the uranium metal data, and a warning message is printed by the SAS4A/SASSYS-1 codes if this is ever required in computation. The linear thermal expansion of uranium during melting at 1408K reported in the Handbook [10-8] is 1.14%, and the coefficient of linear expansion of molten uranium is 25.5 x 10-6/K. In the present method, the post-solidus

uranium thermal expansion is added to Eq. (10.3-50) to obtain the following equation for estimating the linear thermal expansion form 293K to a temperature T above the solidus of the desired alloy:

$$\frac{\Delta L\left(T, W_p, W_z\right)}{L_o} = X_1 \frac{\Delta L\left(T_s, W_p, W_z\right)}{L_o} + X_2 \frac{\Delta L_2\left(T_s, W_p, W_z\right)}{L_o} + X_3 \frac{\Delta L_3\left(T_s, W_p, W_z\right)}{L_o} + 0.0114 \min\left(\frac{T - T_s}{T_\ell - T_s}, 1\right) + 25.5 x 10^{-6}\left(T - T_s\right) \tag{10.3-51}$$

where

T_s, T_ℓ = solidus and liquidus temperatures of the desired alloy.

The fourth term on the right hand side is basically the product of alloy melt fraction and uranium thermal expansion during melting phase change, and the fifth term is an estimate of the molten alloy thermal expansion due to temperature rise above the alloy solidus.

10.3.2.4.5 Subroutine THEXP1 and its Comparison With the Handbook Data

Figure 10.3-40 shows flow diagram of the subroutine THEXP1 developed for calculating the linear thermal expansion, based on this method of regionwise interpolation, of U-Pu-Zr fuel as a function of composition. This subroutine is used, in the SAS4A/SASSYS-1 codes, in the calculation of the theoretical density as a function of temperature and composition, given by Eq. (10.3-44).

Figures 10.3-41 to 10.3-48 show the comparison of calculated linear thermal expansion with all the data in the Metallic Fuels Handbook [10-8] for the 8 basic alloys or components discussed in Section B. It can be noted in Figs. 10.3-41, 10.3-44 and 10.3-48 that the Handbook data for U, Zr and Pu metals over the solid-state transition temperature range differ from the calculated values. As discussed in Section B, the calculated thermal expansion varies linearly with temperature between the first and last solid state transitions. In the case of Zr and Pu (Figs. 10.3-44 and 10.3-48), this linearization has led to ignoring the thermal contractions (taking place during heatup) that occur at solid state transitions. However the behavior of the 3 metals when alloyed is different from their behavior in isolation, and the linearization is the expected behavior when alloyed.

Figures 10.3-49 to 10.3-51 show the variation of linear thermal expansion with temperature for 21 alloy compositions obtained from this subroutine. The Pu and Zr contents each vary from zero to 30 wt % in the alloy compositions plotted in the figures. The solidus and liquidus temperatures required as input to the THEXP1 subroutine were calculated using another subroutine developed by Pelton [10-13]. The linear thermal expansion from 293K to solidus varies over the range 2.4% to 4.0% for the alloy compositions plotted.

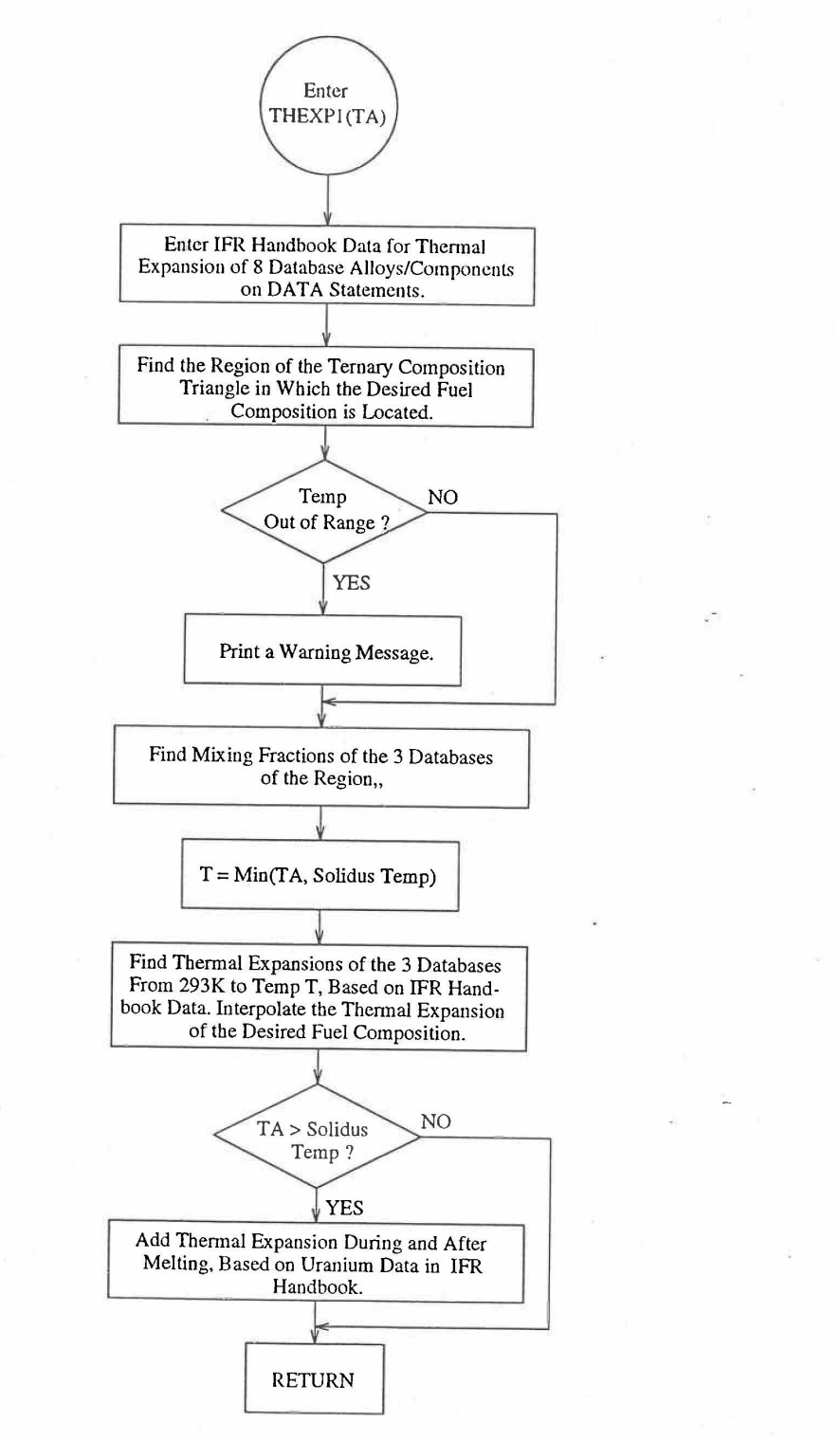

Fig. 10.3-40. Flow Diagram of Subroutine THEXP2 for U-Pu-Zr Thermal Expansion

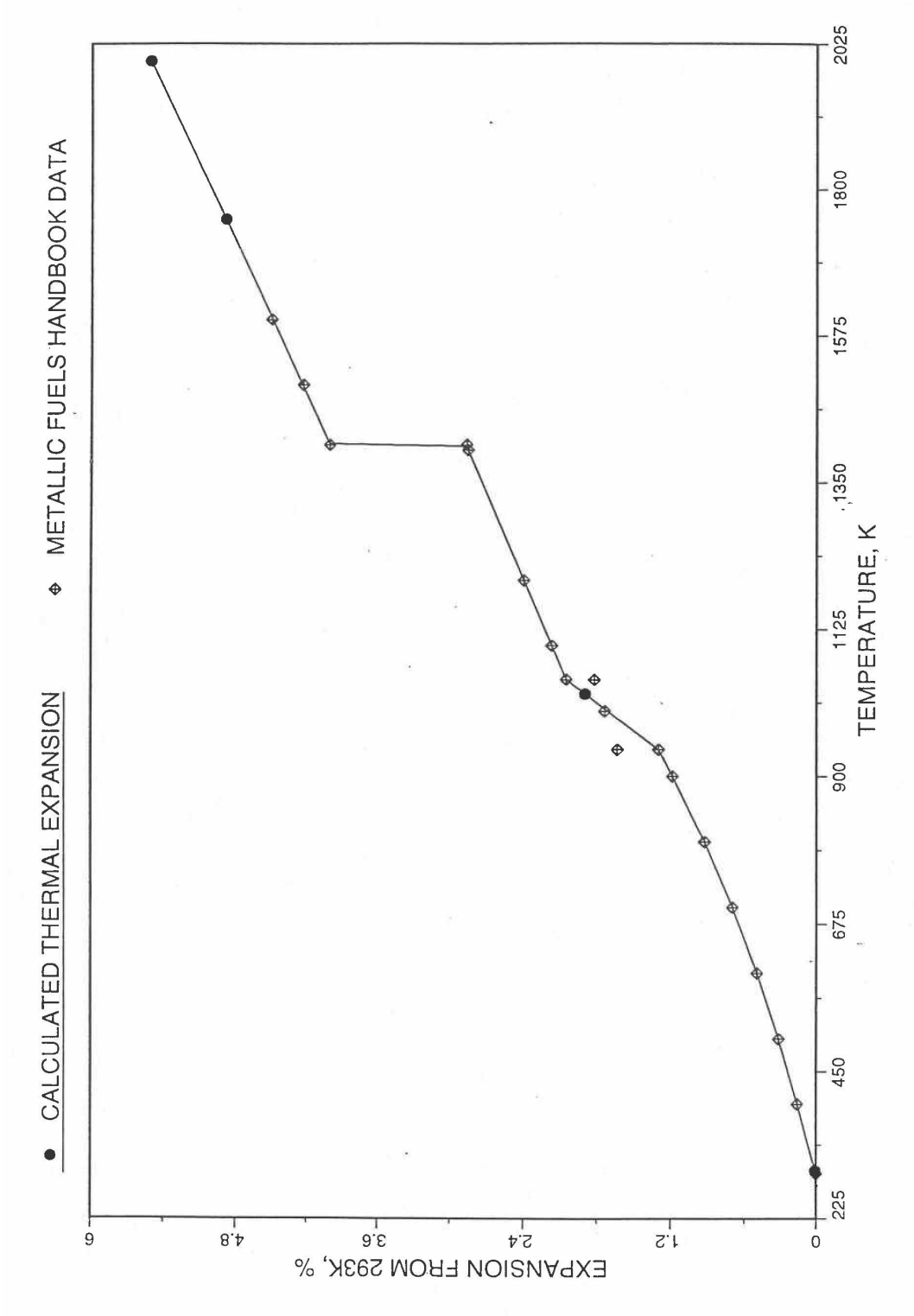

Fig. 10.3-41. Comparison of Uranium Metal Linear Thermal Expansion Data in IFR Handbook With Those Calculated by the Regionwise Interpolation Subroutine THEXP1

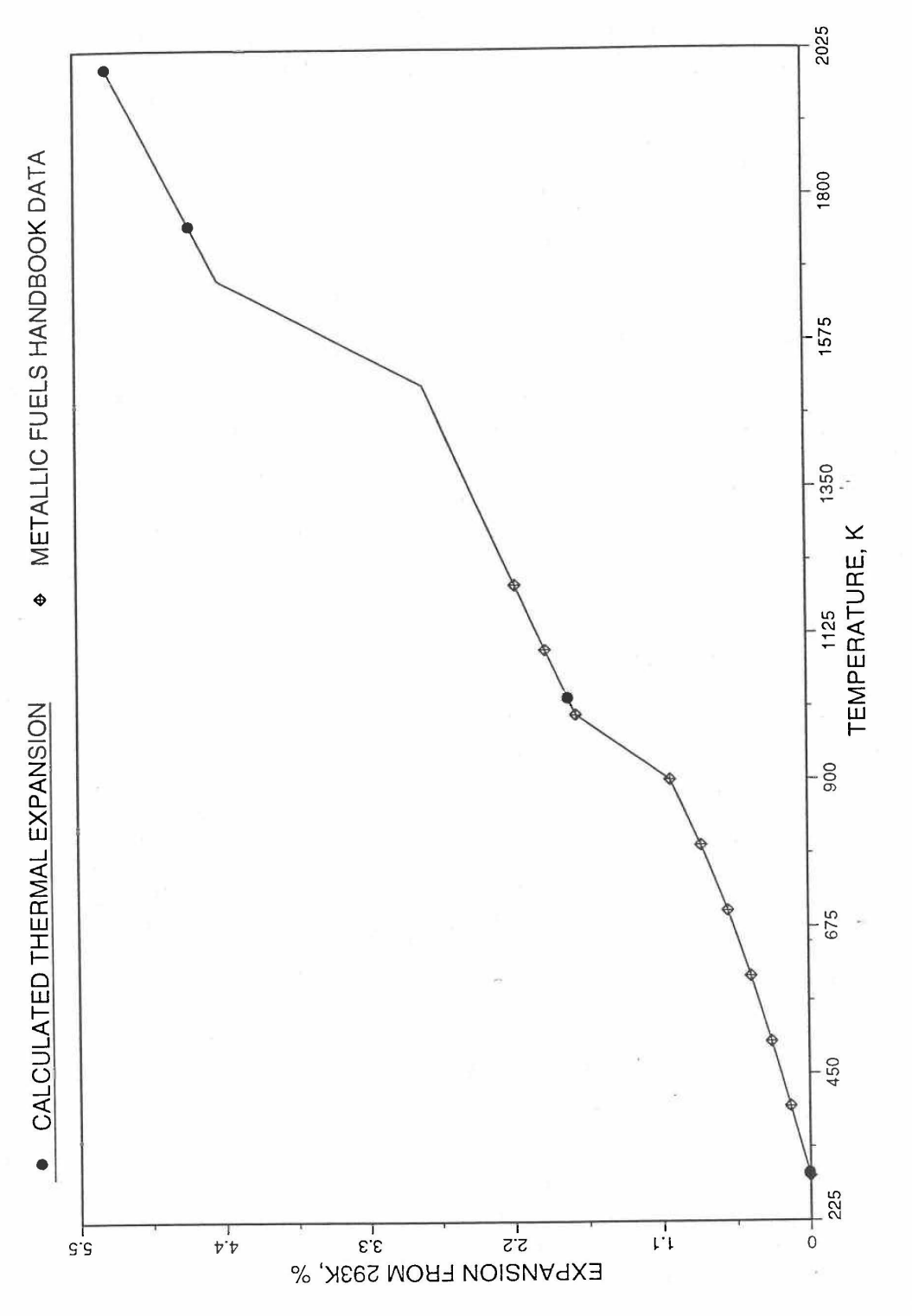

Fig. 10.3-42. Comparison of U-10Zr Alloy Linear Thermal Expansion Data in IFR Handbook With Those Calculated by the Regionwise Interpolation Subroutine THEXP1

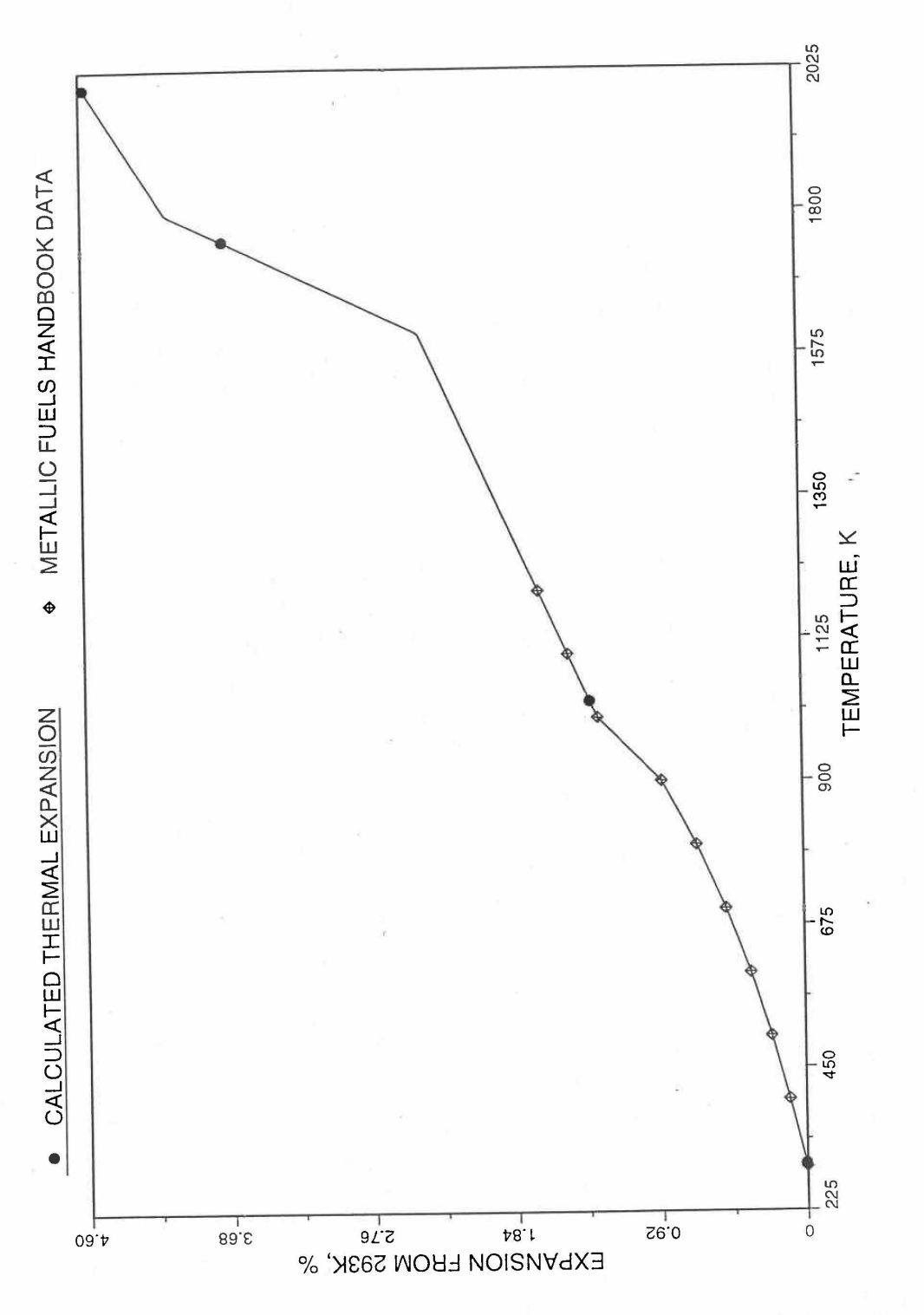

Fig. 10.3-43. Comparison of U-20Zr Alloy Linear Thermal Expansion Data in IFR Handbook With those Calculated by the Regionwise Interpolation Subroutine THEXP1

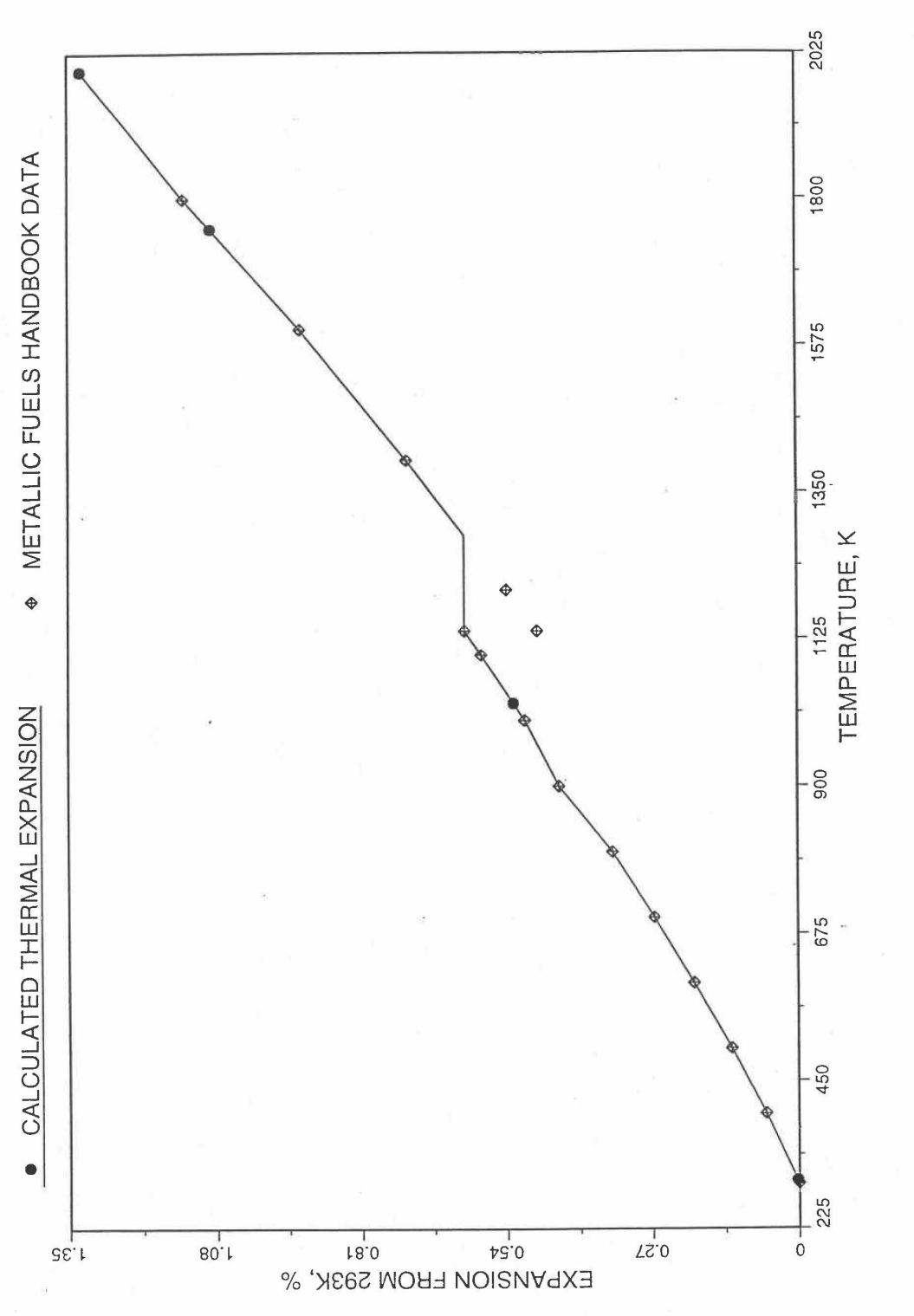

Fig. 10.3-44. Comparison of Zirconium Metal Linear Thermal Expansion Data in IFR Handbook With Those Calculated by the Regionwise Interpolation Subrountine THEXP1

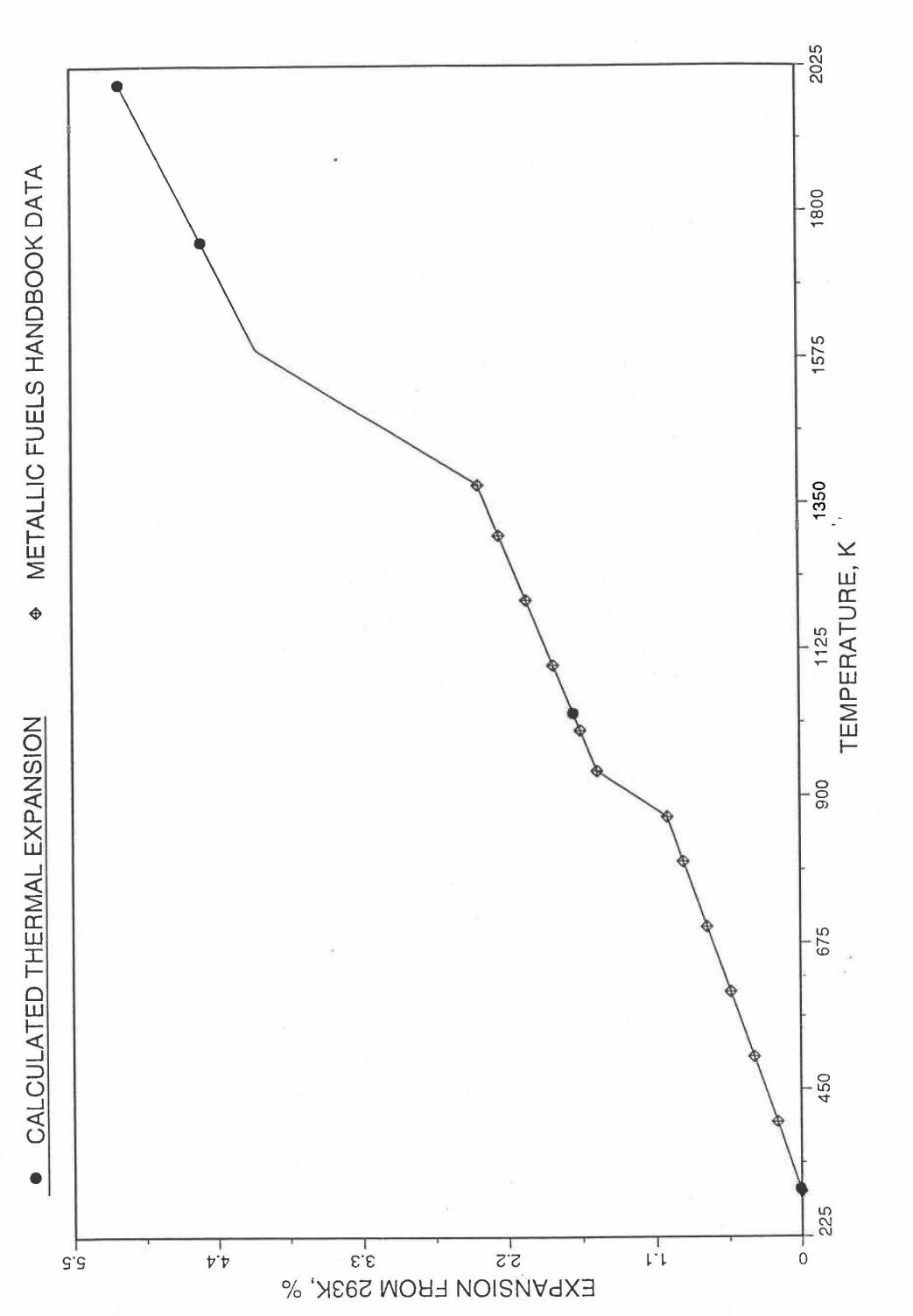

Fig. 10.3-45. Comparison of U-15Pu-10Zr Linear Thermal Expansion Data in IFR Handbook With Those Calculated by the Regionwise Interpolation Subroutine THEXP1

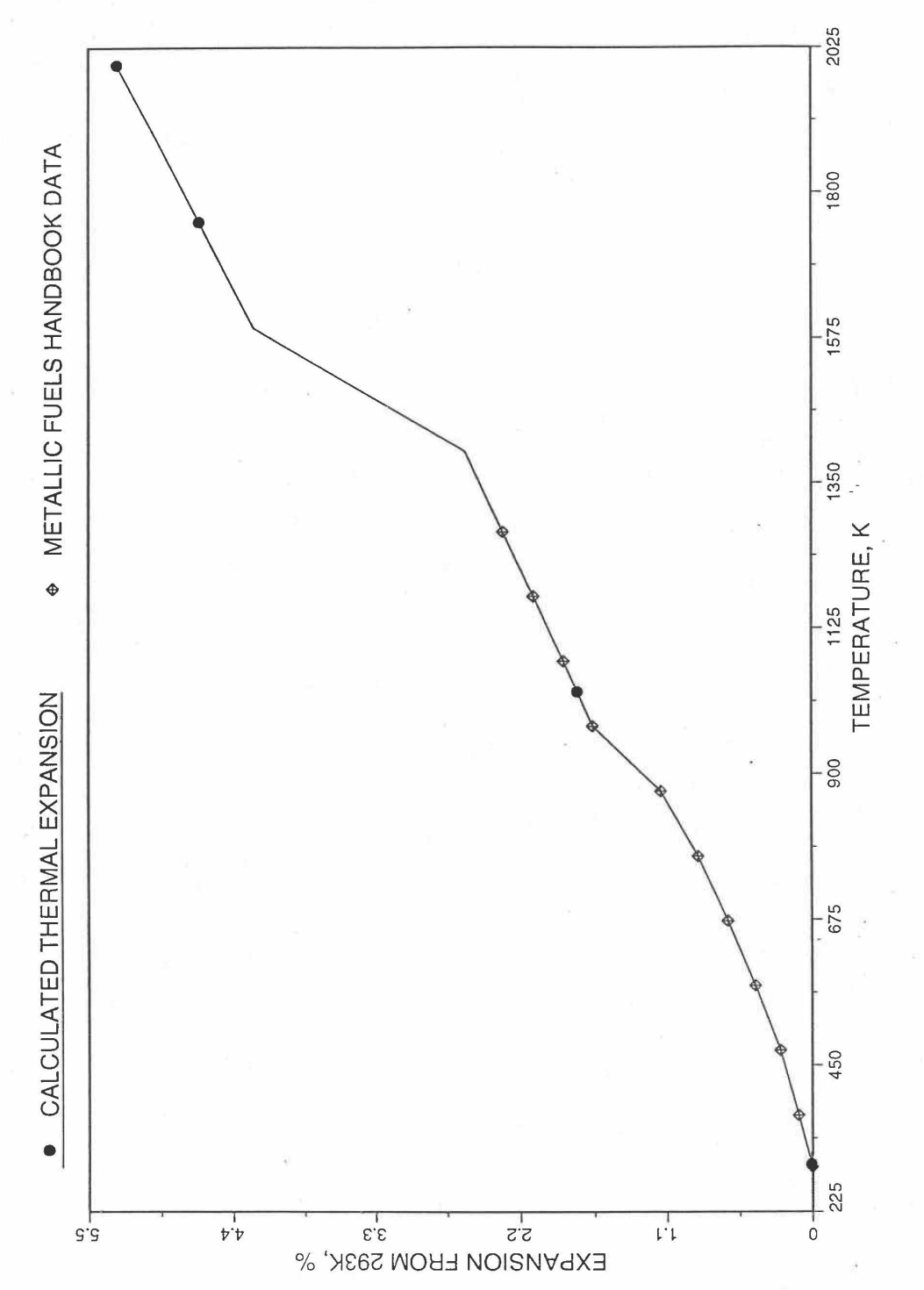

Fig. 10.3-46. Comparison of U-19Pu-10Zr Linear Thermal Expansion Data in IFR Handbook With Those Calculated by the Regionwise Interpolation Subroutine THEXP1

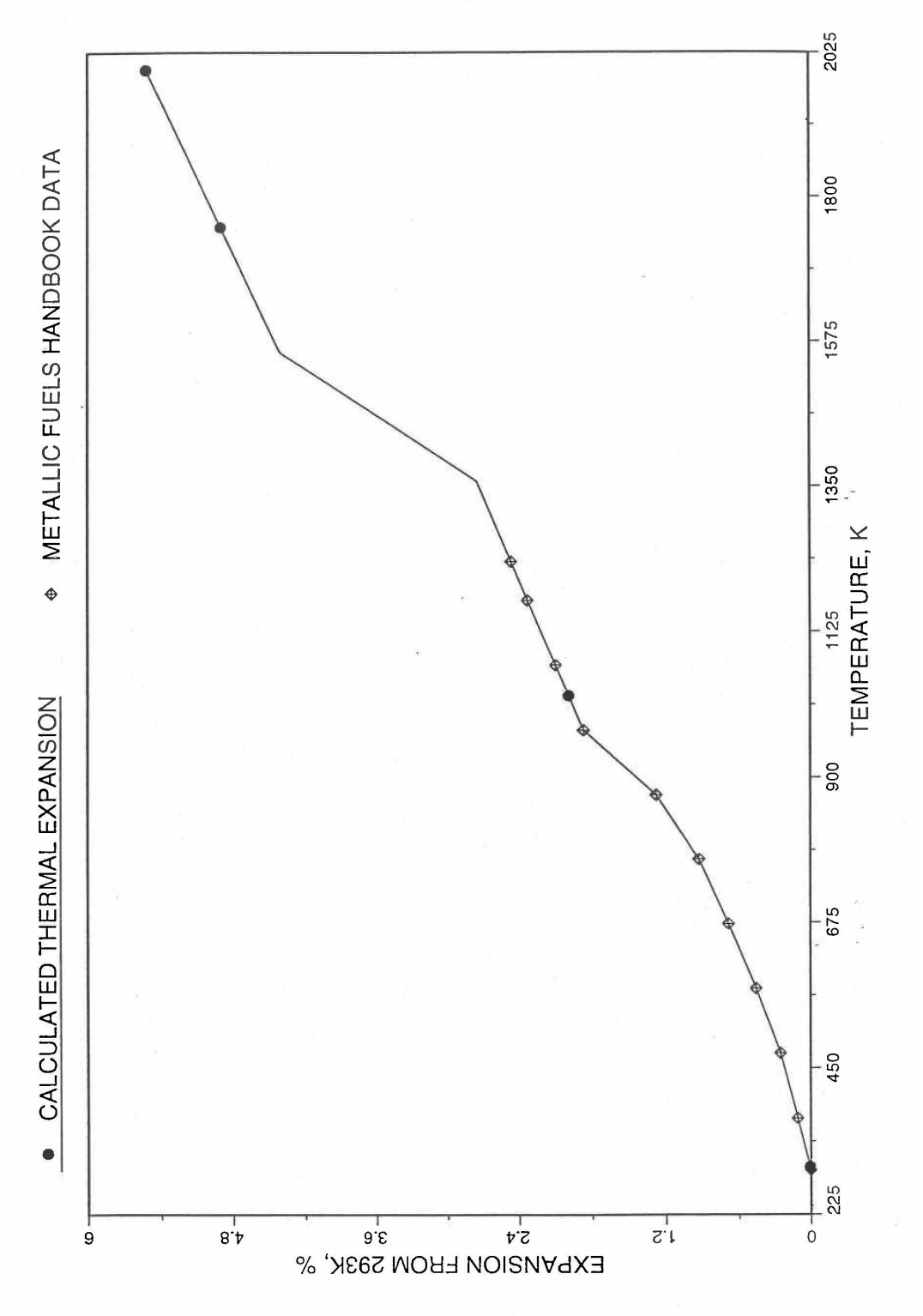

Fig. 10.3-47. Comparison of U-26Pu-10Zr Linear Thermal expansion Data in IFR Handbook With those Calculated by the Regionwise Interpolation Subroutine THEXP1

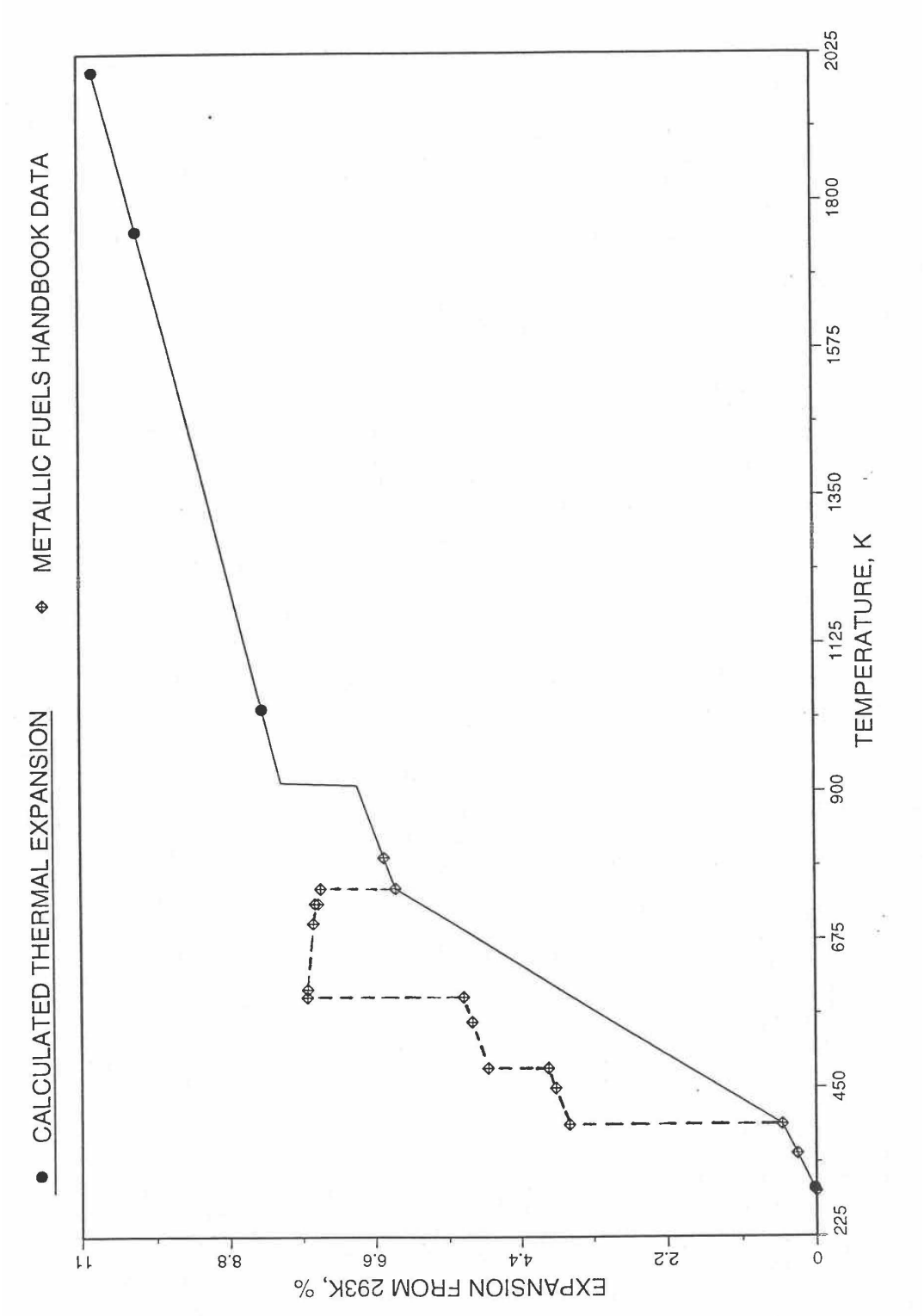

Fig. 10.3-48. Comparison of Plutonium Metal Liner Thermal Expansion Data in IFR Handbook With Those calculated by the Regionwise Interpolation Subroutine THEXP1

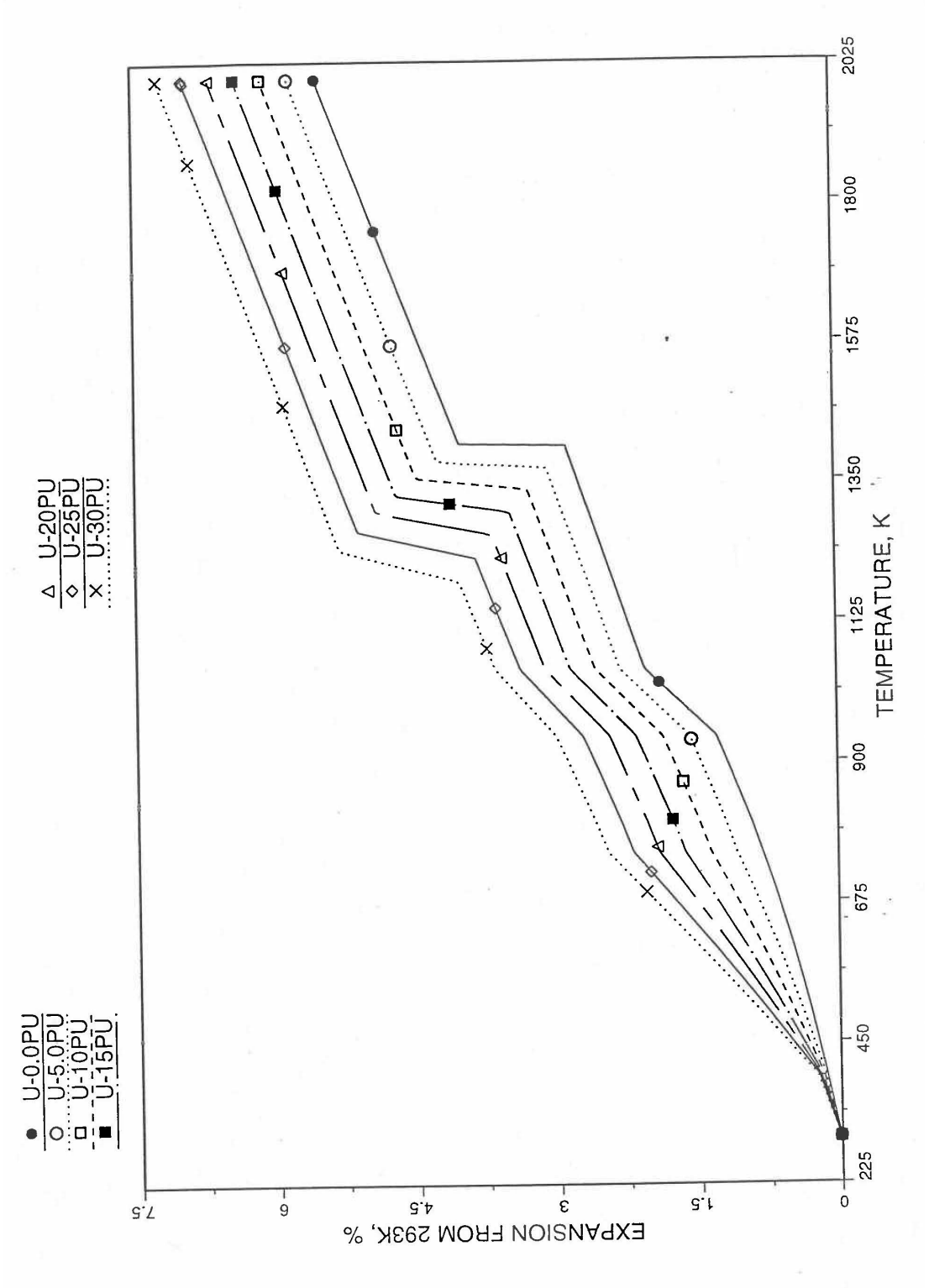

Fig. 10.3-49. Linear Thermal Expansion of U-Pu Fuel Without Fission Products, Obtained From Regionwise Interpolation of IFR Handbook Data

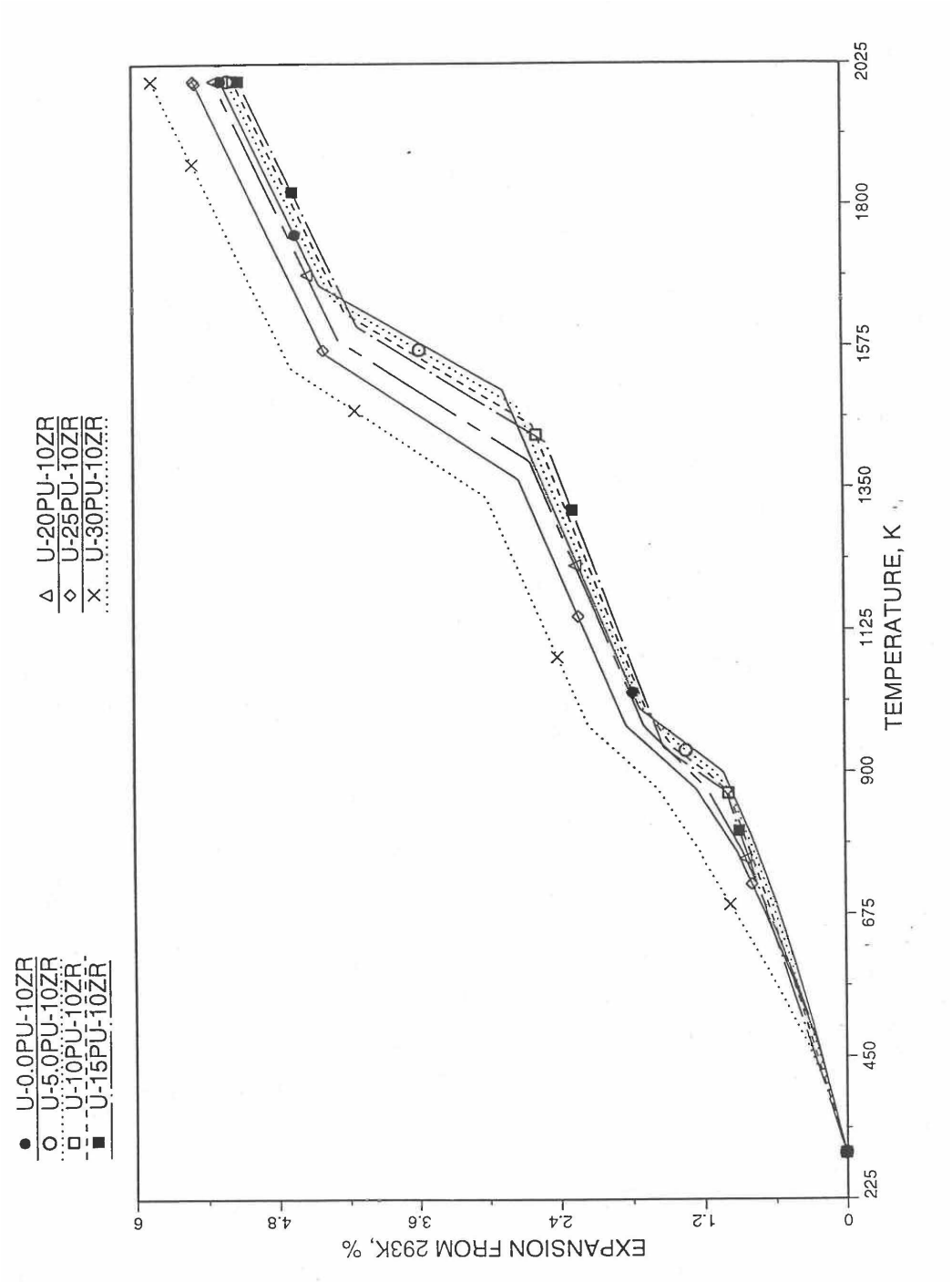

Fig. 10.3-50. Linear Thermal Expansion of U-Pu-10Zr fuel Without Fission Products, Obtained From Regionwise Interpolation of IFR Handbook Data

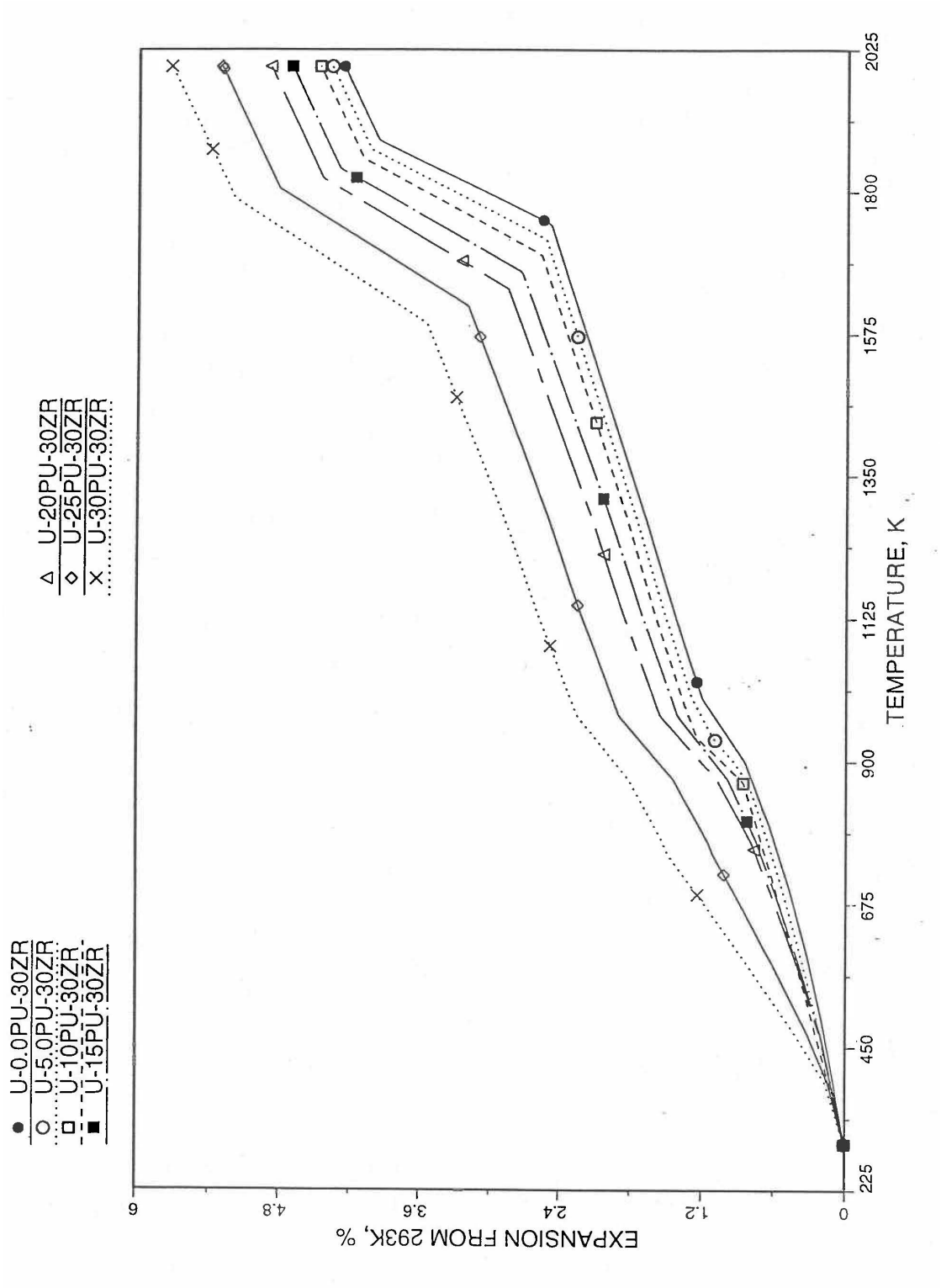

Fig. 10.3-51. Linear Thermal Expansion of U-Pu-30Zr Fuel Without Fission Products, Obtained From Regionwise Interpolation of IFR Handbook Data

10.3.2.5 Thermal Conductivity of Unirradiated 100% Dense U-Pu-Zr Fuel

10.3.2.5.1 Introduction

To perform calculations for the Mark-V fuel (U-20Pu-10Zr), and other metallic alloy fuels to different compositions, especially the fuel compositions across the pin radius resulting from the migration of alloy constituents during steady state irradiation, there is a need for modeling and correlation development for the thermal conductivity of U-Pu-Zr fuels as a function of composition, using the data presented in the IFR Metallic Fuels Handbook [10-8, 10-9].

Earlier, before the preparation of the Metallic Fuels Handbook [10-9], a correlation was developed to estimate the composition- and temperature-dependent thermal conductivity of 100% dense solid U-Pu-Zr alloy fuel [10-4]. In this correlation, the thermal conductivity of the U-Zr binary alloy having the uranium-to-zirconium atomic ratio of the desired U-Pu-Zr fuel was first evaluated from the data for U metal and U-50 at. % Zr alloy. This thermal conductivity was then adjusted for the presence of Pu by subtracting a term linearly proportional to Pu atom fraction where the coefficient of proportionality was determined (as a function of temperature and zirconium atom fraction) by fitting to the thermal conductivity data available for three U-Pu-Zr alloys, i.e., U-16.2Pu-6.2Zr, U-14.7Pu-9.7Zr and U-18.4Pu-11.5Zr. This correlation is valid when Pu atom fraction is less than 0.2, and Zr atom fraction is less than 0.5. The variation of thermal conductivity obtained from this correlation has been plotted for alloy compositions having 0.0 to 30 wt % Pu and 1.5 to 40 wt % Zr [10-17]. A drawback of this correlation [10-4] is that, for some alloy compositions, the thermal conductivity becomes negative (unphysical) at room temperature, and shows a maximum when plotted as a function of temperature (an unexpected behavior [10-18] for temperatures greater than 300 K). Although the allow compositions showing this unphysical/unexpected behavior are out of the noted region of validity, the correlation has another drawback that the thermal conductivity data used in obtaining the correlation were taken from sources [10-14, 10-19, 10-20] other than the Metallic Fuels Handbook.

The Metallic Fuels Handbook [10-8, 10-9] presents thermal conductivity data for U metal and a number of U-Zr and U-Pu-Zr alloys. It also gives a correlation to estimate the composition- and temperature-dependent thermal conductivity of 100% dense solid U-Pu-Zr alloys. In addition, Billone has developed, based on the data reported in the IFR Handbook [10-8], two other correlations [10-21, 10-22] for use in the analysis of EBR-II Mark-V fuel core, and so the following 3 correlations based on the Handbook data are available to estimate 100% dense solid U-Pu-Zr fuel thermal conductivity:

1. The correlation in the IFR Handbook [10-8, 10-9],
2. The correlation in Billone's memorandum [10-21] of March 8, 1991,
3. The correlation in Billone's memorandum [10-22] of October 21, 1991.

The above 3 correlations are summarized here in Appendix 10.2 for easy reference. The variation of thermal conductivity obtained form these 3 correlations have been

plotted for alloy compositions having 0.0 to 30 wt % Pu and 1.5 to 40 wt % Zr [10-17]. The correlation in March 8 memorandum should not be used because it is not well-behaved, and so recommended by Billone [10-22]. The thermal conductivity obtained from this correlation, with increasing Pu content at a fixed Zr content, first increases above the U-Zr binary value, then starts decreasing and goes below the binary value, and finally starts increasing again and becomes much greater than the binary value. A drawback of the other two correlations (i.e., the correlations in the IFR Handbook and in the October 21 memorandum) is that the thermal conductivities become negative (unphysical) at room temperature for Pu and Zr contents greater than 20 wt %. Another drawback of the correlation in October 21 memorandum is that the thermal conductivity shows a maximum when plotted as a function of temperature (an unexpected behavior [10-18] for temperatures greater than 300 K). A comparison of these 3 correlations with the Handbook data for U-Zr binary alloys shows that the 3 correlations are almost identical for binary alloys [10-17], and that they agree with the data closely. The correlation in the IFR Handbook can be reliably used for binary alloys containing 1.5 to 20 wt. % Zr.

Recently, the method of estimating U-Pu-Zr alloy enthalpy by regionwise interpolation has been extended to estimate thermal conductivity of 100% dense solid U-Pu-Zr alloy fuels as a function of composition. Based on this method of calculating composition- and temperature-dependent thermal conductivity, a subroutine KFUEL1 has been developed that removes all the drawbacks mentioned above. The subroutine makes use of the thermal conductivity data of 9 basic alloys/components, compressing of all the data in the IFR Handbook [10-8, 10-9]. The U-10Pu data used in the method are obtained from Billone [10-21], and the Pu data are reported in the Plutonium Handbook [10-23]. The 9 basic alloy compositions are used to divide the ternary composition triangle into 10 regions of interpolation as shown in Fig. 10.3-52. The method is flexible enough to make use of the thermal conductivity data of additional alloys (as they become available) to divide the composition triangle into a larger number of smaller regions, thus improving its accuracy. The subroutine KFUEL1 has been incorporated into the SAS4A/SASSYS-1 codes.

The technique used at present to estimate the fuel thermal conductivity during and after melting is also discussed in this section. Since all the thermal conductivity data reported in the IFR Handbook lies in the 293 K to 1173 K temperature range, a warning message is printed by the codes whenever fuel thermal conductivity is calculated at a temperature smaller than 293 K or greater than 1200 K.

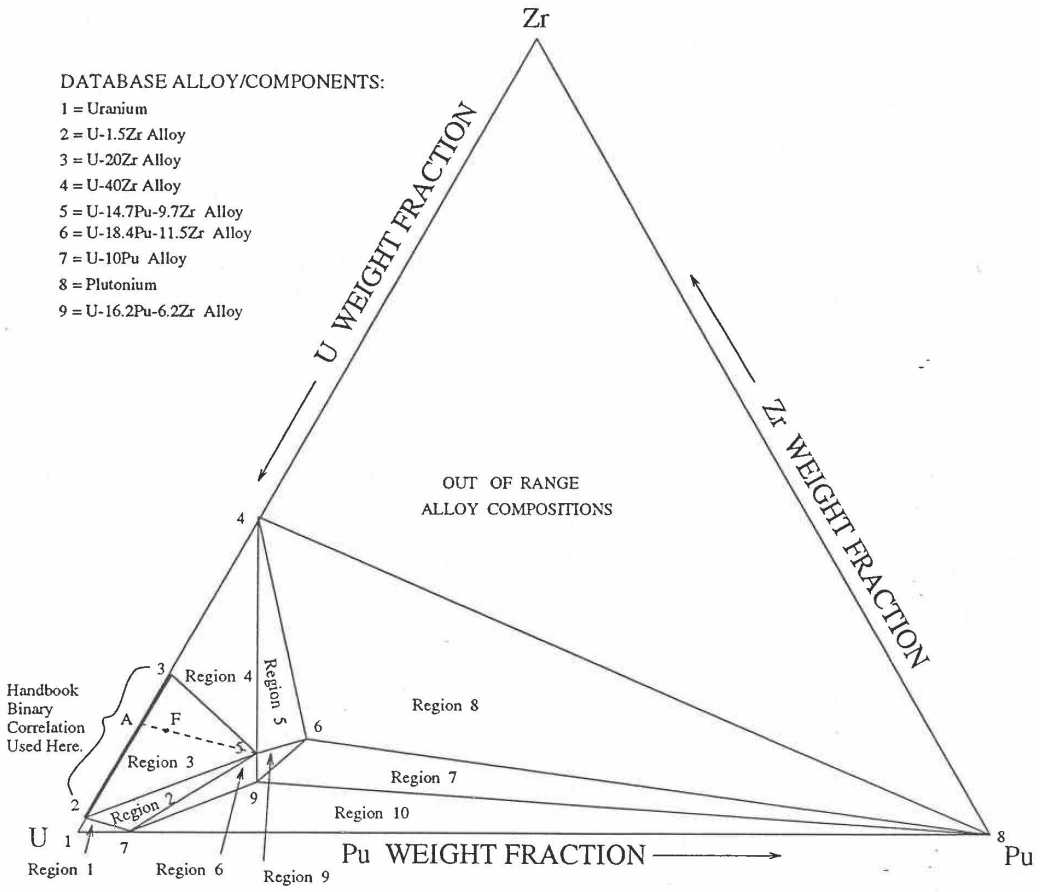

Fig. 10.3-52. Diagram Showing Thermal Conductivity Interpolation Regions for 100% Dense Solid U-Pu-Zr Fuels

10.3.2.5.2 Description of the Method

Figure 10.3-52 shows the U-Pu-Zr ternary composition triangle marked with the points representing 9 basic alloys/components comprising of all the thermal conductivity data reported in the IFR Handbook [10-8, 10-9]. The U-10Pu data used here are obtained from Billone [10-21], and the Pu data are reported in the Plutonium Handbook [10-23], and a warning message is printed by the codes when these two data are actually used in any calculation. The composition points of these 9 database alloys/components are used to divide the whole ternary composition triangle into 10 triangular regions of interpolation as shown in Fig. 10.3-52. For evaluating the thermal conductivity of a desired solid U-Pu-Zr alloy represented by a point located in any region of interpolation, the method consists of mixing the 3 database alloys represented by the corners of the region of interpolation. The proportions or weight fractions of the 3 database alloys in mixing are so calculated in the method that the resulting mixture has the composition of the desired alloy. The calculated mixing fractions are then used as weight factors in making a linear combination of (or linear interpolation between) thermal conductivity data of the 3 database alloys, and the linear combination gives the interpolated thermal conductivity of the desired alloy. The thermal conductivity data of each basic alloy/component are least-square fitted by aquadratic function of temperature.

$$K_{0i} = A_{i1} + A_{i2}\,T + A_{i3}\,T^2 \qquad (10.3\text{-}52)$$

where

K_{0i} = thermal conductivity of the ith 100%-dense solid database alloy/component, W/m-K,

A_{i1}, A_{i2}, A_{i3} = coefficients of the quadratic for the thermal conductivity of the ith database alloy,

T = alloy temperature, K.

The interpolation of the thermal conductivity data of the 3 basic alloys is performed by interpolating between the coefficients (of like terms) of the quadratics for the 3 basic alloys. The calculated mixing fractions are never negative and the linear combination never requires extrapolation because the desired alloy composition point is always inside the triangle with corners at the 3 database alloy points. If the desired alloy composition point were outside this triangle, the linear combination would involve negative mixing fractions and extrapolation which are avoided entirely in the present method.

A different method of interpolation is used in region 3 (Fig. 10.3-52) in order to employ the Handbook U-Zr binary correlation for composition points on the side joining corners 2 and 3, i.e., for binary compositions containing 1.5 to 20 wt % Zr. This is done because the Handbook binary correlation (Eq. A.10.2-1) with Pu content set to zero) is accurate for Zr content in this range, as discussed in Appendix 10.1. The thermal conductivity of a desired U-Pu-Zr alloy in region 3 (represented by point F in

Fig. 10.3-52) is interpolated between only two compositions, the database alloy 5 and binary alloy represented by point A. The point A is the intersection of the side 23 with the line F5 that joins the desired alloy and the database alloy 5. Here also, the interpolation between the database alloy 5 and the binary correlation is performed in terms of the coefficients (of like terms) of the quadratics for thermal conductivity.

10.3.2.5.3 Thermal Conductivity Data of Basic Alloys

Table 10.3-4 gives the thermal conductivity data of the 9 basic solid alloys or components that are used in the present method of evaluating composition- and temperature- dependent thermal conductivity of 100% dense solid U-Pu-Zr fuels. Table 10.3-5 gives the coefficient of the quadratic functions of temperature fitted to the data given in Table 10.3-4. The 9 basic alloys/components are: (1) U metal, (2) U-1.5Zr, (3) U-20Zr, (4) U-40Zr, (5) U-14.7Pu-9.7Zr, (6) U-18.4Pu-11.5Zr, (7) U-10Pu, (8) Pu metal, and (9) U-16.2Pu-6.2Zr. The coefficients of the quadratics for all database alloys except U-1.5 Zr and U-20 Zr are obtained by the method of least-squares fit. The coefficients of the quadratics for U-1.5 Zr an U-20 Zr are evaluated form the Handbook binary correlation. This is required to make the thermal conductivity continuous at the boundary lines of interpolation region 3 (Fig. 10.3-52). All the data available in the Metallic Fuels Handbook [10-8, 10-9] have been included in the database used in the present method. Data for two non-Handbook alloys/components, i.e., U-10 Pu data obtained from Billone [10-21] and Pu data reported in the Plutonium handbook [10-23], have also been included in the database of the present method. The U-Pu data is the only intermediate point on the U-Pu binary side of the ternary composition triangle (Fig. 10.3-52), and has been included to account for thermal conductivity variation of U-Pu binary as Pu content increases from zero to 100 wt. %. The Pu data has been included to be able to interpolate Mark-V fuel (U-10Pu-10Zr) thermal conductivity because all the other database alloys/components contain les than 20 wt. % Pu. Without the Pu data, the evaluation of thermal conductivity of fuels containing more than 18.4 wt. % Pu will involve extrapolation, which is avoided in the present method.

The quadratic functions given in Table 10.3-5 are used in the temperature range of 293 K to the solidus temperature of the desired U-Pu-Zr alloy. Since the thermal conductivity data of the 9 basic alloys/components (Table 10.3-4) used in the present method go only up to 1173 K, a warning message is printed by the code when the method is used to calculate thermal conductivity at temperatures above 1200 K. A similar warning message is also printed when the method is used at temperatures below 293 K. The thermal conductivity at temperatures above the desired alloys solidus temperature is assumed to be equal to the value at the solidus temperature as discussed in Section E.

Table 10.3-4. Thermal Conductivity Data of the 9 100%-Dense Basic Solid Alloys/Components Used in the Method of Regionwise Interpolation

1. Uranium		2. U-1.5Zr		3. U-20Zr		4. U-40Zr		5. U-14.7Pu-9.7Zr	
Temp, K	Cond, W/m-K	Temp, K	Cond, W/m-K	Temp, K	Cond, W/m-K	Temp, K	Cond, W/m-K	Temp, K	Cond, W/m-K
293	27	293	22.6	293	11	293	7	373	10
373	29.1	373	24	373	13	373	8	473	13.2
473	31.1	473	26	473	15	473	10	573	16.4
573	33.4	573	38.5	573	17	573	12	673	19.6
673	35.8	673	31	673	20	673	14	773	22.5
773	38.2	773	34	773	22	773	17	873	25.3
873	40.6	873	37	873	25	873	20	973	27.8
973	43.2	973	40.5	973	28	973	24	1073	30.1
1073	45.7	1073	44.5	1073	31	1073	28	1173	32.3
1173	48.3			1173	34	1173	33		
6. U-18.4Pu-11.5Zr		7. U-10Pu		8. Plutonium		9. U-16.2Pu-6.2Zr			
373	9.2	473	23.9	293	4.1 ± 6.1%	373	10.9		
473	11.7	673	28.9	400	10.2 ± 9.2%	473	14.2		
573	14.4	873	36.4	500	12.3 ± 6.5%	573	17.7		
673	17.1	1073	41.9	600	15.8 ± 5.4%	673	21		
73	19.7			700	18.2 ± 4.4%	773	24.1		
873	21.9			800	18.2 ± 2.5%	873	26.4		
973	23.4			900	20.8 ± 2.5%	973	28		
1073	24.8			2000[a]	47.1	1073	29.3		
1173	26					1173	30.1		

[a]This is linearly extrapolated data point used in least-square curve fitting.

Table 10.3-5. Coefficients of Quadratic Functions of Temperature Fitted to Thermal Conductivity Data of the 9 100%-Dense Basic Solid Alloys/Components Used in the Method of Regionwise Interpolation

		Coefficients of Quadratic[a]				
No.	Database Alloy/Component	A_{i1}	A_{i2}	A_{i3}	RMS[b] Error, %	Maximum Error, %
1	Uranium	20.931	0.020407	2.4968×10^{-6}	0.30	0.72
2	U-1.5Zr,c	16.516	0.015051	9.3800×10^{-6}	1.94	3.85
3	U-20Zr,c	7.336	0.011791	9.3800×10^{-6}	2.07	5.40
4	U-40Zr	6.0734	-0.0025711	2.1589×10^{-5}	1.78	3.13
5	U-14.7Pu-9.7Zr	-4.3462	0.041352	-8.5931×10^{-6}	0.58	1.18
6	U-18.4Pu011.5Zr	-4.3270	0.040293	-1.2208×10^{-5}	1.71	2.57
7	U-10Pu	10.716	0.025919	3.1250×10^{-6}	1.83	2.34
8	Plutonium	-4.6825	0.033747	-3.9751×10^{-6}	14.6	19.9
9	U-16.2Pu-6.2Zr	-7.6844	0.057035	-2.1028×10^{-5}	1.69	2.74

[a]Thermal conductivity $K_{oi} = A_{i1} + A_{i2}T + A_{i3}T^2$ where i is database alloy number.

[b]RMS Error is root mean square error or the standard deviation.

[c]The coefficients of the quadratic function for these two database alloys are obtained from Handbook binary correlation whereas the coefficients for all the other database alloys are found by least-squares fit.

10.3.2.5.4 Method of Interpolation

The method of interpolation to evaluate the thermal conductivity of a 100%-dense U-Pu-Zr fuel composition at and below its solidus temperature consists of first determining the region of the ternary composition triangle (shown in Fig. 10.3-52) in which the desired fuel composition lies, and then finding the weight fractions in which the 3 database alloys of the region are required to be mixed to obtain the desired fuel composition. From the mass balance of U, Pu and Zr, the following equations have been obtained in Section 10.3.2.1 for the weight fractions, X_i, of the database alloys that are assumed to be numbered 1, 2 and 3.

$$X_i = D_i / D,\ i = 1,2,3 \tag{10.3-53}$$

$$D = (W_{z1} - W_{z2})(W_{p3} - W_{p1}) - (W_{p1} - W_{p2})(W_{z3} - W_{z1}) \tag{10.3-54}$$

$$D_1 = (W_z - W_{z2})(W_{p3} - W_p) - (W_p - W_{p2})(W_{z3} - W_z) \tag{10.3-55}$$

$$D_2 = (W_{z1} - W_z)(W_{p3} - W_{p1}) - (W_{p1} - W_p)(W_{z3} - W_{z1}) \tag{10.3-56}$$

$$D_3 = (W_{z1} - W_{z2})(W_p - W_{p1}) - (W_{p1} - W_{p2})(W_z - W_{z1}) \tag{10.3-57}$$

where

W_{ui}, W_{pi}, W_{zi} = weight fractions of U, Pu and Zr in database alloy I of the region in which the desired fuel composition lies,

W_u, W_p, W_z = weight fractions of U, Pu and Zr in the desired fuel composition.

The sum of X_1, X2 and X_3 is always 1. In case of interpolation, the values of X_1, X_2 and X_3 are always positive. If any extrapolation were involved, the value of a least one weight fraction would be negative which is entirely avoided in the present method. The coefficients of the Quadratic for the thermal conductivity of the desired 100%-dense U-Pu-Zr fuel composition are then evaluated by mass-weighted averaging of the coefficients (of like terms) of the quadratics for the thermal conductivities of the 3 database alloys.

$$A_{f1} = X_1 A_{11} + X_2 A_{21} + X_3 A_{31} \tag{10.3-58}$$

$$A_{f2} = X_1 A_{12} + X_2 A_{22} + X_3 A_{32} \tag{10.3-59}$$

$$A_{f3} = X_1 A_{13} + X_2 A_{23} + X_3 A_{33} \quad (10.3\text{-}60)$$

here

A_{f1}, A_{f2}, A_{f3} = coefficients of the quadratic for thermal conductivity of the desired fuel composition,

A_{i1}, A_{i2}, A_{i3} = coefficients of the quadratic for thermal conductivity of the ith database alloy/component.

The thermal conductivity of the desired 100%-dense U-Pu-Zr fuel composition at a temperature T at or below its solidus is then calculated using its quadratic.

$$K_0(T) = A_{f1} + A_{f2} T + A_{f3} T^2 \quad (10.3\text{-}61)$$

where

$K_0(T)$ = thermal conductivity of the desired 100%-dense U-Pu-Zr fuel composition.

It should be noted that the method of interpolation given by Eqs. (10.3-58) to (10.3-61), in which first the coefficients of the quadratic for the desired alloy are calculated and then the thermal conductivity, is equivalent to interpolating the desired alloy thermal conductivity directly from the thermal conductivities of the database alloys.

$$K_0(T) = X_1 K_{01}(T) + X_2 K_{02}(T) + X_3 K_{03}(T) \quad (10.3\text{-}62)$$

where

$K_{0i}(T)$ = thermal conductivity of 100%-dense solid database alloy I of the region in which the desired fuel composition lies.

As described in Section B, the thermal conductivity of a desired U-Pu-Zr fuel composition in region 3, represented by point F (Fig. 10.3-52), is interpolated between only tow compositions, the database alloy 5 and the U-Zr binary alloy represented by point A. The point A is the interaction of the side 23 (of region 3) with the line F5 that joins the desired alloy and the database alloy 5. The Zr content of the binary alloy A is given by

$$W_{za} = W_{z5} - W_{p5}(W_z - W_{z5})/(W_p - W_{p5}) \quad (10.3\text{-}63)$$

where

W_{za} = weight fraction of Zr in the binary alloy A,

W_{p5}, W_{z5} = weight fractions of Pu and Zr in the database alloy 5,

W_p, W_z = weight fractions of Pu and Zr in the desired fuel composition.

The coefficients of the quadratic for thermal conductivity of the U-Zr alloy A are found from the IFR Handbook binary correlation [10-8, 10-9], by setting the Pu weight fraction to zero and the Zr weight fraction to W_{za} in Eq. (A10.2-1).

$$A_{a1} = 17.5\left(1 - 2.23\ W_{za}\right)/\left(1 + 1.61\ W_{za}\right) \tag{10.3-64}$$

$$A_{a2} = 0.0154\left(1 + 0.061\ W_{za}\right)/\left(1 + 1.61\ W_{za}\right) \tag{10.3-65}$$

$$A_{a3} = 9.38\,x10^{-6} \tag{10.3-66}$$

where

A_{a1}, A_{a2}, A_{z3} = coefficients of the quadratic for thermal conductivity of binary alloy A.

The coefficients of the quadratic for thermal conductivity of the desired fuel composition in region 3 are then interpolated between the coefficients of the quadratic for binary alloy A and those for database alloy 5.

$$A_{fj} = A_{aj} + \left(A_{5j} - A_{aj}\right) W_p\ /\ W_{p5},\ j = 1,2,3 \tag{10.3-67}$$

where

A_{f1}, A_{f2}, A_{f3} = coefficient of the quadratic for thermal conductivity of the desired fuel represented by point F in region 3.

10.3.2.5.5 Thermal Conductivity During and After Melting

The quadratic functions of temperature, given in Table 10.3-5, are used to interpolate thermal conductivity of a desired U-Pu-Zr alloy in the temperature range of 293 K to the solidus temperature of the desired alloy. The thermal conductivity at temperatures above the desired alloy solidus temperature is assumed to be equal to the value at the solidus temperature because of two reasons: (1) U-Pu-Zr alloy thermal conductivity data during and after melting are not available, and (2) molten uranium thermal conductivity estimated form its electrical resistivity [10-24] using Wiedermann-Lorenz law, as described below, is nearly equal to solid uranium thermal conductivity evaluated at its melting point using the quadratic function given in Table 10.3-5.

Wiedermann-Lorenz law [10-25] gives the following relation between thermal conductivity and electrical resistivity of metals and alloys at temperatures above 150 K.

$$\frac{\rho K_o}{T} = L \tag{10.3-68}$$

where

K_o = thermal conductivity of 100% dense metal or alloy, W/m-K,

ρ = electrical resistivity of the material, Ω-m,

L = a constant called Lorenz number determined from theoretical considerations to be 2.45 x 10^{-4} W-Ω/K^2 for all metals.

Table 10.3-6 gives the electrical resistivity data [10-24] for uranium at temperatures from 293 K to 1573 K. The thermal conductivities at lower (than melting) temperatures, i.e., 293 K, 873 K, 973 K and 1073 K, are also included in Table 10.3-6 to examine the difference between the experimentally determined Lorenz numbers and the theoretical value of 2.45 x 10^{-8} W-Ω/K^2. The Lorentz numbers determined from data at these four lower (than melting) temperatures are approximately equal to the theoretical value. The thermal conductivities of uranium at and above the melting temperature have been calculated using the theoretical value of the Lorenz number, and found to be 54.2, 55.3 and 56.8 W/m-K at 1406 K, 1473 K and 1573 K. These thermal conductivity estimates are nearly equal to the value of 54.6 W/m-K calculated for solid uranium at its melting point (of 1408 K that is used in SAS4A/SASSYS-1 codes) using the quadratic function given in Table 10.3-5. From this comparison, it is concluded that there is no discontinuity in uranium thermal conductivity at its melting point. It should be noted from plots [10-18] of thermal conductivity as a function of temperature that several other metals do show a sharp discontinuity at the melting point.

At present, the thermal conductivity of all alloy compositions at temperatures above the solidus are assumed to remain constant and equal to the value at the solidus, and a warning message is printed by the code whenever this assumption is used.

10.3.2.5.6 Subroutine KFUEL1 and Its Comparison With the Handbook Data

Figure 10.3-53 shows flow diagram of the subroutine KFUEL1 for calculating the thermal conductivity, based on this method of regionwise interpolation, of a 100% dense U-Pu-Zr fuel as a function of composition and temperature. This subroutine has been incorporated into the SAS4A/SAASSYS-1 codes. For improving the computational speed, the coefficients of the quadratic for thermal conductivity of 100% dense U-Pu-Zr alloy of each input fuel type is pre-calculated before steady-state calculation, and used later in the steady-state and transient calculations of the codes.

Table 10.3-6. Estimation of 100%-Dense Molten Uranium Thermal Conductivity Using Wiedermann-Lorenz Law

Temperature, K	Electrical Resistivity, Ω-m	Thermal Conductivity,[a] W/m-K	Computed Value of L, W-Ω/K^2
293	30.0×10^{-8}	27.0	2.76×10^{-8}
873	59.0×10^{-8}	40.6	2.74×10^{-8}
973	55.5×10^{-8}	43.2	2.46×10^{-8}
1073	54.0×10^{-8}	45.7	2.30×10^{-8}
1406[b]	63.6×10^{-8}	54.2	2.45×10^{-8}
1473	65.3×10^{-8}	55.3	2.45×10^{-8}
1573	67.8×10^{-8}	56.8	2.45×10^{-8}

[a]The first four values are obtained from IFR Handbook data summarized in Table 10.3-4, and the next three values at 1406 K, 1473 K and 1573 K, are calculated using Wiedermann-Lorenz Law with constant L = 2.45×10^{-8} W-Ω/K^2.

[b]Uranium melting point reported in Ref. [10-24] compared to 1408 K given in the IFR Handbook and used in SAS4A/SASSYS-1 codes. The value 1406 K is used only in this table for estimating molten uranium thermal conductivity.

Figures 10.3-54 to 10.3-64 show the comparison of calculated thermal conductivity with all the data in the Metallic Fuels Handbook [10-8] and with the data for U-10Pu alloy [10-21] and Pu metal [10-23] given in Table 10.3-4. There is a close agreement between the calculated and the measured thermal conductivities of all these alloys except U-11.4 Zr and Pu metal. In the case of u-11.4 Zr, there are two outlying data points, one at 673 K and the other at 1173 K, and the rest of the data points are in fair agreement with the calculated curve (Fig. 10.3-57). It should be noted that the calculated curve for this alloy basically arises from the Handbook binary correlation [10-8], which is accurate for both the neighboring binary alloys (i.e., U-5Zr and U20Zr plotted in Figs. 10.3-56 and 10.3-58) for which data are available. Based on the degree of confidence in the Handbook binary correlation, the two outlying data points at 673 K and 1173 K are not believed to be reliable enough to require a revision of the subroutine KFUEL1. In the case of Pu metal, the scatter of the data points about the calculated curve is caused by a number of solid-state phase transitions. However, the behavior of Pu when alloyed with U and Zr is different from its behavior in isolation, and the smooth quadratic function of temperature use in calculation (in the subroutine KFUEL1) is closer to the expected behavior when alloyed.

Figures 10.3-65 to 10.3-67 show the variation of thermal conductivity with temperature for 20 100%-dense alloy compositions obtained from this subroutine. The Pu content varies from zero to 30 wt. % and the Zr content varies from 1.0 to 30 wt. % in the alloy compositions plotted in the figures. The solidus and liquidus temperatures required as input to the KFUEL1 subroutine were calculated using another subroutine developed by Pelton [10-13]. It should be noted that each thermal conductivity curve is flat at temperatures above the solidus temperature of the alloy. The thermal conductivities do not show any unphysical or unexpected behavior.

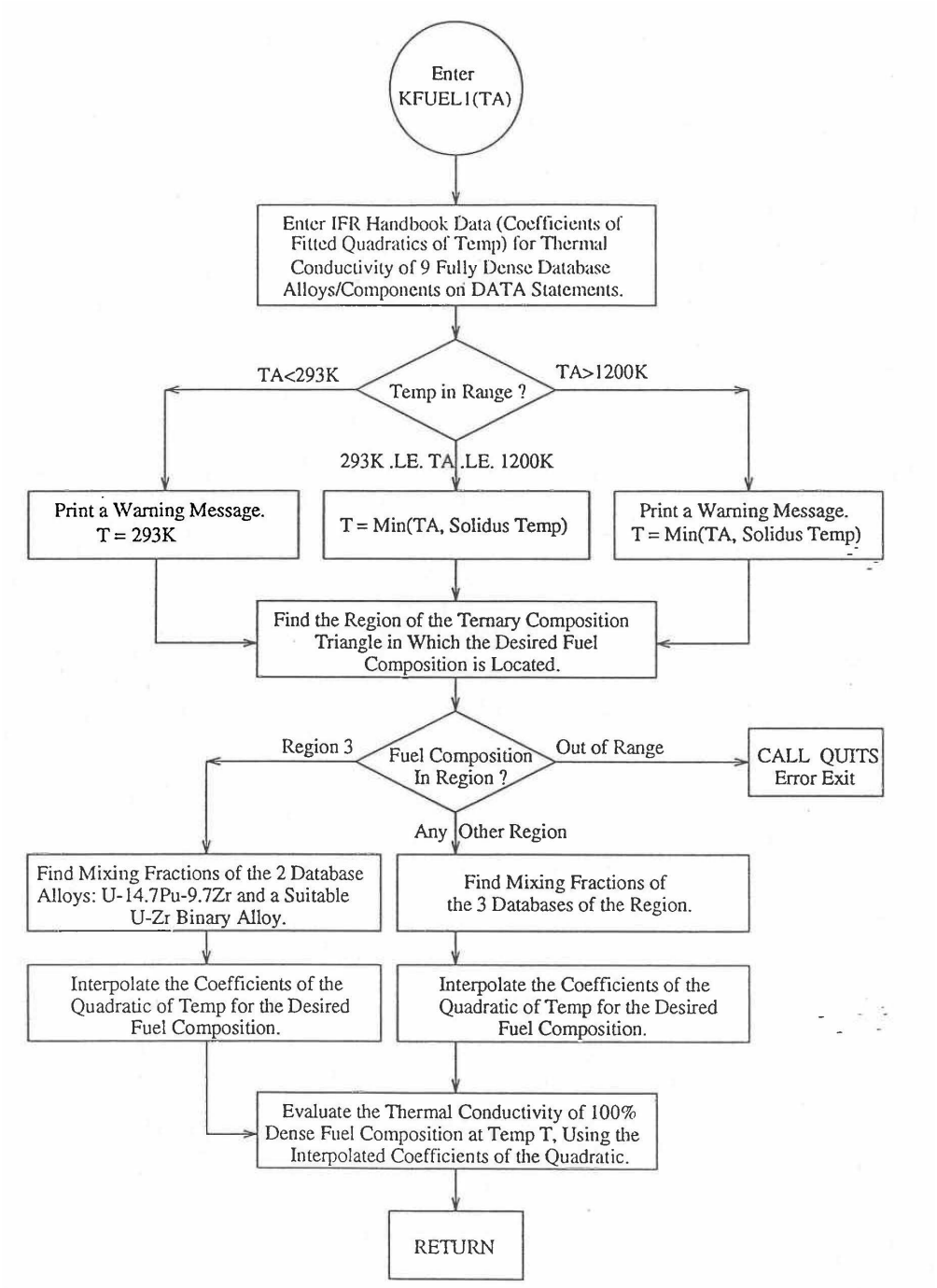

Fig. 10.3-53. Flow Diagram of Subroutine KFUEL1 for 100% Dense U-Pu-Zr Thermal Conductivity

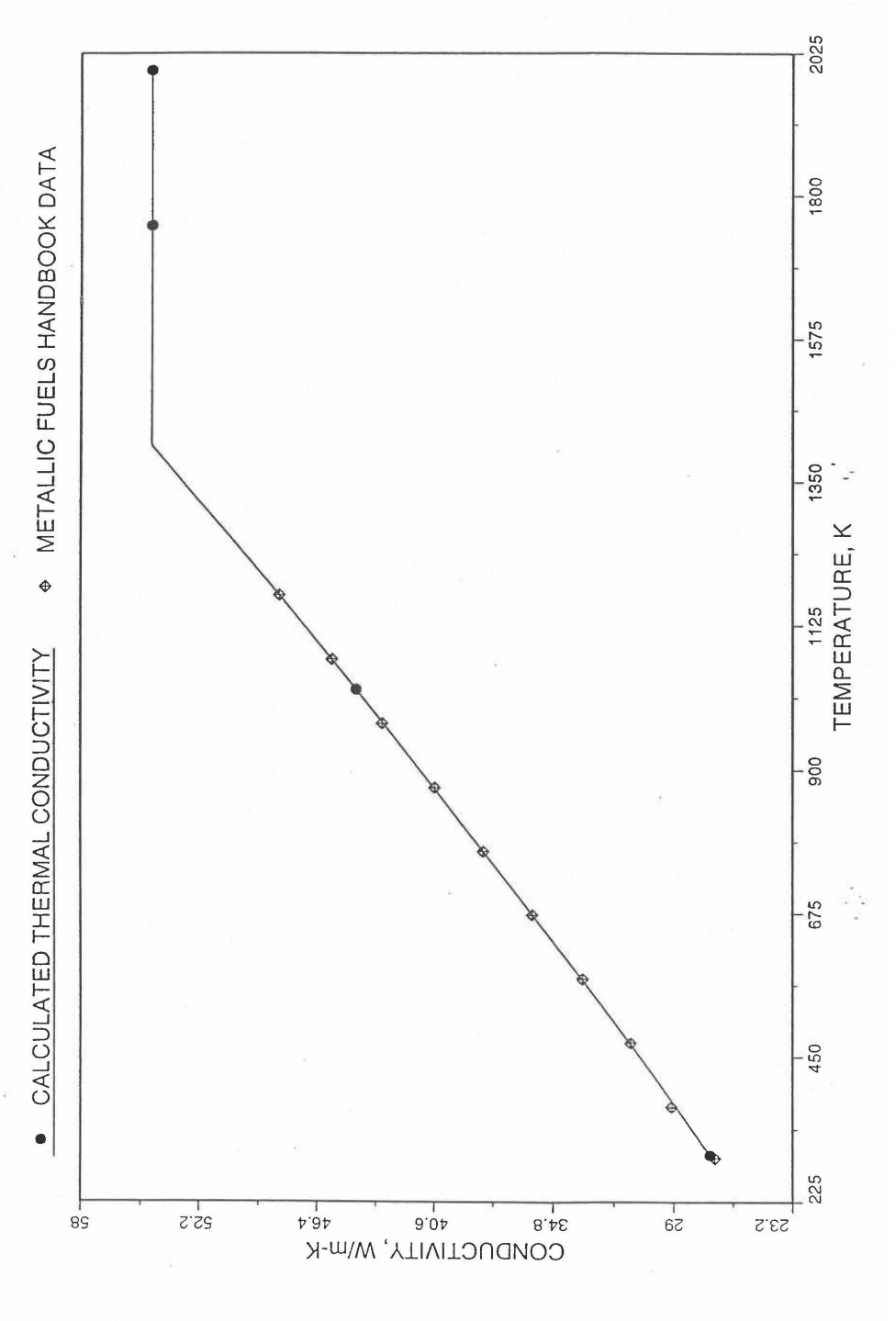

Fig. 10.3-54. Comparison of 100% Dense Uranium Metal Thermal Conductivity Data in IFR Handbook With Those Calculated by Subroutine KFUEL1

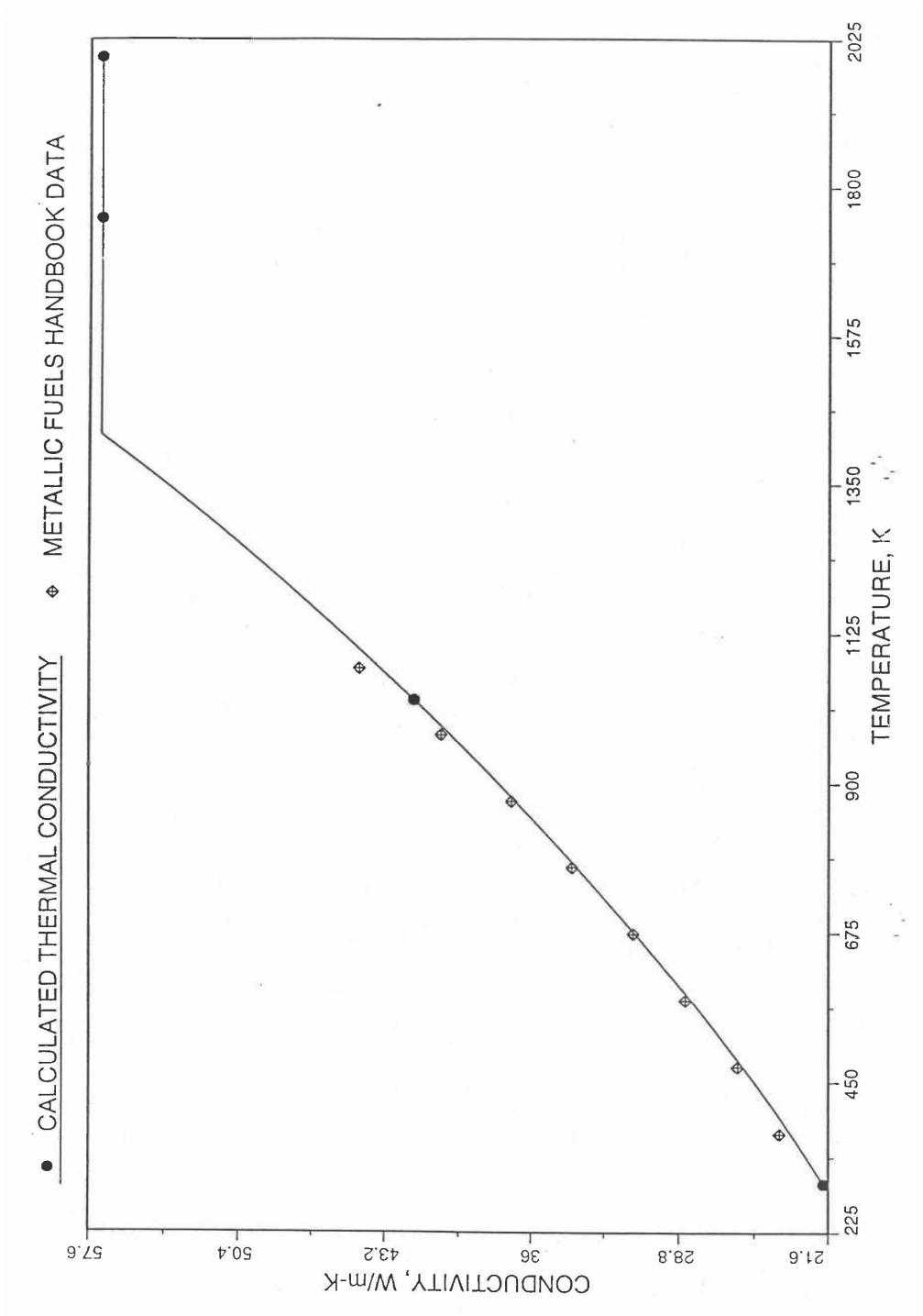

Fig. 10.3-55. Comparison of 100% Dense U-1.5Zr Fuel thermal Conductivity Data in IFR Handbook With Those Calculated by Subroutine KFUEL1

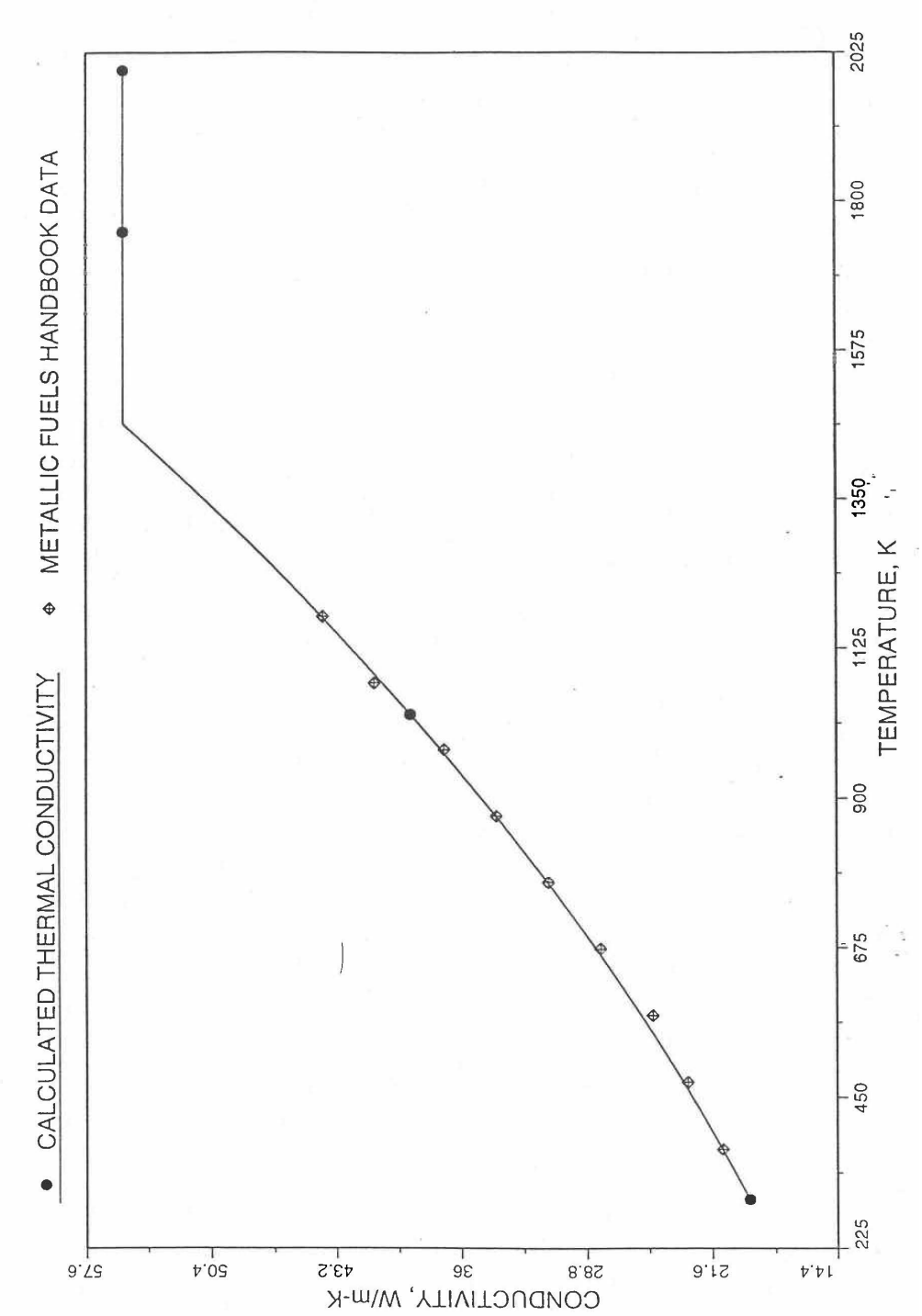

Fig. 10.3-56. Comparison of 100% Dense U-5.9Zr Fuel Thermal Conductivity Data in IFR Handbook With Those Calculated by Subroutine KFUEL1

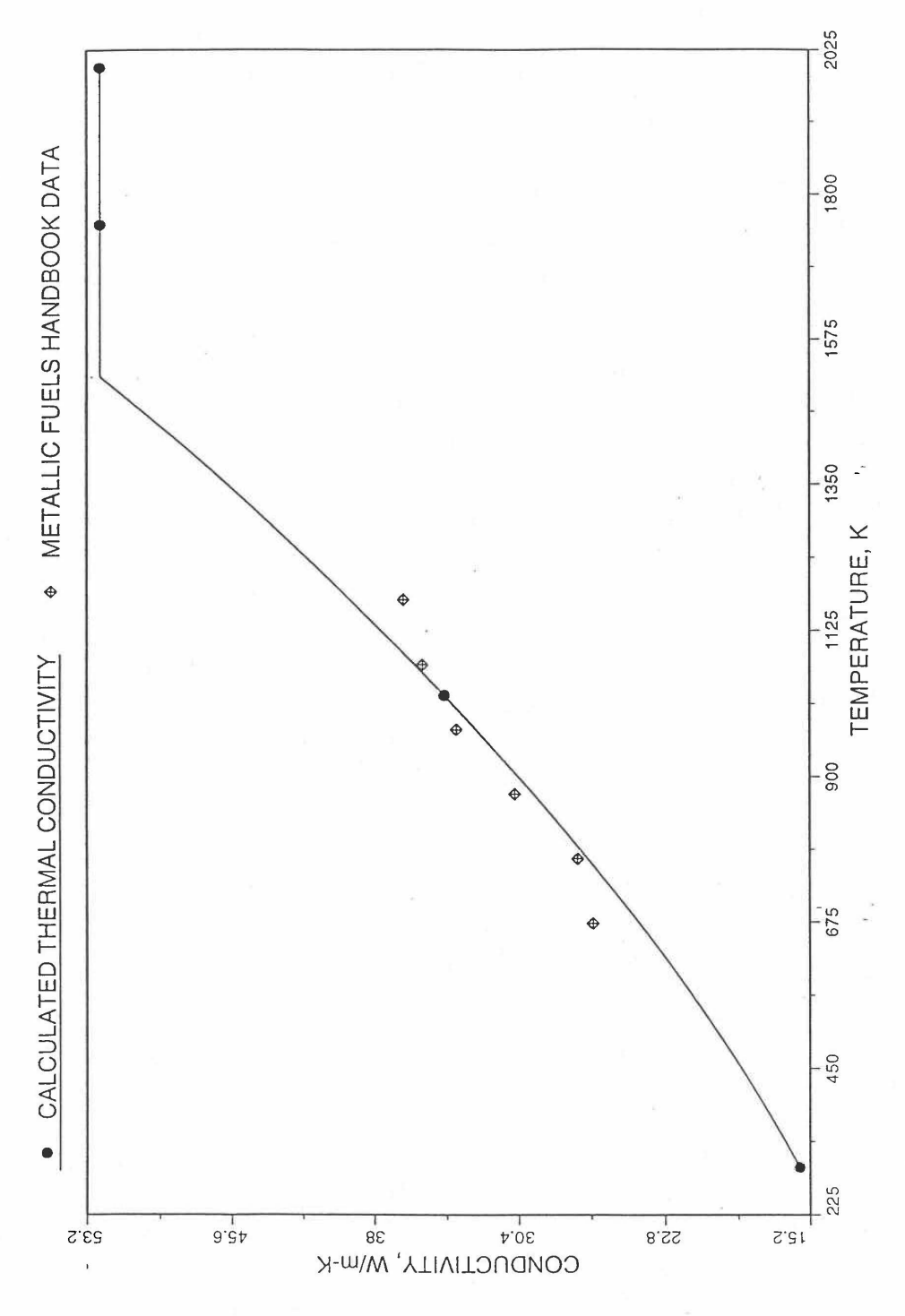

Fig. 10.3-57. Comparison of 100% Desense U-11.4Zr Fuel Thermal Conductivity Data in IFR Handbook With Those Calculated by Subroutine KFUEL1

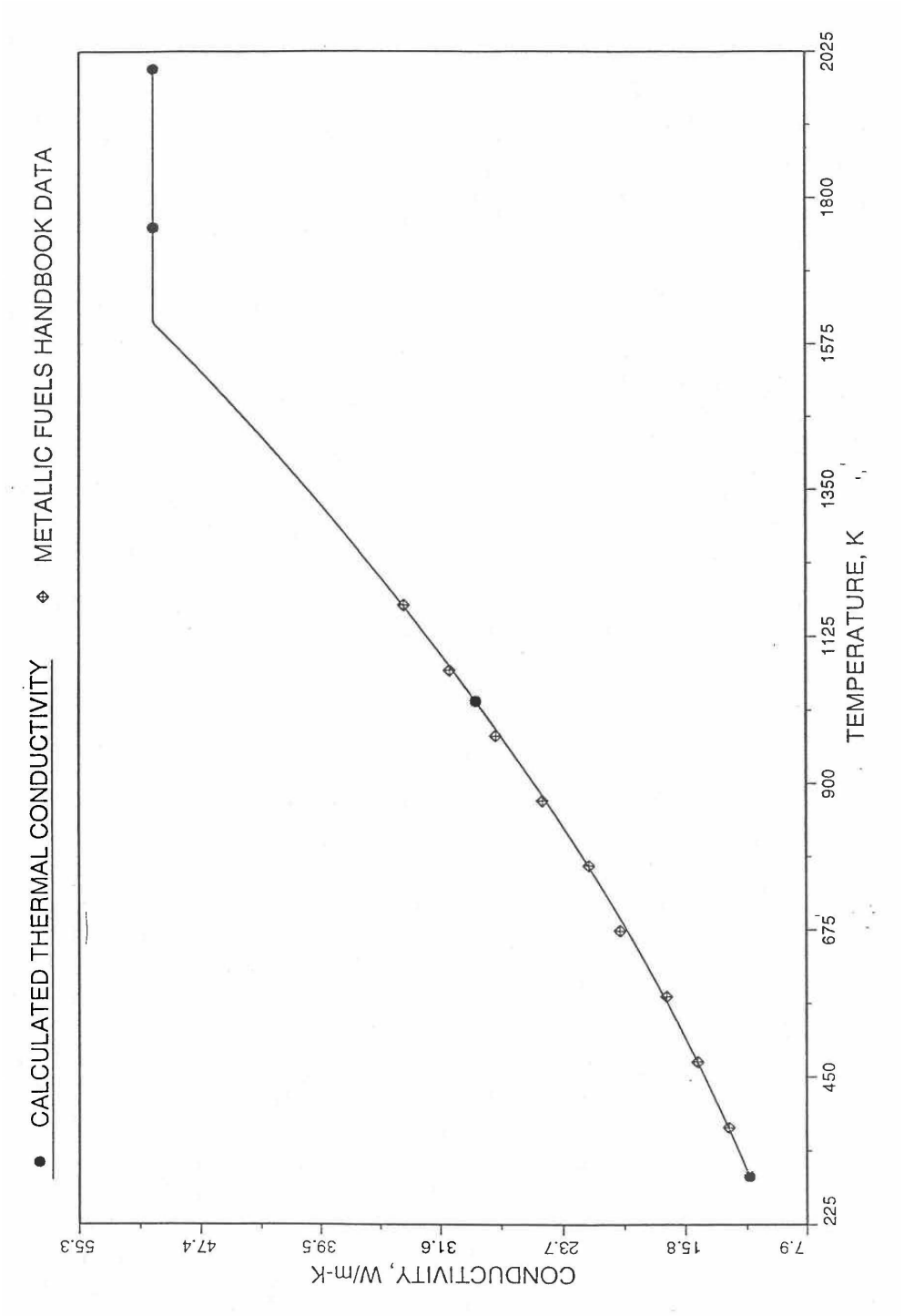

Fig. 10.3-58. Comparison of 100% Dense U-20Zr Fuel Thermal Conductivity Data in IFR Handbook With Those Calculated by Subroutine KFUEL1

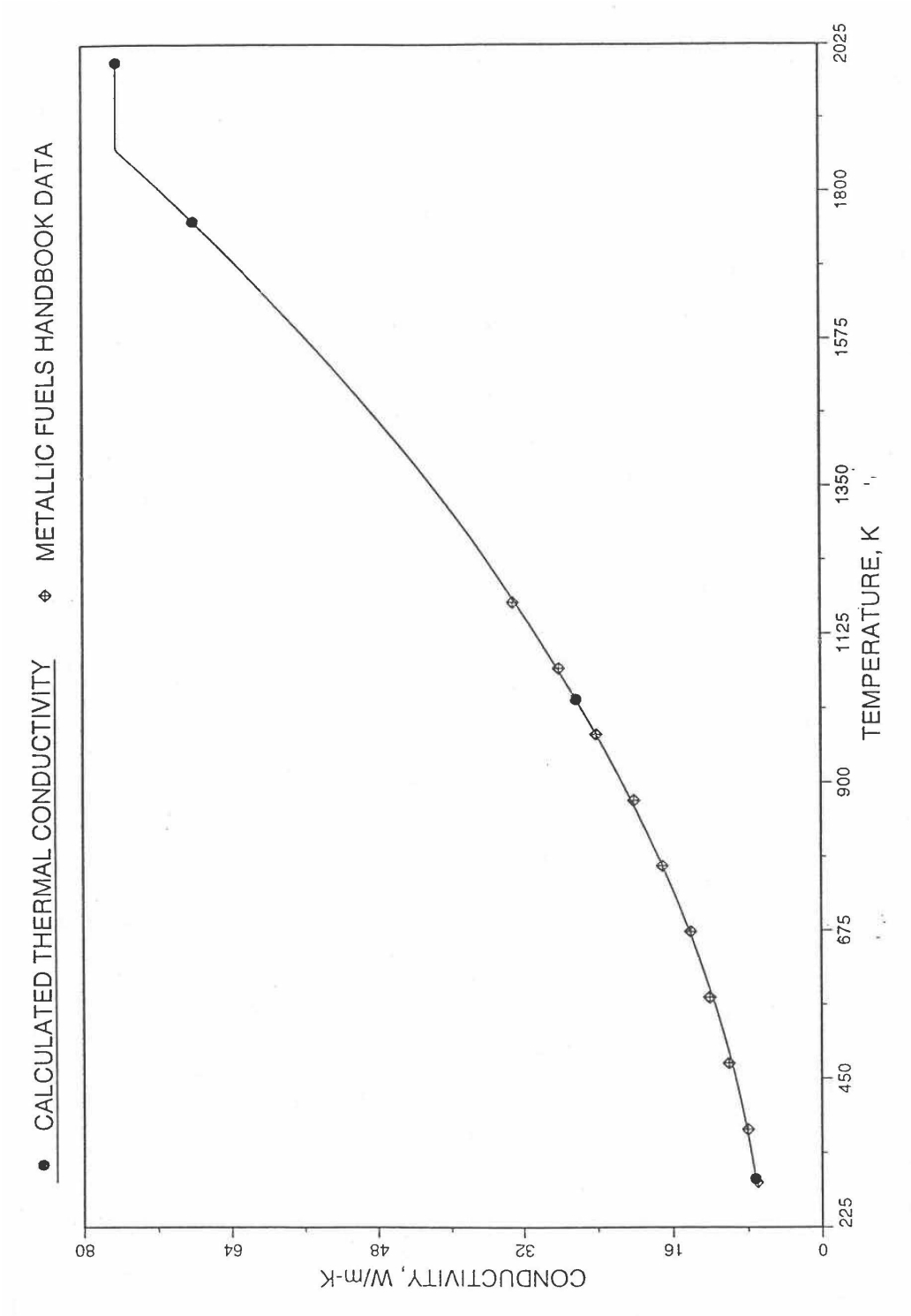

Fig. 10.3-59. Comparison of 100% Dense U-40Zr Fuel Thermal Conductivity Data in IFR Handbook With Those Calculated by Subroutine KFUEL1

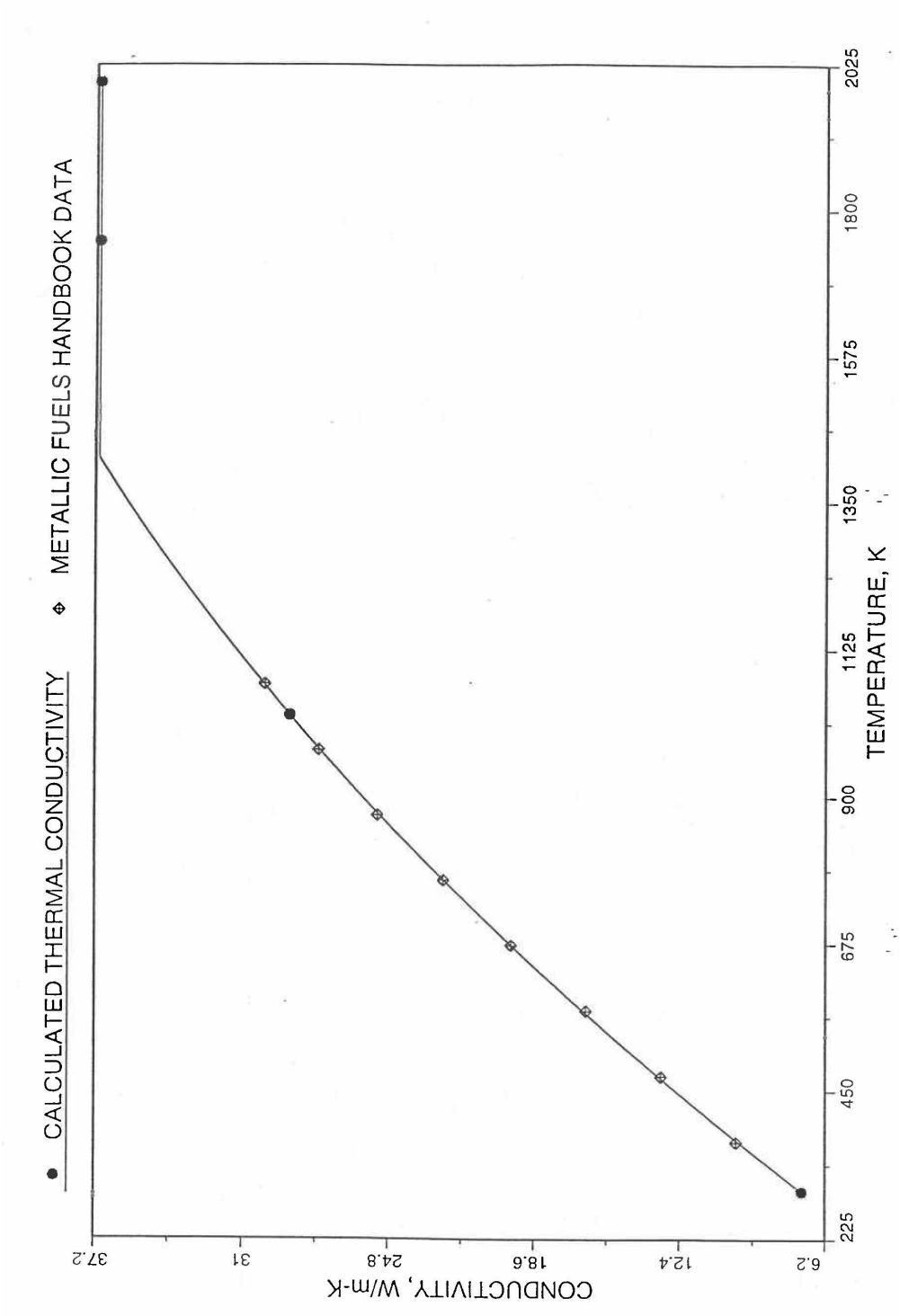

Fig. 10.3-60. Comparison of 100% Dense U-14.7Pu-9.7Zr Fuel Thermal Conductivity Data in IFR Handbook With Those Calculated by Subroutine KFUEL1

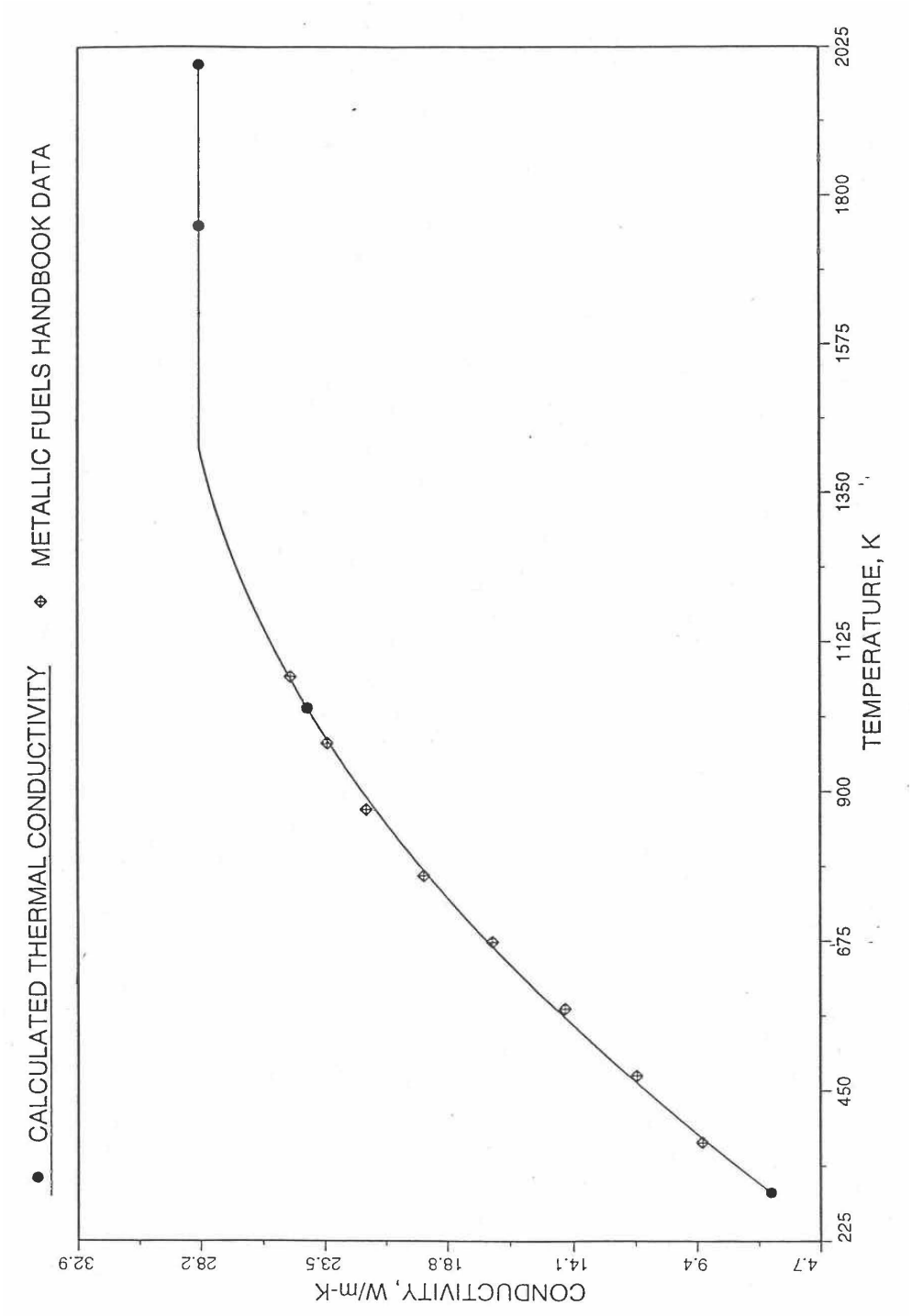

Fig. 10.3-61. Comparison of 100% Dense U-18.4Pu-11.5Zr Fuel Thermal Conductivity Data in IFR Handbook With Those Calculated by Subroutine KFUEL1

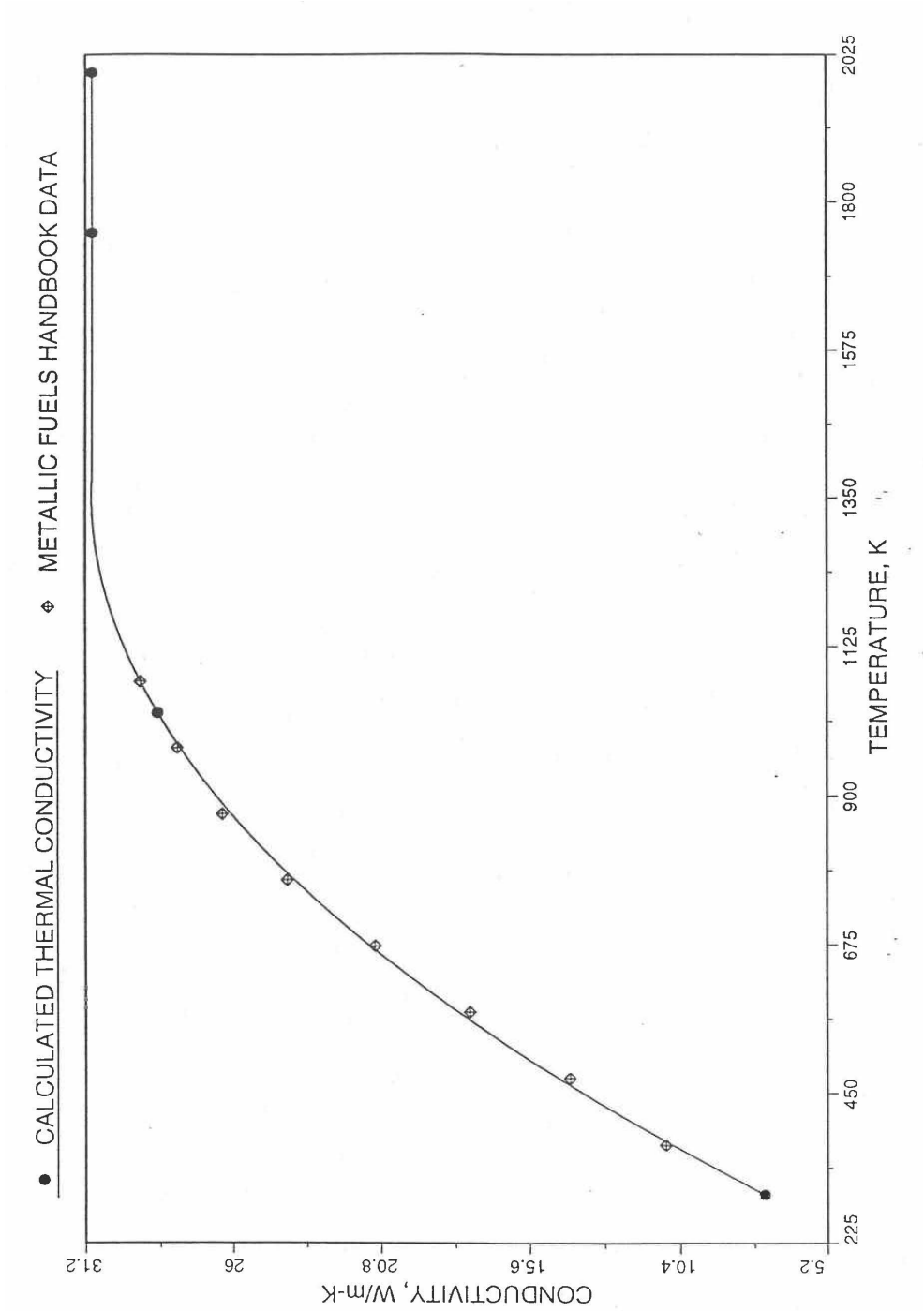

Fig. 10.3-62. Comparison of 100% Dense U-16.2Pu-6.2Zr Fuel Thermal Conductivity Data in IFR Handbook With Those Calculated by Subroutine KFUEL1

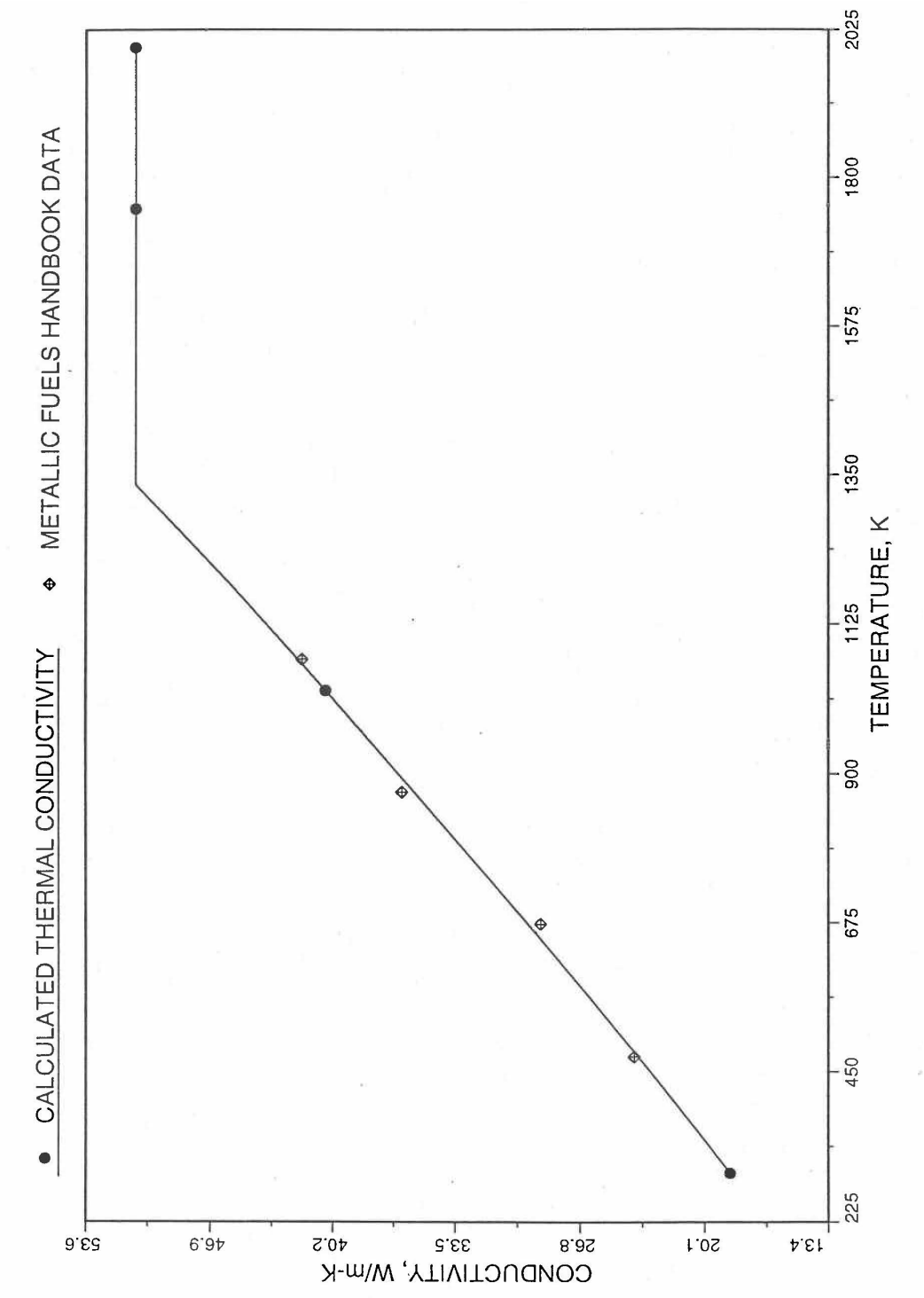

Fig. 10.3-63. Comparison of 100% Dense U-10Pu Fuel Thermal Conductivity Data With Those Calculated by Subroutine KFUEL1

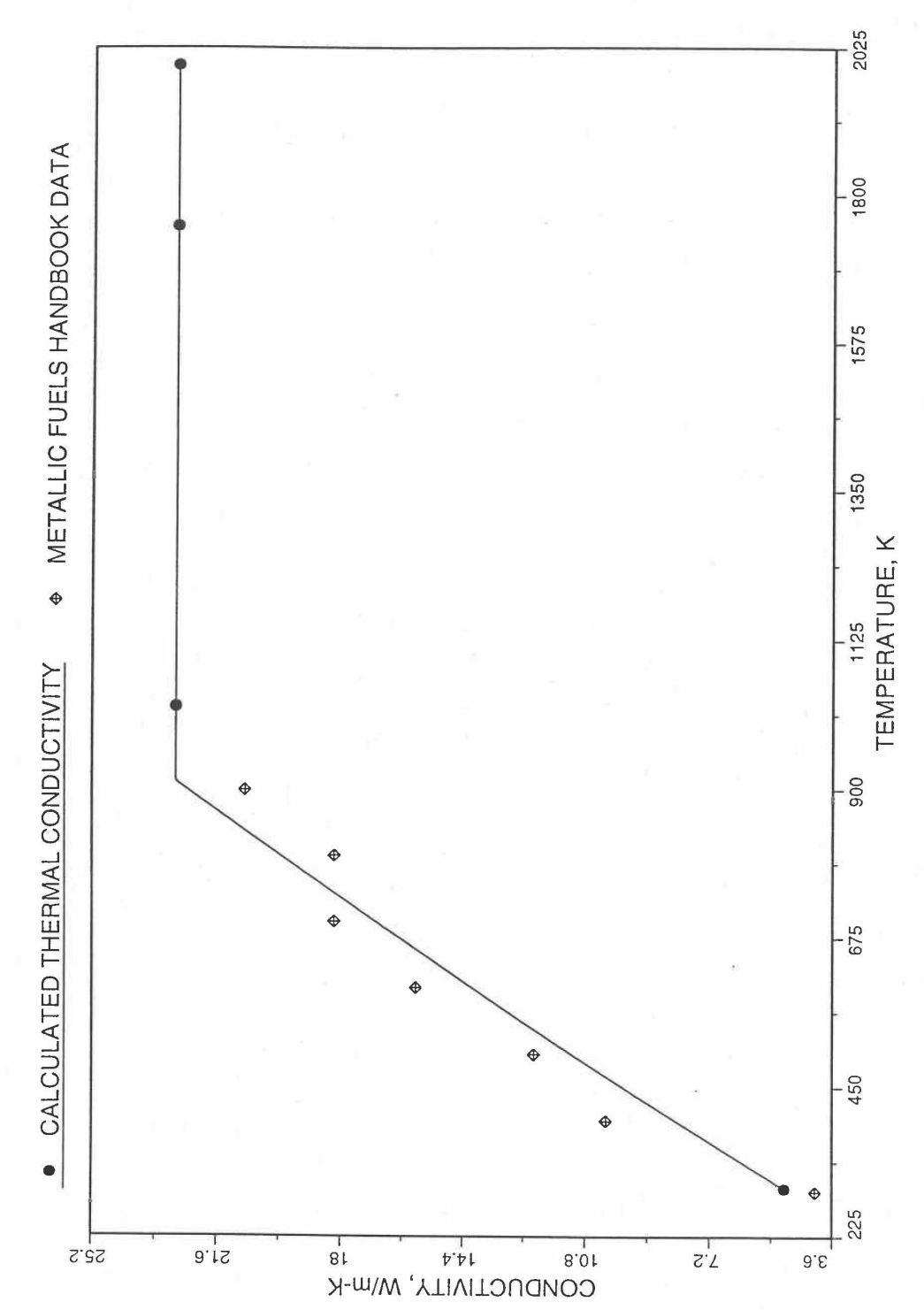

Fig. 10.3-64. Comparison of 100% Dense Pu Metal Thermal Conductivity Data in Plutonium Handbook With Those Calculated by Subroutine KFUEL1

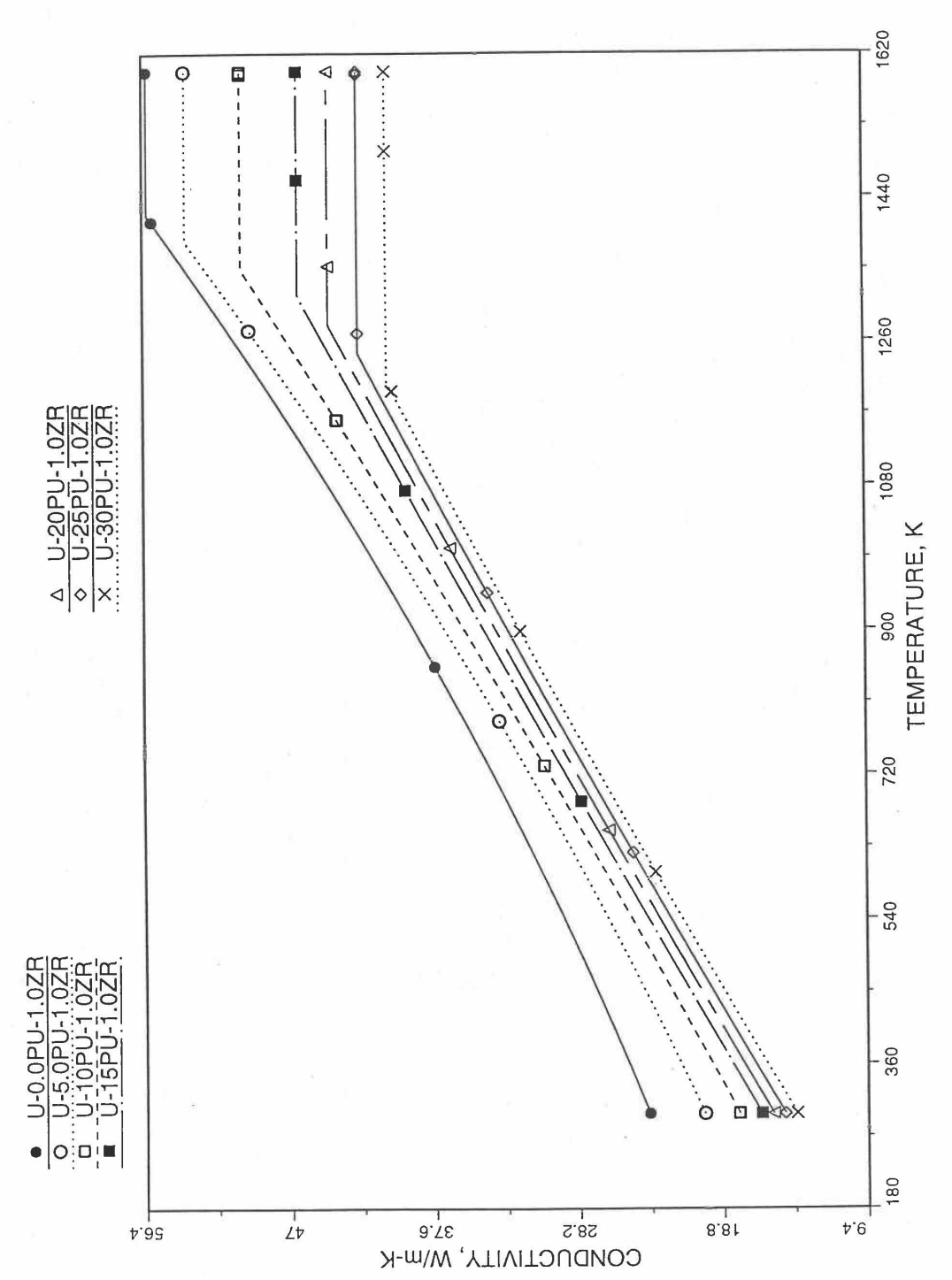

Fig. 10.3-65. Thermal Conductivity of 100% Dense U-Pu-1.0Zr Alloy Fuel, Obtained From Regionwise Interpolation of IFR Handbook Data

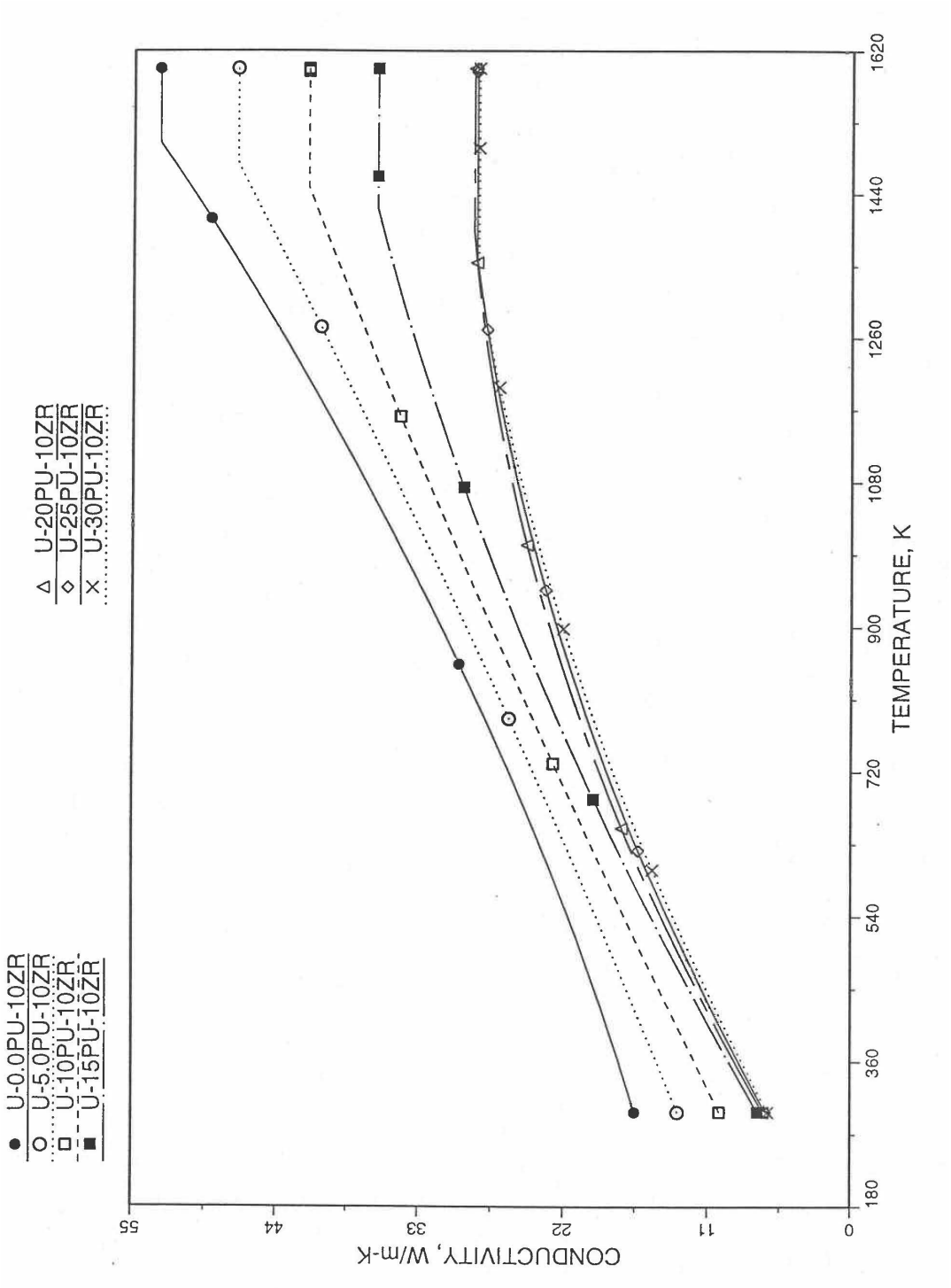

Fig. 10.3-66. Thermal Conductivity of 100% Dense U-Pu-10Zr Alloy Fuel, Obtained From Regionwise Interpolation of IFR Handbook Data

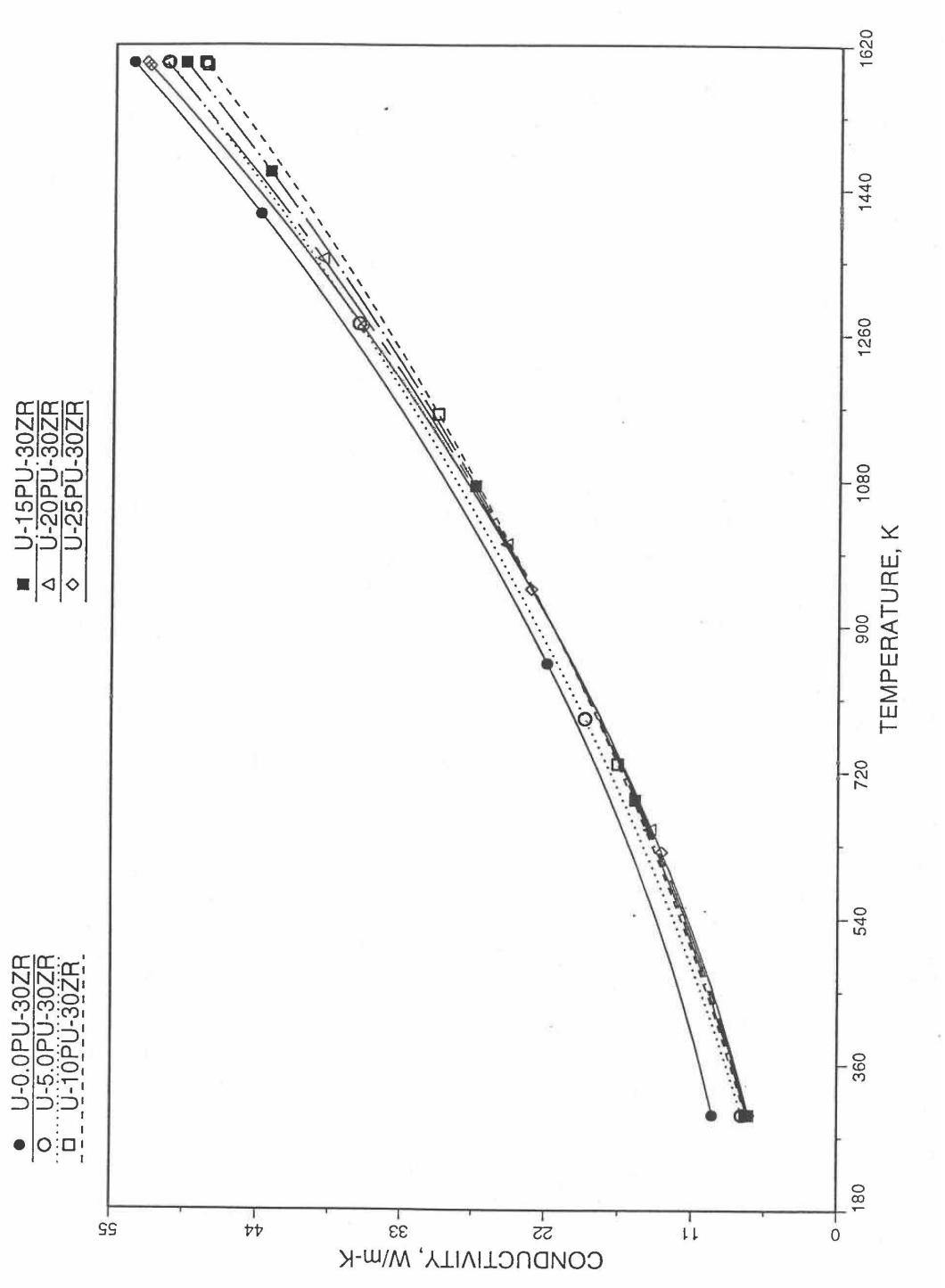

Fig. 10.3-67. Thermal Conductivity of 100% Dense U-Pu-30Zr Alloy Fuel, Obtained From Regionwise Interpolation IFR Handbook Data

10.3.2.6 Burnup or Porosity Correction of Thermal Conductivity

The calculation of thermal conductivity of unirradiated 100% dense U-Pu-Zr alloy fuel as a function of composition and temperature is described in Section 10.3.2.5. The thermal conductivity also depends strongly on the fission gas-filled and logged sodium-filled porosities that form in the fuel during normal steady-state irradiation. This section describes the following two methods that are used in the SAS4A/SASSYS-1 codes to correct the thermal conductivity of 100% dense U-Pu-Zr alloy fuel for fission gas-filled and logged sodium-filled porosities:

(i) an empirical method based on experimental data for U-Fs alloy fuel thermal conductivity change with burnup in EBR-II,
(ii) a theoretical method [10-4, 10-26] that explicitly accounts for the gas-and sodium-filled porosities.

These two options are controlled through the input parameter KFIRR.

10.3.2.6.1 Empirical Correction Based on Average Burnup

No experimental data are available for the effects of irradiation on the thermal conductivity of U-Pu-Zr ternary or U-Zr binary alloy fuel. It is assumed that U-Pu-Zr ternary and U-Zr binary alloy fuels behave during steady-state irradiation in a similar manner to U-5Fs fuel Fig. 10-3-65 (for which data re available) with regard to fission gas-induced swelling and sodium logging. The empirical correction factor, i.e., the irradiated-to-unirradiated thermal conductivity ratio, obtained from the analysis of experimental data [10-27 to 10-29] for the effects of irradiation on U-5Fs fuel thermal conductivity, is also used in the Metallic Fuel Handbook [10-8] for the U-Pu-Zr alloy and U-Zr alloy fuels.

A number of irradiation-induced phenomena tend to lower the thermal conductivity of U-5Fs fuel from start-up to about 2 at. % burnup. During this period irradiation, the fuel porosity is not interlinked. Fission gas bubbles and thermal stress-induced microcracking lower the fuel density and thermal conductivity; solid and liquid fission-products buildup tends to lower the thermal conductivity in much the same way as increasing amounts of fissium lower the conductivity; and irradiation damage tends to degrade the thermal conductivity. But the dominant mechanism accounting for the degradation of U-5Fs thermal conductivity from start-up to about 2 at. % burnup is assumed to be the decrease in fuel density due to fission gas-induced swelling and microcracking. Based on the experimental data of diNovi [10-27] and Beck and Fousek [10-28] reviewed in the Metallic Fuels Handbook [10-8], the recommended porosity correction factor, i.e., the irradiated-to-unirradiated thermal conductivity ratio is

$$\frac{K}{K_o} = \frac{1 - P'}{1 + 1.7P'} \tag{10.3-69}$$

where

P' = porosity fraction relative to the initial 100% dense fuel volume,

K = thermal conductivity of irradiated fuel,

K_o = thermal conductivity of unirradiated 100% dense fuel.

The interlinkage of fission gas bubbles is assumed to occur at 2 at. % burnup. Beyond 2 at. % burnup, the effective thermal conductivity tends to increase due to sodium logging and fuel hot pressing, and tends to decrease due to solid and liquid fission-products buildup. But the ingress of bond sodium into the bubbles dominates and improves the thermal conductivity somewhat, as suggested by the in-core measurements of Betten [10-29]. He has reported U-5Fs fuel and coolant thermocouple measurements in an instrumented subassembly, as a function of time to a peak subassembly burnup of 8.8 at. %. From startup to 2 at. % burnup, U-5Fs fuel thermal conductivity shows the expected decrease with burnup due to porosity formation, and the irradiated-to-unirradiated thermal conductivity ratio takes a minimum value of 0.475 with a standard deviation of 0.111. Beyond 2 at. % burnup, the thermocouple measurements show an improvement in the effective thermal conductivity, which levels off, after about 5 at. % burnup, to a steady-state value. The long-time value of U-Fs fuel irradiated-to-unirradiated thermal conductivity ratio is 0.72 with a standard deviation of 0.06.

The minimum value (just before porosity interlinkage at 2 at. % burnup) of irradiated-to-unirradiated thermal conductivity ratio, recommended in the Metallic Fuels Handbook [10-9], for U-Zr binary and U-Pu-Zr ternary fuels is 0.5. The porosity fraction P', corresponding to this value (i.e., 0.5) of the ratio K/K_o is obtained from Eq. (10.3-69) to be 0.27. Following a recent recommendation by Billone [10-21] used in Mark-V fuel safety calculations, the porosity fraction is assumed to vary linearly with burnup during early irradiation before porosity interlinkage, equaling 0.27 at 2 at. % burnup.

$$P' = 0.135 Bu, \qquad Bu \le 2\, at,\% \tag{10.3-70}$$

where

Bu = fuel burnup, at. %.

The long-time value (after porosity interlinkage, sodium logging and fuel hot pressing at burnups beyond 5 at. %) of irradiated-to-unirradiated thermal conductivity ratio, recommended in the IFR Handbook, for U-Zr and U-Pu-Zr fuels is 0.7.

The above conclusions about the empirical correction of U-Pu-Zr alloy fuel thermal conductivity for the effects of steady-state irradiation can be summarized as follows:

$$\frac{K}{K_o}=\begin{cases}\left(1-P'\right)/\left(1+1.7P'\right), & Bu\le 2\,at.\% \\ 0.5+0.0667\left(Bu-2\right), & 2<Bu\le 5\,at.\% \\ 0.7, & Bu>5at.\%\end{cases} \tag{10.3-71}$$

10.3.2.6.2 Theoretical Correction Based on Sodium- and Gas-Filled Porosities

The fuel develops fission gas-filled porosities during steady-state operation of the reactor. The bond sodium used in the fuel-cladding gap of U-Pu-Zr alloy fuel pins can also migrate into the fuel and fill some of the porosities of the fuel after porosity interlinkage. The gas-filled porosities tend to decrease the fuel thermal conductivity whereas the sodium-filled porosities tend to increase it. The empirical correction based on average fuel burnup is suitable for transient calculations in which fuel porosity and sodium logging fraction do not change during the transient. If the distributions of fuel porosity and sodium logging fraction change during the transient, a method of correcting fuel thermal conductivity for irradiation effects that explicitly accounts for sodium- and gas-filled porosities is required. In this section a formula is derived for the evaluation of these two effects using a generalization of the method given in Ref. [10-26] for single type of porosity.

Assuming all the gas-filled pores to be cubes of the same size (side a_1) and all the sodium-filled pores to be cubes of another size (side a_2), a unit cell of the porous metallic fuel is constructed that contains a single gas-filled pore and a single sodium-filled pore as shown in Fig. 10.3-68. The unit cell is a cube of side L and contains fully dense fuel surrounding the pores. In a real material the pores are not uniformly arranged like atoms in a crystal lattice; so the amount of solid fuel in the unit cell represents an average value. Assuming the heat flow in the y-direction only, the total heat flow through the front x-z face of the unit cell passes through three heat flow paths in parallel: (1) the pore tube containing the gas-filled pore (see Fig. 10.3-68), (2) the pore tube containing the sodium-filled pore, and (3) the remaining frontal are of the fully dense fuel of thermal conductivity K_s. The effective thermal conductivity of the unit cell in the y-direction is given by

$$K = P_{c1}\,K_{pt1} + P_{c2}\,K_{pt2} + \left(1-P_{c1}-P_{c2}\right)K_s \tag{10.3-72}$$

where

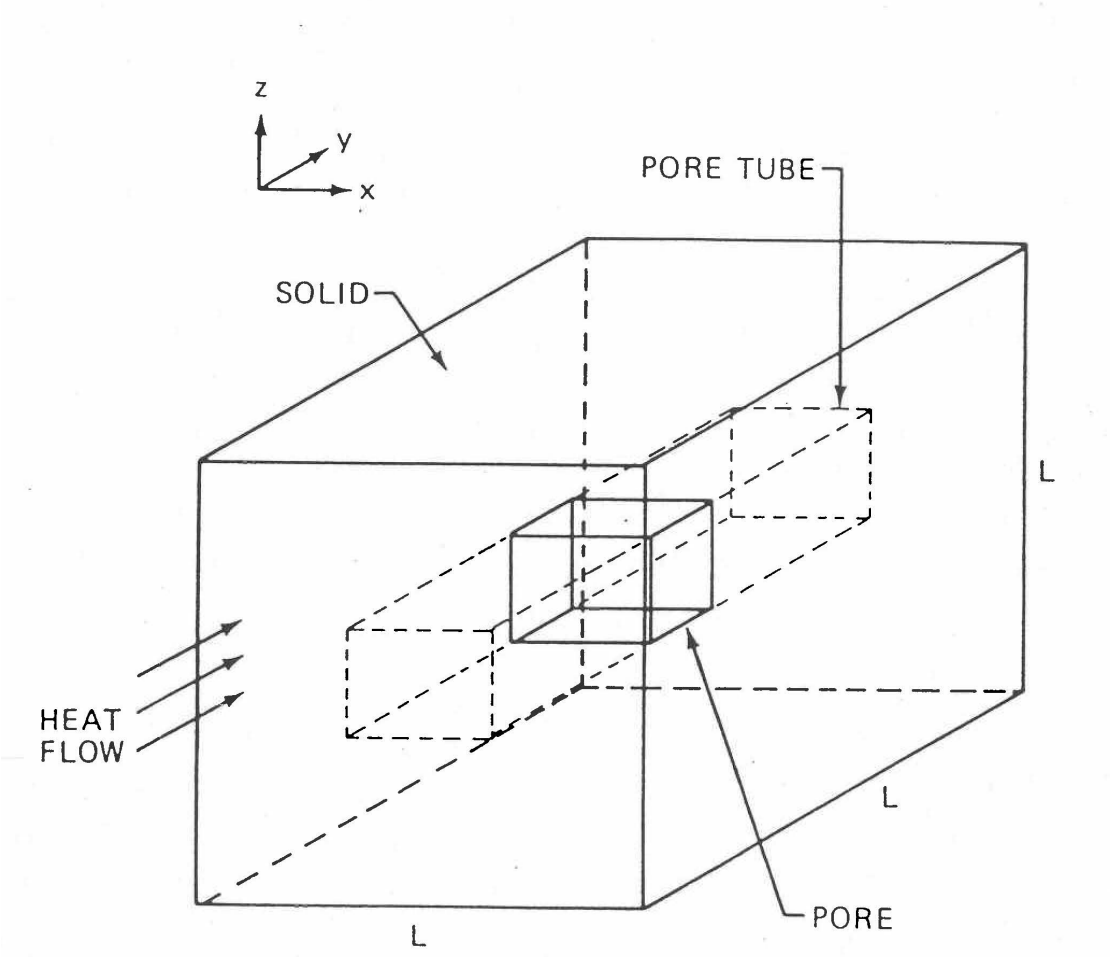

Fig. 10.3-68. A Unit Cell of Porous Metallic Fuel Containing a Sodium-Filled Pore and a Gas-Filled Pore (Only One Pore is Shown for Clarity)

K = effective thermal conductivity of the fuel containing sodium-and gas-filled porosities.

P_{c1}, P_{c2} = fractions of the area of the x-z face of the unit cell that are occupied respectively by the gas-filled pore and the sodium-filled pore,

K_{pt1}, K_{pt2} = apparent thermal conductivities of the pore tubes containing the gas-filled pore and the sodium-filled pore.

The apparent thermal conductivity of a pore tube can be evaluated from the formula for two thermal resistances in series in the y-direction: (1) the pore proper, and (2) the solid fuel contained in the pore tube. For the two pore tubes one obtains the following equations:

$$\frac{1}{K_{pt1}} = \frac{P_{L1}}{K_g} + \frac{1 - P_{L1}}{K_s} \tag{10.3-73}$$

$$\frac{1}{K_{pt2}} = \frac{P_{L2}}{K_{Na}} + \frac{1 - P_{L2}}{K_s} \tag{10.3-74}$$

where

P_{L1}, P_{L2} = fractions of the side of the unit cell in the y-direction that are occupied respectively by the gas-filled pore and the sodium-filled pore,

K_g = thermal conductivity of the fission gas contained in the gas-filled pore,

K_{Na} = thermal conductivity of the sodium contained in the sodium-filled pore.

Neglecting K_g in comparison to K_s and K_{Na}, and solving Eq. (10.3-73) for K_{pt1}, it is found that K_{pt1} is zero. Substituting this value of K_{pt1} and the value of K_{pt2} obtained from Eq. (10.3-74) into Eq. (10.3-72), the effective thermal conductivity of the pours fuel can be written

$$\frac{K}{K_s} = \frac{P_{c2} K_{Na}}{K_s P_{L2} + \left(1 - P_{L2}\right) K_{Na}} + 1 - P_{c1} - P_{c2} \tag{10.3-75}$$

The gas-filled volume porosity, P_g, and the sodium-filled volume porosity, P_{Na}, can be written as

$$P_g = P_{c1} P_{L1} \tag{10.3-76}$$

$$P_{Na} = P_{c2}\, P_{L2} \tag{10.3-77}$$

For the cubic gas-filled pore of side a_1 shown in Fig. (10.3-68),

$$P_{c1} = \frac{a_1^2}{L^2} \tag{10.3-78}$$

$$P_{L1} = \frac{a_1}{L} \tag{10.3-79}$$

Equations (10.3-76), (10.3-78) and (10.3-79) give the following relations of P_{c1} and P_{L1} to the gas-filled volume porosity P_g.

$$P_{c1} = P_g^{2/3} \tag{10.3-80}$$

$$P_{L1} = P_g^{1/3} \tag{10.3-81}$$

Similarly, P_{c2} and P_{L2} can be related to the sodium-filled volume porosity, P_{Na}, as follows:

$$P_{c2} = P_{Na}^{2/3} \tag{10.3-82}$$

$$P_{L2} = P_{Na}^{1/3} \tag{10.3-83}$$

Substituting Eqs. (10.3-80), (10.3-82) and (10.3-83) into Eq. (10.3-75), the effective thermal conductivity of the porous fuel can be written as

$$\frac{K}{K_s} = 1 - P_g^{2/3} + \frac{P_{Na}^{2/3}}{\left(K_s / K_{Na}\right) P_{Na}^{1/3} + \left(1 - P_{Na}^{1/3}\right)} - P_{Na}^{2/3} \tag{10.3-84}$$

Equation (10.3-84) gives the effect of sodium- and gas-filled porosities on fully dense fuel thermal conductivity. It is noted that Eq. (10.3-84) satisfies two limiting conditions: (1) in the absence of any logged sodium in the fuel, the ratio K/K_s equals the known reduction factor of $1 - P_g^{2/3}$ [10-26], and (2) if K_{Na} is set equal to K_s in Eq. (10.3-84), the last two terms on the right-hand side cancel to make K/K_s again equal to $1 - P_g^{2/3}$ which is expected when the sodium and the fully dense fuel behave alike and gas-filled porosity is the only nonconductive porosity in the material.

10.3.2.7 Uncertainties of U-Pu-Zr Fuel Thermal Conductivity

The uncertainties of U-Pu-Zr fuel thermal properties are important in the design and safety analyses of the Integral Fast Reactor (IFR). The purpose of the present section is to set the uncertainties of U-Pu-Zr fuel thermal conductivity that are used in the SAS4A/SASSYS-1 codes.

The uncertainties of U-Pu-Zr fuel thermal conductivity depend on burnup, and therefore the discussion of the subject is divided into two parts: (1) unirradiated U-Pu-Zr fuel, and (2) irradiated U-Pu-Zr fuel. As it will be seen below, the subject of uncertainties of U-Pu-Zr fuel thermal conductivity is a difficult one because of the limited data, and technical judgment has been used in the IFR Metallic Fuels Handbook [10-8, 10-9] to estimate uncertainties in a number of cases.

10.3.2.7.1 Unirradiated U-Pu-Zr Fuel

For evaluating composition- and temperature-dependent U-Pu-Zr fuel thermal conductivity, the IFR Handbook [10-8, 10-9] data have been incorporated into the SAS4A/SASSYS-1 codes. This evaluation uses a method of regionwise interpolation among quadratic fits to 9 basic unirradiated alloy/component data and Handbook U-Zr binary correlation [10-8]. The quadratic fits of the basic alloy data are done in the temperature variable. Table 10.3-7 lists the accuracy of the data for these 9 basic alloys/components, the maximum errors in the quadratic fits to these data, and the accuracy of the binary correlation. It should be pointed out that two of the required database alloys/components are taken from sources other than the Handbook, and a warning message is printed by the codes then these data are actually used in any calculation. The accuracy of data given in Table 10.3-7 is taken to represent 2 standard deviations (95% confidence limits) because accuracy implies that almost all the data lies within the accuracy band [10-31]. Assuming the accuracy to represent 1 standard deviation would imply that only about two-thirds of the data lies inside the accuracy band and about one-third of the data lie outside, and under this assumption almost all the data would not lie within the accuracy band. The maximum error in quadratic fits given in Table 10.3-7 is also taken to represent 2 standard deviations because all the data actually lies within the maximum error band above and below the fitted quadratic equation in temperature. Assuming the maximum error to represent 3 standard deviations is also justified but this is not done here. Statistically combining the accuracy of data and the error in quadratic fit for each database alloy/component (i.e., square-root of the sum of squares of percent accuracy and percent error), one obtains the combined uncertainty given in the last column of Table 10.3-7. The Pu metal has the largest combined 2-sigma uncertainty of 21.9% but most of this uncertainty arises from the error in the quadratic fit. If the 19.9% maximum error in Pu metal quadratic fit were assumed to represent 3 standard deviations, the combined 1-sigma uncertainty would become $[(19.9/3)^2 + (9.2/2)^2]^{1/2} = 8.1\%$. Thus Table 10.3-7 shows that the combined 1-sigman uncertainty can be taken as 10% for unirradiated U-Pu-Zr fuels. This also agrees with the conclusion of Ref. [10-21].

Table 10.3-7. Accuracy of Unirradiated 100% Dense U-Pu-Zr Alloy/Component Thermal Conductivity Data Used in the Method of Regionwise Interpolation

No.	Alloy/Component	Source of Data	Accuracy of Data	Max. Error in Quadratic Fit	Combined 2-sigma Uncertainty, %
1	U metal	Handbook	±20% [a]	0.72%	20.0
2	U-1.5 Zr	Handbook	±20% [a] ±5% [Ref 10-18]	0.41%	20.0
3	U-20 Zr	Handbook	±20% [a]	1.71%	20.1
4	U-40 Zr	Handbook	±20% [a]	3.13%	20.2
5	U-14.7Pu-9.7Ar	Handbook	±20% [a]	1.18%	20.0
6	U-18.4Pu-11.5Zr	Handbook	±20% [a]	2.57%	20.2
7	U-10Pu	Ref. [10-21]	Not reported	2.34%	--
8	Pu metal	Ref. [10-23]	±9.2% [b]	19.9%	21.9
9	U-16.2Pu-6.2Zr	Handbook	±20% [a]	2.74%	20.2
10	Handbook Binary Correlation	Handbook	±20% [a]	[c]	20.0

[a]Assumed in the Metallic Fuels Handbook [10-8].

[b]Based on two theoretical calculations of conductivity.

[c]The quoted accuracy includes fitting error also.

10.3.2.7.2 Irradiated U-Pu-Zr Fuel

No data is available for the thermal conductivity of irradiated U-Zr binary or U-Pu-Zr ternary fuel [10-8, 10-9]. But data are available for irradiated U-5Fs fuel from 3 experimental sources that are reviewed in the Handbook. It is assumed in the Handbook that U-Zr and U-Pu-Zr fuels behave similar to U-5Fs fuel during irradiation, and the same burnup correction factor may be used for all these fuels. The minimum value (just before porosity interlinkage) for irradiated-to-unirradiated thermal conductivity ratio, K/K_o, recommended in the Handbook for U-Zr binary and U-Pu-Zr ternary fuels is 0.5 ± 0.1. This recommendation is based on rounding off the mean value of this ratio (K/K_o just before porosity interlinkage) and its standard deviation, 0.475 ± 0.111, reported by Betten [10-29] in one of the 3 experimental sources. This implies a standard deviation of 23.4%. The porosity interlinkage occurs in the 1-2 at. % burnup range [10-8, 10-9, 10-29], and it is assumed to occur at 2 at. % burnup in the SAS4A/SASSYS-1 codes, following a recent recommendation by Billone [10-21] used in Mark V fuel safety calculations. The standard deviation is assumed to vary linearly with burnup between unirradiated fuel and porosity interlinkage, i.e., zero to 2 at. %.

The long-time value (after porosity interlinkage, sodium logging and fuel hot pressing) for irradiated-to-unirradiated thermal conductivity ratio, K/K_o, recommended in the Handbook [10-9] for U-Zr and U-Pu-Zr fuels is 0.7 ± 0.1. This implies a standard deviation of 14.3%. The plots of K/K_o versus burnup given in Betten's experimental work [10-29] show that this long-time value is practically attained at about 5 at. % burnup. This value has also been recommended for Mark V fuel safety calculations [10-21]. The value of K/K_o and its standard deviation remain constant above this burnup as shown by the plots given in Betten's experimental work [10-29]. The standard deviation is assumed to vary linearly with burnup between porosity interlinkage and the long-time value attainment, i.e., 2 at. % to 5 at. %.

The conclusions made above about 1-sigma uncertainty can be summarized as follows:

$$1-\sigma \text{ uncertainties} = \begin{cases} \text{Varies linearly from 10\% to 23.4\% as burnup} \\ \qquad \text{varies from 0 to 2 at.\%,} \\ \text{Varies linearly from 23.4\% to 14.3\% as burnup} \\ \qquad \text{varies from 2 to 5 at.\%,} \\ \text{14.3\% for burnup greater than 5 at.\%.} \end{cases} \tag{10.3-85}$$

At present the following values of 1-sigma uncertainty have been incorporated in the SAS4A/SASSYS-1 codes. These values are rounded off and slightly higher than those concluded above. These values are also identical to the uncertainties recommended for Mark V fuel safety calculations [10-21].

$$1-\sigma \text{ uncertainties} = \begin{cases} \text{Varies linearly from 10\% to 25\% as burnup} \\ \text{varies from 0 to 2 at. \%,} \\ \text{Varies linearly from 25\% to 15\% as burnup} \\ \text{varies from 2 to 5 at. \%,} \\ \text{15\% for burnup greater than 5 at. \%.} \end{cases} \quad (10.3\text{-}86)$$

10.3.3 Correlations of the Report ANL/RAS 85-19

This section describes the composition and temperature-dependent correlations for thermal properties of U-Pu-Zr alloy fuel which are used by the earlier SSCOMP model [10-4] and other SAS4A/SASSYS-1 modules. These correlations were developed prior to the issuing of the Metallic Fuels Handbook [10-9] in order to provide an early SAS4A/SASSYS-1 capability to compute U-Pu-Zr fuel behavior. These correlations for evaluating fuel thermal properties are specified by setting the input parameter IRHOK =1 and the input parameter IFUELM =1 in a channel.

10.3.3.1 Theoretical Density of U-Pu-Zr Fuel at 298K

The theoretical density of U-Pu-Zr fuel at a room temperature of 298K is estimated from the theoretical densities of U, Pu and Zr by assuming that there is no volume change due to alloying of the constituents. This assumption is discussed in more detail below. The theoretical densities of natural (isotopic composition) U at 298K. 239Pu at 294K, and Zr at 293K are found from their crystal structures to be 19.04 g/cm^3, 19.816 g/cm^3 and 6.52 g/cm^3, respectively [10-14]. The minor corrections required in the densities of Pu and Zr due to the small differences between the quoted temperature and the room temperature 298K are made by using the following coefficients of linear expansion given in the same reference.

$$\alpha\left(^{239}Pu\right) = \left(46.85 + 0.0559\,T_c\right)x10^{6}, \qquad -186 < T_c < 100 \quad (10.3\text{-}87)$$

$$\alpha\left(Zr\right) = \left(5.768 + 0.006154\,T_c\right)x10^{-6}, \qquad 0 < T_c < 600 \quad (10.3\text{-}88)$$

where

α = coefficient of linear thermal expansion per °C,

T_c = temperature on the Centigrade scale.

The theoretical density of ^{239}Pu at 298K after the temperature correction turns out to be 19.805 g/cm^3, and that of Zr at 298K is about 6.51 g/cm^3 because its temperature correction is negligible for the 5K difference. The theoretical densities of U and Pu can be further corrected for the difference between the actual isotopic average atomic weight and the quoted atomic weight, by multiplying by the ratio of these atomic weights.

$$\rho_{th,u}(298K) = 19040\ a_u/238.07 \tag{10.3-89}$$

$$\rho_{th,p}(298K) = 19805\ a_p/239.13 \tag{10.3-90}$$

where

$\rho_{th,u}\ \rho_{th,p}$ = theoretical densities of U and Pu at 298K, kg/m^3,

a_u = uranium atomic weight averaged over its actual isotopic composition in fuel,

a_p = plutonium atomic weight averaged over its actual isotopic composition in the fuel.

The denominators 238.07 and 239.13 of Eqs. (10.3-89) and (10.3-90) are the atomic weights of natural uranium and ^{239}Pu.

The volume of one kilogram of U-Pu-Zr alloy at 298K can be found from Eqs. (10.3-89) and (10.3-90) by summing the volumes of its constituents.

$$V_s = \frac{238.07\ W_u}{19040\ a_u} + \frac{239.13\ W_p}{19805\ a_p} + \frac{W_z}{6510}, \tag{10.3-91}$$

where

V_a = volume of one kilogram of U-Pu-Zr alloy at 298 K, m^3/kg,

W_u, W_p, W_z = weight fractions of U, Pu and Zr in the alloy.

The theoretical density of U-Pu-Zr alloy at 298K in units of kg/m^3 is obtained from Eq. (10.3-91).

$$\rho_{th}\left(298K, W_p, W_z\right) = 1000 / \left(\frac{238.07\ W_u}{19.04\ a_u} + \frac{239.13\ W_p}{19.805\ a_u} + \frac{W_z}{6.51} \right) \tag{10.3-92}$$

where

ρ_{th} (T, W_p, W_z) = theoretical density of U-Pu-Zr alloy at temperature T°K, kg/m^3.

Table 10.3-8. Comparison of Measured and Estimated Theoretical Densities of U-Pu-Zr Alloy at 298K

Quantity	Batch R250	Batch R253Z
U, Pu and Zr weight ratios	73.4/13.8/12.2	75.9/14.8/9.4
U, Pu and Zr weight fractions	0.738/0.139/0.123	0.758/0.148/0.094
Isotopic composition of U, $^{235}U/^{238}U$ wt %	93.19/6.81	93.19/6.81
Isotopic composition of U, $^{239}Pu/^{240}Pu/^{242}Pu$ wt %	91.35/7.85/0.77/0.035	91.35/7.85/0.77/0.035
Average atomic weight of U	235.32	235.32
Average atomic weight of Pu	239.22	239.22
Estimated (using Eq. 10.3-92) theoretical density of U-Pu-Zr fuel, kg/m^3	15360	16080
Measured density averaged over all the fuel slugs in the batch, kg/m^3	15280	15750

Table 10.3-8 shows a comparison of measured densities of two batches of injection cast U-Pu-Zr fuel slugs [10-3] with the theoretical densities estimated from Eq. (10.3-92). The comparison is satisfactory for these two fuel compositions although further comparison for alloys of other compositions, specifically the alloy compositions in the annular zones formed at the end of steady-state irradiation of U-Pu-Zr fuel pins, is required to test the validity of the assumption of no volume change during alloying. The small difference may be due to measurement error, small voids left during the injection casting process or some volume change taking place during alloying.

10.3.3.2 Thermal Expansion of U-Pu-Zr Fuel

The U-Pu-Zr alloys show strong discontinuities in the coefficient of linear thermal expansion when the alloys are heated through the phase transformation temperatures [10-15]. There is some variation between the coefficients of linear expansion of alloys of different compositions but there is not enough data available to correlate this variation as a function of composition. This fuel properties option assumes the coefficient of linear expansion to be independent of composition, and uses the thermal expansion of U-15 wt % Pu-10 wt % Zr for all alloy compositions. The measured values of U-15 wt % Pu-10 wt % Zr alloy linear thermal expansion have been correlated as follows:

$$\frac{\Delta L(T)}{L_1} = \begin{cases} 1.76\ x\ 10^{-5}\left(T - 298\right), & T \le 873K \\ 1.012\ x\ 10^{-2} + 1.05\ x\ 10^{-4}\left(T - 873\right), & 873 < T \le 923K \\ 1.537\ x\ 10^{-2} + 2.04\ x\ 10^{-5}\left(T - 923\right), & T > 923K \end{cases} \qquad (10.3\text{-}93)$$

where

$\frac{\Delta L(T)}{L_1}$ = linear thermal expansion from a fixed temperature 298K to any temperature T, exp

Using Eqs. (10.3-92) and (10.3-93), the following equation for the theoretical density of U-Pu-Zr alloy fuel at any temperature T in units of kg/m^3 is obtained:

$$\rho_{th}(T, W_p, W_z) = \frac{1000}{\left(\frac{238.07\, W_u}{19.04\, a_u} + \frac{239.13\, W_p}{19.805\, a_p} + \frac{W_z}{6.51}\right)} \cdot \frac{1}{\left[1 + \frac{\Delta L(T)}{L_1}\right]^3} \qquad (10.3\text{-}94)$$

10.3.3.3 Enthalpy and Specific Heat of U-Pu-Zr Fuel

The composition-dependent enthalpy and specific heat of U-Pu-Zr alloy at any temperature up to is solidus temperature are estimated by mass-weighted averaging of the enthalpy and specific heat data of U, Pu and Zr metals, assuming that the heat of formation of the alloy is negligible. The heat of formation of the alloy is assumed negligible due to lack of data.

Each of the constituent metals of the U-Pu-Zr alloy undergoes certain crystallographic phase transformations in the solid state which require considerable heat addition and enthalpy increase at the transformation temperatures. The specific heat data of U, Pu, and Zr excluding these heats of solid-state transformations [10-10] are given in Tables 10.3-9 to 10.3-11, and plotted in Figs. 10.3-69 to 10.3-71. In each plot, the value of specific heat between the highest solid-state transformation temperature and the melting point is shown extrapolated to a temperature of 2000K for curve-fitting purposes, although the fitted equations are used only up to a solidus temperature of the U-Pu-Zr alloy. Because the heat transfer routines of the SAS4A/SASSYS-1 codes were initially written for the mixed-oxide fuel without any heat of solid-heat transformation, the heats of solid-state transformations of U, Pu and Zr are required to be included in their specific heats by spreading the corresponding enthalpy jumps over a temperature range. This spreading is not all artificial because these solid-state transformations actually occur over a temperature range in the U-Pu-Zr alloy. Hence the equations fitted to the specific heat and enthalpy data of U, Pu and Zr metals are required (1) to be continuous (no sudden jumps at any temperature) for the purpose of accuracy and convergence of the numerical solution in the SAS4A/SASSYS-1 heat transfer routines, (2) to include the heats of solid-state transformations such that the fitted equations cross the enthalpy jumps close to their midpoints, and (3) to closely reproduce the enthalpy and specific heat data away from the solid-state transformations. When one polynomial could not be fitted over the whole temperature range, the data for each metal was fitted in two parts: a polynomial over the lower temperature range covering most of the solid-state transformations, and an equation of the form $a+b/T^n$ over the higher temperature range. The following equations for the specific heats (in units of J/kg-K) of U, Pu and Zr metals and the U-Pu-Zr alloy are obtained.

$$C_{pu}(T)=\begin{cases}0.72516T-1.4232\,x10^{-3}T^2+1.0134\,x10^{-6}T^3, & T\le 1000K\\ 160.9+154.5(1000/T)^8, & T>1000K\end{cases} \quad (10.3\text{-}95)$$

$$C_{pp}(T)=\begin{cases}-1202.3+9.0307T-0.018232T^2+1.1616\,x10^{-5}T^3, & T\le 753K\\ 147.0+72.65(753/T)^9, & T>753K\end{cases} \quad (10.3\text{-}96)$$

$$C_{pz}(T)=\begin{cases}-7.0215+1.5493T-2.4845\,x10^{-3}T^2+1.3587\,x10^{-6}T^3, & T\le 1136K\\ 344.2+196.4(1136/T)^9, & T>1136K\end{cases} \quad (10.3\text{-}97)$$

$$C_p(T,W_p,W_z)=W_u\,C_{pu}(T)+W_p\,C_{pp}(T)+W_z\,C_{pz}(T) \quad (10.3\text{-}98)$$

where

$C_{pu}(T)$, $C_{pp}(T)$, $C_{pz}(T)$ = specific heats of U,Pu and Zr metals at temperature T, J/kg-K,

$C_p(T, W_p, W_z)$ = composition-dependent specific heat of the U-Pu-Zr alloy, J/kg-K,

W_u, W_p, W_z = weight fractions of U,Pu and Zr in the U-Pu-Zr alloy.

Equations (10.3-95) to (10.3-97) for the specific heats of U, Pu and Zr metals are compared with the data of Tables 10.3-9 to 10.3-11 in Figs. 10.3-69 to 10.3-71. The lower and the higher temperature-range-fitted equations join without any discontinuity at the range interface temperature. The enthalpies obtained by integrating Eqs. (10.3-95) to (10.3-97) are compared with the measured data of Tables 10.3-9 to 10.3-11 in Figs. 10.3-72 to 10.3-74. The enthalpy obtained from the higher temperature-range-fitted equation merges asymptotically with the data. A comparison of the enthalpy obtained from Eq. (10.3-98) for alloys of several compositions (e.g., those formed in the annular zones) is required to test the validity of this technique.

10.3.3.4 Thermal Conductivity of U-Pu-Zr Fuel

The thermal conductivity of U-Pu-Zr alloy (up to its solidus temperature) as a function of temperature and composition has been obtained by evaluating the effect of alloying plutonium on the thermal conductivity of U-Zr binary alloy. The thermal conductivity of U-Zr binary alloy is known for the full range of composition [7-14] and is shown in Fig. 10.3-75. Alloying usually reduces the thermal conductivity substantially. The reduction in the U-Zr binary thermal conductivity due to alloying Pu with it is evaluated using the thermal conductivity data available for three U-Pu-Zr ternary alloys prepared in casting numbers D-44, D-54 and D-50 [10-19, 10-20] and given in Table 10.3-12.

Figure 10.3-75 shows that the thermal conductivity of U-Zr binary alloy decreased linearly with Zr atom fraction in the range of zero to 0.5. Therefore, quadratic functions

are least-square fitted to the pure uranium thermal conductivity data and to the U-50 atom % zr binary alloy data of Fig. 10.3-75, and then the thermal conductivity of any U-Zr binary alloy in the composition range of zero to 50 at. % Zr is linearly interpolated between these two quadratics. The resulting equations are as follows:

$$K_u = 0.22173 + 1.8562\,x10^{-4}\,T_c + 1.3278\,x10^{-7}\,T_c^2 \qquad (10.3\text{-}99)$$

$$K_{u50} = 0.074766 + 1.6738\,x10^{-4}\,T_c + 1.1599\,x10^{-7}\,T_c^2 \qquad (10.3\text{-}100)$$

$$K_{uz} = K_u + \frac{2A_z}{A_u + A_z}\left(K_{u50} - K_u\right) \qquad (10.3\text{-}101)$$

Table 10.3-9. Enthalpy and Specific Heat Data of Uranium Metal [10-10]

Temperature, K	Specific Heat cal/mol-K	J/kg-K	Enthalpy Above 298.15K, cal/mol
298.15	6.61	116.2	0.0
400.0	7.10	124.8	698
500.0	7.65	134.5	1434
600.0	8.31	146.1	2231
700.0	9.08	159.7	3099
800.0	9.99	175.7	4050
900.0	11.02	193.8	5103
941.0 (α)	11.47	201.7	5563
941.0 (β)	10.26	180.4	6230
1000.0	10.26	180.4	6836
1048.0 (β)	10.26	180.4	7327
1048.0 (γ)	9.15	160.9	8464
1100.0	9.15	160.9	8939
1200.0	9.15	160.9	9854
1300.0	9.15	160.9	10769
1400.0	9.15	160.9	11684
1500.0	9.15[a]	160.9[a]	12599[a]
2000.0	9.15[a]	160.9[a]	17174[a]

[a] The constant value of the γ-U-phase specific heat has been extrapolated to temperatures up to 2000K for curve-fitting purposes.

Table 10.3-10. Enthalpy and Specific Heat Data of Plutonium Metal [10-10]

Temperature, K	Specific Heat cal/mol-K	J/kg-K	Enthalpy Above 298.15K, cal/mol
298.15	7.64	133.7	0.0
395.0 (α)	8.20	143.5	772
395.0 (β)	8.00	140.0	1612
400.0	8.03	140.6	2277
480.0 (β)	8.60	150.5	2417
480.0 (γ)	8.30	145.3	2585
500.0	8.53	149.3	3378
588.0 (γ)	9.50	166.3	3508
600.0 (δ)	9.00	157.5	3616
700.0	9.00	157.5	4516
730.0 (δ)	9.00	157.5	4786
730.0 (δ′)	9.00	157.5	4806
753.0 (δ′)	9.00	157.5	5013
753.0 (ε)	8.40	147.0	5453
800.0	8.40	147.0	5848
900.0	8.40	147.0[a]	6688
1000.0	8.40[a]	147.0[a]	7528[a]
2000.0	8.40[a]	147.0[a]	15928[a]

[a] The constant value of the ε-U-phase specific heat has been extrapolated to temperatures up to 2000K for curve-fitting purposes.

Table 10.3-11. Enthalpy and Specific Heat Data for Zirconium Metal [10-10]

Temperature, K	Specific Heat cal/mol-K	J/kg-K	Enthalpy Above 298.15K, cal/mol
298.15	6.06	278.1	0.0
400.0	6.54	300.1	646
500.0	6.78	311.1	1313
600.0	7.01	321.7	2003
700.0	7.23	331.8	2714
800.0	7.45	341.9	3449
900.0	7.68	352.4	4205
1000.0	7.90	362.5	4984
1100.0	8.13	373.1	5785
1136.0 (α)	8.20	376.3	6079
1136.0 (β)	7.50	344.2	7020
1200.0	7.50	344.2	7500
1400.0	7.50	344.2	9000
1600.0	7.50	344.2	10500
1800.00	7.50	344.2	12000
2000.0	7.50	344.2	13500

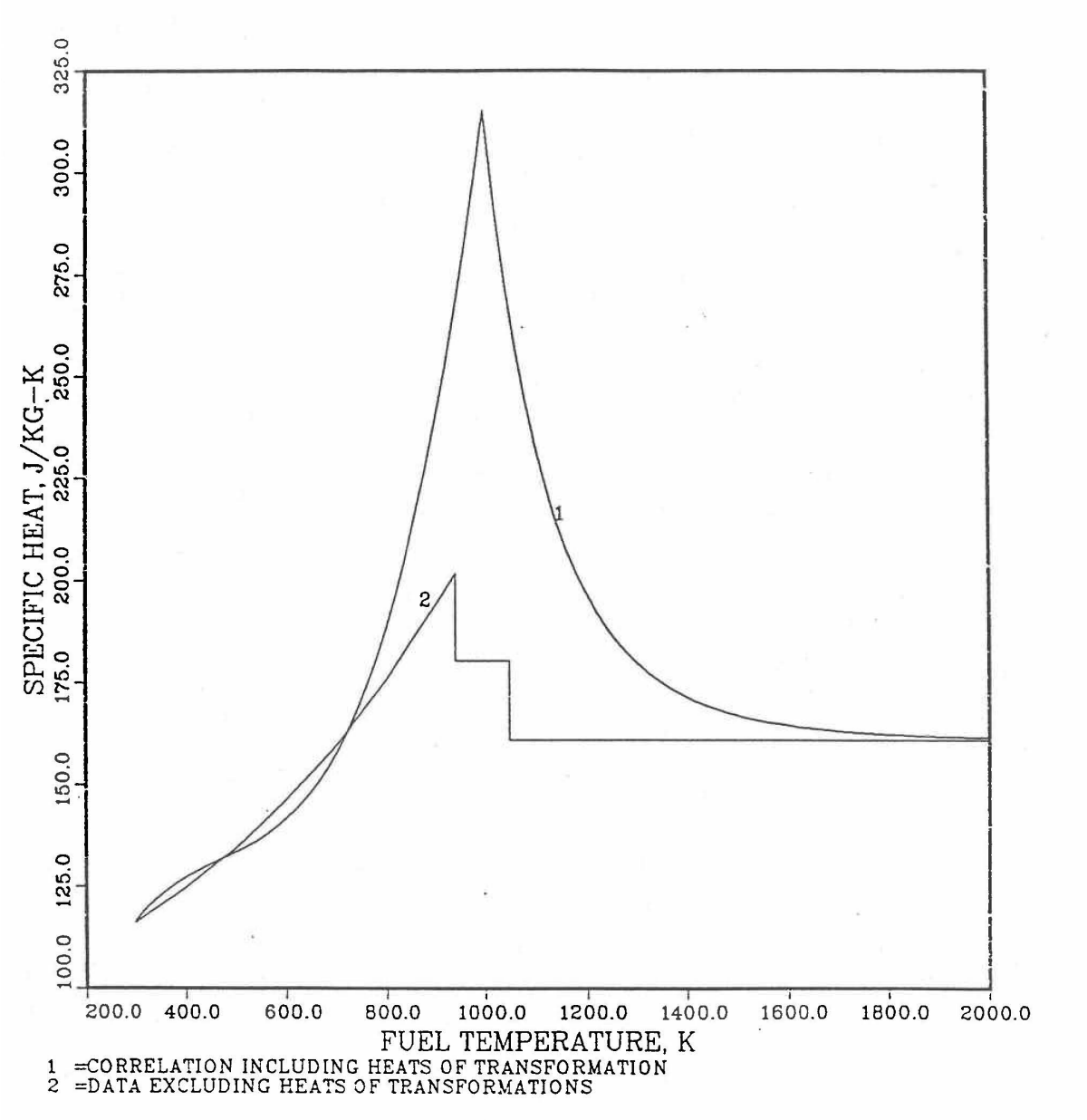

Fig. 10.3-69. Uranium Specific Heat Correlation Including the Heats of Solid-State Transformations

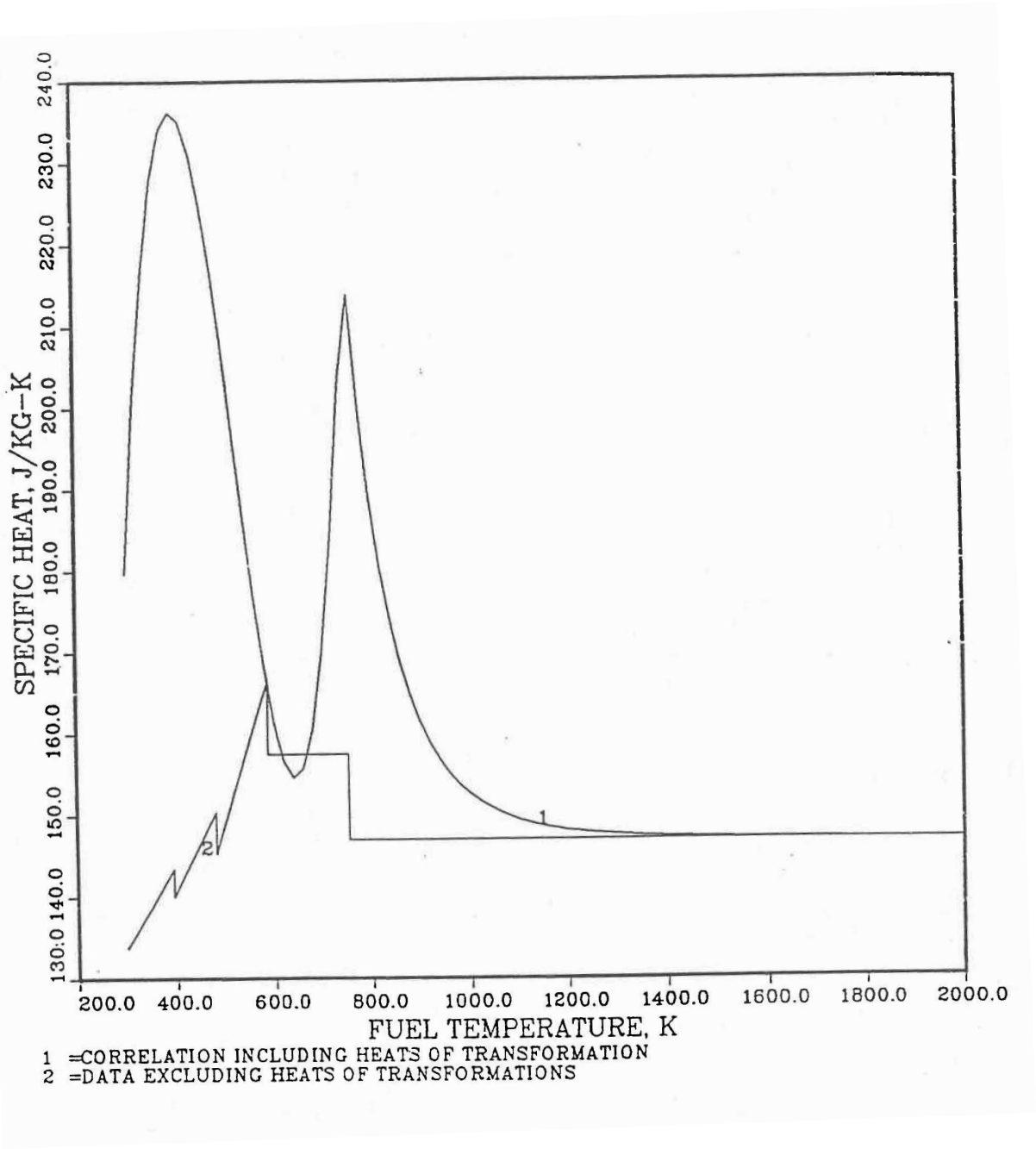

Fig. 10.3-70. Plutonium Specific Heat Correlation Including the Heats of Solid-State Temperature

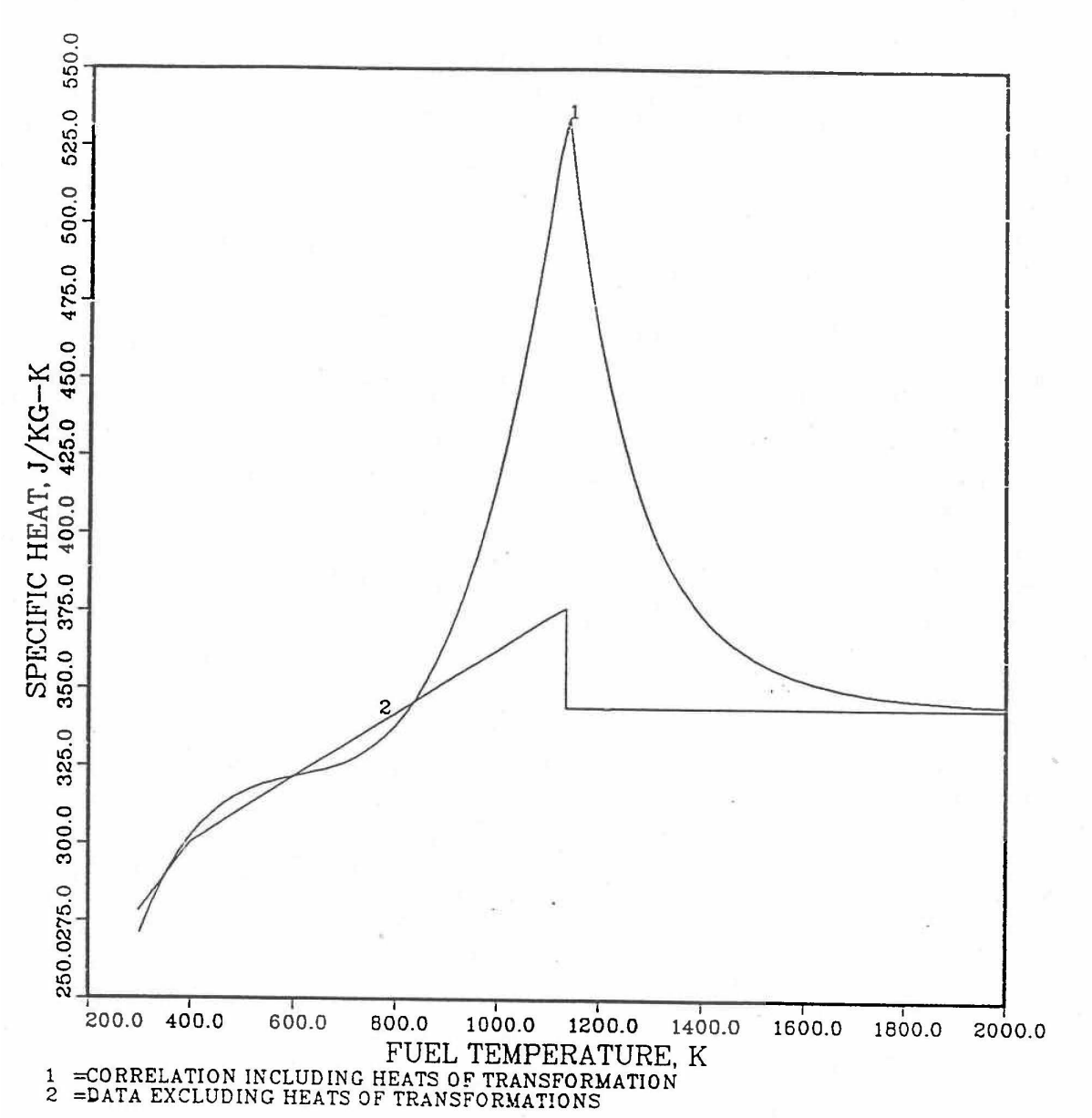

Fig. 10.3-71. Zirconium Specific Heat Correlation Including the Heats of Solid-State Transformations

where

T_c = temperature of the alloy, °C,

A_u, A_p, A_z = atom fractions of U, Pu and Zr in the U-Pu-Zr ternary alloy. For a U-Zr binary alloy, A_p is zero.

K_u = thermal conductivity of pure uranium, W/cm-°C,

K_{u50} = thermal conductivity of U-50 atom % Zr binary alloy, W/cm°C,

K_{uz} = thermal conductivity of any U-Zr binary alloy in the composition range of zero to 50 atom % Zr, W/cm-°C.

Equations (10.3-99) and (10.3-100) reproduce the thermal conductivity data shown in Fig. 10.3-75 for pure uranium and U-50 atom % Zr binary alloy with a maximum error of 1.5%. Equation (10.3-101) for the thermal conductivity of U-Zr binary alloys has been compared in Table 10.3-13 with the data [10-18] for U-20 wt. % Zr (U-39.5 atom & Zr) binary alloy and the maximum error is about 5%. Equation (10.3-101) is so written that it determines the thermal conductivity of the U-Zr binary alloy to which Pu can be added to obtain the desired U-Pu-Zr ternary alloy with U, Pu and Zr atom fractions equal to A_u, A_p and A_z. The addition of Pu to the U-Zr binary alloy decreases the thermal conductivity. Because of a lack of the ternary alloy thermal conductivity data at widely spaced Pu atom fractions, only a linear dependence on Pu atom fraction is assumed in this evaluation.

$$K_o\left(T_c, A_p, A_z\right) = K_{uz} - CA_p \qquad (10.3\text{-}102)$$

where

$K_o(T_c, A_p, A_z)$ = thermal conductivity at temperature T_c °C of the solid (i.e., nonporous) U-Pu-Zr

In Eq. (10.3-102), the coefficient C is independent of A_p and models the effect of alloying Pu with the U-Zr binary.

Table 10.3-12. Thermal Conductivity Data for Three U-Pu-Zr Alloys Prepared in Casting Numbers D-44, D-54 and D50

Temperature, °C	Thermal Conductivity, W/cm-°C		
	Casting D-44[a]	Casting D-54[a]	Casting D-50[a]
100	0.109	0.100	0.092
200	0.142	0.132	0.117
300	0.177	0.164	0.144
400	0.210	0.196	0.171
500	0.241	0.225	0.197
600	0.264	0.253	0.219
700	0.280	0.278	0.234
800	0.293	0.301	0.248
900	0.301	0.323	0.260
1100[b]	0.322	0.368	0.286
1300[b]	0.343	0.413	0.312
1500[b]	0.364	0.458	0.338
1700[b]	0.385	0.503	0.364
1900[b]	0.406	0.548	0.390
2000[b]	0.417	0.571	0.403

[a] The composition of castings:
D-44 is U-16.2 wt & Pu-6.2 wt % Zr (U-14.7 at. % Pu-14.7 at.% Zr
D-54 is U-14.7 wt & Pu-9.7 wt % Zr (U-12.7 at. % Pu-21.9 at.% Zr
D-50 is U-18.4 wt & Pu-11.5 wt % Zr (U-15.5 at. % Pu-25.3 at.% Zr

[b] The data in Ref. [10-19, 10-20] have been extrapolated linearly to temperatures up to 2000°C for curve fitting purposes.

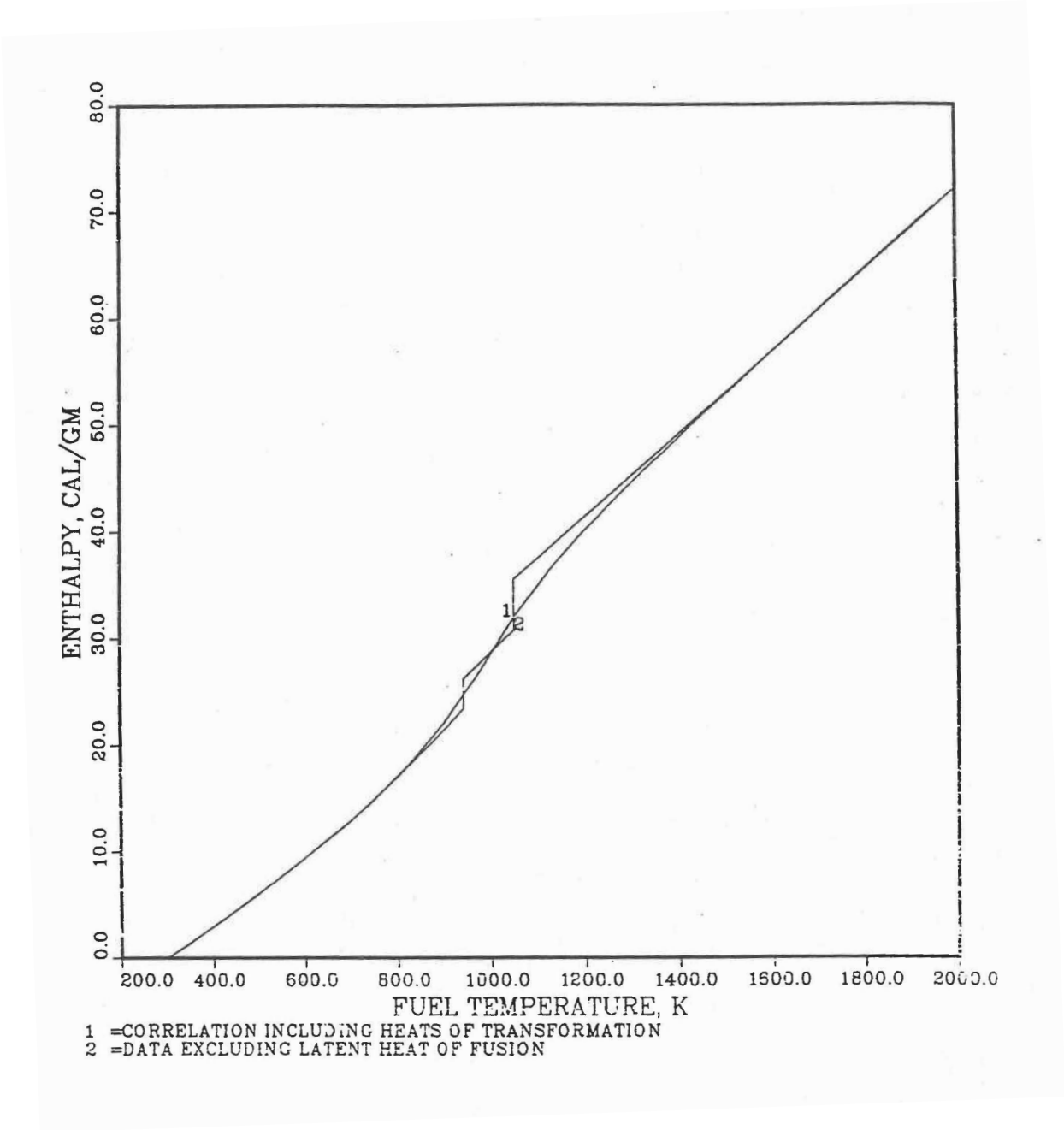

Fig. 10.3-72. Uranium Enthalpy Obtained by Integrating its Specific Heat Correlation

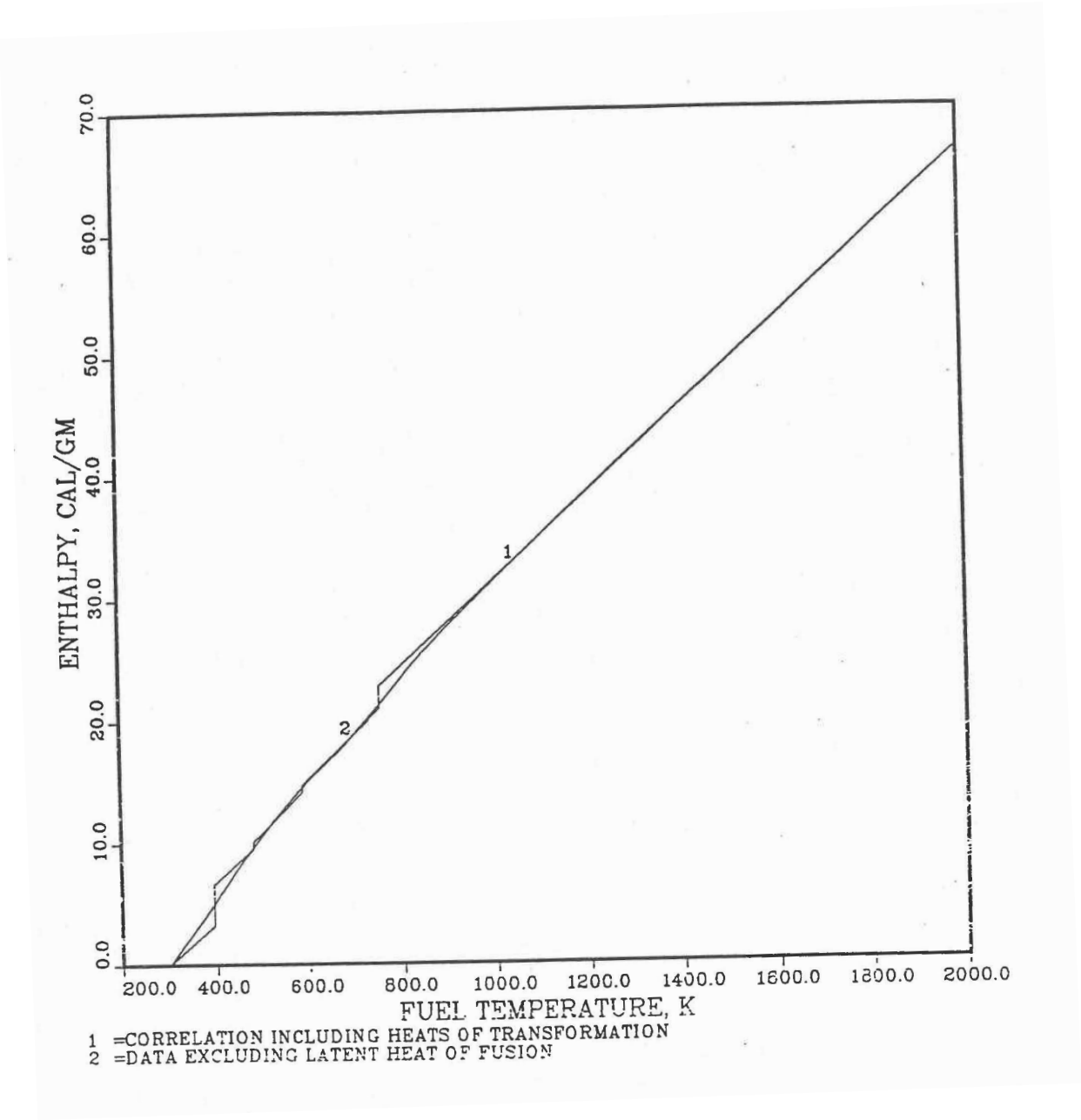

Fig. 10.3-73. Plutonium Enthalpy Obtained by Integrating its Specific Heat Correlation

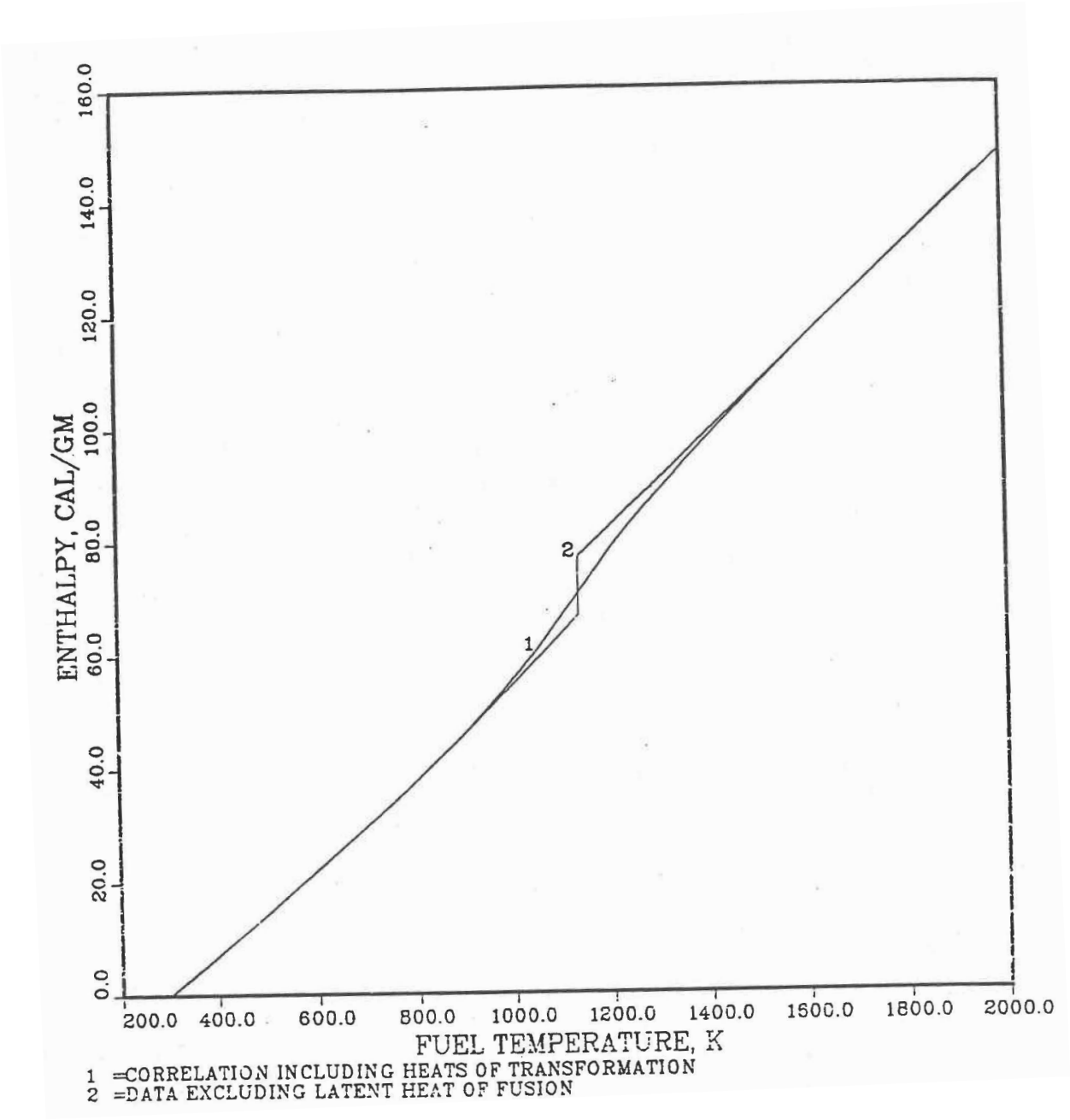

Fig. 10.3-74. Zirconium Enthalpy Obtained by Integrating its Specific Heat Correlation

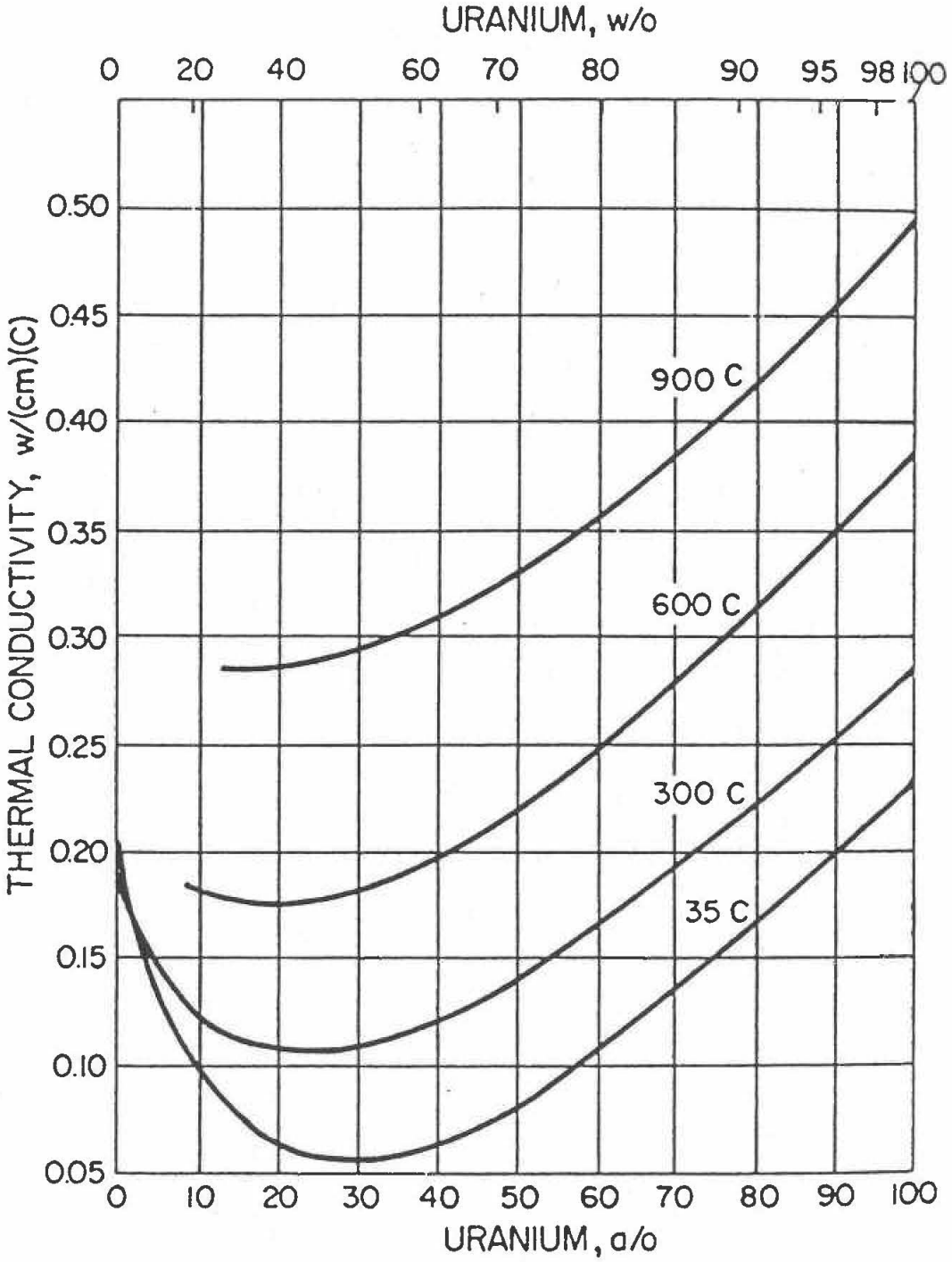

Fig. 10.3-75. Thermal Conductivity of the Uranium-Zirconium Binary Alloy for the Full Range of Composition

Table 10.3-13. Comparison of Thermal Conductivity Evaluated Using Eq. (10.3-101) With the Data [10-18] for U-20Zr Binary Alloy

	Thermal Conductivity, W/cm-°C		
Temperature, °C	**Data**	**Equation**	**% Error**
20	0.11	0.109	-0.8
100	0.13	0.124	-4.6
200	0.15	0.145	-3.5
300	0.17	0.168	-1.3
400	0.20	0.193	-3.4
500	0.22	0.221	0.5
600	0.25	0.251	0.6
700	0.28	0.284	1.5
800	0.31	0.319	2.9
900	0.34	0.357	4.9

Table 10.3-14. Temperature Variation of the Plutonium Alloying Coefficient *C* Evaluated from the Thermal Conductivity Data for Three U-Pu-Zr Alloys Prepared in Casting Numbers D-44, D-54 and D-50

	Thermal Conductivity, W/cm-°C		
Temperature, °C	U-Pu-Zr Casting	U-Zr Binary With U to Zr Atom Ratio Same as Casting	Coefficient C
Casting Number D-44, U-14.7 at.% Pu-14.7 at.% Zr Alloy			
100	0.109	0.190	0.554
200	0.142	0.212	0.477
300	0.177	0.236	0.404
400	0.210	0.263	0.362
500	0.241	0.292	0.351
600	0.264	0.324	0.412
700	0.280	0.359	0.537
800	0.293	0.396	0.701
900	0.301	0.435	0.916
Casting Number D-54, U-12.7 at.% Pu-21.9 at.% Zr Alloy			
100	0.100	0.167	0.529
200	0.132	0.188	0.445
300	0.164	0.212	0.381
400	0.196	0.238	0.336
500	0.225	0.267	0.335
600	0.253	0.299	0.361
700	0.278	0.332	0.431
800	0.301	0.369	0.536
900	0.323	0.408	0.668
Casting Number D-50, U-15.5 at.% Pu-25.3 at.% Zr Alloy			
100	0.092	0.152	0.390
200	0.117	0.173	0.365
300	0.144	0.197	0.344
400	0.171	0.223	0.337
500	0.197	0.252	0.354
600	0.219	0.283	0.412
700	0.234	0.316	0.531
800	0.248	0.352	0.673
900	0.260	0.390	0.843

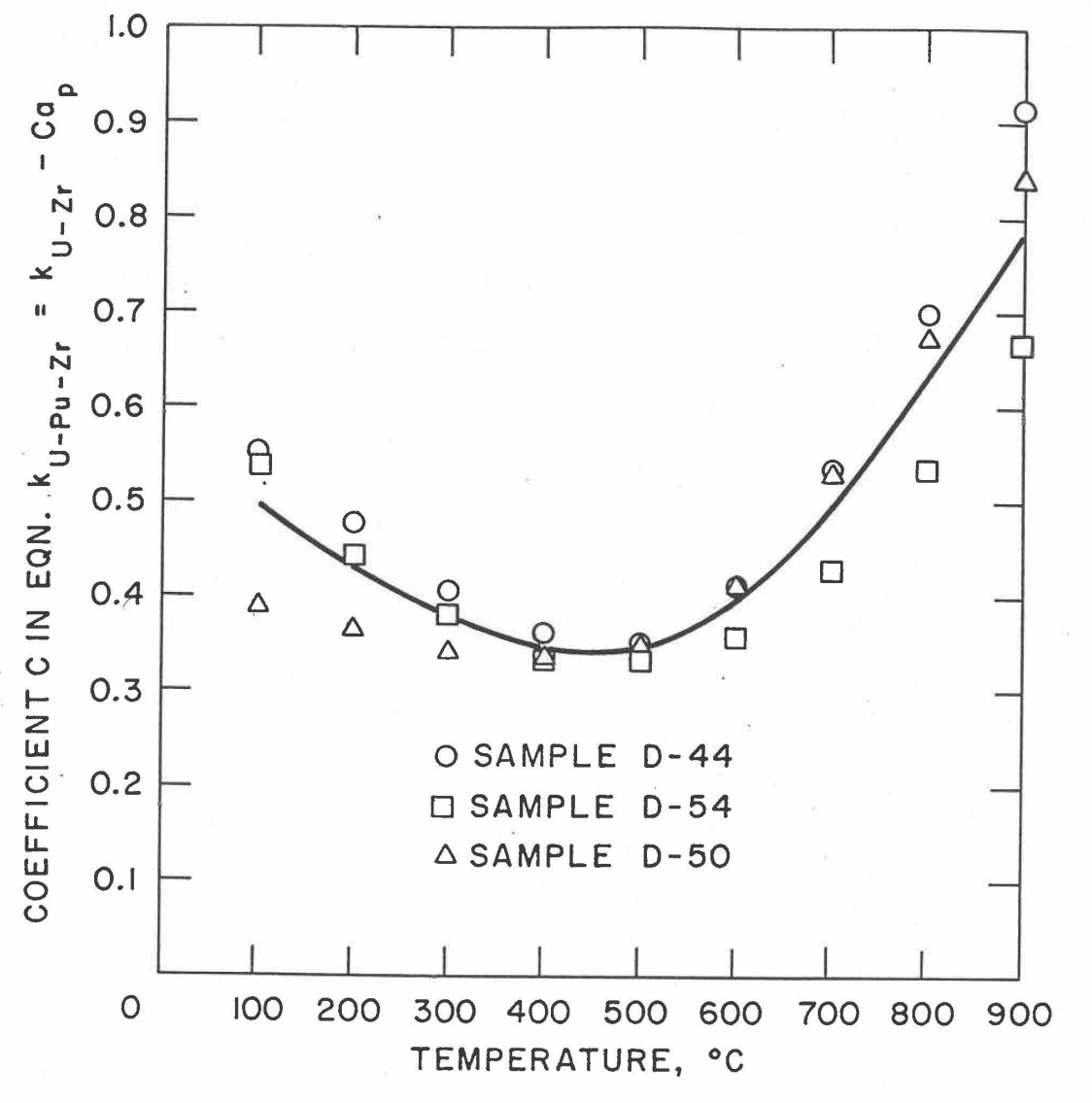

Fig. 10.3-76. Plot of Coefficient C vs. Temperature Obtained from Thermal Conductivity Data for U-Pu-Zr Samples D-44, D-54 and D-50

The coefficient C has been evaluated (see table 10.3-14) from the thermal conductivity data given in Table 10.3-12 for three U-Pu-Zr alloys prepared in casting numbers D-44, D-54 and D-50 [10-19, 10-20], and Fig. 10.3-76 shows a plot of these values of the coefficient C versus temperature. The scatter in Fig. 10.3-76 indicates that the coefficient C may have a weak dependence on Zr atom fraction in addition to the main dependence on temperature. The following two equations have been developed for evaluating the coefficient C: (1) a second degree polynomial of temperature only (ignoring the weak dependence on Zr atom fraction) least-squared fitted to the data given in Table 10.3-12 up to 900°C using A_p^2 as the weighting factor, and (2) a second degree polynomial of temperature with its coefficients linearly depending on Zr atom fraction least-square fitted to all the data given in Table 10.3-12 up to 2000°C using $[K_o(T_c,A_p,A_z)]^{-2}$ as the weighting factor. The A_p^2 weighting factor was used to reduce the errors in the first fitting equation at higher Pu atom fractions and make them nearly equal to the errors at lower Pu atom fractions. The $1/K_p^2$ weighting factor was used in the second case for the purpose of minimizing the mean fractional error in thermal conductivity. The fitted equations are given below with their expected ranges of validity.

$$C = 0.63477 - 1.4980x10^{-3}\,T_c + 1.8878x10^{-6}\,T_c^2,\ 100 \le T_c \le 1200,\quad 0.0 \le A_p \le 0.16,\ 0.0 \le A_z \le 0.50 \tag{10.3-103}$$

$$C = (0.89079 - 1.6757A_z) - T_c(1.7437x10^{-3} - 4.0008x10^{-3}A_z) + T_c^2(1.9608\ x\ 10^{-6} - 3.1043\ x\ 10^{-6}A_z),\ 100 \le T_c \le 1500,\quad 0.0 \le A_p \le 0.20,\ 0.0 \le A_z \le 0.50 \tag{10.3-104}$$

Figures 10.3-77 to 10.3-79 compare the U-Pu-Zr alloy thermal conductivity obtained from Eqs. (10.3-102) and (10.3-104) with the data for the three U-Pu-Zr alloys prepared in casting numbers D-44, D-54 and D-50 [10-19, 19-20]. The correlation compares well with all the base data with a root mean square error of 5% and a maximum error of about 10%. Equation (10.3-104) for evaluating the coefficient C covers a wider range of composition and temperature than Eq. (10.3-103) and is preferred. Further comparison for alloys of other compositions (i.e., those formed in the annular zones) and at temperatures higher than 900°C is required to test the validity of the assumptions used in this correlation.

The IFR Handbook correlation given by Eq. (A10.2-1) reproduces all the base data of Table 10.3-12 over the temperature range 100-900°C with a maximum error of about 20% compared to the maximum error of about 10% in the correlation Eqs. (10.3-102) and (10.3-104).

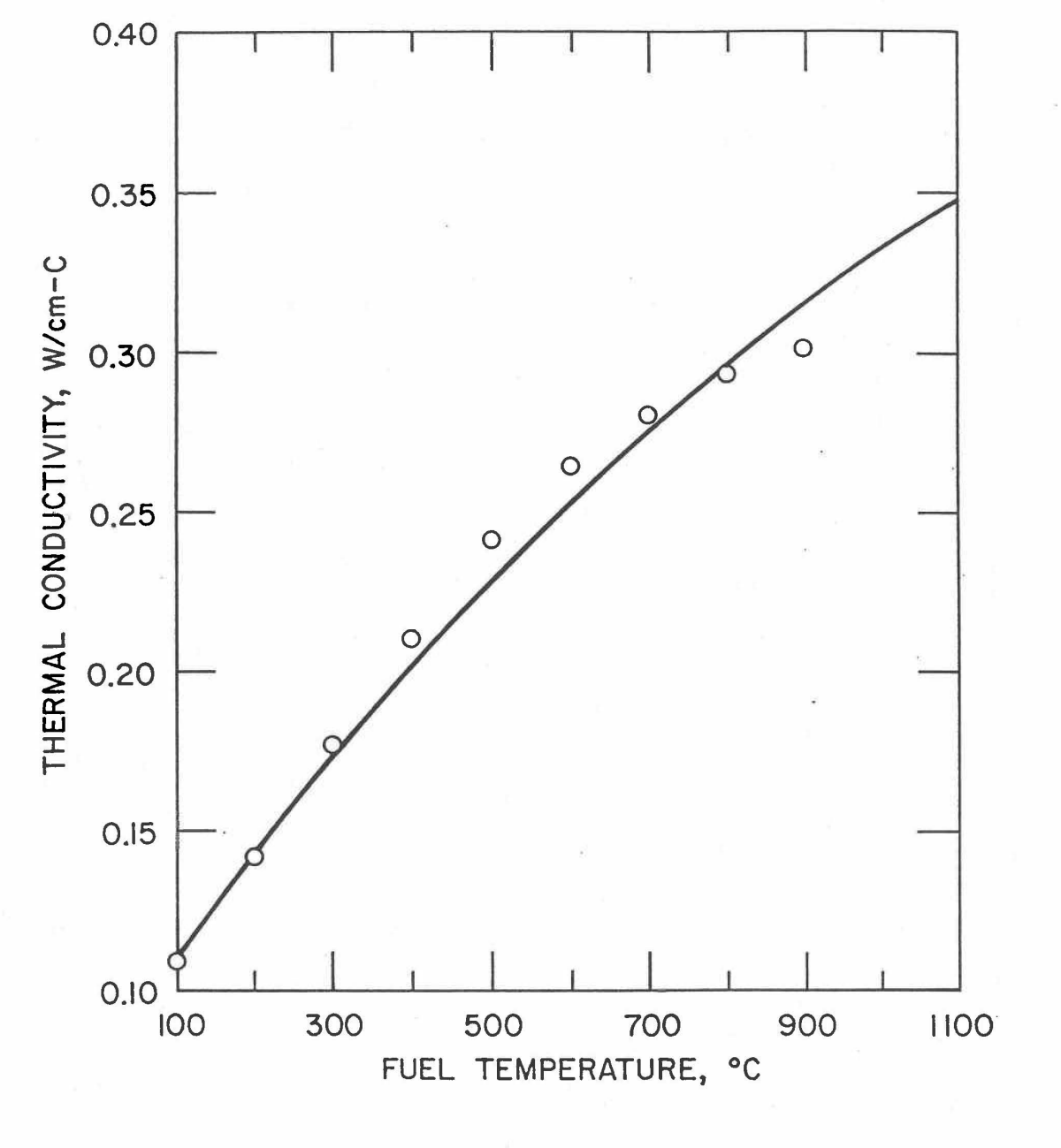

Fig. 10.3-77. Comparison of the Thermal Conductivity Correlation Eqs. (10.3-102) and (10.3-104) with the Data for the U-Pu-Zr Sample D-44

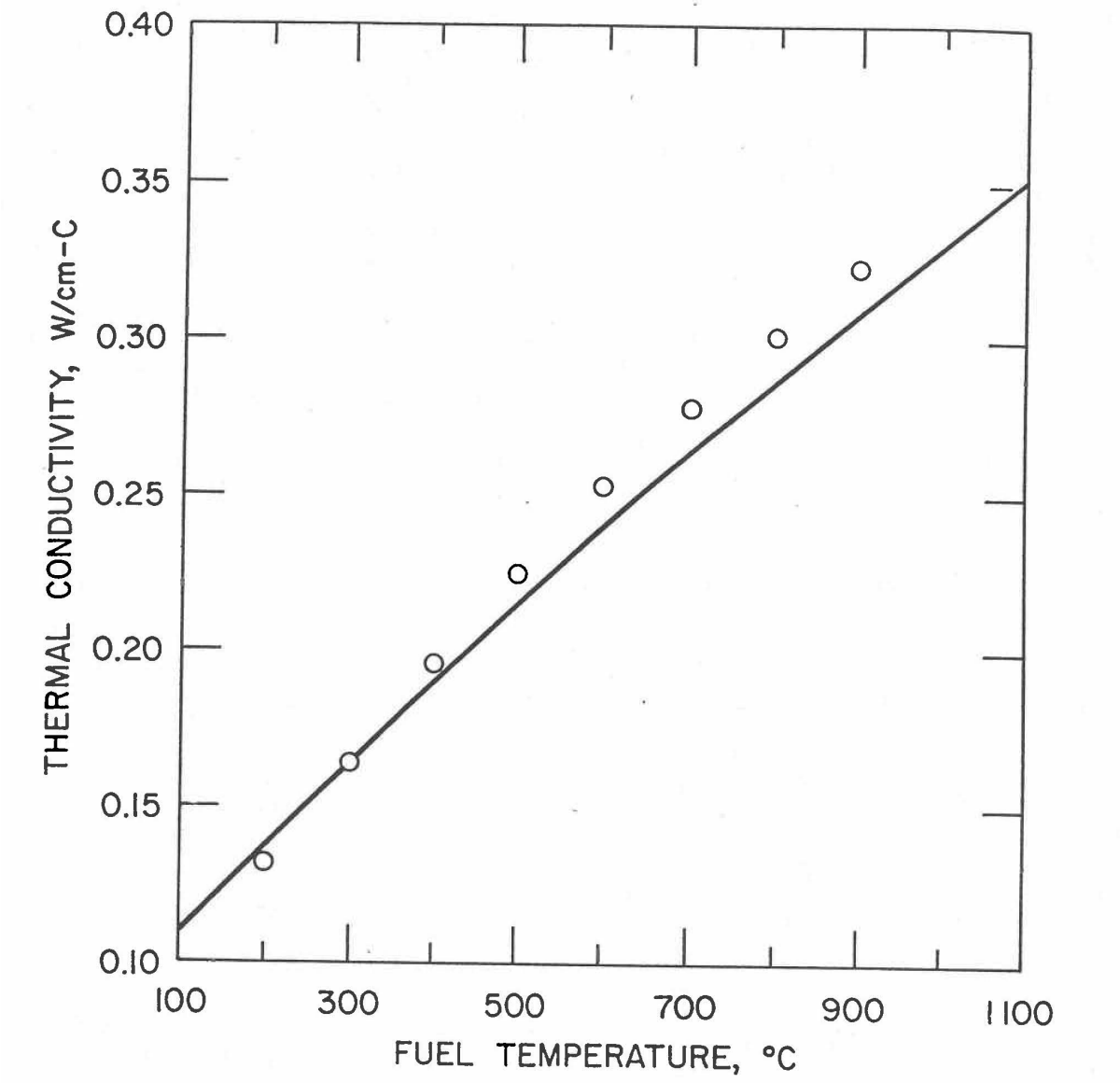

Fig. 10.3-78. Comparison of the Thermal Conductivity Correlation Eqs. (10.3-102) and (10.3-104) with the Data for the U-Pu-Zr Sample D-54

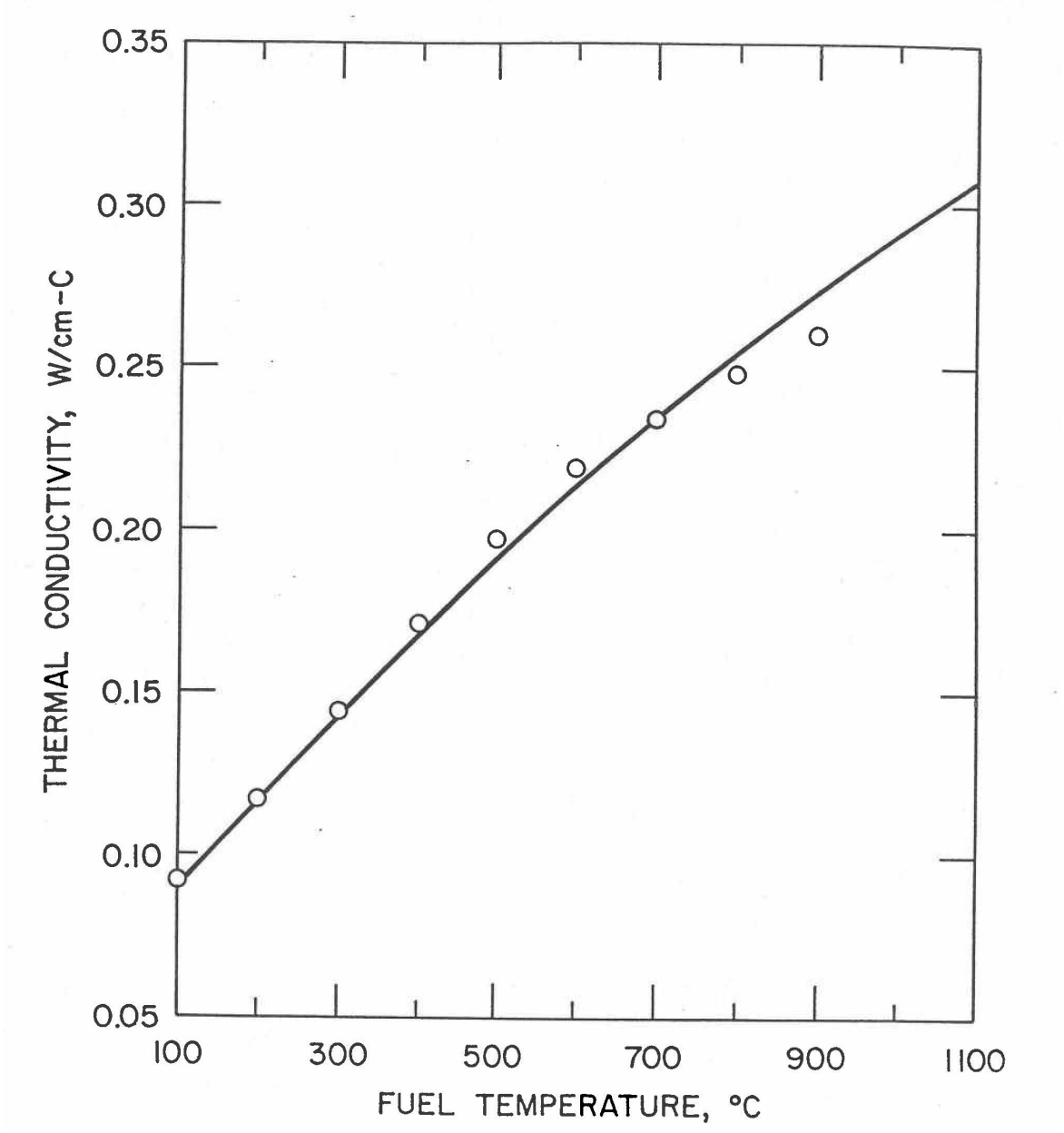

Fig. 10.3-79. Comparison of the Thermal Conductivity Correlation Eqs. (10.3-102) and (10.3-104) with the Data for the U-Pu-Zr Sample D-50

10.3.3.5 Porosity Correction of Fuel Thermal Conductivity

The correlation for the thermal conductivity of unirradiated 100%-dense U-Pu-Zr alloy fuel is described in Section 10.3.3.4 for the fuel properties option specified by setting the input parameter IRHOK=1 and the input parameter IFUELM=1 in a channel. The thermal conductivity also depends strongly on the fission gas-filled and logged sodium-filled porosities that form in the fuel during normal steady-state irradiation. Two methods to correct the thermal conductivity of 100%-dense U-Pu-Zr alloy fuel for fission gas-filled and logged sodium-filled porosities have been described in Section 10.3.2.6: (i) an empirical method based on experimental data for U-5Fs alloy fuel, and (ii) a theoretical method that explicitly accounts for the gas- and sodium-filled porosities. Only the theoretical method is available for irradiation-effects correction in this fuel properties option as shown by the flow diagrams of subroutines FK and KFUEL in Figs. 10.3-3 and 10.3-4.

10.3.4 Properties of Some Specific Fuels

Before the implementation in SAS4A/SASSYS-1 codes of composition- and temperature- dependent fuel thermal properties by the method of regionwise interpolation [10-31] of the Metallic Fuels Handbook [10-8] data, thermal properties of two specific fuels, i.e., Mark-V (U-20Pu-10Zr) ternary and U-10Zr binary alloy fuels, were incorporated into the codes by Briggs [10-32] to perform EBR-II Mark-V fuel safety calculations. These thermal properties are in the form of temperature-dependent correlations that were developed by Billone [10-12, 10-21, 10-22] based on data reported in the Metallic Fuels Handbook [10-8]. For the purpose of reproducing these safety calculations if required in future, these thermal property correlations have been retained in the codes and are used by setting the input parameter IRHOK-1 and the input parameter IFUELM-2 in a channel. In this fuel properties option, the specific heat and theoretical density of Mark-V ternary and U-10Zr binary fuels (specified by setting the input parameter IMETAL = 2 or 3 respectively) are evaluated using the following correlations:

Mark-V (U-20Pu-10Zr) Fuel (IMETAL=2)

$$C_p(T)=\begin{cases} 94.62+0.1301\,T, & T<873K \\ 792.6, & 873\le T<923K \\ 42.82+0.1276T, & 923\le T<1379K \\ 440.1, & 1379\le T<1488K \\ 217.2, & T\ge 1588K \end{cases} \qquad (10.3\text{-}105)$$

$$\rho_{th}(T)=15730 \Big/ \left[1+\frac{\Delta L(T)}{L_o}\right]^3 \tag{10.3-106}$$

$$\frac{\Delta L(T)}{L_o}=\begin{cases} 1.73x10^{-5}(T-293), & T\le 859K \\ \frac{\Delta L(859)}{L_o}+\frac{5.8x10^{-3}}{69}(1.655-6.55W_z)(T-859), & 859\le T\le 928K \\ \frac{\Delta L(928)}{L_o}+2.29x10^{-5}(1+0.567W_z-7.42W_z^2)(T-928), & T\ge 928K \end{cases} \tag{10.3-107}$$

U-10Zr binary Fuel (IMETAL=3)

$$C_p(T)=\begin{cases} 6.625+0.3066T+4.58x10^6/T^2, & T<1000K \\ 180.1, & 1000\le T<1506K \\ 580.7, & 1506\le T<1669K \\ 221.9, & T\ge 1669K \end{cases} \tag{10.3-108}$$

$$\rho_{th}(T)=16.02x10^3\left(1.0122-4.629x10^{-5}T+2.438x10^{-8}T^2 - 2.805X10^{-11}T^3\right) \tag{10.3-109}$$

where

C_p = specific heat, J/kg-K

T = fuel temperature, K

ρ_{th} = theoretical density, kg/m^3

$\frac{\Delta L(T)}{L_o}$ = linear thermal expansion from 293K to temperature T, expressed as a fraction of lengt

W_z = 0.1, the zirconium weight fraction in the fuel.

It is important to note that the specific heats of Mark-V and U-10Zr fuels over the melting range, obtained from Eqs. (10.3-105) and (10.3-108), are the actual values, and are not consistent with the method of Section 3.3.5 for adjusting fuel temperature (computed without accounting for heat of fusion during the main heat transfer calculation) to account for heat of fusion of any radial mesh interval that is going through the melting range. To be consistent with the method (see subroutine TSHTN5), the fuel specific heat used here must be the value for solid fuel just below solidus or the value for molten fuel just above liquidus.

The unirradiated 100%-dense fuel thermal conductivity, for both Mark-V and U-10Zr fuels, is evaluated using Eq. (A10.2-2) from the atom fractions of Pu and Zr in the fuel. These atom fractions are evaluated in the SAS4A/SASSYS-1 codes, using the following relations in this fuel properties option.

$$A_p = W_p / \left(1.0101 - 0.0101\, W_p + 1.611\, W_z\right) \tag{10.3-110}$$

$$A_z = 1.627\, W_z / \left(0.6272 - 0.006297\, W_p + W_z\right) \tag{10.3-111}$$

where

A_p, A_z = atom fractions of Pu and Zr in the fuel,

W_p, W_z = weight fractions of Pu and Zr in the fuel.

As discussed in Appendix 10.2, this thermal conductivity correlation should not be used for any other alloy composition besides Mark-V and U-10Zr fuels because it is ill-behaved, and so recommended by Billone [10-22]. For these two fuels, this correlation has been found to be correct. The correction of the 100% dense fuel thermal conductivity for the effects of steady-state irradiation is done using the empirical method described in Section 10.3.2.6. For the purpose of reproducing EBR-II Mark-V fuel safety calculations if required in future (which is the main purpose of providing this fuel properties option), the theoretical method of correcting for irradiation effects is not available in this option. Finally, to account for the uncertainties in the U-Pu-Zr thermal conductivity data forming the basis of this correlation (i.e., Eq. A10.2-2), the thermal conductivity obtained after correcting for irradiation effects is divided by an input uncertainty factor FUNKFU.

10.3.5 Computer Implementation

The U-Pu-Zr alloy composition in each computational cell of the fuel is at present specified both axially and radially by input data determined from the examination fuel pins with similar irradiation histories. Input data are handled by annular fuel zones (central, middle and outer composition zones) but the codes internally have arrays by radial node to store U-Pu-Zr fuel composition and composition-dependent quantities.

The choice of input data by fuel zone is based on the fact that analysts communicate commonly in terms of zones, and that this simplifies input data preparation. The use of storage by radial node is based on the fact that this reduces logical IF statements from coding, especially in molten material motion models. This should simplify the codes and improve the running time. The addition of composition-dependent fuel thermal properties in the input data is an option in the codes, and the user should be able to run no-zone formation cases without preparing the input data for multiple fuel zones. This section describes the functions of all the fuel thermal property subroutines, the related input data, and internal arrays.

10.3.5.1 List of Fuel Thermal Property Subroutines

The following is a list of all the fuel thermal property subroutines with a brief description of their functions:

CFUEL	Computes specific heat of mixed-oxide, U-Fs and U-Pu-Zr alloy fuels for a range of fuel radial nodes in an axial segment, with specified temperatures and U-Pu-Zr compositions.
CFUEL1	Computes U-Pu-Zr alloy fuel specific heat as a function of composition and temperature by regionswise interpolation of Metallic Fuels Handbook enthalpy data.
FK	Computes thermal conductivity of mixed-oxide, U-Fs and U-Pu-Zr alloy fuels for a single fuel radial node in an axial segment, with specified temperature, porosity and U-Pu-Zr composition. In the case of metal fuels, it also accounts for the effect of sodium logging.
HFUEL1	Computes U-Pu-Zr alloy fuel enthalpy as a function of composition and temperature by regionwise interpolation of Metallic Fuels Handbook enthalpy data.
KFUEL	Computes thermal conductivity of mixed oxide, U-Fs and U-Pu-Zr alloy fuels for a range of fuel radial nodes in an axial segment, with specified temperatures, porosity and U-Pu-Zr compositions. In the case of metal fuels, it also accounts for the effect of sodium logging.
KFUEL1	Computes thermal conductivity of unirradiated 100%-dense U-Pu-Zr alloy fuel as a function of composition and temperature, by the method of regionwise interpolation of Metallic Fuels Handbook thermal conductivity data.
PELTON	Computes solidus and liquidus temperatures of U-Pu-Zr alloy fuel as a function of composition, by the method of chemical thermodynamic equilibrium between conjugate solid and liquid solutions.
PRECAL	Ppre-calculates, before steady-stat calculation, a number of parameters stored for fast evaluation of U-Pu-Zr specific heat, theoretical density and thermal conductivity by fuel type.
RHOF	Computes theoretical density of mixed-oxide, U-Fs and U-Pu-Zr alloy fuels

for a specified temperature and U-Pu-Zr composition.

RHOFM Computes theoretical density of U-Pu-Zr fuel as function of composition and temperature, and also returns the fractional linear thermal expansion over the input temperature range.

THEXP1 Computes fractional linear thermal expansion of U-Pu-Zr alloy fuel as a function of composition and temperature, by the method of regionwise interpolation of Metallic Fuels Handbook data.

TRTEMP Evaluates the first and last solid-state transition temperatures of U-Pu-Zr alloy fuel as a function of composition.

10.3.5.2 Input Data Related to Fuel Thermal Properties

Table 10.3-15 gives the SAS4A/SASSYS-1 input variables required to use (i) U-Pu-Zr fuel thermal properties obtained by regionwise interpolation of IFR Handbook data, and (ii) multiple radial fuel zones option of the codes. The first column of the table gives the location of the variable in a complete input deck of the codes. The second column gives the Fortran variable name used in the codes and the standard input description (see Appendix 2.2). Suggested values of some of these input variables are shown in column 3.

The suggested value, 5.0K, of the input variable DTFUEL (i.e., the maximum fuel temperature change per heat transfer time step) is based on a preliminary study of errors in computed fuel temperatures due to specific heat discontinuity at solid-state transitions. A utility program was developed and used to find the maximum temperature difference between two SAS4A/SASSYS-1 calculations with a main time step of 0.5 sec., differing only in the values used for the input variable DTFUEL, 50.0K and 1.0K in the two calculations. Errors of up to 16K, or up to 32% of the temperature rise in the main time step were found. A value of 5.0K for the input variable DTFUEL should reduce the maximum error in fuel temperatures printed at main time steps to (16 x 5.0/50.0) 1.6K.

By setting the input variable IRHOK=1 and the input variable IFUELM=0 in a channel, one uses the method regionwise interpolation of IFR Handbook data to obtain U-Pu-Zr fuel thermal properties as a function of composition and temperature, and this is the recommended option among the built-in fuel thermal property options. By setting the input variable IFUELC=1, one uses the multiple radial fuel zones option instead of the single radial fuel zone, and then assigns fuel types to central, middle and outer fuel zones using the input array MFTZN instead of the input variables IFUELV and IFUELB.

Table 10.3-16 gives the internal arrays in SAS4A/SASSYS-1 common blocks that are required for implementing IFR Handbook U-Pu-Zr fuel properties data and multiple radial fuel zones option in the codes. Arrays FUFEMS and FUNIMS, for iron and nickel mass distribution in the fuel, have been included in the common block for future modeling work on radial migration of cladding constituents into the fuel. Arrays ACPF, AKFU and ADFU for pre-migration coefficients in equations for fuel specific heat, thermal conductivity and theoretical density, have a first dimension of 8 to represent the 8 fuel types allowed in the codes. The second dimension of each of these arrays

represents the number of coefficients that can be stored for each fuel type. The 7 coefficients in the specific heat equation, stored as array elements ACPR(*,1), ACPR(*,2),…ACPF(*,7), are defined in Fig. 10.3-15. Only 3 array elements AKFU(*,1), AKFU(*,2) and AKFU(*,3) are currently used to store the 3 pre-calculated coefficient of the quadratic for 100% dense fuel thermal conductivity, given by Eq. (10.3-61). Only one array element ADFU(*,1) is currently used to store pre-calculated theoretical density without fission products at 293K, for each fuel type, given by Eq. (10.3-32).

Table 10.3-15. Input Data Required to Use IFR Handbook U-Pu-Zr Fuel Properties Data and Multiple Radial Fuel Zones Option

Input Location	Fortran Variable	Suggested Value	Definition/Comments
Block 1, INPCOM			
92	KHDBK	0	controls printing of messages if any extrapolation of Handbook data is used.
93	KFIRR	0	Option of method for correcting thermal conductivity for irradiation effect.
94	KDENBU		controls whether theoretical density is corrected for the presence of fission products or not.
Block 11, OPCIN			
10	DTFUEL	5.0	This value of DTFUEL is suggested to keep below 1.6K, the errors in computed fuel temperatures due to specific heat discontinuity at solid-state transitions.
Block 13, PMATCM			
786-793	TFSOL		Solidus temperature by fuel type. If Handbook U-Pu-Zr fuel properties option is used, then a zero entry implies that the code will internally evaluate solidus temperature.
794-801	TFLIQ		Liquidus temperature by fuel type. If Handbook U-Pu-Zr tuel properties option is used, then a zero entry implies that the code will internally evaluate liquidus temperature.
802-809	UFMELT		Heat of fusion by fuel type. If the IFR Handbook U-Pu-Zr fuel properties option is used, then the input is replaced by a value internally calculated by the code.
1073-1080	PRSTY		Total (i.e., fission gas-filled and logged sodium-filled) porosity by fuel type.
1300-1315	PUZRTP		Pu and Zr weight fractions by fuel type.

Input Location	Fortran Variable	Suggested Value	Definition/Comments
1316-1323	RHOZN	-1.0	U-Pu-Zr fuel theoretical density at the reference temperature TR, by fuel type. If RHOZN = 0.0 for a fuel type, then the implication is that this fuel type does not use the Handbook U-Pu-Zr fuel properties of input option IFUELM=0.
1324-1331	XLOGNA		Porosity fraction logged by bond sodium by fuel type
1332	XSIGMC	0.0	To account for uncertainties in Handbook data for U-Pu-Zr fuel specific heat, this input is the number of standard deviations to be added to the best estimate. It is not currently used.
1333	XSIGMK	0.0	To account for uncertainties in Handbook data for U-Pu-Zr fuel thermal conductivity, this input is the number of standard deviations to be added to the best estimate.
1334	XSIGMD	0.0	To account for uncertainties in Handbook data for U-Pu-Zr fuel theoretical density, this input is the number of standard deviations to be added to the best estimate. It is not currently used.
Block 51, INPCHN			
3	IRHOK	1	Selection parameter for the form (i.e., input tables or built-in correlations) of fuel thermal properties.
15	IFUELV		Fuel type or properties table number to be used for core fuel, in each channel.
16	IFEULB		Fuel type or properties table number to be used for blanket fuel, in each channel.
189	IMETAL	2	Input parameter to indicate whether the fuel is a mixed oxide or a metallic alloy of some kind, i.e., U-Fs, U-Pu-Zr or U-Zr binary.
191	IFUELO	0	Option to indicate whether annular fuel zone formation data (i.e., zonal compositions and radii) at the end of steady-state irradiation is obtained form user input or computed form the SSCOMP physical model.

Input Location	Fortran Variable	Suggested Value	Definition/Comments
192	IFUELM	0	Option to indicate the source of fuel thermal properties data. A zero entry implies the regionwise interpolation of IFR Handbook data.
193	IFUELC	1	An input flag to specify whether there is a single radial fuel zone, or there are multiple radial fuel zones.
366-389	IZNC		Outermost radial mesh interval of central zone in each axial segment. This input determines central zone boundary only if the input RIZNC, central zone outer radius, is set to zero.
390-413	IZNM		Outermost radial mesh interval of central zone in each axial segment. This input determines central zone boundary only if the input RIZNM, central zone outer radius, is set to zero.
414-485	MFTZN		This input array is used (instead of IFUELV and IFUELB) to assign fuel types to 3 radial fuel zones in each axial segment if the input parameter IFUELC=1.
Block 61, GEOMIN			
224-247	RIZNC		Outer radius of central zone in each axial segment. The steady-state initialization routine makes this radius correspond to the input IZNC.
248-271	RIZNM		Outer radius of middle zone in each axial segment. The steady-state initialization routine makes this radius initialization routine makes this radius correspond to the input IZNM.
Block 65, FUELIN			
54	BURNFU		Axially averaged fuel pin burnup in atom percent.

10.4 Future Directions for Modeling Efforts

Multiple annular fuel zones of different compositions formed at the end of steady-state irradiation in U-Pu-Zr alloy fuel can not be supplied to the SAS4A/SASSYS-1 codes through the input data. The codes are capable of using the input zone formation data in the steady-state and transient temperature calculations. U-Pu-Zr fuel thermal properties can now be evaluated by the codes as a function of composition and temperature, using the method of regionwise interpolation of IFR Handbook data. Besides the U-Pu-Zr fuel specific heat, theoretical density and thermal conductivity, the codes can now evaluate the zonal solidus and liquidus temperatures and heat of fusion. The effect of radial migration of fuel constituents on in-pin radial power shape is yet to be modeled.

The purpose of the SSCOMP module is to provide SAS4A/SASSYS-1 codes with the modeling of all those phenomena that describe the transition of a U-Pu-Zr fuel pin from cold clean as-manufactured conditions to hot irradiated swollen initial conditions for the transition fuel mechanics module FPIN2 [10-6]. As described in Section 10.1, listed below are the important in-pin phenomena occurring during steady-state irradiation, that need to be modeled in order to characterize a U-Pu-Zr fuel pin at the beginning of a transient calculation:

(1) Thermal expansion of fuel and cladding,

(2) Fuel constituent radial migration,

(3) Fission gas behavior, and porosity formation and distribution,

(4) Irradiation-induced radial and axial swelling of fuel and cladding,

(5) Bond sodium migration into fuel and pin plenum,

(6) Cladding constituent migration into fuel.

The modeling of the above phenomena will provide all the needed initial conditions for the transient fuel mechanics module FPIN2. Future modeling efforts will be directed towards modeling the above phenomena. Detailed comments are made below about some of the above six phenomena.

10.4.1 Fuel constituent Radial Migration

As discuss in Section 10.2, the zone formation calculation method of the earlier SSCOMP model [10-4] is not incorporated into SAS4A/SASSYS-1 Version 3.0 codes due to its limitation. The study of fuel constituent radial migration leading to zone formation was not at that time developed to a state where an appropriate dynamic model could be developed. It is expected that a dynamic model for calculating fuel constituent radial migration, available in the literature or developed on the basis of available zonal composition and radial boundary data, will be incorporated into the codes. Such a dynamic model will be based on pin power history during steady-state irradiation. If neither a dynamic model nor a zonal composition and radial boundary database is available in the near future, the earlier SSCOMP model will be implemented in the codes.

Table 10.4-1. Internal Arrays Required for Implementing IFR Handbook U-Pu-Zr Fuel Properties Data and Multiple Radial Fuel Zones Option

Definition/Comments	Array Name
Arrays by Radial Node and Axial Segment in Block COMC	
1. Fuel mass	FUELMS(11,24)
2. Pu mass in fuel	FUPUMS(11,24)
3. Zr mass in fuel	FUZRMS(11,24)
4. Fe mass in fuel	FUFEMS(11,24)
5. Ni mass in fuel	FUNIMS(11,24)
6. Total porosity in fuel	PRSTY2(11,24)
7. Logged sodium mass in fuel	FUNAMS(11,24)
Arrays by Fuel Type in Block FPTVAR	
8. First solid-state transition temperature of fuel	TEMALF(8)
9. Last solid-state transition temperature of fuel	TEMGAM(8)
10. Pre-calculated coefficients in the quadratic equation for fuel thermal conductivity	ACPF(8,7)
11. Pre-calculated coefficient in the quadratic equation for fuel thermal conductivity	AKFU(8,5)
12. Pre-calculated parameters in fuel theoretical density equation	ADFU(8,2)

10.4.2 Fission Gas Behavior, and Porosity Formation and Distribution

The modeling of the following aspects of fission gas behavior is required for calculation the initial conditions of FPIN2 transient calculation: (a) fission gas generation, (b) fission gas retained with grains, (c) fission gas retained in grain boundary bubbles that are not linked, (d) fission gas contained in grain boundary bubbles that are interlinked, and (e) fission gas released to pin plenum. The need for modeling these three types of fission gas contained in fuel (gas within grains, in unliked grain boundary bubbles, and in interlined grain boundary bubbles) has also been expressed by the pre-failure in-pin fuel motion module PINACL development [10-7].

10.4.3 Irradiation-Induced Radial and Axial Swelling of Fuel and Cladding

Regarding irradiation-induced fuel swelling, the axial swelling will contribute to pre-transient fuel column length, a needed initial condition of the FPIN2 module. Radial swelling of fuel and cladding will determine fuel-cladding gap closure and bond sodium migration into pin plenum, a needed initial condition of the FPIN2 module. The modeling of fuel swelling phenomenon has two important aspects: swelling due to solid fission products, and fission gas induced swelling. Swelling of a cladding material is mainly determined by neutron fluence which is also a parameter in determining cladding rupture life used in the FPIN2 transient fuel mechanics calculation.

The SSCOMP module is being developed to model the above listed in-pin phenomena during steady-state irradiation of metallic fuel pins. After the fuel pin has been characterized at the end of steady-state irradiation, the calculation of the relevant ones of these phenomena during the transient will be performed by the DEFORM-5 model.

REFERENCES

NOTICE

Several references in this document refer to unpublished information. For a list of available open-literature citations, please contact the authors.

APPENDIX 10.1:
Equivalency of Interpolation in Terms of Weight Fractions and Atom Fractions

As described in Section 10.3.2.1, the enthalpy of a desired U-Pu-Zr fuel composition is evaluated by mixing 3 basic alloys with enthalpy data known and reported in the Metallic Fuels Handbook [10-8]. The proportions or weight fractions of the 3 database alloys in mixing are so calculated that the resulting mixture has the composition of the desired fuel. The purpose of this appendix is to show that it makes no difference whether this mixing or linear interpolation is carried out by expressing composition in terms of weight fractions or atom fractions, and correspondingly enthalpy in terms of J/unit mass or J/mol.

Let

a_1, a_2, a_3 = average atomic weights of the 3 database alloys,

h_1, h_2, h_3 = enthalpy (J/gm) of the 3 database alloys at a desired temperature.

H_1, H_2, H_3 = enthalpy (J/mol) of the 3 database alloys at the desired temperature,

X_1, X_2, X_3 = weight fractions of the 3 database alloys to be mixed to produce the desired fuel composition.

Y_1, Y_2, Y_3 = atom fractions of the database alloys to be mixed to produce the desired fuel composition.

The desired fuel enthalpy interpolated in terms of weight fractions is given by

$$h = X_1 h_1 + X_2 h_2 + X_3 h_3 \qquad \text{(A10.1-1)}$$

where h is in units of J/gm. The desired fuel enthalpy interpolated in terms of atom fractions is given by

$$H = Y_1 H_1 + Y_2 H_2 + Y_3 H_3 \qquad \text{(A10.1-2)}$$

where H is in units of J/mol. The enthalpies given by Eqs. (A10.1-1) and (A10.1-2) will be the same if it is shown that

$$h = H / a \qquad \text{(A10.1-3)}$$

where

a = average atomic weight of the desired fuel composition.

The average atomic weight of the desired fuel composition is related to the atomic weight of the 3 database alloys and their weight fractions in the desired fuel as follows:

$$a = 1/\left(\frac{X_1}{a_1}+\frac{X_2}{a_2}+\frac{X_3}{a_3}\right) \tag{A10.1-4}$$

The atom fraction Y_1 of database alloy 1 in the desired fuel is related to the weight fractions X_1, X_2, X_3 of the 3 database alloys in the desired fuel as follows:

$$Y_1 = \left(\frac{X_1}{a_1}\right)/\left(\frac{X_1}{a_1}+\frac{X_2}{a_2}+\frac{X_3}{a_3}\right) \tag{A10.1-5}$$

With the help of Eq. (A10.1-4), the atom fraction Y_1 given by Eq. (A10.1-5) simplifies to

$$Y_1 = \frac{aX_1}{a_1} \tag{A10.1-6}$$

Similarly, the atom fractions Y_2 and Y_3 can be written as

$$Y_2 = \frac{aX_2}{a_2} \tag{A10.1-7}$$

$$Y_3 = \frac{aX_3}{a_3} \tag{A10.1-8}$$

The enthalpies of the 3 database alloys in units of J/mol are related to their enthalpies in units of J/gm and their atomic weights as follows:

$$H_1 = a_1\, h_1, H_2 = a_2\, h_2, H_3 = a_3\, h_3 \tag{A10.1-9}$$

Substituting the values of Y_1, Y_2, Y_3 and H_1, H_2, H_3 from Eqs. (A10-1-6) to (A10.1-9) into Eq. (A10.1-2), one obtains

$$H = a\, X_1\, h_1 + a\, X_2\, h_2 + a\, X_3\, h_3 \tag{A10.1-10}$$

With the help of Eq. (A10.1-1), the desired fuel enthalpy interpolated in terms of atom fractions given by Eq. (A10.1-10) becomes

$$H = ah \tag{A10.1-11}$$

Equation (A10.1-11) proves what Eq. (A10.1-3) required.

APPENDIX 10.2:
Correlations in the IFR Handbook and Some Other Sources

The following 4 correlations are available to estimate 100% dense solid U-Pu-Zr fuel thermal conductivity, K_o(W/m-K):

1. The correlation in the IFR Metallic Fuels Handbook [10-8, 10-9] is written as

$$K_o = B_1 + B_2 T + B_3 T^2 \qquad \text{(A10.2-1)}$$

where

$B_1 = 17.5\,[(1 - 2.23\,W_z)/(1 + 1.61\,W_z) - 2.62\,W_p]$

$B_2 = 0.0154\,[(1 + 0.061\,W_z)/(1 + 1.61\,W_z) + 0.90\,W_p]$

$B_3 = 9.38 \times 10^{-6}\,(1 - 2.70\,W_p)$

W_p, W_z = weight fractions of Pu and Zr

T = fuel temperature, K.

2. The correlation in Billone's memorandum [10-21] of March 8, 1991 is written as

$$K_o = B_4 + B_5 T + B_6 T^2 \qquad \text{(A10.2-2)}$$

where

$B_4 = 17.5\,[1 - 1.471\,A_z + 44.083\,A_p\,(1 - 16.198\,A_p + 55.290\,A_p^2)]$

$B_5 = 0.0154\,[1 - 0.5935\,A_z - 158.88\,A_p\,(1 - 14.865\,A_p + 49.478\,A_p^2)]$

$B_6 = 9.38 \times 10^{-6}\,[1 + 215.78\,A_p\,(1 - 14.421\,A_p + 47.158\,A_p^2)]$

A_p, A_z = atom fractions of Pu and Zr.

3. The correlation in Billone's memorandum [10-22] of October 21, 1991 is written as

$$K_o = B_7 + B_8 T + B_9 T^2 \qquad \text{(A10.2-3)}$$

where

$B_7 = 17.5\,(1 - 1.417\,A_z - 6.8174\,A_p)$

$B_8 = 0.0154\,(1 - 0.5935\,A_z + 15.108\,A_p)$

$B_9 = 9.38 \times 10^{-6}\,(1 - 18.778\,A_p)$

4. The correlation reported in ANL/RAS 85-19 can be written as

$$K_o = K_u + 2A_z\left(K_{u50} - K_u\right)/\left(A_u + A_z\right) - CA_p \qquad \text{(A10.2-4)}$$

where

K_u = 22.173 + 0.018562 T_c + 1.3278 x 10^{-5} T_c^2

K_{u50} = 7.4766 + 0.016738 T_c + 1.1599 x 10^{-5} T_c^2

C = (89.079 – 167.57 A_z) – T_c(0.17437 – 0.4008 A_z) +

T_c^2 (1.9608 x 10^{-4} – 3.1043 x 10^{-4} A_z), 100 ≤ T_c ≤ 1500,

0.0 ≤ A_p ≤ 0.2, 0.0 ≤ A_z ≤ 0.5 (A10.2-5)

T_c = fuel temperature, °C

Correlations 1, 2 and 3 have been developed based on the thermal conductivity data presented in the Metallic Fuels Handbook. Detailed plots of these correlations are available in Ref. [10-17]. Correlation 2 should not be used because it is ill-behaved, and so recommended by Billone [10-22]. A drawback of correlations 1 and 3 is that the thermal conductivities become negative (unphysical) at room temperature for Pu and Zr contents greater than 20 wt %. In addition, the thermal conductivity obtained from correlation 3 shows a maximum when plotted as a function of temperature (an unexpected behavior [10-18] for temperatures above 300 K).

The comparison of these 3 correlations with the Handbook data for 3 ternary alloys (U-16.2Pu-6.2Zr, U-14.7Pu9.7Zr and U-18.4Pu-11.5Zr) shows that there are significantly large differences among the 3 correlations at temperatures above 1200 K where there is no thermal conductivity data. Below 1200 K, the difference among the data and the 3 correlations are smaller.

The comparison of these 3 correlations with the Handbook data for 3 U-Zr binary alloys (U-1.5Zr, U-5Zr and U-20Zr) shows that the 3 correlations are almost identical at all temperatures, and that they agree with the data closely. The agreement is not so good with the data for U-40Zr, as shown by a plot given in the Handbook [10-8, 10-9]. The Handbook correlation for U-Zr binary alloys, i.e., Eq. (A10.2-1) with W_p set to zero, is found to be reliable for Zr content in the 1.5 to 20 wt % range.

The thermal conductivity obtained from correlation 4 for the some alloy compositions becomes negative (unphysical) at room temperature, and shows an unexpected maximum when plotted as a function of temperature. Although the alloy compositions showing this unphysical/unexpected behavior are out of the noted region of validity, the correlation has another drawback that it was derived using data from sources [10-14, 10-19, 10-20] other than the IFR Metallic Fuels Handbook [10-8, 10-9].